DOCTOR OF SCIENCES

CtrA-dependant cell cycle regulation of Brucella abortus in culture and during infection

Francis, Nayla

Award date:
2015

Awarding institution:
University of Namur

UNIVERSITÉ DE NAMUR

URBM

Investigating the CtrA-dependent cell cycle regulation of the pathogen *Brucella abortus*

Nayla Francis

Dissertation presented in preparation
of the degree of PhD in Sciences

Jury members

Pr. Sean Crosson, University of Chicago, USA
Dr. Emanuele Biondi, University of AIX-Marseille, France
Pr. Jean-François Collet, UCL, Belgium
Pr. Patsy Renard, President, University of Namur, Belgium
Pr. Xavier De Bolle, Promoter, University of Namur, Belgium

2015

"Science is a way of life. Science is a perspective.
Science is the process that takes us from confusion
to understanding in a manner that's precise, predictive
and reliable – a transformation, for those lucky enough to
experience it, that is empowering and emotional."

Brian Green

"Time has been transformed, and we have changed;
it has advanced and set us in motion;
it has unveiled its face, inspiring us with bewilderment and exhilaration."

Khalil Gibran

Acknowledgements

First I would like to thank the jury members Pr. Sean Crosson, Dr. Emanuele Biondi, Pr. Jean-François Collet and Pr. Patsy Renard for accepting to be part of this jury, for reading the manuscript and sharing their comments to improve it.

Je voudrais ensuite remercier les membres du comité d'accompagnement, Dr. Sébastien Rigali et Pr. Jean-Jacques Letesson pour leurs remarques et commentaires constructifs lors de nos réunions. Un tout grand merci à mon promoteur, Pr. Xavier De Bolle pour sa bonne humeur, pour sa présence malgré un horaire chargé et pour nos discussions. Merci de m'avoir donné l'oportunité de vivre cette belle expérience enrichissante au plan intellectuel aussi bien qu'humain.

I would also like to thank Dr. Emanuele Biondi and his team for welcoming me in their lab and for teaching me new techniques in biochemistry. Antonella, Francesco and Saswat thanks a lot for your help! Anto I was happy to see you on a regular basis in the European meetings we attended. And I am very happy to see you soon in Brussels ;).

Merci à l'URBM, ce labo unique en son genre! Merci aux URBMiens pour votre bonne humeur, nos sorties, nos rigolades, nos soupers de noel bien arrosés… Je voudrais remercier tout particulièrement Emeline non seulement pour son soutien tout au long du mémoire et des quatre années de thèse, mais aussi pour les moments inoubliables passés ensemble au labo, aux wallos, aux congrès, etc. Merci à Jérôme, Lio et Julien, mémos URBM! Jéjé et Séverin, merci d'être passés au bureau pendant la période de rédaction; ça m'a fait du bien de pouvoir papoter pendant cette période d'isolement (quasi) total :p. Sans oublier la bonne humeur de Moumou, Kéké, Arnaud et Doudou. Merci à Aurélie et Kéké pour le coup de main donné avec les manips durant ces derniers mois, je ne sais pas ce que j'aurais fait sans vous… Merci à Mathieu pour l'organisation des sorties labo et pour toute la logistique instaurée au labo, merci à Françoise aussi! Sans vous, le labo ne serait pas ce qu'il est aujourd'hui. Merci à la Xa Team, Katy, Vicky, Phuong, JF, Rosa, Nicolas et, la nouvelle recrue ;), Mathilde. Merci aux anciens, Mike Caro, Miche-Miche, Mira et Dédé. Je voudrais aussi remercier le labo Gémo, Julie, Oli, Carlo, Constant et Valérie, pour les beers hours; cette petite routine du vendredi après-midi va bien me manquer…

Merci à JY et aux filles de bio, Caro, Mimi, Evelyne, Laura, Thérèse, Elo et Virginie d'avoir gardé contact et merci pour toutes ces sorties organisées. J'espère qu'il y en aura encore plein d'autres dans l'avenir! Merci à Christina et Sandy, le petit bout de Liban ici en Belgique ☺. Je suis super contente de vous avoir rencontrées! Merci à Florent aussi! Florence et Denis, merci pour les chouettes moments passés ensemble, à Namur ou Bruxelles; Flo merci pour nos "séances psy" à la péda. J'ai vraiment eu de la chance de t'avoir comme voisine de chamber ☺. Merci aussi aux autres filles de la péda, Faty, Pauline, Nath, Marie, Catherine. Je n'oublierai jamais ce premier chapitre de ma vie belge. Sarah, mon amie d'enfance, merci d'avoir été là pour moi à tout moment, malgré la distance.

Un tout grand merci à ma famille à Bruxelles, Saad, Rima, Lara et Elie. Tous les mots ne pourraient exprimer à quel point je vous suis reconnaissante pour tout ce que vous avez

fait. Merci d'avoir été là pour moi et de m'avoir aidée et soutenue à mon arrivée en Belgique et bien après. Merci à ma famille belge, Marc, Myriam, Martin, Aline et Béné, ainsi qu'aux cousins tantes et oncles. Vous m'avez si bien accueillie et je suis très heureuse d'avoir fait votre connaissance et de faire partie de votre famille. Merci à mon meilleur ami et mon âme soeur. Hubert merci d'avoir été là pour moi pendant cette période pas si facile, merci d'avoir supporté mon stress, mes doutes, d'avoir été à l'écoute, d'avoit toujours trouvé les bons mots pour me rassurer. Merci d'avoir lu et corrigé la thèse. Merci pour tous les bons moments passés ensembles, et pour tous ceux à venir…

Merci à ma famille au Liban, à toutes ces personnes sans lesquelles je ne serais pas ce que je suis aujourd'hui. D'abord Papi, merci d'avoir été toujours là pour moi, de m'avoir soutenue dans tous mes projets, de m'avoir offert ce beau voyage qu'est mon séjour en Belgique. Merci à Nadine et Georges d'avoir été là pour moi, de m'avoir fait rire, de pouvoir tout partager avec vous. Merci à mon ange gardien, je sais que tu es avec moi à tout moment de la journée et de la nuit. Merci à mes autres mamans, Téta Saideh, Téta Yolla, Jocy, Amto Norma et Amto Hanan. Sans votre amour et votre présence à mes côtés, je ne serais pas arrivée là je suis aujourd'hui. Jocy, I know French is not your best friend ;). So here is a little switch to English if you read these lines one day. Thank you for having been there for me on a daily basis while I was growing up. Thank you for reading and correcting the thesis. Andrew, I am so lucky for having you as a cousin and a godson. Mary, Nicholas, Joe, Jad and Jawad, thank you for all the great moments we spent together. More than cousins, you are sisters and brothers to me. Amo Georges and Amo Garo, thank you for the great moments and for taking care of us. Amto Nahla, Amo Jamil, Mimi and G, I wish I could see you more often, but it's nice to know I have family in the States. I hope I can come visit you soon ☺.

Pour terminer, je voudrais dire que je suis tellement chanceuse d'avoir été si bien entourée durant ces dernières années. Et je suis infiniment reconnaissante à toute personne qui a contribué de près ou de loin à ma réussite.

Investigating the CtrA-mediated cell cycle regulation of *Brucella abortus*

How a conserved transcription factor is adapted to the intracellular lifestyle of a pathogen

Coordinating growth with chromosome replication and division is a basic condition for the survival of any living organism, be it unicellular or multicellular, prokaryote or eukaryote. For this coordination to occur correctly, several external and internal cues have to be sensed and integrated into the complex system that is a living cell. During evolution, bacteria have selected a conceptually simple but robust system to sense signals and respond accordingly, the two-component system (TCS). As the name implies, a TCS is composed of two actors, a sensor and an effector. The sensor, often a histidine kinase, is activated by recognizing various physical or chemical stimuli. It transmits the signal to the effector component, often a transcription factor that initiates a specific gene expression program in response to the signal sensed by the histidine kinase. In *Caulobacter crescentus*, a model organism for studying bacterial cell cycle and differentiation, a TCS regulating the phosphorylation status of a central transcription factor called CtrA was thoroughly studied. Together with other essential regulators, CtrA coordinates, among other processes, chromosome replication with division and polar morphogenesis. Most interestingly, this TCS and CtrA are conserved among *Alphaproteobacteria* members, to which *C. crescentus* belongs, even in those devoid of polar organelles. This class brings together bacteria with diverse lifestyles, ranging from free-living organisms to pathogens of plants and mammals, as well as symbionts of plants and arthropods.

During this thesis, we aimed at investigating the role of CtrA and the TCS regulating its phosphorylation in *Brucella abortus,* a pathogen of mammals. We performed kinase assays and showed that the PdhS sensor kinase can modulate the phosphorylation status of the response regulator DivK. CtrA being essential, we constructed a depletion strain and analysed its growth, morphology, DNA content and virulence in a HeLa cell infection model. We showed that CtrA is essential for *B. abortus* division and intracellular survival, but not for bacterial elongation. Indeed, in absence of CtrA, *B. abortus* cells continue elongating and form branched morphologies. A ChIP-seq assay allowed the mapping of CtrA binding sites on the whole genome of *B. abortus* and the identification of two main functional categories for CtrA potential target genes, cell cycle-related genes and genes involved in envelope biogenesis and homeostasis. The latter putative function of CtrA was of particular interest for us, as it distinguishes CtrA of the pathogen *B. abortus* from the one of the free-living bacterium *C. crescentus*.

All along this manuscript, we attempt to compare the TCS and CtrA of *C. crescentus*, *B. abortus* and *Sinorhizobium meliloti*, an alphaproteobacterium symbiont of legume plants. A substantial amount of data has been published during the last few years concerning the events regulating the cell cycle of *S. meliloti*. These data together with those obtained along this thesis give a more extensive insight of how a highly conserved phosphorylation cascade was exploited and adapted by microorganisms with different lifestyles.

Abbreviations

BCV	Brucella containing vacuole
BMDM	Bone marrow-derived macrophage
Bvr	*Brucella* virulence related
CA	Catalytic and ATP-binding domain
CACHE	Ca^{2+} channels, chemotaxis receptors
CbrA	Calcofluor bright regulator A
CcrM	Cell cycle regulated methyltransferase
CHASE	Cyclase/Histidine kinase-associated sensing extracellular
ChIP-seq	Chromatin immunoprecipitation followed by deep-sequencing
C*ori*	*Caulobacter crescentus* origin of replication
CtrA	Cell cycle transcriptional regulator A
DHp	Dimerization and histidine phosphotransfer domain
ER	Endoplasmic reticulum
ECM	Extracellular matrix
EEA1	Early endosomal antigen 1
EMSA	Electrophoretic mobility shift assay
ERES	Endoplasmic reticulum exit site
GST	Glutathione S transferase
GTA	Gene transfer mechanism
HK	Histidine kinase
HPt	Histidine phosphotransferase
IT	Infection thread
Lamp1	Lysosomal-associated membrane protein1
LPS	Lipopolysaccharide
MBP	Maltose Binding Protein
MDH	Malate dehydrogenase
OM	Outer membrane
OMP	Outer membrane protein
ORF	Open reading frame
Pal	Peptidoglycan-associated protein
PAS	Per-ARNT-Sim = Period, Aryl hydrocarbon receptor nuclear transporter, Single-minded
PBP	Penicillin binding protein
PdhS	PleC-DivJ homologous sensor
PG	Peptidoglycan
PI	Post-infection
REC	Receiver domain
RR	Response regulator
SwaPS	Swarmer progeny-specific
T4SS	Type 4 secretion system
TCA	Tricarboxylic acid
TCS	Two-component system
TM	Transmembrane
TRSE	Texas red succinimidyl ester
Trx	Thioredoxin
TS	Thermosensitive
Y2H	Yeast two-hybrid

Table of contents

Introduction

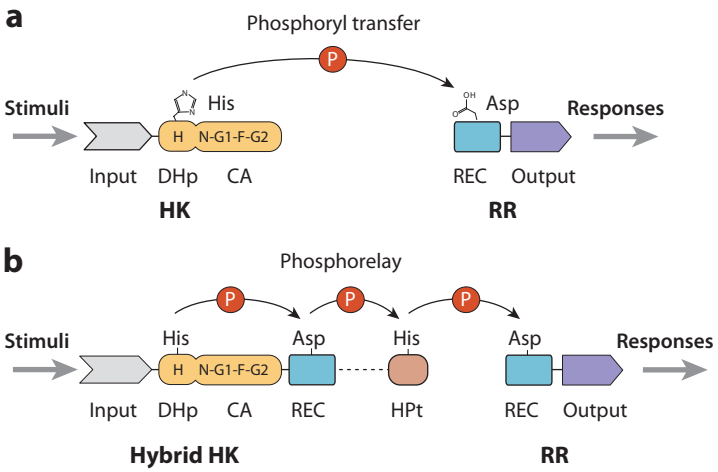

Figure 1- Schematic representation of a two-component system and a phosphorelay (Gao and Stock, 2009)

The modular structure of TCS proteins is represented by coloured boxes depicting conserved domains.

a- A TCS involves a histidine kinase (HK) and a response regulator (RR). The input domain of the HK senses a stimulus, leading to the autophosphorylation on a conserved histidine in the DHp domain then the phosphotransfer to a conserved aspartate in the receiver domain (REC) of the RR. The phosphorylated RR is activated and can fulfil a biological response.

b- A phosphorelay is a more complex version of a TCS. It involves a hybrid HK that contains a REC domain and performs intra-molecular phosphotransfer before transferring the phosphoryl group to a histidine phosphotransefrase (HPt) that can be part of the hybrid HK or encoded separately (dashed line). The HPt serves as an intermediate between the hybrid HK and the final RR with an output domain.

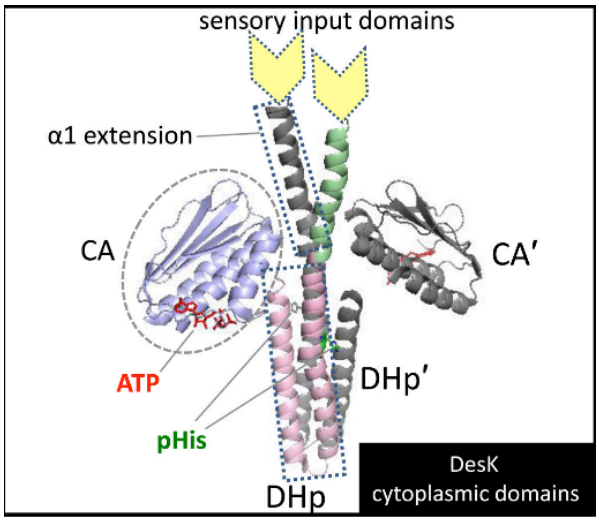

Figure 2- Crystal structure of the cytoplasmic domain of a dimer of *Bacillus subtilis* DesK histidine kinase (Stewart, 2010)

This crystal structure shows a dimer of DesK cytoplasmic domain. The two monomers interact at the level of the DHp domain. The back monomer is in grey. The front monomer is coloured. Color code for the front monomer: DHp helices in pink, extension of α1 helix in green, CA domain in purple.

Chapter I- Two-component systems and phosphorelays

A- Two-component systems (TCS)

All living organisms have to adapt to their changing environment. Bacteria have selected an efficient apparatus composed of a multitude two-component systems (TCSs), allowing them to sense diverse stimuli and to respond accordingly (Nixon et al., 1986). The prototype of a TCS consists of a membrane-bound receptor protein, a histidine kinase (HK), and a cytoplasmic effector protein, a response regulator (RR). HKs are associated to the cytoplasmic membrane via 2 to 20 transmembrane (TM) domains. Phosphorylation reactions are at the basis of the functioning of a TCS. When a HK senses a stimulus, it is activated by autophosphorylation on a histidine residue and transmits the signal by transferring the phosphoryl group to an asparate residue on its cognate RR (Figure 1-a). This phosphotransfer induces conformational changes in the RR, switching it to its active form and leading to a specific biological response. Motility, development, nutrient uptake, nodulation and virulence are a few examples of processes regulated by TCSs in bacteria. TCSs based on His-Asp phosphotransfer are not specific to bacteria. Archea, yeast and plants also code for several TCSs while such an apparatus is quite rare in animals (Stewart, 2010). Indeed, signal transduction cascades in animals are based on serine, threonine and tyrosine phosphorylation.

1. Autophosphorylation of a histidine kinase and phosphotransfer to its cognate response regulator

HKs have a modular organisation, with highly variable N-terminal input or sensor domains and conserved C-terminal catalytic domains. In typical membrane-bound HKs (83% of all known HKs) (Cock and Whitworth, 2007), the input domain is located in the periplasmic space. The cytoplasmic part of a HK contains two domains: a conserved catalytic ATP-binding (CA) domain and a less conserved dimerization and histidine phosphotransfer (DHp) domain (Figure 2) (Gao and Stock, 2009). The DHp domain contains a conserved sequence motif "H" comprising a histidine residue that receives the phosphoryl group (Figure 1-a). The CA domain contains four conserved sequence motives called N, G1, F and G2 (Figure 1-a). These conserved boxes define the ATP-binding cavity of the CA domain and the F and G2 boxes are separated by a flexible loop named ATP lid that changes conformation upon nucleotide binding. Most HKs occur in homo-dimers, and the dimerization zone is localized to the DHp α1 and α2 helices, forming a four-helix bundle (Figure 2) (Casino et al., 2014). Crystallizing a full-length histidine kinase and visualizing autophosphorylation are challenging processes given the obvious difficulty of purifying a membrane-associated protein, but also because of the high dynamics of the autophosphorylation reaction. However, the model presented in Figure 3 was inferred from several experimental observations. Recognition of a signal is thought to induce changes in the sensor domain, releasing inhibitory interactions (in orange) and inducing movements in the helices of the DHp domain. These conformational changes bring the ATP molecule close to the conserved histidine residue and promote the transfer of the γ-phosphate from the ATP to the histidine. HKs autophosphorylate either in *cis* (the CA domain of a monomer phosphorylates the conserved histidine of the same monomer) or in *trans* (the CA domain of a monomer phosphorylates the conserved histidine of the other monomer) (Cai and Inouye, 2003; Casino et al., 2009; Ninfa et al., 1993). Depending on the orientation and the length of the loop connecting the helices α1 and α2 of the DHp domain, the CA domain of a monomer

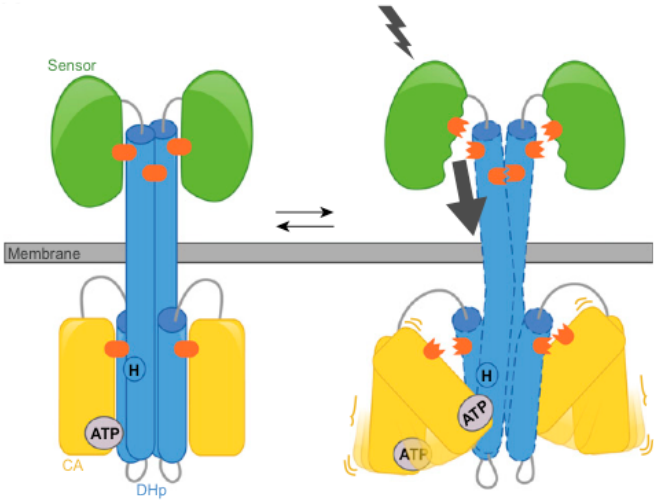

Figure 3- Model for the autophosphorylation of a histidine kinase dimer (Rivera-Cancel et al., 2014)
The sensor domain is in green, the DHp domain in blue and the CA domain in yellow. Orange elongated circles represent interactions that bloc the dimer in an inactive state (on the left). When a particular signal is detected by the sensor domain (on the right), conformational changes of this domain disrupt the inhibitory interactions and propagate throughout the DHp domain, allowing the ATP molecule to come close to the conserved histidine.

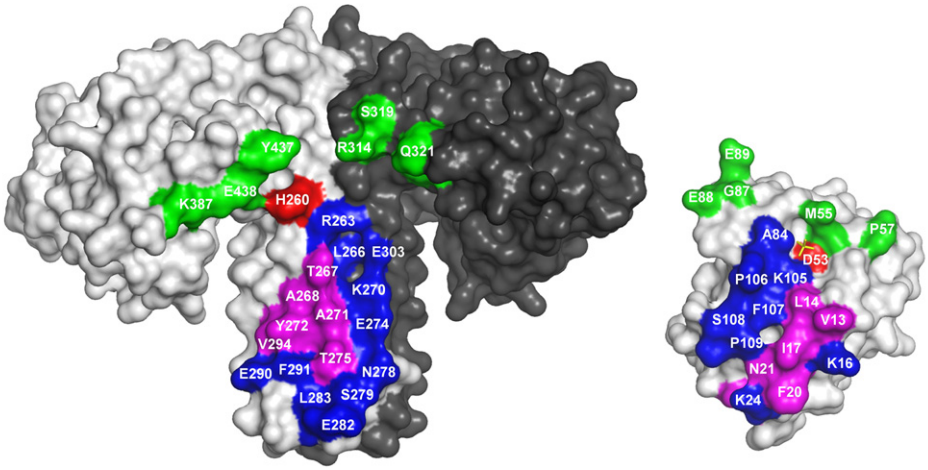

Figure 4- Residues involved in a HK-RR interaction (Casino et al., 2009)
This surface representation shows the crystal structure of the cytoplasmic portion HK853 (on the left) from *Thermotoga maritima* and and its cognate RR, RR468 (on the right). The phosphoacceptor residue H260 and the phosphoreceiver residue D53 are highlighted in red. Residues of HK853 painted in green, purple and blue interact with residues of RR468 of the same colour.

is positioned close to the conserved histidine of the same monomer or of the other monomer, determining by that the mode of autophosphorylation of the HK (Casino et al., 2014; Casino et al., 2010).

Unlike the phospho-ester bonds formed in serine/threonine and tyrosine kinases, the phospho-amidate formed in histidine kinases between the phosphoryl group and the imidazole ring of the histidine is less stable and thus more suitable as a phosphotransfer intermediate (Gao and Stock, 2009). A typical RR contains a N-terminal receiver domain (REC) with a conserved aspartate residue and a C-terminal output domain. Often, the output domain is a DNA binding domain. An activated RR thus acts as a transcription factor, regulating gene expression in response to the stimulus sensed by the HK. A bacterial genome can encode dozens of two-component proteins (Gao and Stock, 2009). A specific recognition between the phosphorylated HK dimer and its cognate RR is thus needed to ensure the development of a correct answer and avoid crosstalks. The identification of co-evolving amino acid patterns by large multiple alignments followed by mutagenesis experiments and crystallisation of HK-RR complexes allowed the identification of poorly conserved residues in the HK and the RR that contact each other in the complex and confer HK-RR interaction specificity (Figure 4) (Casino et al., 2009; Skerker et al., 2008). Two experiments exemplify the robustness of HK-RR recognition specificity. Yamamoto et al. purified the kinase domain (DHp+CA) of 27 HKs and the full length of 34 RRs from *E. coli* and tested the phosphotransfer between cognate HKs and RRs but also between 692 non-cognate pairs (Yamamoto et al., 2005). Twenty-four of the 27 HKs showed phosphotransfer towards their cognate RR while only 22 out of the 692 non-cognate pairs harboured phosphotransfer. In another experiment, EnvZ was shown to phosphorylate 11 RRs after an incubation of 60 minutes. However when given a 10 second-reaction time, EnvZ was only able to efficiently phosphorylate OmpR, its cognate RR (Skerker et al., 2005).

2. Histidine kinases sense diverse stimuli

Signals sensed by HKs can be of physical nature (light, temperature, turgor pressure) or chemical molecules such as chemoattractants (serine, aspartate), small inorganic compounds (CO_2, CO, NO) or metabolites (citrate, 2-ketoglutarate, glutamine) (Krell et al., 2010). For most TCSs, the signals sensed by the HKs remain unknown. It is indeed difficult to predict the stimuli sensed by a HK given the poor conservation of the amino acid sequence and structure of sensor domains. Furthermore, predictions are rendered even more challenging by the fact that in some cases the stimulus is sensed indirectly, via a periplasmic protein that binds to a given molecule and subsequently interacts with the sensor domain of the HK. For instance, *Agrobacterium tumefaciens* VirA HK is activated by interacting with the glucose-binding protein ChvE (Shimoda et al., 1993).

Despite the huge variability in the sequence and structure of input domains, they can still be classified according to some common features. Analysis of periplasmic domains allowed the identification of some common sequences and secondary structures, namely GAF and PAS domains. GAF domains are found in cyclic GMP phosphodiesterases, adenylyl cyclases and FhlA (Formate hydrogenlyase A). PAS domains are present in bacteria, Archea and eukaryotes (Taylor and Zhulin, 1999). PAS is an acronym originating from the names of three eukaryotic proteins in which this domain was first identified: the drosophila period clock protein (PER), vertebrate aryl hydrocarbon receptor nuclear translocator (ARNT) and the drosophila single-minded protein (SIM) (Taylor and Zhulin, 1999). In bacteria, PAS domains can be periplasmic or cytoplasmic

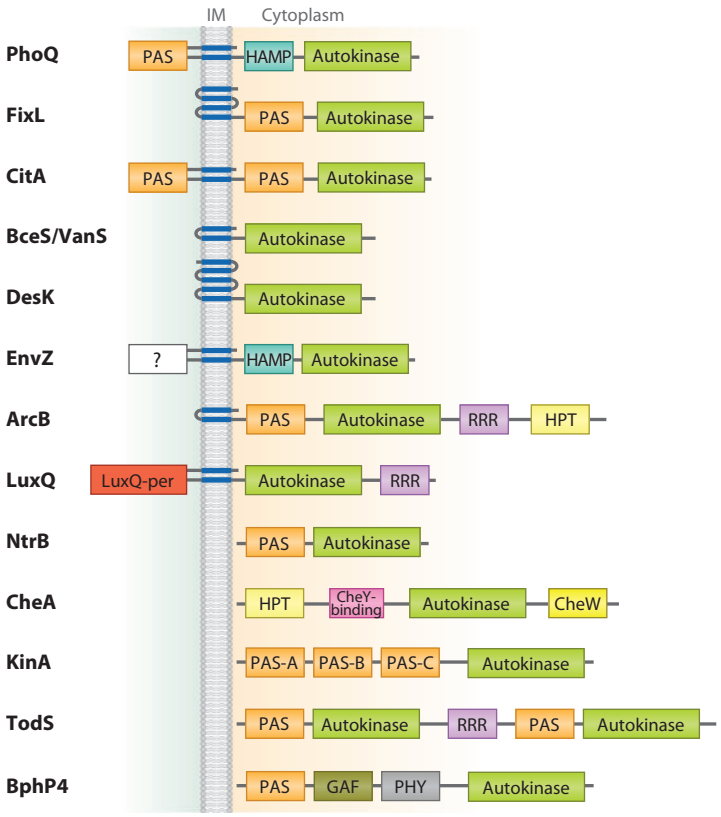

Figure 5- Domain organization of representative HKs (Krell et al., 2010)
Examples of membrane-bound kinases with two to five TM domains (blue) are represented in the upper part of the scheme, while cytoplasmic HKs are depicted in the lower part. PAS domains are shown to be located in the periplasmic space or in the cytoplasm. EnvZ has no predicted sensor domain in the periplasm (?). "Autokinase" refers to the DHp and CA domains. Some HKs harbour yet other domains such as the HAMP (HKs, adenylyl cyclases, methyl binding proteins, phosphatases), RRR (Response regulator receiver) and PHY (Phytochrome) domains.

(Figure 5) and are involved in sensing oxygen and redox state. For instance, in *Sinorhizobium meliloti*, a soil bacterium and a symbiont of legume plants, the PAS domain of FixL HK binds oxygen. When nitrogen sources become scarce in the soil, a complex molecular interplay is launched between the root hair of legume plants and *S. meliloti* (Figure 19). Bacteria invade the root hair and are endocytosed by plant cells where they are confined in a microaerobic environment. Oxygen is displaced from FixL PAS domain, leading to activating conformational changes. FixL autophosphorylates and transfers the phosphoryl group to the REC domain of FixJ, its cognate RR. Phosphorylated FixJ acts as a transcriptional activator of genes involved in nitrogen fixation. Products of these genes are necessary for reducing atmospheric N_2 to NH_3, metabolically usable by the host plant (Gibson et al., 2008; Taylor and Zhulin, 1999).
Identification of PAS domains is based on the presence of two repeated sequences (Taylor and Zhulin, 1999). However, in some cases sequence similarity is not enough to detect PAS domains. Some input domains harbour a structure similar to PAS domains but with little sequence similarity (Mascher et al., 2006). This is the case of PhoQ of *Salmonella*. The PhoQ/PhoP TCS of *Salmonella enterica* serovar Typhimurium controls virulence, Mg^{2+} homeostasis and resistance to acidic pH and to antimicrobial cationic peptides (Park and Groisman, 2014). These peptides have a positive net charge, allowing them to interact with negatively charged lipopolysaccharide (LPS) and membranes, thereby disrupting the bacterial envelope. The PhoQ PAS domain repeats are separated by two negatively charged alpha helices that are thought to interact with Mg^{2+}. These ions are proposed to form cationic bridges between the helices of the PAS domain and the negatively charged groups on the cytoplasmic membrane, blocking PhoQ in an inactive state. Cationic peptides are thought to displace these divalent cations and to disrupt the interaction of the PAS domain with the inner membrane. Activation of the PhoQ/PhoP TCS leads to the expression of genes involved in lipid A modifications (See paragraph III-C and figure 27) that render the LPS resistant to the action of cationic peptides.
More recently, sequence analyses allowed the identification of other conserved domains called CACHE (Ca^{2+} channels, chemotaxis receptors) (Anantharaman and Aravind, 2000) and CHASE1 to 6 (Cyclase/Histidine kinase-associated sensing extracellular) (Mougel and Zhulin, 2001). CACHE domains are present in methyl-accepting chemotaxis proteins (MCP) of *Bacillus subtilis*. They are thought to bind small molecules and are important for sensing amino acids and carbohydrates by McpB and McpC respectively in *B. subtilis*. A CHASE3 domain was found in VsrA HK of *Pseudomonas solanacearum* and is required for the expression of virulence factors (Schell et al., 1994). Other pathogens, such as *Legionella pneumophila* and *Bacillus anthracis*, code for CHASE3-containing HKs (Zhulin et al., 2003).

Despite the continuous progress in understanding signal sensing by periplasmic domains, the way many HKs are activated remains elusive. EnvZ is a good example of a HK for which the mechanism of activation is not well understood even though the EnvZ-OmpR pair is one of the most studied TCSs. EnvZ is a prototype for studying membrane-bound HK dimerization and phosphorylation and its cytoplasmic domain has been crystallized. The EnvZ-OmpR TCS regulates the expression of *ompF* and *ompC*, two genes coding for outer membrane porins, in response to changes in the osmolarity of the environment (Russo and Silhavy, 1991). In low osmolarity conditions, low levels of phosphorylated OmpR activate the expression of *ompF* (Harrison-McMonagle et al., 1999). When osmolarity increases, the accumulation of phosphorylated OmpR activates

the expression of *ompC* and inhibits the expression of *ompF*. Activation of EnvZ by the increase of osmolarity is thought to be independent of the sequence of EnvZ periplasmic domain as replacing it with the periplasmic domain of PhoR HK did not alter the expression of *ompF* and *ompC* (Leonardo and Forst, 1996). It was suggested that the integrity of the periplasmic domain as a whole is important (Mascher et al., 2006). When the osmolarity increases, movements in the TM domains occur, leading to autophosphorylation (Leonardo and Forst, 1996).

Stimulus sensing is not limited to the periplasmic domain of a HK (Mascher et al., 2006). In some cases, TM regions are the input domain, especially in HKs where the (extra)cytoplasmic linkers between two TM domains are very short. HKs with a TM-based stimulus sensing mechanism were classified in six groups based on their function, the number of TM regions and the sequence conservation of the TM regions: (1) small HKs of two TM domains sensing envelope stress in Gram positive bacteria; (2) DesK-like thermosensors that possess 4-5 TM domains and sense membrane fluidity; (3) RegB-like global sensor kinases with 6 TM regions; (4) quorum-sensing kinases with 6 to 10 TM regions occurring more often in Gram positive bacteria; (5) HKs with 12 to 20 TM domains, showing homology to transport proteins and (6) HKs with unknown conserved input domains of 6 to 8 TM domains.

Some proteins sense signals via a portion of their cytoplasmic part (Figure 5). These HKs are (1) membrane-bound in which case they sense a stimulus from the N-terminus or the C-terminus, (2) cytoplasmic proteins associated with membrane-bound proteins or (3) cytoplasmic proteins with no connection to the membrane (Mascher et al., 2006). Proteins of the first group harbour PAS or GAF domains but it is difficult to predict the sensed stimulus based on the sequence of the input domain. PhoR from *B. subtilis* and *E. coli* is an example of such a HK. Its sensing activity was attributed to a cytoplasmic domain located between the TM domain and the DHp domain (Scholten and Tommassen, 1993; Shi and Hulett, 1999). CheA is one of the most studied HKs of the group 2. Together with the RR CheY, it regulates flagellar motor rotation in proteobacteria. CheA is activated by interacting with MCP, which is localized to the membrane. Cytoplasmic HKs harbour a huge diversity in their domain architecture, rendering their classification impossible. They often contain one to several PAS domains. Figure 5 summarizes the different types of HKs mentioned above.

3. Some histidine kinases are also phosphatases

Some HKs harbour a phosphatase activity towards their cognate RR (Alves and Savageau, 2003). They are referred to as bifunctional, in contrast to monofunctional HKs that show only a kinase activity. Inactivation of the RR by dephosphorylation allows the fine-tuning of the response and prevents crosstalks (Alves and Savageau, 2003). When unphosphorylated, bifunctional HKs have an enhanced phosphatase activity towards their phosphorylated RR. This activity resides in the DHp domain even though the expression of this domain by itself is not sufficient for an optimal phosphatase activity (Carmany et al., 2003). Interaction with the CA domain as well as conformational changes transmitted from the sensor and TM domains are essential to ensure an effective dephosphorylation of the RR (Carmany et al., 2003; Gao and Stock, 2009). Furthermore, the ATP lid might be an important determinant of this activity. It was indeed shown to have a highly conserved structure that is distinctive between monofunctional and bifunctional HKs (Alves and Savageau, 2003).

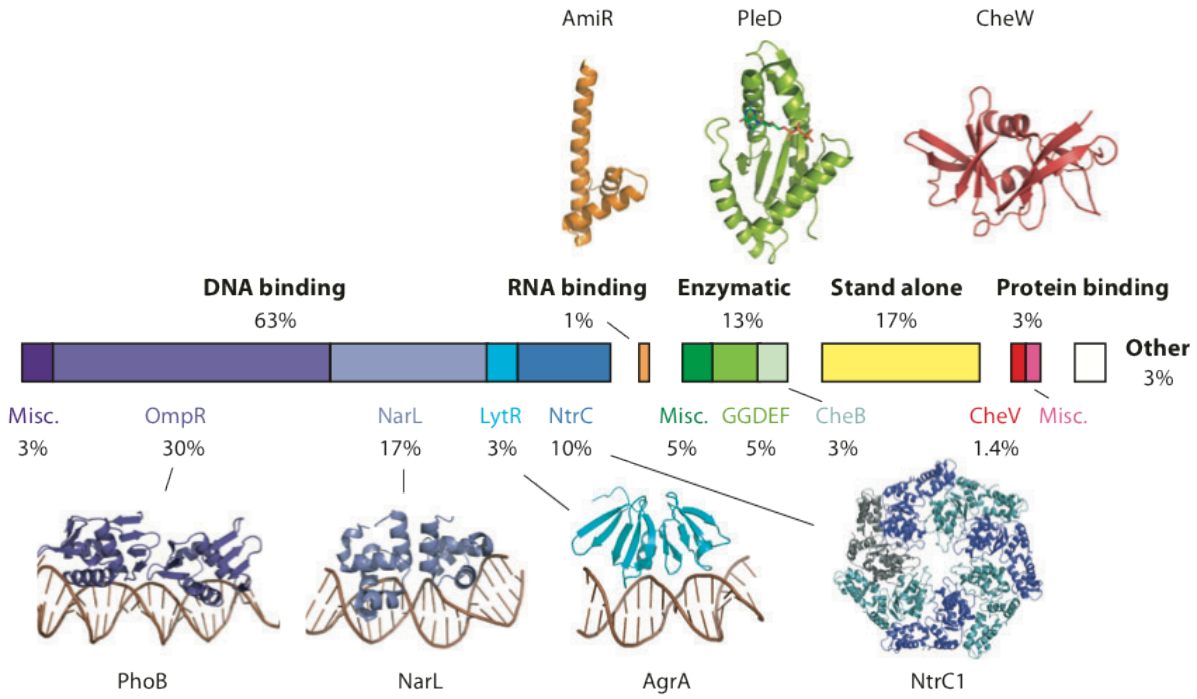

Figure 6- Functional distribution of RRs output domains (Gao and Stock, 2009)
Output domains are distributed along a colour-coded horizontal bar in different families according to their activities. The percentile functional distribution is indicated above the horizontal bar. RRs subfamilies are indicated beneath the bar. Ribbon diagrams illustrate the structure of representative members of some subfamilies.

Identifying the amino acids involved in the dephosphorylation of the RR is not straightforward. Hsing et al. suggest that, in the case of EnvZ, as for its kinase activity, the H box plays a critical role for the phosphatase activity (Hsing and Silhavy, 1997). Mutating the conserved histidine of EnvZ into several other amino acids resulted in a more or less important loss of the phosphatase activity, without completely abolishing it. This suggests that the conserved histidine is important for the phosphatase activity albeit non-essential, and that several other residues might contribute to define an active site (Hsing and Silhavy, 1997). RRs also harbour an intrinsic phosphatase activity. The acyl-phosphate link formed on the aspartate is of high energy and thus very unstable (Gao and Stock, 2009).

4. Response regulators elicit different biological responses

RRs can be divided into three distinct groups depending on the activity of the output domain: nucleic acid binding, enzymatic and protein/ligand binding proteins (Gao and Stock, 2009) (Figure 6). The majority of RRs (63%) have DNA-binding effector domains. They are themselves classified in different subfamilies according to the structure of the DNA-binding domain. These subfamilies are named after extensively studied RRs, representative of each subfamily. There is for example the OmpR/PhoB subfamily with a winged-helix domain (30% of all RRs) and the NarL/FixJ four-helix helix-turn-helix domain (Gao and Stock, 2009) (Figure 6). A small subgroup of RRs (1%) binds to RNA and functions as anti-termination factors. For instance, the RR AmiR of *Pseudomonas aeruginosa* allows the synthesis of a full-length mRNA at the aliphatic amidase operon in the presence of small-molecule inducers, by preventing the formation of a stem-loop structure (O'Hara et al., 1999).

Output domains with an enzymatic activity are found in 13% of RRs (Gao and Stock, 2009) (Figure 6). Most of them are involved in regulating the level of cyclic diguanylate (c-di-GMP). They include c-di-GMP synthases with GGDEF diguanylate cyclase domains and/or EAL phosphodiesterases. Other known enzymatic activities associated to output domains include chemotaxis methyltransferases, HKs and phosphatases.

Three percent of the RRs harbour diverse output domains that bind other proteins or ligands. These include chemotaxis proteins, regulators of the stress sigma factor RpoS, histidine phosphotransferases (see paragraph I.B-Phosphorelays), PAS and GAF domains.

Finally, 17% of the RRs do not harbour any effector domain, and they are therefore referred to as single-domain RRs. As will be detailed in the following paragraph, they play a major role in a more complex version of TCSs, called phosphorelays.

RRs of the transcription factors family are commonly known to dimerize upon phosphorylation (Gao and Stock, 2009). In the case of OmpR-PhoB RRs, dimerization of the REC domains brings the DNA binding domains close together, allowing them to bind to direct repeat half-sites that form a conserved binding site for the RR (Bachhawat et al., 2005). Binding of RRs to promoters can either activate or repress the expression of the downstream gene.

B- Phosphorelays

Phosphorelays are a more elaborate and complex version of TCSs. They harbour an initial sensor component and a final output protein but involve several intermediate actors and multiple His-Asp phosphotransfers (Gao and Stock, 2009) (Figure 1-b). In phosphorelays, the sensory HKs contain, in addition to the input, DHp and CA domains, a REC domain with a conserved aspartate residue and form so-called hybrid HKs that show intra-molecular phosphotransfer. Alternatively, the REC domain is not connected to the HK and constitutes a single-domain RR already mentioned above (Mitrophanov and Groisman, 2008). Hybrid HKs constitute about 25% of all known HKs and function together with individual or linked histidine phosphotransferases (HPt) (Figure 1-b). HPts do not have any kinase or phosphatase activity. Thus they do not serve to amplify the signal, as is the case in eukaryotic phosphorylation cascades. Instead, a multistep cascade in bacteria is thought to allow different regulatory checkpoints to occur as intermediate RRs or HPts can be targeted by additional phosphatases. HPts serve as phosphodonors to the final RR with an output domain. For instance, sporulation in *Bacillus subtilis* is regulated by a phosphorelay (Piggot and Hilbert, 2004). Five HKs, KinA to KinE, phosphorylate Spo0F, a single-domain RR. Spo0F then transfers the phosphoryl group to the HPt Spo0B, which serves as a phosphodonor to the RR and transcription factor Spo0A. Spo0A regulates the expression of genes involved in sporulation. Spo0A is inactivated by several phosphatases, Spo0E, YisI and YnzD. This phosphorelay is turned on by several internal and external stimuli such as cell density, cell cycle progression and nutrient starvation but the exact stimuli sensed by the HKs are still unknown (Hilbert and Piggot, 2004).

To sum up, during evolution, bacteria have developed, used, adapted and shaped a conceptually simple but efficient way of sensing the environment and elaborating an appropriate behaviour. The modular nature of TCS proteins could have facilitated their evolution (Whitworth and Cock, 2009). The accumulation of large numbers of TCSs in a single genome could result from gene duplications followed by point mutations and domain shuffling. Such mechanisms can indeed give rise to endless input-output combinations. Only those with a significant advantage are retained in the population. The huge diversity accumulated during evolution is best exemplified by the poor conservation of input domains both at the sequence and structure level. As a direct consequence of such diversity, and despite the development of reliable prediction tools, defining common structures for sensor domains and inferring the precise stimulus recognized by a HK are still a challenge for scientists.

A particular TCS and a phosphorelay have been studied in several bacteria of the *Alphaproteobacteria* class and they will be the subjects of the following chapter. Their role in cell cycle regulation was first investigated in *Caulobacter crescentus*, a model organism for studying bacterial cell cycle and differentiation. More recently, experiments have shown that this phosphorylation cascade is widely conserved among alphaproteobacteria but was nevertheless adapted by each genus to its lifestyle.

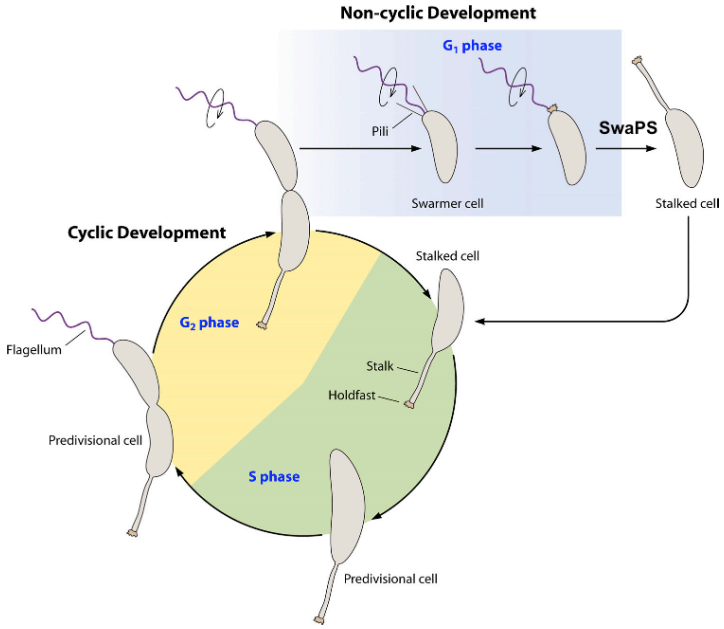

Figure 7- *Caulobacter crescentus* cell cycle is biphasic (Curtis and Brun, 2010)
Each division gives rise to two daughter cells with different cell fates. The large stalked cell enters directly the S phase and thus undergoes a cyclic development. At each cycle, a stalked cell elongates, replicates its chromosome, synthesizes a flagellum at the new pole and divides. The flagellated cell is, on the contrary, stuck in G1 phase unable to grow and to replicate its chromosome. It has first to differentiate into a stalked cell before entering the cyclic phase.

Chapter II- Cell cycle regulation in alphaproteobacteria

A- The case of Caulobacter crescentus

1. Its cell cycle

For reviews:
(Curtis and Brun, 2010), (Jacobs-Wagner, 2004), (Thanbichler, 2009)

a) Morphological and functional asymmetry

Caulobacter crescentus is by far one of the most studied Gram-negative bacteria in regards to cell cycle regulation and differentiation. It is a free-living alphaproteobacterium growing in oligotrophic environments. What makes *C. crescentus* an interesting model organism for studying developmental processes is the presence, in an asynchronous population, of different bacterial subtypes with distinct morphological features. Indeed, each division event is asymmetric and gives rise to two daughter cells of different size and harbouring different appendixes at their old poles. The large daughter cell has a stalk at one pole. A sticky material known as the holdfast is located at the tip of the stalk and is partially composed of a polysaccharide of *N*-acetylglucosamine allowing the bacterium to adhere to a solid surface (Merker and Smit, 1988). The small bacterium has a flagellum and pili at its old pole; it is thus motile and can explore new environments to colonize. In the following section, the large bacterium will be referred to as the stalked cell and the small bacterium as the swarmer cell.

The morphological differences of *C. crescentus* daughter cells are intrinsically linked to a difference in their cell fate. Each one of them has a specific task to fulfil in the bacterial community. This observation can be associated to cellular differentiation of eukaryotic cells. The large stalked cell can be seen as a stem cell, a "producer" of small flagellated cells. During each cell cycle, it grows and replicates its chromosome; a flagellum is synthesized at the pole opposite to the stalked pole; finally division occurs and pili are produced at the flagellated pole, giving rise to a small flagellated cell (Figure 7). After each cell division, the stalked cell is able to initiate a new round of chromosome replication, growth and septation. As for the flagellated cell, it can be considered as a "scout". Its rotating flagellum and its chemotactic system allow it to look for an environment suitable for growth once the current niche has become overcrowded for example. It is blocked in G1 phase and it is thus unable to replicate its DNA (Figure 7) (Degnen and Newton, 1972). It first has to undergo a complex program of differentiation called the SwaPS (Swarmer progeny-specific) during which it differentiates into a stalked cell (Matroule et al., 2004). The transition from the flagellated to the stalked state involves first a contact between the pili and a surface, shedding of the flagellum, retraction of the pili and synthesis of the stalk. Studying *C. crescentus* cell cycle progression was made possible thanks to a synchronization protocol based on the separation of different bacterial subtypes on a density gradient (Evinger and Agabian, 1977). Flagellated cells have a higher density, allowing their separation from stalked and predivisional cells. Fractions enriched in flagellated cells can then be inoculated in fresh medium and sampled at critical time points of the cell cycle.

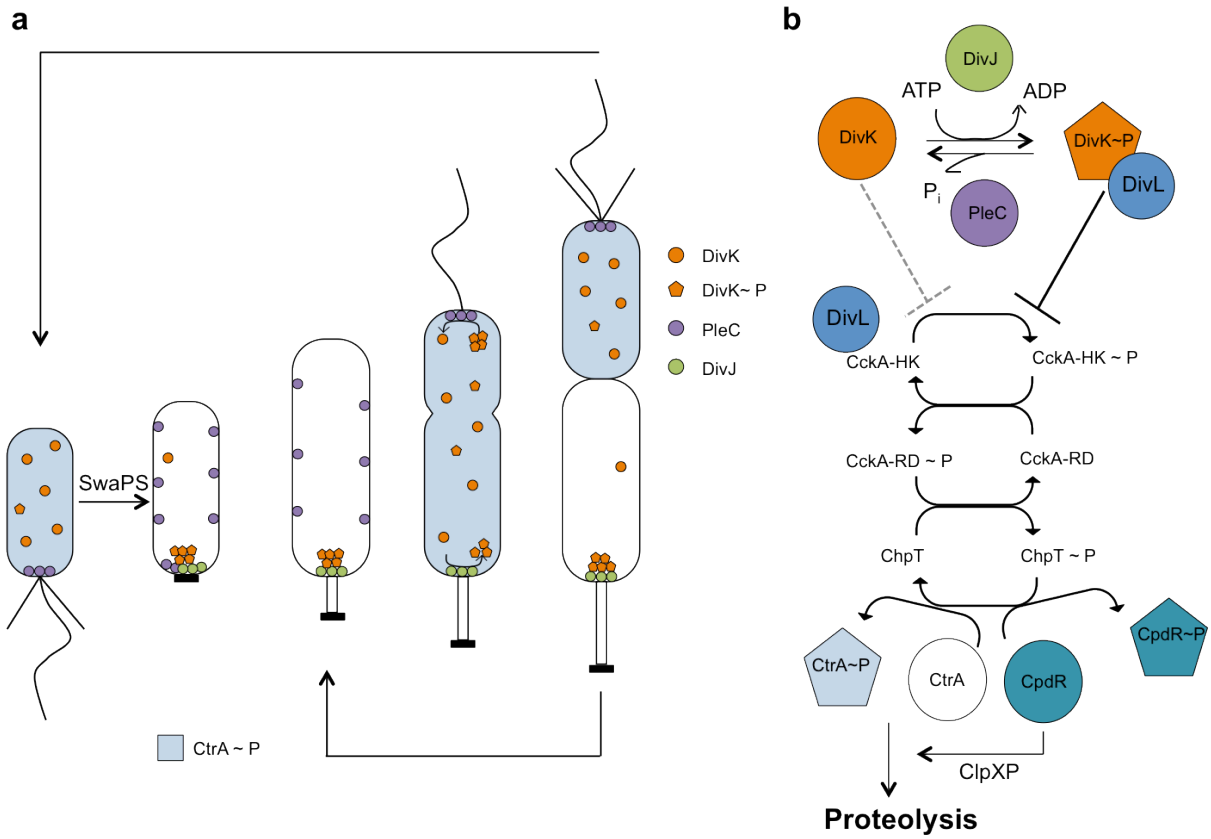

Figure 8 – Schematic representation of CtrA phosphorylation status during the cell cycle and the subcellular localization of several actors of the phosphorylation cascade upstream of CtrA

a- The scheme represents the different stages of *C. crescentus* cell cycle, starting from a flagellated cell, going through the stalked cell and finally to the predivisional cell. Bacterial subtypes coloured in blue are those in which CtrA is present and phosphorylated. Circles represent the histidine kinases DivJ and PleC and the response regulator DivK. They show their dynamic subcellular localization throughout the cell cycle.

b- The scheme represents the PleC/DivJ-DivK TCS that governs the phosphorelay involving CckA, ChpT, CtrA and CpdR.

b) The molecular mechanisms governing C. crescentus cell cycle regulation

The molecular mechanisms underlying the asymmetric division of *C. crescentus*, the synthesis of polar appendixes and the G1 block of flagellated cells involve two histidine kinases, DivJ and PleC, and an essential single-domain response regulator, DivK (Hecht and Newton, 1995; Ohta et al., 1992; Wang et al., 1993). DivJ acts as a kinase on DivK whereas PleC has a dual activity. Depending on the stage of the cell cycle, PleC either phosphorylates or dephosphorylates DivK. The phosphorylation status and the localization of these proteins are dynamic throughout the cell cycle of *C. crescentus* (Figure 8-a) (Wheeler and Shapiro, 1999). In swarmer cells, PleC is localized to the flagellated pole where it acts as a phosphatase for DivK. DivK is diffused in the cytoplasm. During the SwaPS, DivJ is synthesized, co-localizes with PleC at the old pole and replaces it progressively (Figure 8-a) (Wheeler and Shapiro, 1999). DivJ phosphorylates DivK, leading to its polar localization. In the meantime, the pole is undergoing important morphological changes: the flagellum is shed, the pili are retracted and a stalk is formed. Polar phosphorylated DivK (DivK~P) enhances PleC kinase activity and inhibits its phosphatase activity while it is still localized to the old pole (Paul et al., 2008). DivK thus creates a positive feedback loop that results in the accumulation of more DivK~P. In stalked cells, DivK pool is phosphorylated and PleC delocalizes from the old pole. In predivisional cells, PleC localizes to the new pole opposite to DivJ. DivK shuttles from the old pole, where it gets phosphorylated by DivJ, to the new pole where its phosphate is removed by PleC (Matroule et al., 2004). Finally, after cytokinesis, DivJ and PleC are physically separated: DivJ in the stalked cell keeps DivK in its phosphorylated state whereas PleC in the flagellated cell dephosphorylates DivK. Despite the essentiality of DivK, *pleC* and *divJ* can be deleted separately or together, and a basal level of phosphorylated DivK is still present. This observation suggests that *C. crescentus* might possess another, yet to identify, kinase for DivK.

The importance of DivK activity resides in its ability to modulate a phosphorelay regulating both the phosphorylation and degradation of a master regulator called CtrA (Cell cyle transcriptional regulator A) (Figure 8-b). This phosphorelay involves the hybrid histidine kinase CckA (Jacobs et al., 2003; Jacobs et al., 1999) and the phosphotransferase ChpT (Biondi et al., 2006). CckA possesses both a DHp domain with a conserved histidine residue and a REC domain with a conserved aspartate residue. CckA autophosphorylates on the histidine residue, transfers the phosphoryl group to the aspartate residue then to a conserved histidine residue on ChpT. Finally, ChpT activates CtrA by transferring the phosphoryl group on a conserved aspartate residue (Biondi et al., 2006). CtrA is an essential response regulator and transcription factor regulating the expression of almost a 100 different genes involved in various essential processes such as DNA methylation, cell division, polar morphogenesis, etc. Paragraph A-2 of Chapter II is dedicated to the role CtrA plays in regulating *C. crescentus* cell cycle.

The atypical histidine kinase DivL steps in at the hinge between DivJ-PleC-DivK TCS and CckA-ChpT-CtrA phosphorelay (Figure 8-b). DivL promotes CckA autophosphorylation and thus CtrA activation (Iniesta et al., 2010). However, DivK~P binds to DivL and prevents its interaction with CckA. Thus in stalked cells, DivK~P prevents the activation of CtrA whereas in flagellated cells DivK is in its unphosphorylated form and DivL is free to interact with CckA. In predivisional cells, CckA localization to the flagellated pole is essential for its activity (Iniesta et al., 2010; Tsokos et al., 2011). In this subtype of cells, DivK pool is partially phosphorylated as both the kinase and the phosphatase of DivK are present. However PleC dephosphorylates DivK at the flagellated pole and creates a

microenvironment where CckA can autophosphorylate and activate CtrA (Tsokos et al., 2011).

The CckA-ChpT-CtrA phosphorelay regulates not only CtrA phosphorylation but also its proteolysis via a single-domain response regulator called CpdR (Figure 8-b) (Biondi et al., 2006; Iniesta et al., 2006). ChpT can also transfer its phosphoryl group to CpdR, which, unlike CtrA, is inactive when phosphorylated, leading to CtrA stabilization. However, when CckA activity is inhibited by DivK~P, CpdR is not phosphorylated and is thus active. It promotes the polar localization of ClpXP, the protease complex responsible for CtrA degradation.
CckA activity is also regulated by an important second messenger, the cyclic di-GMP (c-di-GMP) (Lori et al., 2015). C-di-GMP is widely used by bacteria to control several processes such as virulence, motility and biofilm formation (Romling et al., 2013). In *C. crescentus*, c-di-GMP amount increases during the differentiation of swarmer cells to stalked cells, leading to a transition from a motile to a sessile lifestyle (Abel et al., 2013). Recently, c-di-GMP was shown to promote the switch of CckA from a kinase to a phosphatase, leading to an inversion of the phosphorylation flux from CtrA to CckA, thus resulting in the inactivation of CtrA (Lori et al., 2015).

In flagellated cells, CtrA and CpdR are both phosphorylated. CtrA is thus activated and stabilized. During the transition to stalked cells, DivK phosphorylation by DivJ inhibits the downstream phosphorelay, preventing the phosphorylation of the two response regulators. As a result, CpdR is activated and CtrA is cleared from the cells by proteolysis. In the predivisional cells, CtrA is produced and phosphorylated. Finally after cell division, CtrA~P is kept in the flagellated cell and is cleared from the stalked cell (Figure 8-a).
The power of such a phosphorylation cascade is its ability to regulate CtrA at two different levels: phosphorylation and degradation. Either it activates and stabilizes this essential transcription factor or it favours its degradation and clearance from the cells.

c) **C. crescentus** *growth and division are coupled with the replication of its chromosome*

Unlike the well-known paradigm of *E. coli* in which multiple initiations of chromosome replication occur between each division, each round of growth and division in *C. crescentus* is accompanied by a single event of initiation of chromosome replication followed by the segregation of the two daughter chromosomes (Marczynski, 1999; Zweiger and Shapiro, 1994). The stalked cell is the only subtype competent for chromosome replication. It can enter the S phase directly after cytokinesis, growing into a predivisional cell in G2 phase. After division, both daughter cells are in G1 phase. However, unlike the stalked cell, the flagellated cell is blocked in this phase and has first to differentiate into a stalked cell to be able to replicate its genome.
As will be detailed in the following paragraph, CtrA plays a major role in regulating the initiation of chromosome replication. CtrA~P can bind to the origin of replication (C*ori*) and prevent the initiation of chromosome replication (Quon et al., 1998). This inhibition is exerted by CtrA~P both in the flagellated cell and in the late predivisional cell. As a result, the flagellated cell is blocked in G1 phase and the predivisional cell cannot initiate a second event of chromosome replication (Schredl et al., 2012).

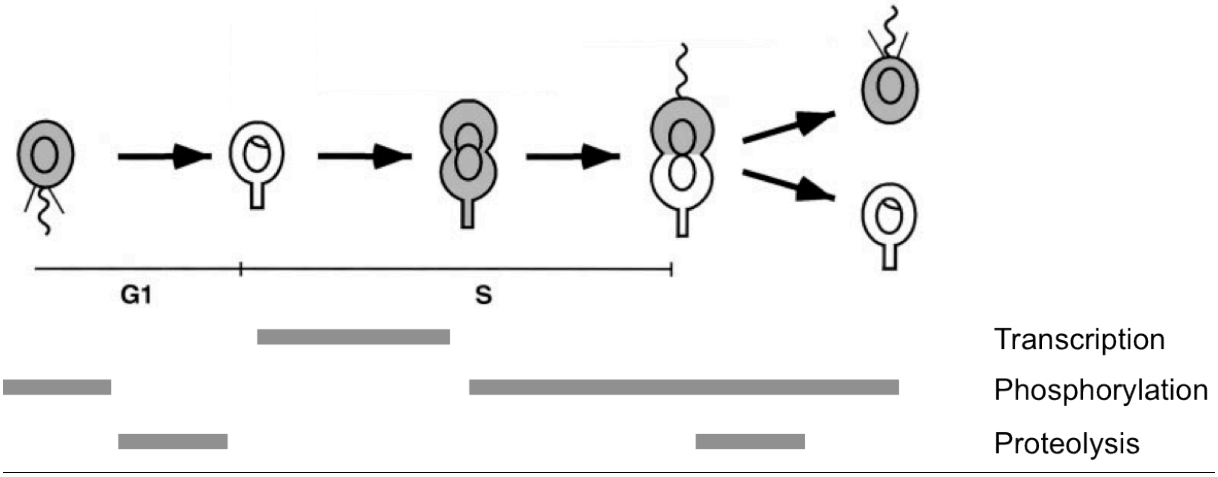

Figure 9 – CtrA amount and activity are cell cycle regulated. (Modified from Jacobs et al., 1999)
The *ctrA* gene is transcribed during the S phase. The protein is subsequently phosphorylated and remains so in the flagellated cell while it is proteolyzed in the stalked cell. CtrA is also degraded during the flagellated to the stalked cell transition.

2. Role of CtrA in *C. crescentus* cell cycle regulation

a) CtrA amount and activity are cell cycle regulated

CtrA is a response regulator of the OmpR family (Quon et al., 1996). It harbours an amino-terminal receiver domain with a conserved phosphorylatable aspartate residue (D51) and a carboxy-terminal DNA binding domain. CtrA is regulated at the transcription, phosphorylation and proteolysis levels throughout *C. crescentus* cell cycle (Figure 9). The *ctrA* gene is transcribed in predivisional cells during the S phase (Quon et al., 1996). The newly synthesized protein is phosphorylated during the late S phase and degraded at two precise time points: (i) during the swarmer-to-stalked cell transition (Domian et al., 1997) and (ii) in the stalked compartment after cytokinesis where it is localized to the stalked pole together with the proteolysis machinery ClpXP (Iniesta et al., 2006; Jenal and Fuchs, 1998). As will be discussed later in this section, CtrA activity is modulated at a fourth level: CtrA interacts with two other transcriptional regulators, SciP (Gora et al., 2010; Tan et al., 2010) and MucR (Fumeaux et al., 2014). These interactions restrain the activation of CtrA target promoters in time, allowing the activation of the corresponding genes at the proper cell cycle stage (G1 or S phase).
The following section will be dedicated to CtrA regulon, its mode of binding to DNA and the way SciP modulates CtrA binding to DNA.

b) CtrA regulon

In vivo genomic binding site analysis showed that CtrA regulates directly 95 different genes (Laub et al., 2002). As already described in the literature, many class II flagellar genes are targeted by CtrA. However, unlike what was expected, CtrA presumably regulates class III and IV flagellar genes as well. CtrA also regulates pili synthesis and chemotaxis. Among the genes of CtrA regulon, there are regulatory genes encoding histidine kinases, response regulators, sigma factors and transcription factors. CtrA binds to the promoter region of *ccrM*, an essential DNA methyltransferase involved in regulating gene expression via a transcription factor called GcrA (Fioravanti et al., 2013) (Paragraph A-3 of Chapter II). CtrA also controls the expression of genes involved in the initiation and progression of cell division such as *ftsZ*, *ftsQ* and *ftsA* as well as genes responsible for cell wall remodeling (*ftsW* and *murG*). CtrA regulates proteolysis by targeting *clpP*, encoding the catalytic component of the ClpXP machinery. Finally, CtrA regulates its own expression; this autoregulation will be detailed below. These findings were later confirmed by ChIP-seq (Chromatin immunoprecipitation followed by deep-sequencing) (Fumeaux et al., 2014).

c) CtrA binds to a conserved sequence

Upon phosphorylation, CtrA binding to DNA is enhanced (Reisenauer et al., 1999). It recognizes the consensus sequence "TTAA(N_7)TTAAC" 9-mer box, with N_7 being a linker of 7 nucleotides (Quon et al., 1998). The length of this linker is critical for optimal binding of CtrA to DNA (Ouimet and Marczynski, 2000). This consensus sequence was identified before CtrA itself in the promoter regions of most of the class II flagellar genes (Quon et al., 1996) and was found to be essential for their normal activity. It was also identified in the promoter of *ccrM* and of *hemE,* which lies within the origin of replication of *C. crescentus* chromosome (Quon et al., 1996). Later, bioinformatics analyses identified another consensus sequence for CtrA binding, termed the 8-mer box, for "TTAACCAT" (Laub et al., 2002). It is actually an extension of a unique "TTAA" half site.

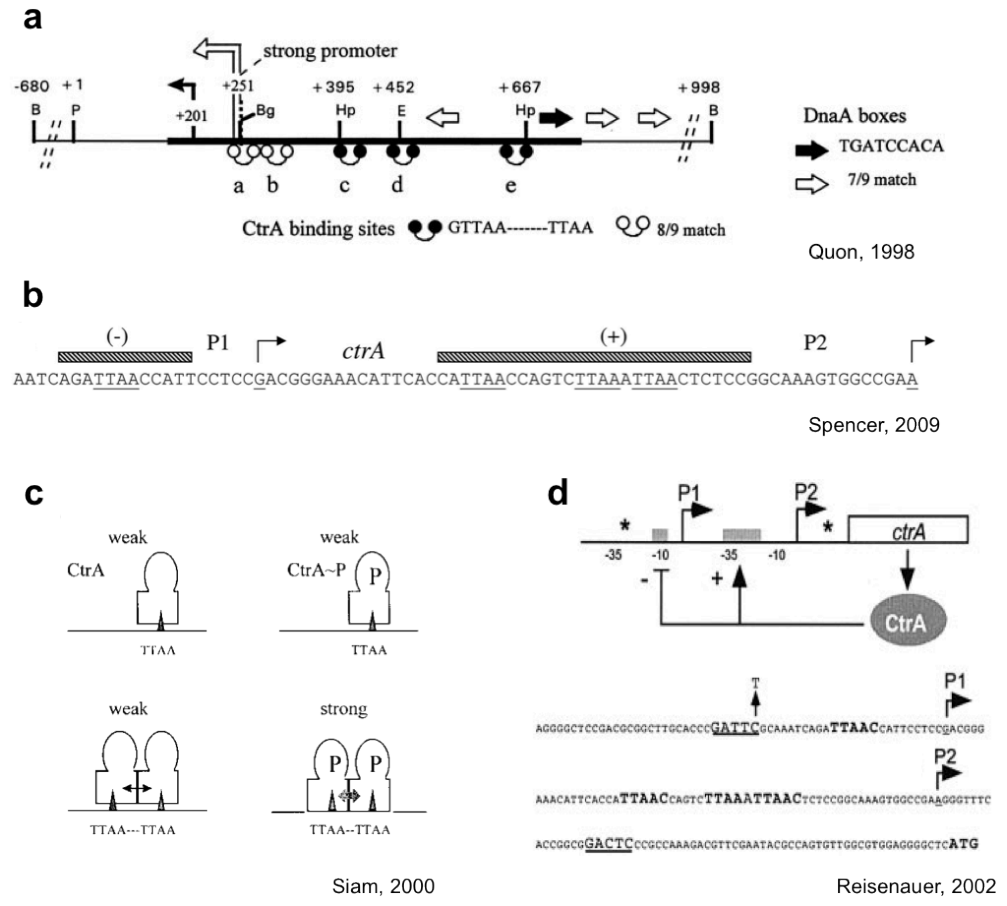

Figure 10 – Structure of the origin of replication (a) and of *ctrA* promoter (b-d) and schematic representation of the "cooperative interaction" model (c) (Quon et al., 1998; Reisenauer and Shapiro, 2002; Spencer et al., 2009)

a- The C*ori* region contains a strong promoter (tall white bent arrow) and a weak promoter (short black bent arrow) regulating the expression of the *hemE* gene. The thick horizontal line represents the minimal sequence required for C*ori* replication. White and black arrows represent DnaA consensus boxes. White and black dumbbell shapes represent CtrA consensus boxes. Restriction enzymes: *B: Bam*HI, *Bg: Bgl*II, *E: Eco*RI, *Hp: Hpa*I, *P: Pst*I.

b- Bent arrows represent *ctrA* P1 and P2 promoters. Underlined nucleotides correspond to CtrA consensus boxes. Dashed rectangles highlight the regions protected by CtrA in a DNase I footprinting assay. (-): CtrA binding to this region represses P1; (+): CtrA binding to this region activates P2.

c- Model for CtrA cooperative interaction: binding of a CtrA monomer (phosphorylated or not) to DNA is weak. Binding of an unphosphorylated dimer of CtrA to two "TTAA" half sites is weak. Binding of a phosphorylated dimer of CtrA to two "TTAA" half sites is strong, as phosphorylation strengthens the interaction between two CtrA molecules and between CtrA and DNA.

d- The scheme summarizes *ctrA* promoter region and the feedback loops exerted by CtrA on this regulatory region (grey rectangles represent the regions bound by CtrA). Asterisks represent GAnTC methylation sites.

CtrA both activates and represses gene expression. This can depend on the position of its consensus sequence in the promoter (Domian et al., 1999; Spencer et al., 2009). CtrA-activated genes harbour a CtrA binding site next to the -35 box of their promoter, where CtrA presumably recruits or binds to the RNA polymerase. Genes repressed by CtrA usually have a consensus sequence next to the +1 transcriptional starting site. CtrA binding to this region could prevent the RNA polymerase from transcribing the downstream gene by simple steric hindrance.
Many variations around the consensus "TTAA(N_7)TTAAC" sequence are present in CtrA target promoters. The way CtrA binds to DNA (affinity and multimerization) depends for example on the size of the linker separating two "TTAA" half sites and on the distance separating two binding boxes.

d) CtrA binds to the origin of replication

CtrA binds to five consensus sequences in the C*ori* (Quon et al., 1998). These sequences are referred to as [a], [b], [c], [d] and [e] (Figure 10-a). Given the close location of binding site [e] to an essential DnaA box (DnaA being the initiator of chromosome replication), it was suggested that CtrA binding to this region prevents chromosome initiation of replication by DnaA (Quon et al., 1998). DNase I footprinting assays show that CtrA binds to these boxes in two distinct manners. These assays suggest that one monomer of CtrA binds one "TTAA" half site of each of [c], [d] and [e] binding sites (Siam and Marczynski, 2000). Two monomers of CtrA binding to two "TTAA" half sites of the same box interact with each other. This weak protein-protein interaction enhances DNA binding in a cooperative manner and phosphorylation of CtrA strengthens its own dimerization and the binding of the dimer to two "TTAA" half sites (Figure 10-c).
Binding to boxes [a] and [b] is different (Siam and Marczynski, 2000). These two consensus sequences are separated by only four base pairs, suggesting a cooperative binding of CtrA to [a] and [b]. Increasing the number of nucleotides separating [a] and [b] affected CtrA binding to these boxes to a different extent. Inserting 14 extra base pairs between [a] and [b] completely abolished binding of CtrA to [a] both in its phosphorylated (CtrA~P) and non-phosphorylated form. CtrA still bound [b] but with a decreased affinity, and CtrA~P binding was more affected than CtrA. These data suggest that CtrA binding to [a] and [b] is cooperative and that phosphorylation enhances this cooperative interaction (Figure 10-c). However, this cooperative interaction is local, as disrupting the binding to [a] and [b] did not affect the binding to [c], [d] and [e]. In the same manner, mutating a nucleotide in a "TTAA" half site of either [c], [d] or [e] prevented the binding of CtrA to the mutated site but not to the other boxes.
In the "Discussion" part of their paper, Siam and co-workers argue that three distinct signals cooperate to ensure an optimal binding to the "TTAA(N_7)TTAAC" consensus sequence: (1) the phosphorylation of the conserved D51 residue in the receiver domain, (2) the contact with the adjacent CtrA molecule on the neighbouring half site and (3) the implication of DNA in this contact, as dimers of CtrA are never detected in solution. CtrA binding to C*ori* is crucial in regulating the initiation of chromosome replication. CtrA binds to C*ori* in flagellated cells, blocking them in G1 phase, and in predivisional cells, preventing multiple replication initiation events (Schredl et al., 2012).

e) CtrA regulates its own promoter

The *ctrA* gene is transcribed from two promoters: a weak promoter P1 and a strong promoter P2 (Figrue10-b) (Domian et al., 1999). P1 is active in the stalked cells where it initiates the transcription of low amounts of *ctrA* mRNA while P2 is activated in the predivisional cells, where it boosts the production of high amounts of CtrA protein. P1 and P2 have atypical CtrA binding sites. P1 has a unique "TTAA" half site (corresponding actually to a "TTAACCAT" 8-mer box which was discovered later by Laub et al. in 2002) whereas P2 has three "TTAA" half sites separated by N_6 and N_1 linkers instead of the usual N_7 nucleotide stretch (Figrue10-b).

These atypical binding sites are accompanied by an atypical mode of binding to DNA. As discussed earlier, CtrA binding to C*ori* is enhanced by phosphorylation (Siam and Marczynski, 2000). "TTAA" half sites in P1 and P2 promoters have weak affinity for CtrA binding *in vitro* and phosphorylation of CtrA does not increase this affinity (Spencer et al., 2009). Despite the weak binding of CtrA to its own promoter *in vitro*, *in vivo* results suggest that phosphorylation of CtrA (as well as binding of other factors, to be discussed later) does play an important role and allows cell cycle regulation of *ctrA* promoter activity.

Spencer and co-workers used a Glutathion S transferase (GST)-fused version of CtrA for their electrophoretic mobility shift assays (EMSA) (Spencer et al., 2009). GST-CtrA forms a dimer (thanks to the dimerization of the GST tag) and switches CtrA into its active form as it enhances its binding to C*ori* compared to a non tagged version of CtrA or to CtrA fused to a poly histidine tag. In other words, GST-CtrA mimics the cooperative protein-protein interaction observed upon CtrA phosphorylation. However, unlike the wild type (WT) phosphorylated CtrA, GST-CtrA forms dimers in solution, independently of any DNA molecule. In these conditions, P1 is bound by a dimer of GST-CtrA, showing that an 8-mer box is also bound by a dimer of CtrA.

The three "TTAA" half sites of P2 promoter bind to a tetramer of GST-CtrA: the first and second "TTAA" motifs separated by N_6 bind a GST-CtrA dimer; the third motif binds by itself another GST-CtrA dimer. Both these dimers interact with each other to form a tetramer. This interaction is hierarchical, since mutating the third single "TTAA" motif disrupted the GST-CtrA tetramer but a dimer was still bound to the "TTAA(N_6)TTAA" box. However, mutating the first or second "TTAA" half site abolished binding of GST-CtrA to P2, suggesting that CtrA binding to the first and second half site is essential for its binding to the third half site. This observation also suggests that the interaction between the two GST-CtrA dimers is cooperative; CtrA at motif one is connected to GST-CtrA dimer at motif three via motif two.

CtrA exerts a feedback loop on both promoters. It represses P1 in the swarmer stage (Domian et al., 1999). After the SwaPS, CtrA is cleared from the stalked cell allowing P1 activation in the stalked cell. Ensuing this activation, a small amount of CtrA is produced which then activates the strong P2 promoter and inhibits the weak P1 promoter in predivisional cells (Domian et al., 1999).

The three levels of CtrA regulation (transcription, phosphorylation and degradation) as well as the different modes by which CtrA binds to DNA, do not explain why most CtrA-activated genes are exclusively transcribed in predivisional cells whereas CtrA-repressed genes are expressed in stalked cells and inhibited by CtrA during the rest of the cell cycle. A fourth level of regulation is modulating CtrA transcriptional activity.

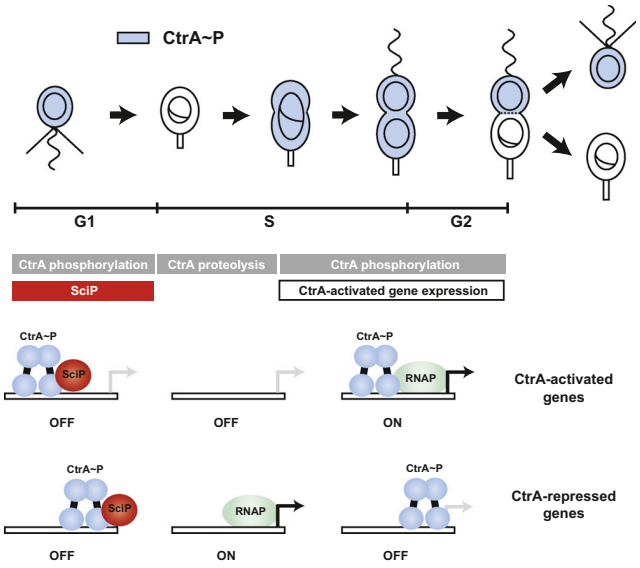

Figure 11 – Schematic representation of SciP mode of action (Gora et al., 2010)
SciP is specific of G1 phase bacteria, as shown by the red rectangle. In these cells, SciP interacts with DNA-bound CtrA. In the case of CtrA-activated genes, SciP prevents their activation in flagellated cells. In stalked cells, CtrA is absent because it is proteolyzed, thus these promoters remain in their "OFF" state. In predivisional cells, CtrA~P accumulates again and, in the absence of SciP, is free to activate the transcription of these genes. In the case of CtrA-repressed genes, their promoters are silenced both by CtrA and SciP in the flagellated cells. They are expressed in stalked cells where both these proteins are absent and repressed in predivisional cells when CtrA~P is present.

f) SciP, a cofactor for CtrA or a transcription factor acting in parallel?

RNA microarrays conducted by Laub et al. in 2002 showed that most CtrA-activated genes are exclusively transcribed in predivisional cells whereas the expression of CtrA-repressed genes is restricted to stalked cells. These findings suggest that an unknown factor might modulate the activity of CtrA, either by preventing it from activating gene expression in flagellated cells or by enhancing transcription of target genes in predivisional cells.

A protein was identified in 2010 by Gora and co-workers and was termed SciP for "small CtrA inhibitory protein" (Gora et al., 2010). SciP is restricted to G1 swarmer cells; it accumulates in this particular subtype of *C. crescentus* and it is rapidly cleared from the cell during the G1-S transition. The regulation of *sciP* expression is crucial for the proper progression in the cell cycle as either depleting cells from SciP or overproducing it disrupts the cell cycle. More specifically, SciP is essential for the G1-S transition as depleting cells from SciP resulted in an elongated G1 stage. Furthermore, overexpressing *sciP* resulted in a filamentation phenotype and an accumulation of multiple chromosomes per cell, typical of an inhibition of cell division.

Perturbing SciP amount during the cell cycle affects the expression level of late S-phase CtrA target genes. The depletion of SciP from flagellated cells (the only cell type where it is normally expressed) resulted in an overexpression of CtrA-activated genes but had no effect on CtrA-repressed genes. Overproducing SciP throughout the cell cycle resulted in a decrease in the expression of CtrA-activated genes but had no effect on CtrA-repressed genes. These data suggest that SciP is a G1-specific inhibitor of CtrA and prevents it from activating its target genes in flagellated cells. Most of the genes activated by CtrA and whose expression is altered by depleting or overexpressing *sciP* are involved in flagellum synthesis, chemotaxis and pilus secretion (Gora et al., 2010). All these processes are indeed activated in predivisional cells, ensuring the later formation of the G1 flagellated compartment (Jones et al., 2001; Quon et al., 1996; Skerker and Shapiro, 2000).

The mechanism by which SciP modulates CtrA transcriptional activity is still debated. Gora and co-workers argue that SciP is a cofactor of CtrA, unable to bind DNA by itself (Gora et al., 2010). Instead, it interacts with CtrA bound to DNA and prevents it from recruiting the RNA polymerase (Figure 11). By interacting with CtrA, SciP can bind an adjacent unspecific DNA sequence. SciP also increases CtrA affinity for DNA, thus stabilizing it by protecting it from the activity of ClpXP protease (Gora et al., 2013). From another point of view, Tan and co-workers maintain that SciP is a transcription factor that binds DNA by itself and recognizes a consensus sequence, "TGTCGCG" (Tan et al., 2010). However, mutating this sequence did not alter the formation of the "SciP-CtrA-DNA" complex *in vitro* and did not alter the expression of a *lacZ*-based reporter system *in vivo* (Gora et al., 2013). Furthermore, the occurrence of this sequence in *Caulobacter* GC-rich genome largely exceeds the predicted CtrA target promoters with CtrA boxes (over 1460 "TGTCGCG" sequences versus 50 CtrA-bound promoters with one to four CtrA boxes) (Fumeaux et al., 2014).

A ChIP-seq analysis was performed on a mid-exponential phase culture of *C. crescentus* using antibodies against SciP (Fumeaux et al., 2014). This analysis showed that SciP binds only S-phase promoters and not G1-phase promoters, contradicting the model proposed by Gora and co-workers (Figure 11) (Gora et al., 2010). Indeed the latter model suggests that both G1 phase-repressed promoters and S phase-activated promoters are bound by SciP. However, this model was inferred by comparing gene

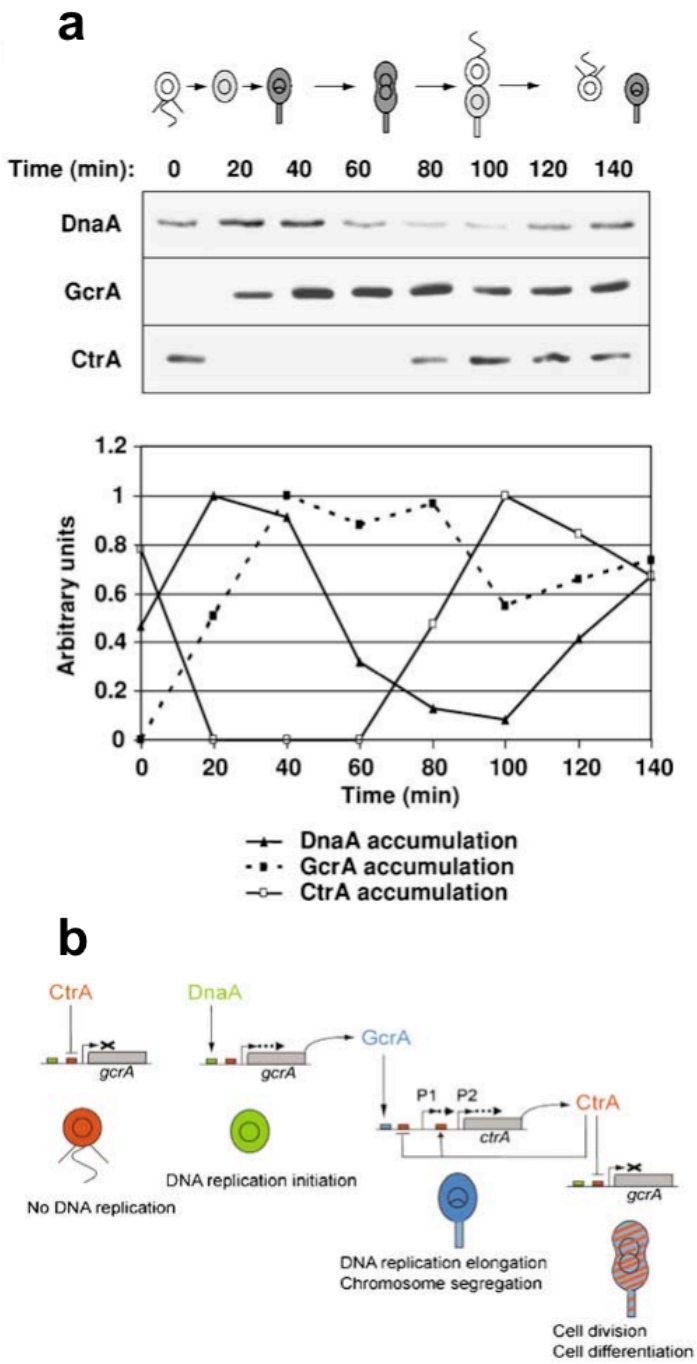

Figure 12 – Oscillation of DnaA, GcrA and CtrA during the cell cycle (Collier et al., 2006)

a- Schematic representation of *C. crescentus* cell cycle. GcrA accumulation is shown in gray Western blots with antibodies recognizing specifically DnaA, GcrA or CtrA were performed on a synchronized *C. crescentus* population. Bands were quantified and represented on the graph.

b- The scheme represents the sequential accumulation of the three transcription factors during the cell cycle as well as their mutual transcriptional regulation.

expression profiles in WT, *sciP*$^{-}$ and *sciP*$^{+}$ strains. The ChIP-seq assay provides direct evidence of *in vivo* binding of SciP to DNA and brings new information to the model proposed by Gora et al. The fact that SciP binds only to a subset of CtrA target genes suggests that SciP might recognize a DNA sequence specific to S-phase promoters. A MEME-based (Multiple EM for motif elicitation) analysis suggested that SciP could bind to a "TTAACCAT" consensus sequence, actually corresponding to the sequence earlier referred to as the CtrA "8-mer" binding box (Fumeaux et al., 2014). Authors suggest that SciP and CtrA could compete for this sequence or that repression by SciP could involve a cooperative binding mode between CtrA and SciP.

3. The DnaA-GcrA-CtrA circuitry and the importance of DNA methylation by CcrM in regulating gene expression

a) On the role of DnaA, GcrA and CtrA

As already mentioned earlier, CtrA regulates the expression of genes involved in essential processes of the cell cycle such as initiation of chromosome replication, polar morphogenesis and division. However, CtrA does not regulate other essential events in *C. crescentus* development, such as formation of the replisome and chromosome segregation (Holtzendorff et al., 2004). This suggests that other regulatory proteins ensure, together with CtrA, proper progression in the cell cycle. Indeed, in addition to CtrA, two other proteins play a major role in regulating *C. crescentus* cell cycle: DnaA and GcrA. DnaA is a protein with a dual function; it is an initiator of chromosome replication (Fuller et al., 1984; Zweiger and Shapiro, 1994) and a transcription factor regulating the expression of 40 genes encoding nucleotide biosynthesis enzymes, proteins of the DNA replication machinery, polarity determinants and GcrA itself (Hottes et al., 2005). GcrA is a transcription factor regulating the expression of 50 genes involved in polar morphogenesis and asymmetry (*podJ*, *pleC*), in DNA replication (*dnaA, gyrA,* Topo IV) and the gene coding for CtrA (Holtzendorff et al., 2004). The tight regulation of CtrA, DnaA and GcrA amounts at the transcriptional and proteolysis levels results in a precise cycling profile of each of these proteins during *C. crescentus* development (Figure 12-a). Each of these three proteins participates in the transcriptional regulation of one of its counterparts. DnaA activates the expression of *gcrA* (Collier et al., 2006). GcrA activates the expression of *ctrA* (Holtzendorff et al., 2004) and CtrA represses the expression of *gcrA* (Collier et al., 2006; Holtzendorff et al., 2004) (Figure 12-c). Starting from the flagellated cell, CtrA is abundant at this stage of the cell cycle, while GcrA is absent and DnaA is present at a basal level (Collier et al., 2006). During the swarmer to stalked cell transition, CtrA is cleared from the cell (Domian et al., 1997) while DnaA peaks before its level decreases again during S phase (Zweiger and Shapiro, 1994). Finally GcrA level rises during the S phase and falls in late S phase cells and after division (Collier et al., 2006; Holtzendorff et al., 2004). When looking at the protein level profiles of GcrA and CtrA (Figure 12-b), one can notice that they are out of phase: the decrease of CtrA amount at the G1-S transition is accompanied by an increase in the amount of GcrA. The opposite occurs in late predivisional cells. This out of phase variation is due to the antagonistic effects CtrA and GcrA exert on each other's promoters, GcrA being an activator of *ctrA* promoter and CtrA an inhibitor of *gcrA* promoter. It is also due to the opposite effect DnaA and CtrA have on *gcrA* expression, the first one being an activator while the other is a repressor (Collier et al., 2006).

To this mutual transcriptional regulation between CtrA and GcrA is added another layer of regulation, that of DNA methylation. This is where the essential and cell cycle

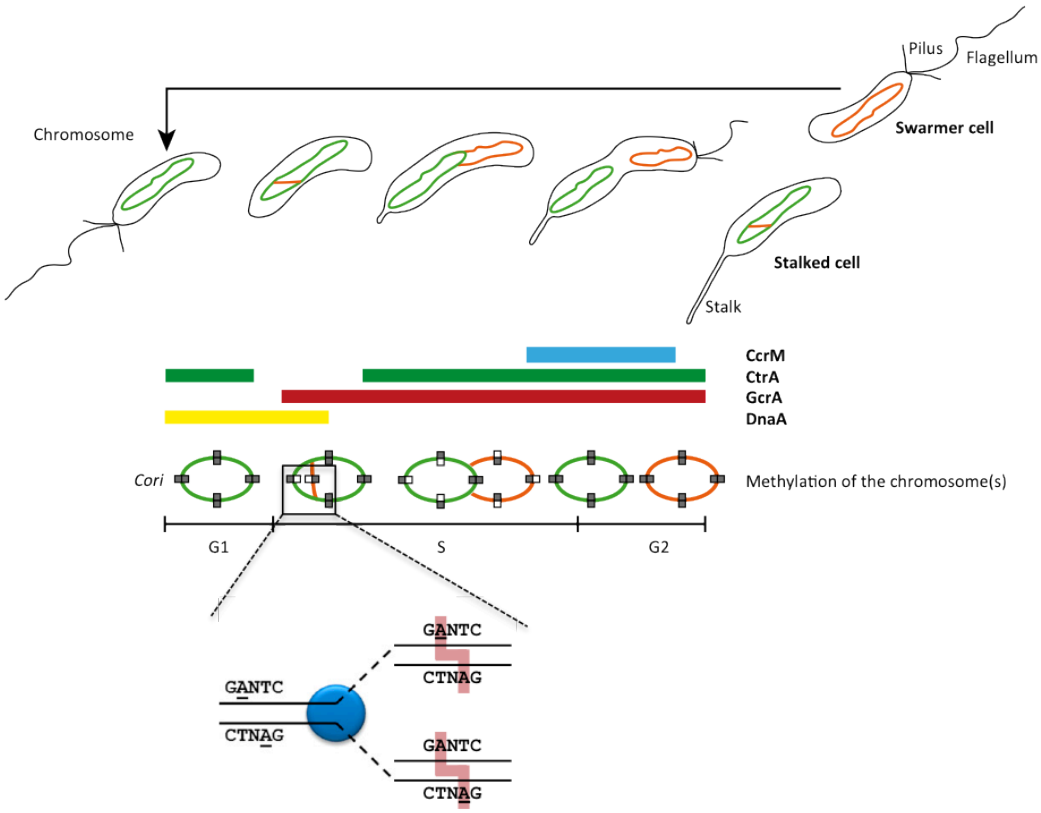

Figure 13- Schematic representation of the methylation status of the chromosome during the cell cycle (Modified from Kozdon et al., 2013 and Mohapatra et al., 2014)
The DNA molecule present in the initial swarmer cell is represented in green while the newly synthesized DNA is in orange. The stages during which the regulators CcrM, CtrA, GcrA and DnaA are present are depicted in coloured boxes. Fully methylated and hemi-methylated DNA double helices are symbolized by grey or grey and white rectangles respectively.

regulated methyltransferase CcrM steps in. The following paragraph (A-3-b) is dedicated to CcrM discovery and to its role in regulating gene expression during cell cycle. Paragraphs A-3-c/d explain how DNA methylation by CcrM affects gene expression in general, and that of *ctrA* in particular, via GcrA and focuse on the regulation of *ccrM* expression by CtrA. The purpose of these paragraphs is to demonstrate how a complex genetic circuitry coordinates chromosome replication and several developmental programmes.

b) On the role of the DNA methyltransferase CcrM, or how epigenetics regulates bacterial gene expression

CcrM was discovered before CtrA and GcrA. Zweiger and co-workers identified CcrM as being a DNA methyltransferase able to methylate the adenine base of GAnTC sites (Zweiger et al., 1994). This sequence corresponds to *Hinf*I recognition site of *Hinf*M methyltransferase from *Haemophilus influenza*. *ccrM* is expressed in late predivisional cells. Concomitantly, authors analysed three methylation sites on *C. crescentus* chromosome. They noticed that these sites were fully methylated in flagellated cells (G1 phase), became hemi-methylated in stalked cells (S phase) and regained their fully methylated state in late predivisional cells (G2 phase), coinciding with *ccrM* expression. Furthermore, when expressing *ccrM* constitutively, the three methylation sites remained fully methylated throughout the cell cycle and cells with aberrant morphologies and several chromosome replication events accumulated in the population. Based on these observations, authors postulated that CcrM might methylate the DNA strands synthesized by the DNA replication machinery on GAnTC sites and that the methylation of these sites at the proper time is crucial for correct gene expression.

The cell cycle-dependent methylation of DNA was later confirmed by Marczynski et al. (Marczynski, 1999) and by Kozdon et al. (Kozdon et al., 2013). After the initiation of chromosome replication, each replication fork passes through the chromosome from the C*ori* to the terminator, synthesizing on its way a new strand of DNA that is not methylated (Figure 13). As a result of *ccrM* late expression in the cell cycle, promoters localized close to the origin of replication, on either side, remain hemi-methylated for a longer time than those located close to the terminator. The time during which promoters subjected to methylation by CcrM remain hemi-methylated is crucial for their activity and thus for *C. crescentus* development. Methylation on both strands of a given promoter can either boost or repress its activity, while a hemi-methylated state always results in the activation of the expression of the downstream gene (Mohapatra et al., 2014). Among the genes whose expression is regulated by CcrM methylation many are involved in division (*mipZ, ftsZ* and *ftsN*), polar morphogenesis and polarity determination (*pleC, podJ, popZ* and *tipF*), chromosome segregation (*parE*), DNA replication (*dnaA, gyrA* and *gyrB*) and cell cycle regulation (*ctrA* and *ccrM*) (Mohapatra et al., 2014).

Restricting the presence of CcrM to the late S phase is thus crucial for normal gene expression. This restriction in time is achieved thanks to three levels of regulation: (i) activation of *ccrM* expression by CtrA (Quon et al., 1996; Stephens et al., 1995), (ii) repression of *ccrM* promoter activity by methylation on GAnTC sites (Stephens et al., 1995) and (iii) degradation of CcrM by Lon protease (Wright et al., 1996).

c) On the link between CtrA and CcrM

As already discussed in paragraph A-2-e of this chapter, *ctrA* is expressed from two promoters, P1 and P2 (Figure 10-b-d). P1 is activated during early S phase while P2 is turned on during late S phase (Domian et al., 1999). CtrA represses P1 and activates P2 (Domian et al., 1999). This regulatory region upstream of *ctrA* harbours two GAnTC sites, one close to the -35 box of P1 promoter and another downstream of the P2 +1 start site (Figure 10-d), suggesting that the activity of these promoters is modulated by methylation. Monitoring the activity of P1 and P2 in a strain constitutively expressing *ccrM* or depleted in its expression showed that P2 activity was insensitive to both conditions (Reisenauer, 2002). On the contrary, P1 activity was reduced when the chromosome remained fully methylated throughout the cell cycle (condition during which *ccrM* is constitutively expressed) and increased in the condition where DNA was hemi- or unmethylated (strain depleted in CcrM). These data suggest that P1 is activated after the passage of the replication fork, when DNA was duplicated into two hemi-methylated molecules.

Further experiments confirm this hypothesis. For instance, changing the position of P1-P2-*ctrA* locus on the chromosome altered its expression profile (Reisenauer and Shapiro, 2002). Indeed, cloning this locus next to the terminator of the chromosome resulted in a delay in the induction of *ctrA* expression, confirming the necessity of having a hemi-methylated DNA for the onset of *ctrA* transcription.

Before the discovery of CtrA itself, Stephens et al. noticed a puzzling resemblance between the sequence of *ccrM* promoter and that of several flagellar genes (Stephens et al., 1995). These promoters shared a consensus sequence: TTAACCAT. At that time, authors concluded that DNA methylation and flagellar synthesis had to be under the control of the same regulatory process. In 1996, Quon et al. published their work describing CtrA as being a transcription factor and part of a TCS (Quon et al., 1996). They showed that in a strain carrying a thermosensitive allele of *ctrA,* the expression of flagellar genes and of *ccrM* is altered. Reisenauer et al. highlighted the presence of a 9-mer TTAA(N_7)TTAAC consensus sequence in the *ccrM* promoter and showed that CtrA∼P can bind this sequence *in vitro* (Reisenauer et al., 1999). The *ccrM* promoter itself contains two GAnTC methylation sites. Mutating either of these sites or both resulted in an increase of *ccrM* expression, suggesting that a fully methylated state is required for turning off *ccrM* promoter (Stephens et al., 1995).

Taken together, these data show that CtrA and CcrM influence the expression of their own genes but also of each other's. Thus *ctrA* and *ccrM* promoters are subjected to the regulation of at least two major regulators. However, as shown earlier (paragraph A-2-f), CtrA transcriptional activity is modulated by SciP (Gora et al., 2010). The *ccrM* and *ctrA* genes are among the downregulated genes in the strain constitutively expressing *sciP* (Gora et al., 2010). They are indeed expressed in late S phase (Domian et al., 1999; Zweiger et al., 1994). Thus SciP also participates in the proper expression of *ccrM* and *ctrA* during the cell cycle.

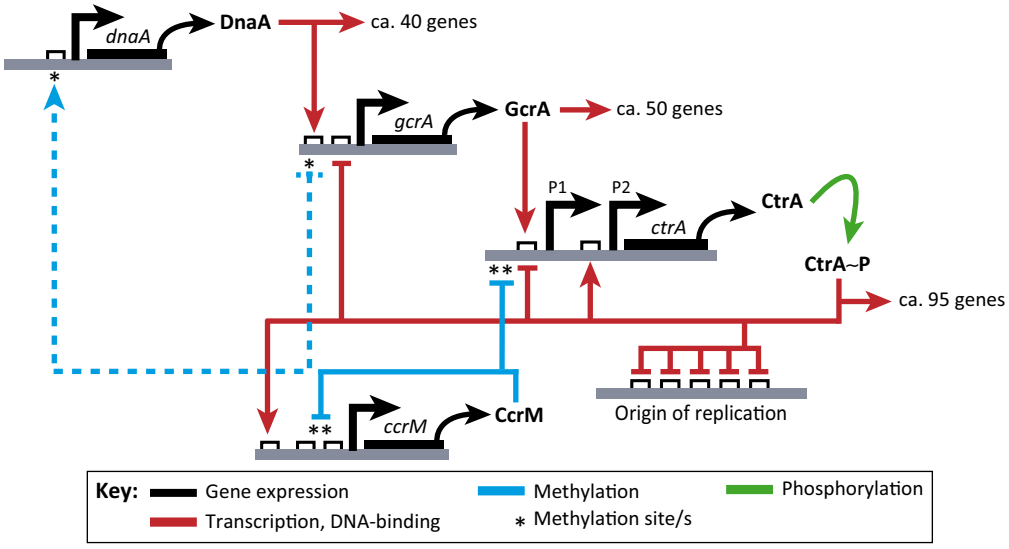

Figure 14- Schematic representation of the DnaA-GcrA-CtrA-CcrM circuitry (Mohapatra et al., 2014)

This scheme represents the highly interconnected transcriptional regulation of *dnaA, gcrA, ctrA* and *ccrM* and the role of methylation in modulating the activity of promoters containing GAnTC sites (*). The dashed blue lines depict the controversial effect of methylation on *dnaA* and *gcrA* expression.

d) On the link between GcrA and CcrM

The co-occurrence of CcrM and GcrA in alphaproteobacteria hinted towards a possible simultaneous implication of both proteins in the regulation of gene expression (Brilli et al., 2010). GcrA was previously shown to bind promoters of cell cycle regulated genes (Holtzendorff et al., 2004). Fioravanti and co-workers showed that GcrA affinity for DNA is dependent on its methylation state (Fioravanti et al., 2013). GcrA forms dimers in solution and has the highest affinity for fully methylated DNA. It can also bind hemi-methylated DNA but with less affinity. Finally binding to unmethylated DNA was the least efficient. A ChIP-seq assay allowed the authors to map GcrA binding sites on *C. crescentus* chromosome. Many already identified targets, such as *podJ*, *mipZ* and *ctrA* were fished out. Most interestingly, regions bound by GcrA were highly enriched in GAnTC sites, further supporting the idea that GcrA binds methylated DNA. However, some GcrA-bound regions do not contain any methylation sites, suggesting that methylation might not be the only modification recognized by GcrA. Furthermore, GcrA does not seem to bind any conserved sequence (Fioravanti et al., 2013).

Figure 14 summarizes the DnaA-GcrA-CtrA-CcrM circuitry. As already shown in Figure 12-b, DnaA activates the expression of GcrA, which in turn activates the expression of CtrA. CtrA inhibits the expression of *gcrA*. CcrM further modulates the activity of this "transcriptional cascade": methylation by CcrM silences the activity of *ctrA* and *gcrA* promoters while it activates *dnaA* promoter. It should be noted though that the effect of methylation on *gcrA* and *dnaA* promoter activity is controversial (Mohapatra et al., 2014).

In light of these informations, DnaA, GcrA and CtrA oscillation during *C. crescentus* cell cycle can be resumed as follows:

In the swarmer cell stage, CtrA is the main transcription factor present in the cell. It prevents initiation of chromosome replication as well as division and polar morphogenesis and represses *gcrA* promoter activity. At the G1-S transition, two major events occur: CtrA is proteolyzed (as a result in the inversion of DivK phosphorylation status) and DnaA is produced. As a consequence of this switch, the transcriptional programme of the cell is modified, allowing the entrance into the S phase. DnaA binds to the C*ori* and initiates chromosome replication, leading to the duplication of DNA and its transition from a fully methylated to a hemi-methylated state. It turns on *gcrA, ftsZ* and *podJ* expression, preparing the cell for the asymmetric division and polar organelle development. After the passage of the replication fork through *ctrA* locus, GcrA activates the hemi-methylated P1 weak promoter, allowing the synthesis of a small amount of CtrA. CtrA then feeds back on both its promoters, repressing the weak P1 promoter and activating the strong P2 promoter. This results in the synthesis of around 22000 molecules of CtrA in one cell (Judd et al., 2003). At that point, CtrA represses *gcrA* transcription and activates *ccrM* hemi-methylated promoter. CcrM accumulates, methylates its target sites and by that silences the *ctrA* P2 promoter as well as its own promoter. After septation, CtrA is maintained in the flagellated compartment and is eliminated from the stalked compartment by degradation, leading to two distinct transcriptional programmes in each cell.

Given its dual function, DnaA can be considered as a coordinator of chromosome replication and several developmental processes. Not only does it regulate the onset of chromosome replication, it also modulates the expression of a transcription factor (GcrA) that itself regulates the expression of a whole set of genes involved in DNA synthesis, polar morphogenesis and cell cycle regulation.

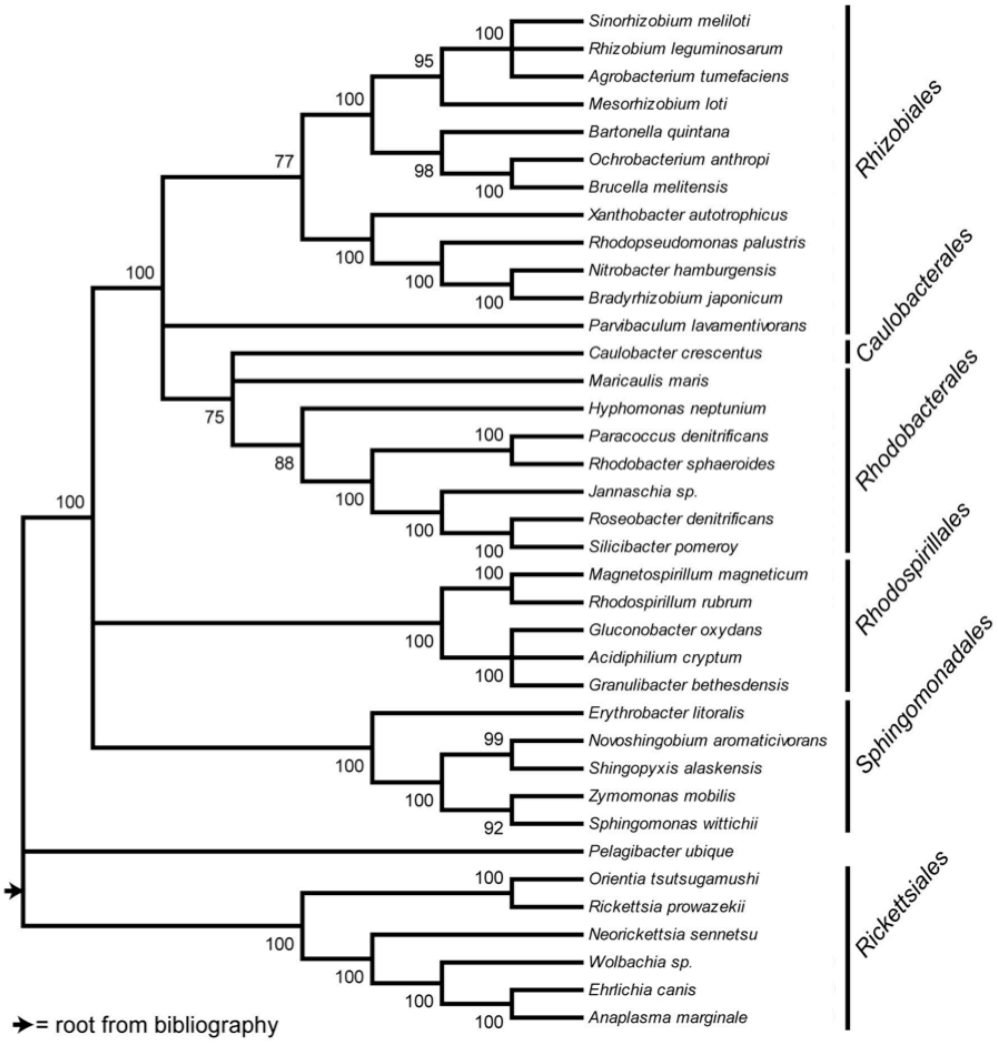

Figure 15- Phylogenetic tree of the *Alphaproteobacteria* class (Modified from Brilli et al., 2010) Numbers correspond to Bootstrap values.

B- Cell cycle regulation in other alphaproteobacteria

The *Alphaproteobacteria* class brings together different bacterial orders harbouring diverse lifestyles. Some are free-living organisms such as the model bacterium *Caulobacter crescentus*. Others, belonging to the order *Rhizobiales*, adopted a lifestyle in association with eukaryotic hosts: this order includes genera symbionts of plants (*Sinorhizobium, Rhizobium, Mesorhizobium*) and others pathogens of plants (*Agrobacterium*) (Batut et al., 2004). To this order belong also facultative intracellular pathogens of mammals (*Brucella* and *Bartonella*) and *Ochrobactrum anthropi*, a bacterium of the soil and opportunistic pathogen. Bacteria of the order *Rickettsiales* are obligate intracellular pathogens of arthropods and mammals whereas *Rhodobacterales* are photosynthetic bacteria (Batut et al., 2004). Figure 15 represents a phylogenetic tree of alphaproteobacteria based on the sequences of eight ribosomal proteins (Brilli et al., 2010).

Many aspects of the cell cycle have been studied in *C. crescentus*, especially regarding the role of the master transcription factor CtrA in the cell cycle progression as well as the different levels of regulation of CtrA activity itself. As already detailed earlier, these levels of regulation include transcription, phosphorelation and proteolysis (paragraph A-2-a of Chapter II) and involve the DivJ-PleC-DivK TCS and the DivL-CckA-ChpT-CtrA/CpdR phosphorelay (paragraph A-1-b). Coordinating the activity of this phosphorylation cascade is crucial to ensure a proper oscillation of CtrA activity throughout the cell cycle of *C. crescentus* and thus to give rise, at the end of each division, to two daughter cells with different morphologies and cell fates.

Despite the discrepancies in the lifestyles of members of the *Alphaproteobacteria* class, several bioinformatics analyses as well as experiments conducted recently have clearly shown that both the phosphorylation cascade leading to CtrA activation/proteolysis, and CtrA regulon are conserved among this class. However, this conservation is partial as other bacteria have diverged from the well known "*Caulobacter* paradigm" by losing part of the phosphorylation cascade or by using CtrA to other ends, i.e. in some orders CtrA regulates unessential processes not related to cell cycle.

1. Conservation of the PleC-DivJ-DivK TCS and the CckA-ChpT-CtrA phosphorelay in alphaproteobacteria

Interest in the cell cycle regulations occurring in alphaproteobacteria is growing. Several projects conducted recently have shown that the CtrA pathway is involved in the establishment of a successful interaction (symbiosis, pathogenicity) between several alphaproteobacteria and their eukaryotic hosts (Cheng et al., 2011; Pini et al., 2013; Willett et al., 2015). These projects show indeed how the CtrA pathway was adapted by each genus to its own lifestyle.

CtrA is restricted to *Alphaproteobacteria* and is widely present within this group of microorganisms (Brilli et al., 2010). Orthologs are indeed present in *Rickettsiales*, *Rhodobacterales*, *Rhizobiales, Rhodospirillales* and *Sphingomonadales*. A first search for orthologs of the TCS and phosphorelay upstream of CtrA in five alphaproteobacteria revealed that this signalling pathway is at least partially conserved among this class of bacteria (Hallez et al., 2004) (Figure 16). Some differences are indeed observed and could be explained by the adaptations developed by the different genera to their diverse habitats. For instance, the obligate intracellular pathogen *Rickettsia prowazekii* lacks

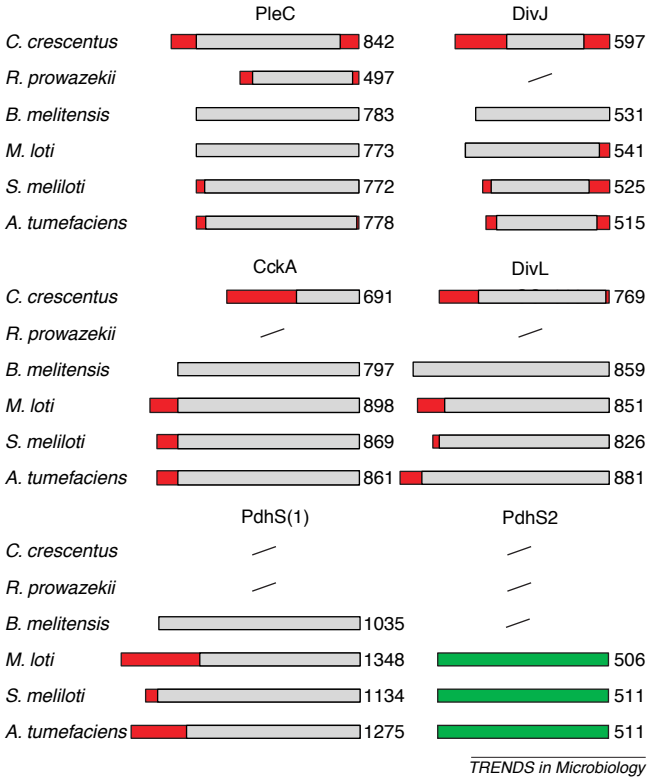

Figure 16- Schematic representation of protein orthologs of the phosphorylation cascade upstream of CtrA in *C. crescentus* and five other *Alphaproteobacteria* (Hallez et al., 2004)

C. crescentus shares orthologs of PleC, DivJ, DivL and CckA with all listed *Rhizobiales*. The latter possess either one or two extra histidine kinases, PdhS1 and PdhS2. PdhS1 is also called CbrA in *S. meliloti* (Gibson et al., 2006). *Rickettsia prowazekii*, an obligate intracellular pathogen, lacks most of these actors.

The number of amino acids of each protein is listed on the right. Grey bars represent the portions of the proteins similar to *B. melitensis* homolog taken as a reference. Red rectangles represent diverging domains and green bars represent proteins absent in *B. melitensis*.

divJ, *divL* and *cckA* orthologs. The absence of these genes can be associated with the reduction in genome size that accompanied the adaptation of this microorganism to an obligate intracellular lifestyle (Batut et al., 2004). Indeed, *Rickettsiales* harbour genomes of 1.1 to 1.3 mega base pairs (Mb), whereas *Brucellae* have genomes of around 3.3 Mb and plant associated bacteria living in the soil have undergone a genome expansion reaching for some 7.6 Mb (*Mesorhizobium loti*) and 9.1 Mb (*Bradyrhizobium japonicum*) in genome size.
The search for orthologs by Hallez et al. also revealed the presence in the *Rhizobiales* order of a gene coding for a third histidine kinase homologous to *pleC* and *divJ*. This gene is either present in one copy (*Brucella abortus*) or two copies (plant-associated *Rhizobiales*) and was dubbed *pdhS* for *pleC-divJ* homologous sensor (Hallez et al., 2004). A wider comparative genomic analysis conducted by Brilli et al. showed that *Rhizobiales* harbour the highest conservation of this phosphorylation cascade in comparison to *C. crescentus* while other orders diverge from this model organism to different extents (Brilli et al., 2010). Some members of the *Rhodobacterales* lack the *pleC-divJ-divK* TCS while some *Rickettsiales* lack this TCS, *cckA* and *chpT*.

2. CtrA regulon

Brilli et al. predicted CtrA regulon in several alphaproteobacteria based on the presence of the consensus sequence known to be bound by CtrA in *C. crescentus* (Brilli et al., 2010). Their results show that the regulon of CtrA is widely conserved in *Alphaproteobacteria*, and this observation concerns genes directly involved in cell cycle regulation as well as genes regulating other processes. CtrA seems indeed to regulate its own expression in almost all analysed genomes. In *Rhizobiales*, where the phosphorylation cascade is mostly conserved in comparison to the one of *C. crescentus*, CtrA exerts a feedback loop sometimes on *divK*, but mostly either on *pleC* or *divJ*. In bacteria lacking this TCS, CtrA regulates the expression of *divL* or *chpT*. More generally, CtrA seems to regulate similar processes as in *C. crescentus*. Indeed, most of CtrA predicted targets are involved in signal transduction, envelope homeostasis, cell division, chromosome partitioning and motility. These bioinformatics analyses suggest that CtrA regulon is partially conserved among *Alphaproteobacteria*.

CtrA is essential in most of the alphaproteobacteria. *Rhodobacter capsulatus* is an exception. In this organism, *ctrA* can be disrupted without affecting *R. capsulatus* viability. Such a disruption showed that CtrA regulates the expression of genes involved in a genetic exchange system called GTA for "gene transfer agent" (Lang and Beatty, 2000). GTAs are phage-like particles produced by *R. capsulatus* in stationary phase culture, probably in response to some stress-related environmental cue(s). In the obligate intracellular pathogen *Ehrlichia chaffeensis* (a member of the *Rickettsiales* order), CtrA is not essential either. It probably plays an important role in establishing the pathogenesis of this microorganism by regulating the expression of several genes involved in membrane homeostasis and in resistance to oxidative stress (Cheng et al., 2011). These examples show that some alphaproteobacteria developed adaptations involving CtrA in particular processes other than cell cycle regulation.
In *Brucella abortus*, a DNase I footprinting assay performed by Bellefontaine et al. suggests that CtrA might regulate similar processes as in *C. crescentus* but via different target genes (Bellefontaine et al., 2002). This *in vitro* assay showed that CtrA binds to the promoters of *pleC, minC* (an inhibitor of Z-ring formation near the poles), *ftsE* (a component of an ABC transporter localized to the Z ring), *ccrM, rpoD* (the major sigma

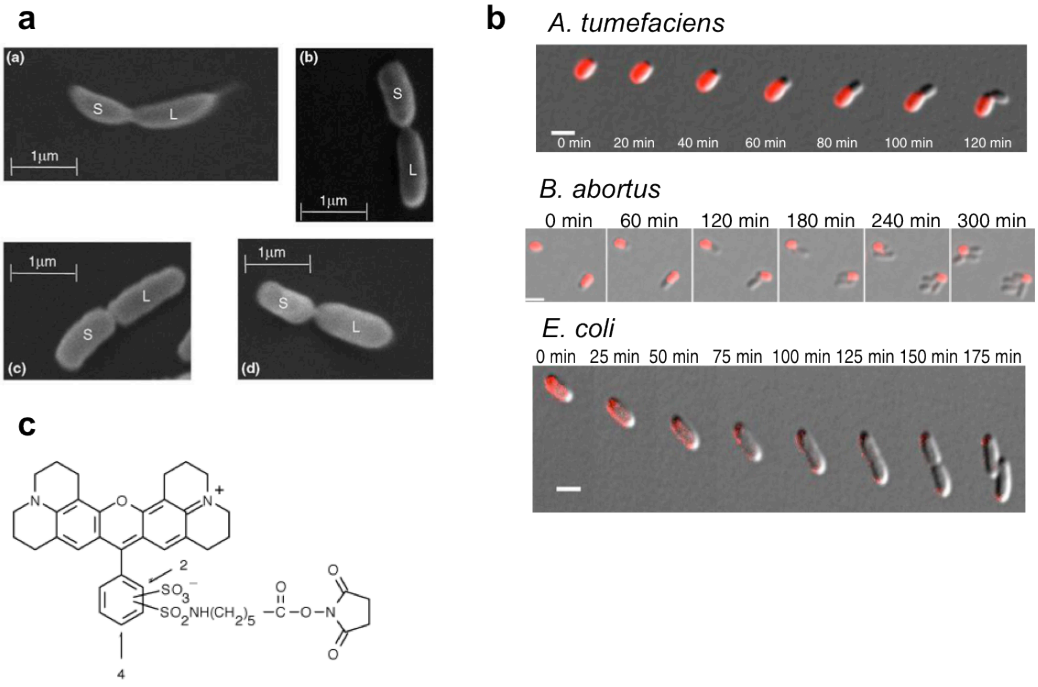

Figure 17 – *Alphaproteobacteria* divide asymmetrically and grow unipolarly (Brown et al., 2012; Hallez et al., 2004)

a- *C. crescentus* (a), *B. abortus* (b), *S. meliloti* (c) and *A. tumefaciens* (d) have an asymmetric division. The small and large cells are annotated S and L respectively.

b- Time lapse microscopy of *A. tumefaciens*, *B. abortus* and *E. coli* previously labelled with Texas Red succinimidyl ester (TRSE).

c- Molecular structure of Texas Red succinimidyl ester (TRSE)

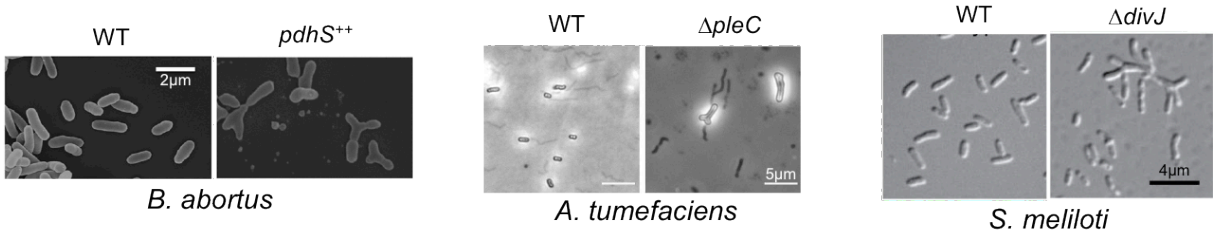

Figure 18- Scanning electron microscopy of *B. abortus* (WT and overexpressing *pdhS*) and light microscopy of *A. tumefaciens* (WT and Δ*pleC*) and *S. meliloti* (WT and Δ*divJ*) (Kim et al., 2013; Pini et al., 2013; Van der Henst et al., 2012)

B. abortus, *A. tumefaciens* and *S. meliloti* have aberrant morphologies (branched cells, mini-cells) when the level of expression of either of the histidine kinases (PdhS, DivJ and PleC) controlling DivK phosphorylation is perturbed.

factor) and *ctrA* but not to the promoter of *divK* or to the origin of replication, two known targets of CtrA in *C. crescentus*. Thus, CtrA probably regulates cell cycle (via *pleC* and *ctrA*), cell division (via *minC* and *ftsE*) and DNA methylation (via *ccrM*). These processes are also regulated by *C. crescentus* CtrA but sometimes via different genes. For instance, CtrA exerts a feedback loop on the phosphorylation cascade leading to its own activation by regulating the expression of *divK* in *C. crescentus* (Laub et al., 2000); CtrA could fulfil the same purpose in *B. abortus* by binding to the promoter of *pleC*.

3. The particular case of *Rhizobiales*

Bacteria of the order *Rhizobiales* have that in particular that they share many features despite their diverse lifestyles. This order brings together mammalian pathogens, *Brucella* and *Bartonella,* symbionts of plants, *Sinorhizobium, Rhizobium* and *Mesorhizobium*, a pathogen of plants, *Agrobacterium*, and a free-living bacterium and opportunistic pathogen, *Ochrobactrum*. Hence, one common feature among most *Rhizobiales* is their ability to establish an interaction with a eukaryotic organism, either in a symbiotic or in a pathogenic way.

Rhizobiales are rod-shaped bacteria sharing three other interesting characteristics: asymmetric division (Hallez et al., 2004) (Figure 17-a), unipolar growth (Brown et al., 2012) (Figure 17-b) and a multipartite genome. Scanning electron micrographs showed that *B. abortus*, *S. meliloti* and *A. tumefaciens* predivisional cells form a septum slightly shifted towards one of the poles. These observations raise the question of whether the asymmetric division in these bacteria also leads to the generation of daughter cells with distinct cell fates.

Unipolar growth has been observed in *B. abortus*, *S. meliloti, A. tumefaciens* and *O. anthropi* (Figure 17-b) (Brown et al., 2012). It was monitored thanks to a fluorescent dye called Texas Red succinimidyl ester (TRSE) (Figure 17-c). The succinimidyl ester group of this molecule reacts with amine groups present at the surface of the bacterial envelope, rendering the bacterial envelope fluorescent. When bacteria are labelled with TRSE and kept to grow, with time appears an unlabelled polar zone corresponding to the growing zone where newly synthesized material is inserted. Hence, the new daughter cell generated at the tip of this growing pole is exclusively made of new material. On the contrary, the old pole and the remaining cellular body of the "mother" cell are inert. *E. coli* displays a different growth pattern. It is known to incorporate new material along its cell body. This results in a dilution of the TRSE labelling during growth, except at the poles (Figure 17-b). As a direct consequence of such a unipolar growth, *Rhizobiales* harbour a branching phenotype when their cell cycle is perturbed in a way that leads to inhibition of division (Figure 18). It is the case of a fraction of *B. abortus* cells when *pdhS* is overexpressed (Van der Henst, 2012) or when a strain harbouring a thermosensitive allele of *ctrA* is grown at restrictive temperature (Willett et al., 2015) (Figure 21). Deleting *pleC*, *pdhS1* or *divK* in *A. tumefaciens* also leads to the formation of so called "Y-shaped" bacteria (Kim et al., 2013). Finally, a *S. meliloti* strain lacking *divJ* also harbours a branched phenotype (Pini et al., 2013).

Rhizobiales are also characterized by a multipartite genome. *A. tumefaciens* genome consists of a circular chromosome, a linear chromosome and two plasmids (Wood et al., 2001). *S. meliloti* genome is divided in a circular chromosome and two megaplasmids, pSymA and pSymB (Galibert et al., 2001). Finally, *B. melitensis* and *B. abortus* genomes are bipartite and consist of a large chromosome or ChrI (2.1 mega base pairs) and a

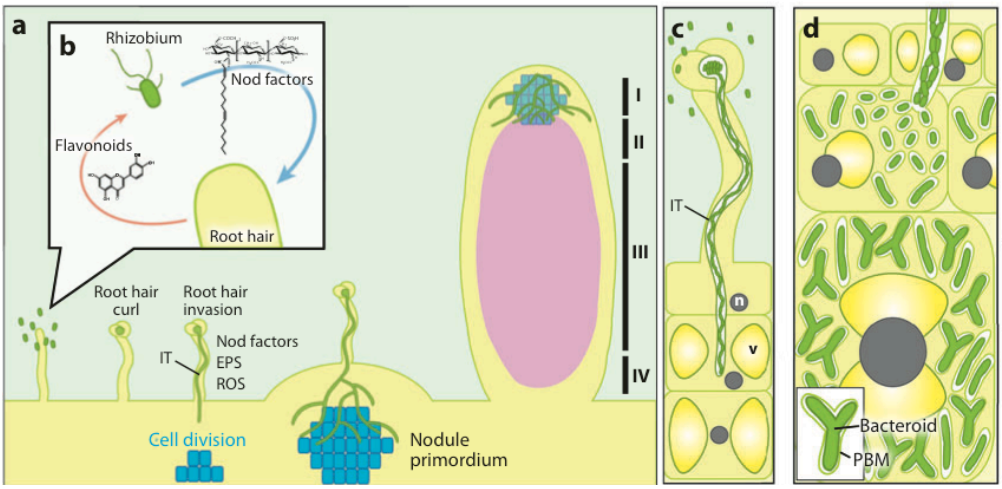

Figure 19- Schematic representation of the infection of a plant root hair by *S. meliloti* (Modified from Gibson et al., 2008)

In nitrogen starvation conditions, plants exude flavonoids recognized by *S. meliloti*. In response to these molecules, bacteria produce Nod factors, which bind to receptors at the surface of the root hair (b). This molecular exchange induces a curling of the root hair and the subsequent uptake of the bacteria invading the plant by dividing in an infection thread (IT) (a-c). After reaching the cortex, bacteria induce the mitosis of the plant cells (in blue) leading to the formation of a nodule (a). This nodule contains four distinct zones: the persistent meristem (I), the invasion zone (II), the nitrogen fixing zone (III) and the senescent zone (IV) present in old nodules. At the tip of the IT, bacteria are endocytosed by post-mitotic cortex cells (d). They are enclosed in a peribacteroid membrane (PBM) where they differentiate into bacteroids, a bacterial form specialized in taking up nitrogen (N2) and metabolizing it into molecules usable by the plant.

small chromosome or ChrII (1.2 mega base pairs) (DelVecchio et al., 2002; Singh et al., 2015). Each chromosome has its own replication machinery. ChrI encodes homologs of the ParAB segregation machinery while ChrII initiation of replication and segregation probably relies on the RepABC system (Deghelt et al., 2014; Pinto et al., 2012). The RepABC system is proper to the *Alphaproteobacteria* class and chromosomes encoding this machinery are referred to as chromids (Pinto et al., 2012). These replicons encode at least one essential gene but their replication and segregation profiles resemble those of plasmids. Recently, Deghelt, Mullier et al. showed that ChrI and ChrII of *B. abortus* are oriented along the cell length axis and that initiation of replication of ChrI starts before ChrII (Deghelt et al., 2014). They also showed that the origin of replication and terminator of ChrI (*ori*I and *ter*I) are closely apposed to the cell poles while *ori*II and *ter*II seem to be loosely associated to the poles and more mobile.

a) Sinorhizobium meliloti cell cycle regulation

Sinorhizobium meliloti is a nitrogen fixing symbiont of legume plants (Horvat, 1986). It is also a free-living bacterium able to colonize the soil. When nitrogen becomes limiting in the environment, leguminous plants secrete flavonoids into the soil. These secondary plant metabolites are perceived by the *Rhizobiales*, which in response to these molecules produce Nod factors (Figure 19). The latter are recognized by receptors present at the surface of host plant root hair, inducing a curling of the root hair and subsequent invasion of the plant tissue by the bacteria through an infection thread (IT). The Nod factors induce mitosis of the root cortex cells, leading to the formation of a nodule. At the tip of the IT, bacteria are endocytosed by post-mitotic cells where they differentiate into nitrogen-fixing bacteroids, able to reduce dinitrogen (N_2) into molecules usable by the host plant. Bacteroids display elongated and branched morphologies and undergo endoreduplication, suggesting profound changes in the cell cycle of these bacteria (Gibson et al., 2008; Kondorosi et al., 2013).

S. meliloti divides asymmetrically (Hallez et al., 2004) and chromosome replication is coupled with growth and division. Each round of growth and division is accompanied by a single event of chromosome replication and segregation (Mergaert et al., 2006). In addition to *pleC* and *divJ*, *S. meliloti* genome contains two genes coding for histidine kinases homologous to PleC and DivJ (CbrA and CbrB, also called PdhS1 and PdhS2 respectively) that might regulate certain aspects of the cell cycle (Hallez et al., 2004). One of these genes was selected in a transpositional mutagenesis screen for genes involved in symbiosis and exopolysaccharide synthesis (Gibson et al., 2006). The protein encoded by this gene was called CbrA for "Calcofluor bright regulator A" as the disruption of this coding sequence by a transposon resulted in an overproduction of succinoglycan, which is detected by the binding to calcofluor. Disrupting this gene also perturbed the cell cycle of *S. meliloti*, since mutant bacteria display branched phenotypes and abnormal genome contents, either <1N or >2N (Sadowski et al., 2013).
As already presented in the previous paragraph, genes involved in the phosphorylation cascade leading to CtrA phosphorylation and degradation are well conserved in *Rhizobiales* in general and in *S. meliloti* in particular. Several experimental data gave further insight into how this phosphorylation cascade functions in *S. meliloti.* In this bacterium, CbrA and DivJ are kinases for DivK while PleC is its phosphatase (Pini et al., 2013). CbrA and DivJ maintain a low level of phosphorylated CtrA, suggesting that, as in *C. crescentus*, DivK~P inhibits the phosphorelay leading to CtrA phosphorylation. DivK localizes to the old pole (Lam et al., 2003) in a CbrA-dependent manner (Sadowski et al.,

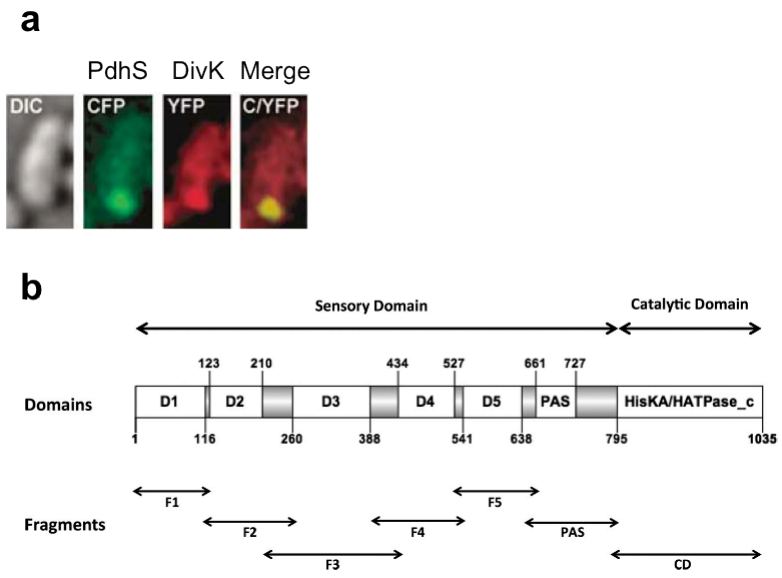

Figure 20- PdhS and DivK polar localization and PdhS domain mapping (Hallez et al., 2007; Van der Henst et al., 2012)

a- Fluorescence microscopy of a *B. abortus* strain expressing a PdhS-CFP fusion and a DivK-YFP fusion. Both proteins localize to one pole of the bacterium.

b- Schematic representation of PdhS domains: 6 fragments constitute the sensory domain while the catalytic domain (CD) comprises the histidine kinase and the ATPase domains.

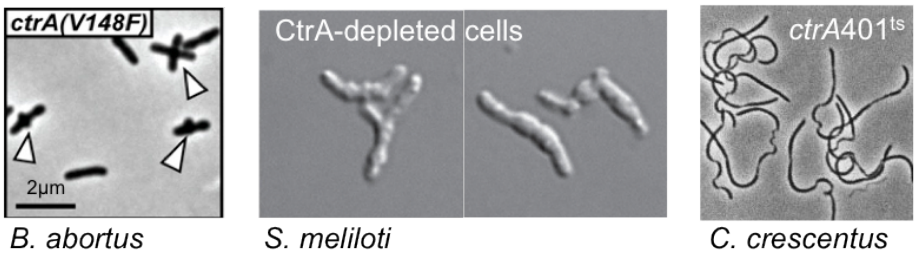

Figure 21- Light microscopy of a *B. abortus* and *C. crescentus* expressing a thermosensitive allele of *ctrA* and *S. meliloti* depleted of CtrA (Pini et al., 2015; Quon et al., 1998; Willett et al., 2015)

When *B. abortus* cells expressing *ctrA(V148F)* allele are incubated at restrictive temperature (37°C) for 24h, they elongate and form buddings at the midcell. CtrA-depleted *S. meliloti* cells elongate and branch, similarly to bacteroids. *C. crescentus* cells expressing a thermosensitive allele of *ctrA* and grown at restrictive temperature filament.

2013). The *divJ* and *cbrA* genes can be disrupted separately, although bacteria lacking one of these genes show branched phenotypes and accumulation of genomic DNA (Pini et al., 2013; Sadowski et al., 2013). However, *divJ* and *cbrA* are co-lethal, showing that DivK phosphorylation is essential. On the contrary, *pleC* cannot be deleted, suggesting that an excess of phosphorylated DivK is deleterious for the bacteria (Fields et al., 2012; Pini et al., 2013). When CtrA is depleted in *S. meliloti*, cells harbour a bacteroid-like phenotype, showing elongation and branching (Pini et al., 2015) (Figure 21).
Cell cycle and symbiosis are intricately linked together. Indeed, although not necessary for viability in culture, *divJ* and *cbrA* are essential for establishing a successful symbiosis with alfalfa host plants. Indeed, Δ*divJ* and *cbrA*::*tn5* mutants accumulate more CtrA than the WT strain and are unable to form efficient nodules (Pini et al., 2013; Sadowski et al., 2013). Furthermore, bacteroids purified from nodules are devoid of CtrA (Pini et al., 2013). Together with the CtrA-depleted cells phenotype, these observations suggest that CtrA has to be cleared from the cells to allow the differentiation into bacteroids.
CtrA predicted regulon is similar, although presents some differences, compared to CtrA regulon in *C. crescentus*. Combining microarray and ChIP-seq data, Pini and co-workers established the direct regulon of CtrA in *S. meliloti*. This regulon includes mainly genes involved in cell cycle regulation (*divJ*, *sciP*), division (*minCD*), motility genes and genes coding for envelope components (Pini et al., 2015).

b) Brucella abortus cell cycle regulation

B. abortus life style will be detailed in Chapter III. Briefly, it is a facultative intracellular pathogen of mammals, able to infect epithelial cells and professional phagocytes. Several cell types have been used in laboratories to study *Brucella* intracellular trafficking. Often they consist of HeLa cells and macrophages.
Major interest has been granted to studying the function of PdhS in *B. abortus* in our lab (Hallez et al., 2007; Mignolet et al., 2010; Van der Henst et al., 2012). PdhS is the only homolog of PleC and DivJ in *B. abortus*. Unlike these two kinases, it is cytoplasmic and it is essential (Hallez et al., 2007). When *pdhS* is overexpressed, *B. abortus* harbours abnormal morphologies, such as Y-shaped bacteria or minicells, suggesting that the accumulation of supernumerary copies of PdhS highly perturbs septum positioning and division (Figure 18) (Hallez et al., 2007). PdhS co-localizes with DivK at the old pole (Figure 20-a) (Hallez et al., 2007). When a *B. abortus* strain expressing a thermosensitive allele of *pdhS* is grown at a restrictive temperature, DivK polar localization is lost suggesting that PdhS controls DivK phosphorylation *in vivo* (Van der Henst et al., 2012). However, it should be noted that this strain generates suppressor mutations at high frequency (C. Van der Henst & X. De Bolle, unpublished).
Multiple alignments of *B. abortus* PdhS with homologs from other *Alphaproteobacteria* revealed seven conserved domains separated by linkers (Figure 20-b) (Van der Henst et al., 2012). Domain 6 is a predicted PAS domain. PAS domains are known to sense changes in several cues such as light, redox potential, oxygen, energy level or small ligands (Taylor and Zhulin, 1999) (See paragraph A2 of Chapter I). Domain 7 is a predicted histidine kinase domain (Kin) with a conserved histidine at position 805 and an ATPase domain. The first five domains at the N-terminus (D1 to D5) are of unknown function. A yeast two-hybrid (Y2H) assay showed that a fragment F3 corresponding to domain D3 is involved in PdhS dimerization while the PAS and Kin domains are required for interacting with DivK. Van der Henst et al. fused several fragments (F1 to F5) of PdhS to YFP on a replicative plasmid and identified that a minimal fragment corresponding to F2 and F3 is required for PdhS polar localization (Van der Henst et al., 2012). They also

showed that overexpressing domain F5 is able by itself to induce aberrant morphologies in *B. abortus*, suggesting that this fragment contains a regulatory region of PdhS activity.

B. abortus DivK is essential and it is the functional homolog of *C. crescentus* DivK as it is sufficient to ensure viability when present as the sole copy of *divK* in *C. crescentus* (Hallez et al., 2007). These two homologs share 79% of identity. DivK phosphorylation is essential for its polar localization, as a DivK(D53A)-YFP fusion does not localize to the pole. DivK interacts with PdhS, DivJ and PleC in a Y2H assay. However, neither PleC nor DivJ are essential for DivK polar localization or for *B. abortus* viability (Hallez et al., 2007).

Recently, Willett et al. showed that the *B. abortus* CckA-ChpT-CtrA/CpdR phosphorelay functions in a similar manner to the one of *C. crescentus* where CckA is a hybrid histidine kinase and ChpT a phosphotransferase able to shuttle the phosphoryl group between CckA on one hand and CtrA or CpdR on the other hand (Willett et al., 2015). They also showed that CckA, ChpT and CtrA are essential while deleting *cpdR* did not affect *B. abortus* viability. By constructing several conditional mutants, Willett and co-workers demonstrated that this phosphorelay regulates chromosome replication and division in culture and is essential for survival inside macrophages. One of these conditional mutants is *ctrA(V148F),* a thermosensitive (TS) allele of *ctrA*. A *B. abortus* strain expressing *ctrA(V148F)* from the chromosomal locus as the only copy of *ctrA* grew normally at 30°C. When shifted to 37°C, bacteria stopped proliferating but remained alive for as long as 72h, as shown by a stable number of CFUs. Twenty four hours after the shift to the restrictive temperature, bacteria were elongated and showed budding at the midcell (Figure 21). These results suggest that the thermosensitive allele is still sufficiently functional to maintain viability in rich culture medium. On the contrary, the *ctrA(V148F)* mutant did not survive in THP-1 macrophages at 37°C, showing a decrease in the CFU number after 24 and 48h of infection. For the sake of comparison, the phenotype of a *C. crescentus* strain with a *ctrA* TS allele is shown (Figure 21). Unlike unipolarly growing *Rhizobiales,* inhibition of *C. crescentus* division by CtrA inactivation results in filamentation (Quon et al., 1998).

Table 1 summarizes the essentiality of the proteins involved in the PdhS/PleC/DivJ-DivK TCS of four alphaproteobacteria. It is interesting to notice that, except for *C. crescentus*, all other cited alphaproteobacteria have at least one essential histidine kinase, and this essential kinase is different from one organism to the other. Finally, it is intriguing that DivK lost its essentiality in *A. tumefaciens*.

Organism	Life style	TCS	Essentiality
C. crescentus	Free living	PleC DivJ DivK	No No Yes
B. abortus	Mammal pathogen	PleC DivJ PdhS DivK	No No Yes Yes
S. meliloti	Plant symbiont	PleC DivJ CbrA DivK	Yes No* No* Yes
A. tumefaciens	Plant pathogen	PleC DivJ PdhS1 PdhS2 DivK	No Yes No No No

Table 1- Summary of the essentiality of the PdhS/PleC/DivJ-DivK TCS in *C. crescentus, B. abortus, S. meliloti* and *A. tumefaciens*
**divJ* and *cbrA* cannot be deleted simultaneously, demonstrating that DivK phosphorylation by DivJ or CbrA is essential.

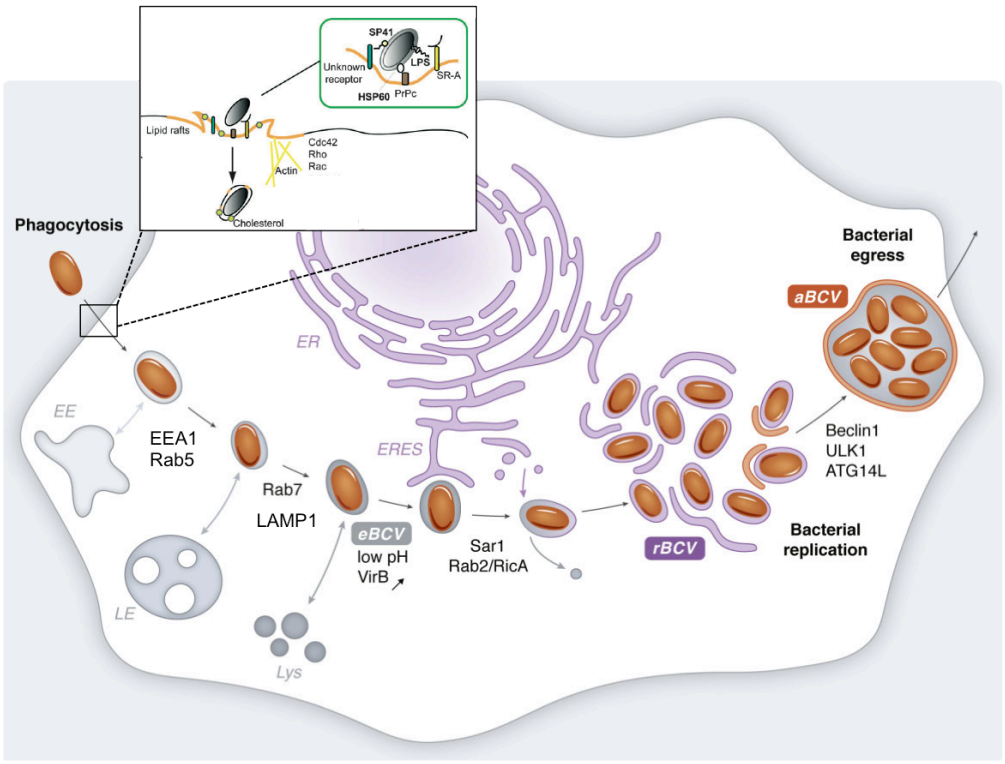

Figure 22- *Brucella* intracellular trafficking, from invasion to dissemination (Modified from Celli et al., 2015 and von Bargen et al., 2012)
Brucella are internalized in mammalian cells by phagocytosis at the level of lipid rafts (orange line in the zoomed image). These are micro-domains of the cytoplasmic membrane of eukaryotic cells enriched in cholesterol and several receptors that bind to proteins present at the surface of bacteria. For example, the surface protein 41 (SP41) of *Brucella* is thought to bind to unknown sialidated receptors. The PrP^C (prion protein) receptor recognizes the bacterial heat-shock protein Hsp60 (Watarai et al., 2003), even though this observation is controversial (Fontes et al., 2005). The scavenger receptor A (SR-A) interacts with LPS (Kim et al., 2004). Once inside the host cell, *Brucella* is enclosed in an endosomal *Brucella* containing vacuole (eBCV) that interacts with early endosomes (EE), acquiring EEA1 and Rab5, then with late endosomes (LE), acquiring Rab7 and Lamp1 and with lysosomes (Lys). Trafficking through the endocytic pathway leads to the acidification of the eBCV, which allows the expression of the *virB* operon. The eBCV interacts with the endoplasmic reticulum exit sites (ERES) in a Sar1-dependent manner, maturating into a replicative BCV (rBCV) where bacteria proliferate actively. Finally, interaction of the rBCV with an autophagosomal nucleation machinery (Beclin 1, ULK1, ATG14L) gives rise to the aBCV, proposed to be involved in the bacterial spreading to neighbouring cells.

Chapter III- Bacteria of the genus *Brucella*

A- *Brucella* species and brucellosis

Bacteria of the genus *Brucella* were first isolated in Malta in the 1880s by David Bruce (Bruce, 1889), a British captain and surgeon. At that time, many British soldiers suffered from an undulant fever. The source of infection was traced back to the ingestion of contaminated milk. *Brucella* are Gram negative coccobacilli, 0.5-0.7 µm wide and 0.6-1.5 µm long (Moreno and Moriyon, 2006). They are members of the alpha-2 proteobacteria class (Moreno et al., 1990). They are the causative agent of brucellosis, a worldwide zoonosis affecting diverse mammals including humans. Ten *Brucella* species have been characterized up to now, and together they can infect a broad range of mammalian hosts including cattle, sheep, goats, swine, dogs, rodents and marine mammals. Humans are accidental hosts for *Brucella* (Atluri et al., 2011), since *Brucella* do not propagate from one person to another. *B. melitensis, B. abortus* and *B. suis* are the most infectious for humans. Symptoms of brucellosis in humans resemble those of a strong cold and consist of fever, chills, weakness and muscle joint pain (Moreno and Moriyon, 2006). In animals, *Brucella* have a tropism for the reproductive tract, trophoblasts being one of their favourite niches (Anderson et al., 1986). Brucellosis induces abortion in females and sterility in males.

Brucellosis has been mostly eradicated in western countries but is still present in some parts of the world, especially in the Mediterranean region, in Latin America and in central Asia (Pappas et al., 2005). However, it should be noted that in some countries located in these regions, brucellosis is controlled by vaccinating healthy herds and culling infected animals (Pappas et al., 2006). As mentioned in the previous paragraph, *Brucella* infect many domestic animals. Brucellosis can thus have an important socio-economical impact as well as public health repercussions (Pappas et al., 2006).

B- *Brucella* intracellular trafficking and its link to virulence

Brucella are "facultatively extracellular, intracellular pathogens" of mammals (Moreno and Moriyon, 2006), meaning that they can survive in the environment (soil, water) but that their favourite niche is the intracellular milieu of mammalian cells. More commonly, they are referred to as facultative intracellular pathogens. *Brucella* can infect a wide range of mammalian cells, both non-phagocytic cells (Detilleux et al., 1990) and professional phagocytes (Archambaud et al., 2010). Epithelial cell lines such as HeLa and Vero cells, trophoblasts, THP1 human monocytes, dendritic cells and murine bone marrow-derived macrophages (BMDM) are a few examples of cell lines used in the laboratory to study *Brucella* pathogenesis (Billard et al., 2007; Detilleux et al., 1990; Moreno and Moriyon, 2006). *B. abortus* is one of the most studied species in regards to its intracellular trafficking and Hela cells and RAW 264.7 murine macrophages are the infection models most commonly used in laboratories. The journey bacteria undergo from the moment they encounter a host cell to the moment they disseminate to other cells can be divided in several distinct steps: (1) adhesion, (2) invasion, (3) survival inside the host cell, (4) proliferation and (5) dissemination to neighbouring cells (Figure 22). Each of these steps has been investigated and data show that bacteria control all stages of their life cycle.

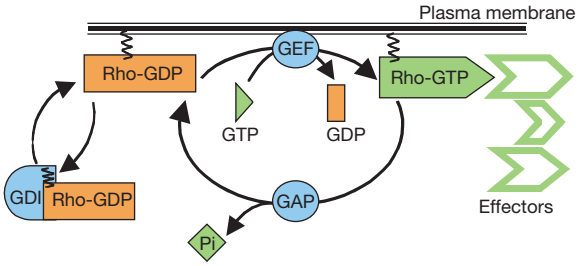

Figure 23- Cycling of small GTPases between their active and inactive form (Etienne-Manneville and Hall, 2002)

Box1- The eukaryotic small GTPases (Etienne-Manneville and Hall 2002)
Small GTPases are molecular switches allowing the regulation of a wide variety of processes such as gene transcription, membrane transport, cell polarity and organization of actin and tubulin cytoskeleton. The Ras superfamily of GTPases brings together five major groups: Rho, Ras, Rab, Arf and Ran. These GTPases cycle between a GTP-bound active state and a GDP-bound inactive state (Figure 23). These proteins are prenylated, which allows their insertion into membranes when activated. Guanine nucleotide exchange factors (GEFs) activate the GTPases by replacing the GDP by a GTP. GTPase-activating proteins (GAPs) stimulate GTP hydrolysis, bringing back the GTPases to their inactive state. Guanine nucleotide exchange inhibitors or GDP dissociation inhibitors (GDIs) extract inactivated GTPases from the membranes. In their active form, GTPases interact with effectors, resulting in a downstream specific biological response. For instance, activated Rho, Rac and Cdc42 (three proteins of the Rho subfamily) interact with a set of effectors and regulate signal transduction pathways, and by that link several membrane receptors to the assembly of actin and myosin filaments (Etienne-Manneville and Hall 2002). By regulating the dynamics of actin cytoskeleton, these GTPases are involved in phagocytosis, pinocytosis, cytokinesis and morphogenesis.
Members of the Rab superfamily are specifically involved in membrane trafficking (Grosshans, Oritz et al. 2006). They regulate vesicle budding from the donor membrane and its delivery, tethering and fusion to the correct target compartment. For instance, by binding to its effector EEA1, Rab5 ensures specific fusion of vacuoles to early endosomes. Replacement of Rab5 by Rab7 leads to the maturation of the vacuole into a late endosome.

1. Adhesion and internalisation

Many aspects of *Brucella* adhesion and entrance into host cells remain unclear but experiments did provide some answers to these aspects of the infection. *Brucella* bind to fibronectin and vitronectin, two components of the extracellular matrix (ECM), as well as to sialic acid present on the surface of HeLa cells (Castaneda-Roldan et al., 2004). Several proteins of *B. abortus, B. suis* and *B. melitensis* were shown to mediate adhesion and/or invasion into host cells. For instance, *Brucella* surface protein 41 (SP41) seems to bind to eukaryotic sialidated receptors (Castaneda-Roldan et al., 2006) (Figure 22). Most intriguingly, *ugpB* gene encoding SP41 is predicted to code for a periplasmic ATP-binding cassette. Yet SP41 was detected on the surface of *B. abortus* by immunofluorescence. Furthermore, monomeric and trimeric autotransporters of *B. suis* were shown to bind components of the ECM such as fibronectin and hyaluronic acid (Posadas et al., 2012; Ruiz-Ranwez et al., 2013). Authors suggest that binding to the ECM allows bacterial dissemination in the infected organism, given the presence of ECM components in multiple organs. However, for many other *Brucella* proteins, the mammalian ligands or receptors to which they bind are unknown and therefore no mechanism of action has been investigated (Czibener and Ugalde, 2012; Hernandez-Castro et al., 2008). Deleting any of the genes coding for these structures (autotransporters, SP41, etc.) separately resulted in a reduced adherence or internalization of bacteria but not their abolishment, suggesting redundancy between the activities of the proteins expressed on the surface of *Brucella*.

Furthermore, *Brucella* internalisation depends on the interaction with components of lipid rafts, particularly cholesterol and ganglioside GM1 (Naroeni and Porte, 2002; Watarai et al., 2002). Following a contact with HeLa cells or macrophages, *Brucella* induce a discrete rearrangement of the actin cytoskeleton and activate the small GTPase Cdc42 (Guzman-Verri et al., 2001) (Figure 22). Activity of Rho and Rac small GTPases (Box1) (Figure 23) is also important for *Brucella* internalization (Guzman-Verri et al., 2001). By modulating the activity of such proteins, *Brucella* binding to the surface of host cells could induce a signal transduction pathway in the mammalian cells resulting in the uptake of bacteria by macropinocytosis (Watarai et al., 2002).

These data show that internalization of *Brucella* by mammalian cells requires recognition between several structures present at the surface of each of the prokaryotic and eukaryotic cell. This recognition could elicit a response on both sides and activate specific phosphorylation cascades leading to the entrance of *Brucella* into their host cells. Indeed, small GTPases are known to regulate phosphorylation pathways by binding to specific effectors and, as will be discussed in the following paragraph (C-*Brucella* envelope), the *Brucella* BvrS/BvrR TCS, regulating the expression of several components of the outer membrane, is essential for virulence (Lopez-Goni et al., 2002). The data summarized in this paragraph also suggest that adhesion to and invasion of host cells by *Brucella* rely on different, partially redundant or synergistic mechanisms. This redundancy could reflect the multiple adaptations developed by *Brucella* while encountering a wide range of mammalian host cells.

2. Intracellular survival and proliferation

Once inside the host cells, *Brucella* reside in a membrane-bound compartment called BCV for "*Brucella*-containing vacuole" (Figure 22). BCVs are modified phagosomes (Starr et al., 2008) that first support *Brucella* survival, then their proliferation by interacting with compartments of the endocytic and secretory pathways of the host cell (Box2) (Figure 24). Thanks to these interactions, BCVs acquire specific markers of the early

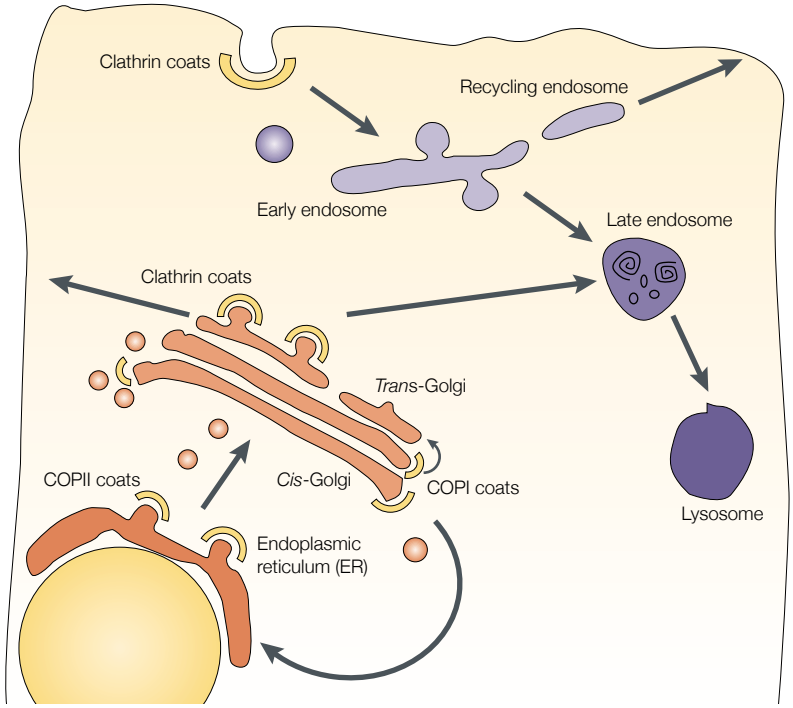

Figure 24- The endocytic and secretory pathways of eukaryotic cells (Kirchhausen, 2000)

Box 2- The endocytic and secretory pathways of eukaryotic cells (Kirchhausen 2000)
Phagocytosis is a mechanism by which eukaryotic cells uptake extracellular material. Ingested particles are engulfed in a vesicle that buds at the plasma membrane and undergoes a multi-step process of maturation leading to the destruction of the cargo in phagolysosomes (Figure 24). The vesicle first interacts with early endosomes also called sorting endosomes. They are characterized by a mildly acidic pH (around 6) and Rab5 and EEA1 are typical markers of these endosomes. The vesicle is then directed either to recycling endosomes recognizable by the presence of Rab11 or to late endosomes. The latter have an acidic pH (5.5) and are enriched in proteases. They are characterized by the presence of Rab7 and Lamp1. The vesicle finally reaches lysosomes, highly acidic (pH<5.5) and containing proteases and lipases.
The secretory pathway involves the ER and the Golgi apparatus. Proteins synthesized by ER-associated ribosomes are translocated to the ER lumen and transported to the Golgi apparatus where they undergo post-translational modifications before being sorted and sent to their final destination (plasma membrane or late endosomes). Budding of vesicles from the ER takes place at the ER exit sites (ERES). This ER to Golgi transport as well as the passage between Golgi cisternae (cis to trans Golgi) is known as the anterograde transport and occurs in COPII-coated vesicles. Some proteins, for example receptors or misfolded peptides, are recycled to the ER through the retrograde transport in COPI-coated vesicles. Several specific protein complexes are required for loading of the appropriate cargo, for the budding of the vesicle and for its targeting to the right compartment. For instance, Sar1 small GTPase is required for vesicular budding from the ERES as its activation triggers coat formation. It also recruits part of the "label" needed for the targeting of the vesicle to the Golgi apparatus.

endosomes such as EEA1 (Early endosomal antigen 1) (Pizarro-Cerda et al., 1998b) and the small GTPase Rab5 already 10 minutes post-infection (PI) (Chaves-Olarte et al., 2002). Around one hour PI, BCVs co-localize with markers of late endosomes such as Lamp1 (Lysosomal-associated membrane protein 1) (Pizarro-Cerda et al., 1998b) and Rab7 (Starr et al., 2008). BCVs then fuse with lysosomes, receiving lysosomal luminal content (Starr et al., 2008). The acquisition of lysosomal membrane and fluid-phase components results in the progressive acidification of the BCVs, reaching a pH of 4-5 (Rittig et al., 2001). Far from being deleterious, this acidification is crucial for BCV proper trafficking and *Brucella* survival. Acidification is indeed essential for the intracellular expression of the *virB* operon composed of 12 open reading frames (ORF) and coding for a type 4 secretion system (T4SS) (Boschiroli et al., 2002; O'Callaghan et al., 1999). This machinery delivers in the cytoplasm of the mammalian cell bacterial proteins known as "effectors", which interact with proteins of the host cell endocytic pathway and modulate the intracellular trafficking of *Brucella* (de Barsy et al., 2011; Dohmer et al., 2014; Marchesini et al., 2011; Myeni et al., 2013). The interactions with lysosomes are transient and tightly controlled by the bacteria (Starr et al., 2008) thanks to its T4SS (Celli et al., 2003; Comerci et al., 2001; Delrue et al., 2001). Indeed, around 8 hours PI, BCVs progressively exclude Lamp1 and concomitantly acquire markers of the rough endoplasmic reticulum (ER) such as calnexin (Pizarro-Cerda et al., 1998a), Sec61 translocon pore (Celli et al., 2003) and Sar1 (Celli et al., 2005) (Box 2). It was proposed that maturation of the BCVs into ER-derived compartments makes them permissive for *Brucella* proliferation (von Bargen et al., 2012).

Differences in *Brucella* intracellular trafficking have been observed depending on the host cells. When infecting macrophages, bacteria undergo an initial killing as shown by a decrease in the number of colony forming units (CFU) after plating extracted bacteria on rich medium (Celli et al., 2003). The few surviving bacteria (10%) are able to continue their intracellular journey as described above and CFU numbers increase around 10 hours PI when bacteria have reached their ER-derived replicative niche. The intracellular growth profile of *Brucella* is slightly different in epithelial cells (Detilleux et al., 1990). In these cells, no killing is observed, as the CFU numbers remain constant during the first hours of infection when the BCVs transit through the early and late endocytic pathway. CFU counts increase when bacteria reach their replicative niche. *Brucella* intracellular trafficking can thus be considered as biphasic: bacteria go through an early non-proliferative phase before entering a late proliferative phase.

The route by which bacteria enter their host cells is determinant for the outcome of the infection. Contact of a *B. abortus* WT strain with the surface of BMDMs induces membrane ruffling by actin polymerization, leading to bacterial internalization by macropinocytosis in a *virB*-dependent manner and through lipid rafts (Watarai et al., 2002). Internalization of a Δ*virB4* mutant into BMDMs is quicker than for the WT and more bacteria are taken up. Also, internalization of Δ*virB4* induces less actin polymerization (Watarai et al., 2002). However, despite a more efficient uptake, the mutant survival in BMDMs was compromised as shown by a decrease in the CFU counts. Furthermore, a Δ*virB10* mutant remains in Lamp1 positive (Lamp1+) compartments for up to 12 hours PI (Comerci et al., 2001), unable to reach an ER-derived replicative niche. Interestingly, Döhmer et al. identified an effector protein named SepA, secreted in a *virB*-dependent manner during the first hours of the infection (Dohmer et al., 2014). A Δ*sepA* mutant showed similar behaviour to the Δ*virB4* and Δ*virB10* mutants, being taken up

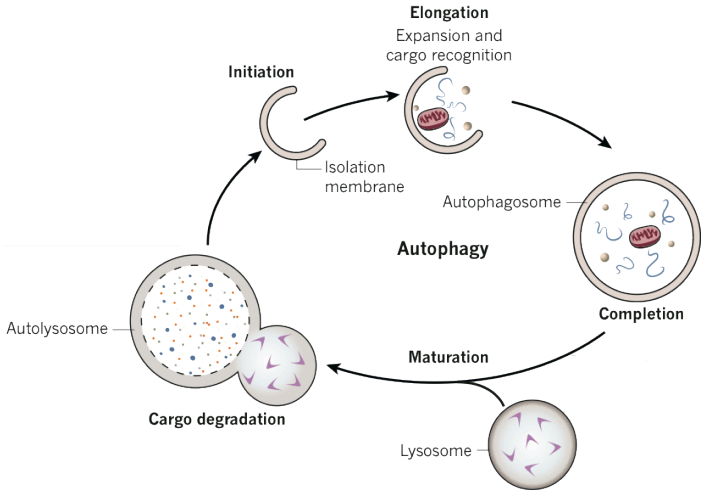

Figure 25- Autophagy: Nucleation, elongation, completion and maturation (Modified from Levine et al., 2011)

Box 3- Autophagy, a way of recycling organelles and eliminating microorganisms (Deretic and Levine, 2009; Levine et al., 2011)

Autophagy is the engulfment of cytoplasmic material, soluble macromolecules or organelles, in an autophagosome that targets its cargo to degradation in phagolysosomes. Synthesis of the autophagosome starts by a membrane "initiation" or nucleation at the ER, followed by its elongation and finally its completion (Figure 25). Autophagosome maturation occurs by fusion with lysosomes, leading to the degradation of the autophagosomal cargo. ULK1, Belcin 1 and PI3-kinase are some of the proteins involved in membrane initiation while ATG5, ATG7 and LC3B are required for membrane elongation. Autophagy is induced by nutrient starvation or by microbes or microbial virulence factors. It can thus serve as a recycling mechanism in times of shortage or as a means of defence against intracellular pathogens. As could be expected, the latter have developed several ways to interfere with autophagosome initiation or maturation by blocking the activity of Beclin 1 or preventing fusion with lysosomes for instance. Some have also evolved to hijack autophagy to facilitate their own intracellular survival, proliferation or spreading. For example, the periodontal pathogen *Prophyromonas gingivalis* takes refuge in autophagosomes to evade the endocytic pathway. *Legionella pneumophila* and *Coxiella burnetii* are enclosed in vacuoles harbouring autophagosomal but not lysosomal markers, suggesting an inhibition or a delay of the autophagosomal maturation.

more efficiently than the WT by J774 A.1 macrophage-like cells but having a lower rate of replication. The Δ*sepA* viability was reduced at early hours PI as BCVs retained Lamp1 marker for a longer time but bacteria were able to proliferate at later times (Dohmer et al., 2014). A Δ*sepA* mutant is thus less able to control the fusion of its BCV with lysosomes.

Brucella LPS was also shown to play an important role in the mode of entry and subsequent intracellular survival. Actually, internalization via lipid rafts depends on the polysaccharidic O-chain of the LPS (Porte et al., 2003) (Figure 27). *Brucella* lacking the O-chain (Rough strains), show an increased uptake but a reduced intracellular survival due to the maturation of their BCV into phagolysosomes (Porte et al., 2003). Treating murine macrophages with cholesterol or ganglioside GM1 sequestering agents prior to infection decreased survival of a *Brucella* Smooth strain (strain expressing the O-chain) but had no effect on the survival of a rough strain (Naroeni and Porte, 2002). This further supports the importance of lipid rafts-mediated entrance in the escape from the late endocytic pathway and pinpoints towards a potential interaction between the LPS and the lipid-rafts. Taken together, these data suggest that the way *Brucella* enter their host cells influences the later outcome of the intracellular trafficking. They also suggest that the LPS, the T4SS and its effectors play an important role in controlling this way of entry.

3. Dissemination to neighbouring cells

After *Brucella* reach the ER and proliferate, the BCVs mature into an autophagosome-like compartment (Box 3) necessary for bacterial spreading to neighbouring cells (Starr et al., 2012) (Figure 22). Besides its well-known function in the recycling of organelles and cytoplasmic content, autophagy is a mechanism used by eukaryotic cells to fight and eliminate internalized bacteria (Figure 25) (Levine et al., 2011). *Brucella* are able to hijack this process. More specifically, the maturation of the BCVs into an autophagosome-like compartment depends on the nucleation machinery involving ULK-1 and Beclin-1 but not on the elongation machinery (Box 3) (Figure 25) (Starr et al., 2012). This final maturation process allows *Brucella* to complete their lifecycle by infecting new cells. The process by which bacteria are released from the cells is still unknown. It could involve exocytosis or programmed cell death. The latter possibility is unlikely as no significant cell death was observed at late times PI (Starr et al., 2012). The signal triggering the recruitment of autophagosomal proteins to the BCVs also needs further investigation.

4. On the link between *Brucella abortus* intracellular trafficking and its cell cycle

The early phase of *Brucella* intracellular trafficking is characterized by a stable number of CFUs in HeLa cells, and in macrophages after an initial killing stage, evidencing a bacterial growth arrest for at least six hours. Deghelt, Mullier et al. asked whether *Brucella abortus* was indeed arrested for its growth and what was its chromosomal replication status (Deghelt et al., 2014). TRSE labelling of bacteria prior to infection showed that *B. abortus* growth was completely arrested for six hours and resumed around 8 h PI in Lamp1+ compartments, showing that bacteria restart their growth while still trafficking through the late endocytic pathway (Figure 26-a-b). Interestingly, newly generated daughter cells are localized in Lamp1 negative (Lamp1-) compartments (Figure 26-b). Labelling the origins of replication of chromosomes I and II showed that at very early times PI (15 minutes), 80% of internalized bacteria were in G1 phase (Figure 26-a) while G1-phase bacteria constitute only 26% of the total

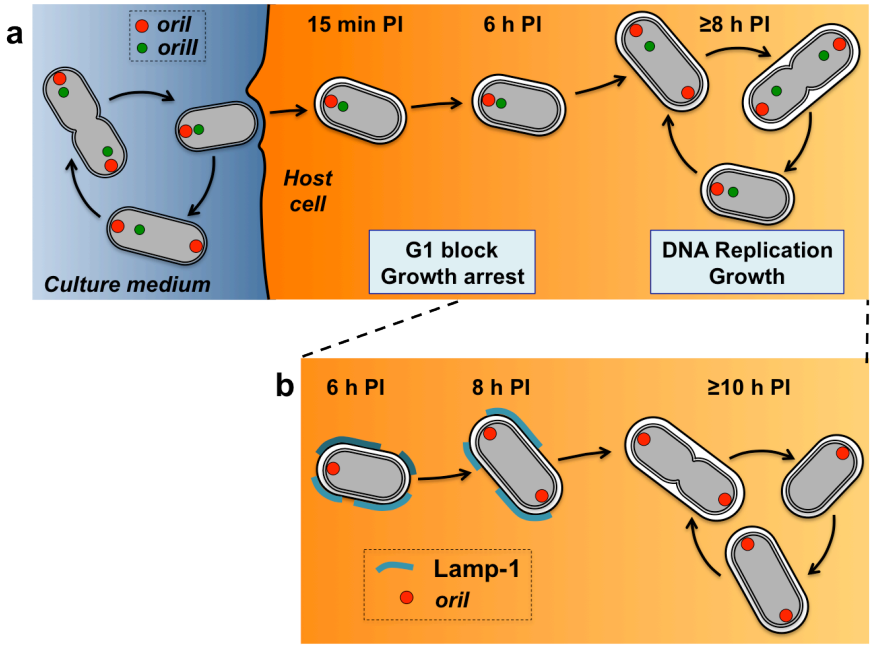

Figure 26- *Brucella abortus* cell cycle during infection (Deghelt et al., 2014)

a- In an asynchronous population of *B. abortus* grown in rich culture medium (blue background), bacteria grow, constrict and divide. Their genome is divided in two chromosomes, the large chromosome I (ChrI) and the small chromosome II (ChrII). The red and green dots depict the origin of replication of ChrI and ChrII respectively (*oriI* and *oriII*). Bacteria with single *oriI* and *oriII* are in G1, while bacteria with two copies of each of the *ori* are in S or G2. At early times PI (15 min and 6 h; orange background), most of the bacteria are in G1 phase and they are arrested for their growth. At 8 h PI, they resume their cell cycle.

b- Bacteria resume their growth while still in Lamp1+ compartments. Newly generated daughter cells are in Lamp1- compartments.

population of bacteria grown in rich culture medium prior to infection (Deghelt et al., 2014). This increase in the proportion of bacteria with one copy of their genome suggests that they are more infectious than bacteria in S or G2 phase. Similarly to growth, chromosome replication is arrested during the early phase of the infection and resumed later during the proliferative phase (Figure 26-a). Authors suggest that this cell cycle arrest protects bacteria from harmful agents present in the endosomes such as reactive oxygen species targeting DNA and acidic pH. Additionally, bacteria could encounter starvation during the early hours of infection, leading to cell cycle arrest. Finally, this work highlights a potential link between the cell cycle status of bacteria and the entrance stage of the infection. Further investigations of surface markers (such as adhesins) specifically expressed in G1 bacteria should shed light into the mechanism(s) underlying their selection at the entrance.

C- *Brucella* envelope

Brucella are Gram negative bacteria. Their cytoplasm is thus defined by an intracellular membrane, a periplasmic space containing the peptidoglycan (PG) and an outer membrane (OM) with an outer leaflet composed of lipopolysaccharide (LSP). LPS is composed of lipid A, which serves to anchor the molecule in the OM, an oligosaccharidic core and the O-polysaccharide chain (Figure 27). Special interest has been dedicated to *Brucella* OM composition given its importance in virulence.

As already discussed earlier, the O-chain of the LPS is involved in *Brucella* entrance into host cells (Figure 22). However, the importance of *Brucella* LPS in its virulence is not limited to the invasion step. Unlike most other bacterial LPS, *Brucella* LPS structure has evolved to avoid recognition by the host immune system and induction of pro-inflammatory responses (Goldstein et al., 1992; von Bargen et al., 2012). Its particularity resides in the Lipid A composition, consisting of a diamino-glucose backbone, instead of the classical glucosamine sugar backbone, and unusually long fatty acid chains (Figure 27). It is also poorly recognized by TLR4 (Lapaque et al., 2005). In addition to its low endotoxicity, this atypical LPS shields *Brucella* from the harmful effect of several anti-microbial agents. For instance, The O-chain prevents the deposition of complement on the bacterial surface. The LPS also makes bacteria resistant to cationic peptides such as polymyxin B (Martinez de Tejada et al., 1995). This resistance is thought to be associated to the absence of negatively charged uronic acid residues in the core, present in the core LPS of other bacteria (Moreno and Moriyon, 2006).

In addition to the LPS, the OM of *Brucella* contains several outer-membrane proteins (OMPs) strongly associated to PG and classified in three groups according to their size: group 1 (~90 KDa), group 2 (36-38 KDa) and group 3 (25-27 and 31-34 KDa) (Cloeckaert et al., 1990; Verstreate et al., 1982). Group 1 proteins represent a minority of the OMPs and have been subsequently poorly investigated (S. Genevrois thesis). OMPs of group 2 and group 3 represent the majority of the proteins present in the outer membrane of *Brucella*. Group 2 OMPs are porins encoded by two homologous genes, *omp2a* and *omp2b*, located close to each other in *Brucella* genome and sharing 85% of DNA sequence identity (Marquis and Ficht, 1993). However *omp2a* does not seem to be expressed in *B. abortus* under laboratory culture conditions. Group 3 consists mainly of Omp25 and Omp31. Omp25 was implicated in the virulence of three *Brucella* species as Δ*omp25* mutants were attenuated in a mouse and cattle infection model (Edmonds et al., 2001; Edmonds et al., 2002). This Omp25-mediated virulence could depend on its ability

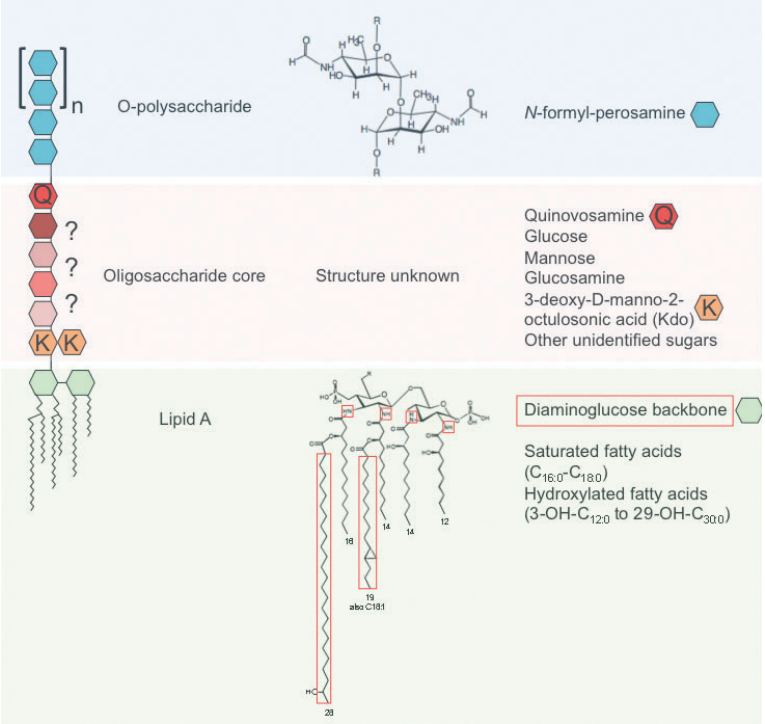

Figure 27- Structure of *Brucella* LPS (von Bargen et al., 2012)
Brucella LPS is composed of a lipid A, an oligosaccharidic core and the O-chain. The backbone of lipid A consists of two diaminoglucose monomers connected by amide linkages to long fatty acid chains (these three features are highlighted in red boxes). The structure of the oligosaccharidic core still needs to be characterized. Glucose, mannose and glucosamine are some of its already identified components, but others remain unknown (represented by question marks on the scheme). The O-chain is a homopolymer of N-formyl-perosamine; each polymer has an average size of 96 to 100 subunits (von Bargen et al., 2012).

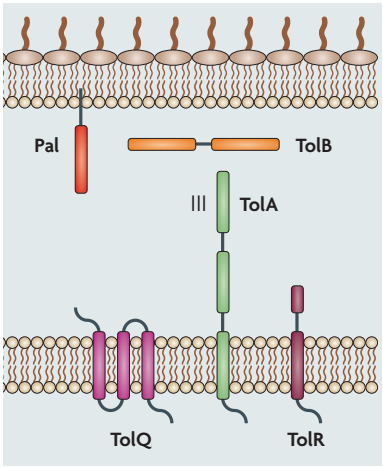

Figure 28- The Tol-Pal system in *E. coli* (Kleanthous, 2010)
The Tol-Pal system is a complex spanning the whole bacterial envelope. TolQ, TolA and TolR are embedded in the inner membrane, TolB is a periplasmic protein tightly interacting with the PG and Pal, a lipoprotein anchored to the OM.

to inhibit the production of the cytokine tumor necrosis factor alpha (TNFα) by human macrophages (Jubier-Maurin et al., 2001).

In addition to these three groups of OMPs, three minor lipoproteins of low molecular weight have been identified: Omp10, Omp16 and Omp19 (Tibor et al., 1999). Omp10 and Omp19 are specific to *Rhizobiales* (Tibor et al., 2002). *Brucella* strains lacking either of these proteins were attenuated in a mouse infection model and were more sensitive to polymyxin B and the detergent sodium deoxycholate, suggesting that these proteins are important for maintaining membrane homeostasis and for *Brucella* virulence (Tibor et al., 2002). Omp16 is thought to be a peptidoglycan-associated lipoprotein or Pal, as it is highly similar to three Pals from other bacteria (Tibor et al., 1994). Pals harbour an N-terminal moiety allowing their anchor to the OM and they are associated to PG by strong, non-covalent interactions. They are part of the Tol system known to be important for maintaining the homeostasis and integrity of the envelope in *E. coli* (Lazzaroni et al., 2002) (Figure 28). The Tol complex is also implicated in the coordination of the OM constriction with the PG synthesis during division in *E. coli* (Gray et al., 2015).

Going back to *Brucella,* one cannot evoke its envelope without introducing the BvrS/BvrR two-component system, where BvrS is a sensory transmembrane histidine kinase and BvrR a response regulator of the OmpR subfamily. This regulatory system was identified in a transpositional mutant library screened for its sensitivity to the cationic peptide polymyxin B (Sola-Landa et al., 1998). Bvr stands for "*Brucella* virulence-related". Not only is it important for resistance to cationic peptides, the BvrS/BvrR TCS is also essential for cell invasion and intracellular replication in murine macrophages and HeLa cells; it is also crucial for establishing an infection in a mouse model (Sola-Landa et al., 1998). The avirulent phenotype of the BvrS/BvrR mutants is associated to alterations of the cell envelope resulting in an increased sensitivity to polymyxin B, permeability to surfactants and hydrophobicity of the OM surface. Several differences in the envelope composition in the BvrS/BvrR mutants and the WT strain could account for these characteristics. For instance, the degree of lipid A acylation was decreased as tri- and tetra-acyl forms appeared in the BvrS/BvrR mutants on top of the penta- and hexa-acyl forms of the lipid A normally present in the WT strain (Figure 27) (Manterola et al., 2005). Furthermore, the expression of *omp*25 gene was down-regulated in the mutant strains (Guzman-Verri et al., 2002). Alteration of lipid A acylation resulted in a higher fluidity of the LPS leading to an increased sensitivity to polymyxin B (Manterola et al., 2005). The absence of Omp25 in the OM could alter its topology and hence the hydrophobicity at its surface. A whole-genome microarray analysis showed that mutation of the BvrS/BvrR TCS altered expression of many genes involved in cell envelope homeostasis (OMPs, lipoporteins, stress response proteins, LPS and fatty acid synthesis) and metabolism (nitrogen and carbon). Furthermore, microarrays showed down-regulation of *vjbR*, a gene coding for a transcription factor. The importance of VjbR resides in the fact that it is a crucial transcriptional regulator activating the expression of the *virB* operon in *Brucella* (Delrue et al., 2005).

Objectives

Brucella pathogenicity has been greatly investigated in regards to its trafficking inside cultivated mammalian host cells and to the immune response elicited in mice models. Data show how this bacterium evolved to become a stealthy pathogen, to survive to harsh conditions inside endosomes and to evade killing inside phagolysosomes. Despite the knowledge accumulated concerning the survival mechanisms developed by this bacterium, very little was known about how the bacterial cell cycle is regulated during infection. Cell elongation, chromosome replication and division are the basic processes that have to be fulfilled to ensure proliferation and they are subjected to multiple regulations. In rich culture medium, *Brucella* undergo a whole cell cycle in about three hours, from the moment a bacterium is generated by division to the moment a new daughter cell is released. The fact that inside host cells bacteria remain in an apparent latent phase for at least six hours suggests that their cell cycle is differentially regulated compared to the culture conditions (Deghelt et al., 2014). Recent data have indeed shown a complete arrest of growth and chromosome replication during the early phase of the infection in HeLa cells and RAW 264.7 macrophages (Deghelt et al., 2014).

In several alphaproteobacteria, cell cycle is regulated by the conserved master transcription factor CtrA, which amount and phosphorylation are controlled by a conserved phosphorylation pathway. In the symbiont *S. meliloti*, the proper functioning of this phosphorylation cascade is essential for establishing a successful interaction with host plants. CtrA could also play an important role in *B. abortus* pathogenicity. In the present project, we aim at investigating the activity of the histidine kinase PdhS (and possibly PleC and DivJ, two histidine kinases homologous to PdhS) on the response regulator DivK, both *in vitro* and *in vivo*. Kinase assays will be conducted to test the possible kinase and phosphatase activities of PdhS on DivK. Given that CtrA is essential, we aim at constructing a *B. abortus* 544 CtrA depletion strain and to analyse the effect of this depletion on the cell cycle and the virulence. We would like indeed to monitor bacterial elongation and division as well as chromosome replication in rich culture medium. We also plan to assess the viability of CtrA-depleted bacteria in a Hela cell infection and to monitor their intracellular elongation and trafficking to evaluate the effect of a cell cycle perturbation on *B. abortus* virulence. In order to identify the direct targets of CtrA *in vivo*, we propose to map CtrA binding sites on the two chromosomes by performing a ChIP-seq assay on *B. abortus* cells grown in rich culture medium. This experiment would confirm the central role of CtrA in *B. abortus* cell cycle regulation, and would identify new targets, specific to *B. abortus* or to *Rhizobiales*. Finally, we would like to develop a methodology to be able to follow gene expression along cell cycle. This will be performed through attempts to synchronize *B. abortus* populations on one side, and to sort bacteria carrying a reporter system according to their cell length on the other side. Such a reporter system could also be useful to follow bacterial gene expression inside host cells.

Altogether, we hope to contribute to a better understanding of the function of the DivK-CtrA network in *B. abortus*, to be able to compare the regulations occurring in this pathogen with those occurring in related symbionts and free-living bacteria. We also wish to better characterize cell cycle progression of *B. abortus* during infection.

Results

1. Manuscript

The PdhS-DivK-CtrA Pathway Controls Cell Division and Outer Membrane Composition in the Pathogen *Brucella abortus*

Nayla Francis[1], Antonella Fioravanti[2], Katy Poncin[1], Luca Rappez[3], Jean-Jacques Letesson[1], Emanuele G. Biondi[4], Xavier De Bolle[1]*

[1] University of Namur, Microorganisms Biology Research Unit, Namur, Belgium

[2] Vrije Universiteit Brussels (VUB), Structural and Molecular Microbiology Department, Brussels, Belgium

[3] European Molecular Biology Laboratory (EMBL), Structural and Computational Biology Department, Heidelberg, Germany

[4] AIX-Marseille University – CNRS, Laboratoire de Chimie Bacterienne, Marseille, France

* Corresponding author
xavier.debolle@unamur.be

Abstract

The well-conserved transcription factor CtrA and its upstream regulatory phosphorylation cascade control cell cycle progression in the model organism *Caulobacter crescentus* and in *Sinorhizobium meliloti*. In the pathogen of mammals *Brucella abortus*, we show that the histidine kinase PdhS controls the phosphorylation state of the single-domain response regulator DivK *in vitro* and modulates indirectly CtrA amount and phosphorylation *in vivo*. CtrA-depleted bacteria formed large branched morphologies, indicating that CtrA is essential for division. This abnormal morphology was also observed during a HeLa cell infection. Indeed, CtrA-depleted bacteria were able to resume their intracellular elongation and to leave late endosomes, but their long-term survival was compromised. A ChIP-seq experiment showed that CtrA regulon is enriched in genes involved in cell cycle progression and in envelope homeostasis and composition. Accordingly, we confirmed that the outer membrane protein Omp25 was depleted in the absence of CtrA. Altogether our data suggest that although the core of the DivK-CtrA pathway is conserved in *B. abortus,* it was adapted to its pathogenic lifestyle.

Author Summary

All living organisms are in constant interaction with their environment. In bacteria, histidine kinases and response regulators form two-component systems and phosphorelays that allow the sensing of intra- and extracellular stimuli and the elaboration of an adapted response. A phosphorylation cascade conserved between *Alphaproteobacteria* involves the single-domain response regulator DivK and the transcription factor CtrA and regulates cell cycle progression in the free-living model organism *Caulobacter crescentus*. We aimed at studying DivK phosphorylation and CtrA functions in the related pathogen of mammals *Brucella abortus*. We showed that DivK phosphorylation state is regulated by the histidine kinase PdhS and that PdhS can also indirectly modulate CtrA amount and phosphorylation *in vivo*. Our results indicate that CtrA is essential for *B. abortus* division and survival in culture and inside host cells. A genome-wide analysis of CtrA binding sites showed that CtrA regulon is enriched in genes involved in cell cycle-related functions and in envelope synthesis and composition. Taken together, data presented here show how a phosphorylation cascade was adapted during evolution to diverging lifestyles.

Introduction

Brucella abortus is a facultative intracellular pathogen [1] preferentially infecting cattle, although humans can be accidental hosts. Infection by *B. abortus* causes a disease called brucellosis, a worldwide zoonosis. *B. abortus* can infect both epithelial cells (such as HeLa and Vero cells) [2] and professional phagocytes (macrophages and dendritic cells) [3]. Once inside its host cell, *B. abortus* resides in a membrane-bound compartment called BCV for *Brucella* containing vacuole. *B. abortus* intracellular trafficking is biphasic, there is first an early non proliferative phase during which the BCV interacts with early and then late endosomes [4-6], as shown by the acquisition of Lamp1, a marker of late endosomes and lysosomes. Then, in most cell types [7], the second phase is characterized by bacterial proliferation in a compartment harbouring endoplasmic reticulum (ER) markers [5,8,9]. After this massive proliferation step, BCVs acquire autophagic markers and bacteria spread to neighbouring cells [10].

Recently, new evidence showed that cell cycle and virulence of *B. abortus* are coordinated [11]. Bacteria in the G1 stage of their cell cycle are more infectious than their counterparts in S or G2 phases. Furthermore, during the early non-proliferative phase of the infection, bacteria remained in G1 phase for up to 6 h and were arrested for their growth. *B. abortus* is thus able to arrest its cell cycle while trafficking through the endocytic pathway. Around 8 h post-infection (PI) in HeLa cells, bacteria resumed chromosome replication and growth while still residing in Lamp1+ compartments. However, the newly generated daughter cells were delivered into Lamp1- BCVs [11].

B. abortus is a member of the *Alphaproteobacteria*, and many key regulators controlling the cell cycle progression of the model organism *Caulobacter crescentus* are conserved in *B. abortus* [12,13]. In particular, the DivK-CtrA regulation network, involving proteins of the two-component systems (TCS), i.e. histidine kinases (HK), response regulators (RR) and histidine phosphotranferases (HPt), is conserved in many *Alphaproteobacteria*, including *Rhizobiales* like *Sinorhizobium meliloti* [14] and *B. abortus*. It was recently reported that a large fraction of this network is functional in *B. abortus* and that it is essential for survival in THP-1 macrophages [15]. However, this network displays also variations between *Alphaproteobacteria*, particularly at the top and at the bottom of the regulation cascade. At the top of the cascade in *C. crescentus*, DivK phosphorylation level is controlled by two HK, DivJ phosphorylating DivK, and PleC acting both as a kinase and a phosphatase for DivK [16]. In *B. abortus*, besides DivJ and PleC, a third histidine kinase

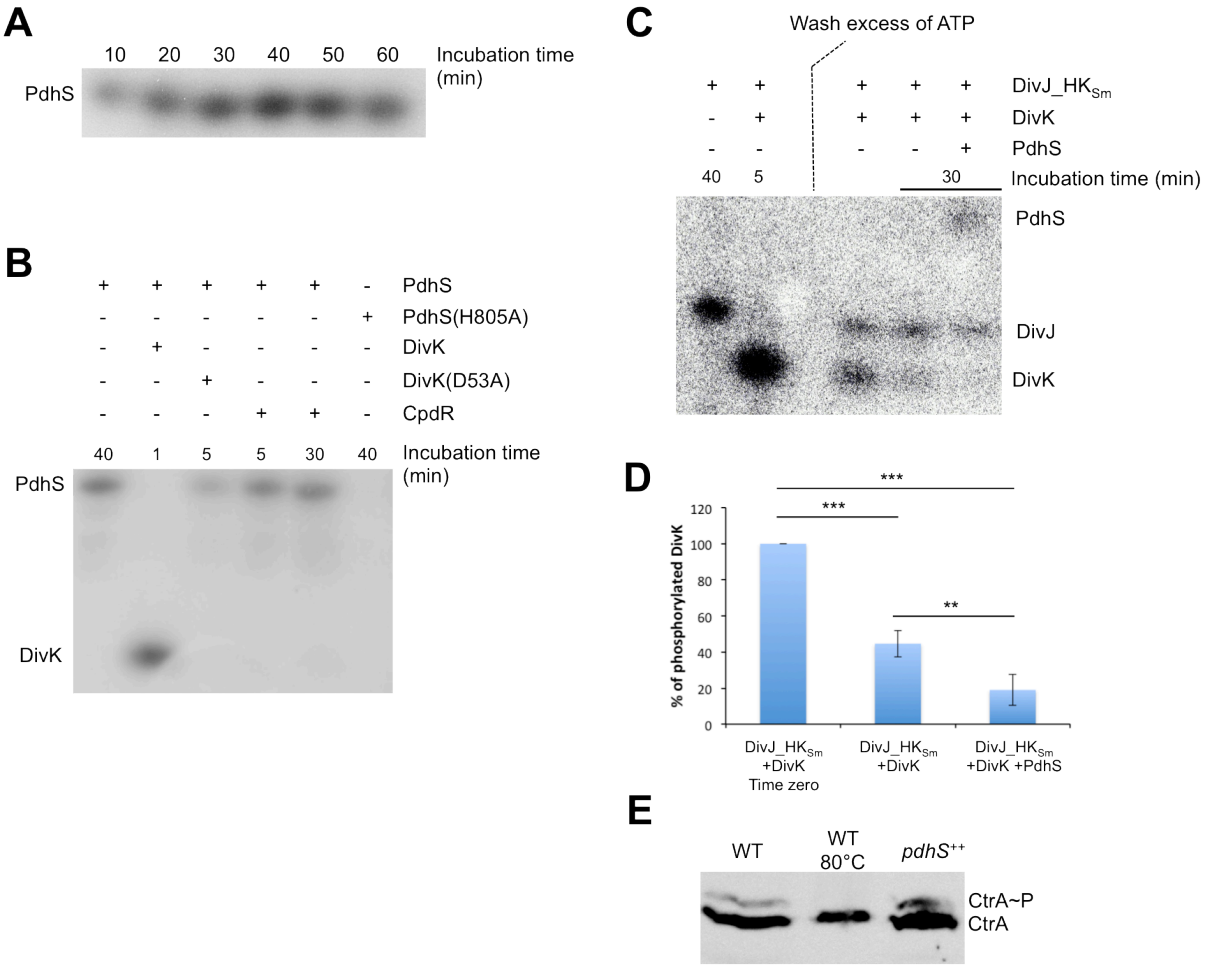

Fig 1. *In vitro* and *in vivo* kinase assays. (A) Autoradiography of a time course of PdhS auto-phosphorylation, showing that autophosphorylation is maximal after 40 min of incubation. (B) Autoradiography showing phosphotransfer from PdhS to DivK in one minute and absence of phosphotransfer from PdhS to CpdR, confirming that PdhS-DivK phosphotransfer is specific. The absence of PdhS(H805A) autophosphorylation and of phosphotransfer to DivK(D53A) shows that phosphorylation occurs on these two conserved residues. (C) Autoradiography and (D) the corresponding quantifications show that PdhS has a phosphatase activity toward DivJ_HK$_{Sm}$-phosphorylated DivK. The significant pairwise comparisons according to Scheffe are indicated by ** ($p < 0.01$) and *** ($p < 0.001$). (E) *In vivo* Phostag assay (repeated thrice) followed by an anti-CtrA Western blot. The upper band is lost when bacteria are heated at 80°C, proving that it corresponds to the phosphorylated form of CtrA. Overexpression of *pdhS* alters CtrA amount and phosphorylation.

called PdhS, homologous to DivJ and PleC, is predicted [13,17]. PdhS is essential and it interacts with DivK [17], suggesting a potential kinase or phosphatase activity of PdhS on DivK. At the bottom of the cascade in *C. crescentus*, the CtrA RR directly controls the expression of 95 genes involved in key events of the cell cycle, like cell division, polar morphogenesis, DNA methylation and chemotaxis [18-20]. CtrA also binds the replication origin of *C. crescentus* chromosome, thereby preventing the initiation of its replication [19]. The CtrA homologue in *B. abortus* was proposed to control similar processes but through different target genes [21]. CtrA phosphorylation by the DivK-CtrA regulation pathway promotes its binding to DNA [20]. CtrA binds two consensus sequences, the "TTAA(N7)TTAAC" 9-mer box [19] and the "TTAACCAT" 8-mer box [18], which are also found in CtrA target promoters in *B. abortus* [13,21].

Here we investigated the main variations in the *B. abortus* DivK-CtrA regulation network, compared to *C. crescentus*. At the top of the cascade, we show that PdhS can have both a kinase and a phosphatase activity towards DivK *in vitro* and that it can modulate CtrA amount and phosphorylation *in vivo*. At the bottom of the cascade, we found that CtrA is dispensable for *B. abortus* elongation but is essential for its division, both in culture and during infection. CtrA is also required for an efficient intracellular trafficking of B. *abortus* in HeLa cells. A detailed analysis of CtrA regulon in *B. abortus* not only reveals that CtrA binds to the promoters of genes involved in cell cycle control and progression, as expected, but it also provides evidence that CtrA controls outer membrane composition.

Results

PdhS is a kinase and a phosphatase for DivK *in vitro*

In vitro autokinase assays showed that a recombinant fusion Trx-His_6-PdhS is able to autophosphorylate and a maximal signal is reached after 40 min of incubation with ATP (Fig 1-A). Acquisition of a phosphate group occurs on a conserved histidine at position 805, since mutating this residue to an alanine abolished autophosphorylation (Fig 1-B). In order to test the potential kinase activity of PdhS on DivK, phosphorylated PdhS was added to purified Trx-His_6-DivK. Phosphotransfer from PdhS to DivK was efficient and quick, as it was apparently complete after one minute of incubation (Fig 1-B). This phosphotransfer occurred on a conserved aspartate residue of DivK at position 53, since replacing Asp-53 by an alanine prevented phosphotransfer from PdhS (Fig 1-B). Finally,

the PdhS-DivK phosphotransfer is specific since the PdhS-dependent phosphotransfer on a different response regulator (CpdR) was not observed; CpdR is another single-domain response regulator of *B. abortus*. As a control, we showed that phosphotransfer was possible between phosphorylated MBP-EnvZ and Trx-His_6-CpdR (data not shown).
In order to assess PdhS phosphatase activity on DivK, we generated phosphorylated DivK by incubation with the histidine kinase domain of DivJ from *Sinorhizobium meliloti* (DivJ_HK_{Sm}) fused to Trx-His_6 [14] (Fig 1-C). The excess of ATP was then washed and the DivJ-DivK~P mix was supplemented or not with PdhS. Both mixes were incubated at room temperature for 30 min and the remaining DivK~P was quantified. The DivJ-DivK mix showed a decrease of DivK~P by 50%, while the addition of PdhS generated 80% dephosphorylation of DivK (Fig 1-D). Those data indicated that PdhS harbours a phosphatase activity towards DivK as well as a kinase activity.

Overexpression of *pdhS* results in an increase of CtrA phosphorylation in *B. abortus*

Recently, Willett *et al.* showed that the *B. abortus* CckA-ChpT-CtrA phosphorelay functions in a similar manner to *C. crescentus* phosphorelay [15]. Furthermore, the conservation of DivL in *B. abortus*, which transmits signal from DivK to CckA, and the fact that *B. abortus* DivL and DivK interact with each other [22], suggests that the whole signalling network is conserved between *B. abortus* and *C. crescentus*. We thus hypothesized that alteration of *pdhS* expression could result in a change of CtrA phosphorylation level. Since *pdhS* is essential, we used a strain overproducing PdhS to compare CtrA phosphorylation status to the wild type (WT) strain [23]. In the *pdhS* overexpressing strain, the overall amount of CtrA, as well as the phosphorylated proportion of the protein were increased compared to the WT strain (Fig 1-E). These results indicate that in *B. abortus* PdhS indeed modulates CtrA abundance and phosphorylation, which is required for DNA binding [21]. This also suggests that the PdhS-CtrA regulation network is "wired".

CtrA is crucial for *B. abortus* cell division

In *C. crescentus*, CtrA is the master regulator controlling many important genes required for cell cycle progression. Here we investigated the *B. abortus* CtrA function *in vivo* by generating a *ctrA* depletion strain, as this gene was suggested to be essential [21]. First,

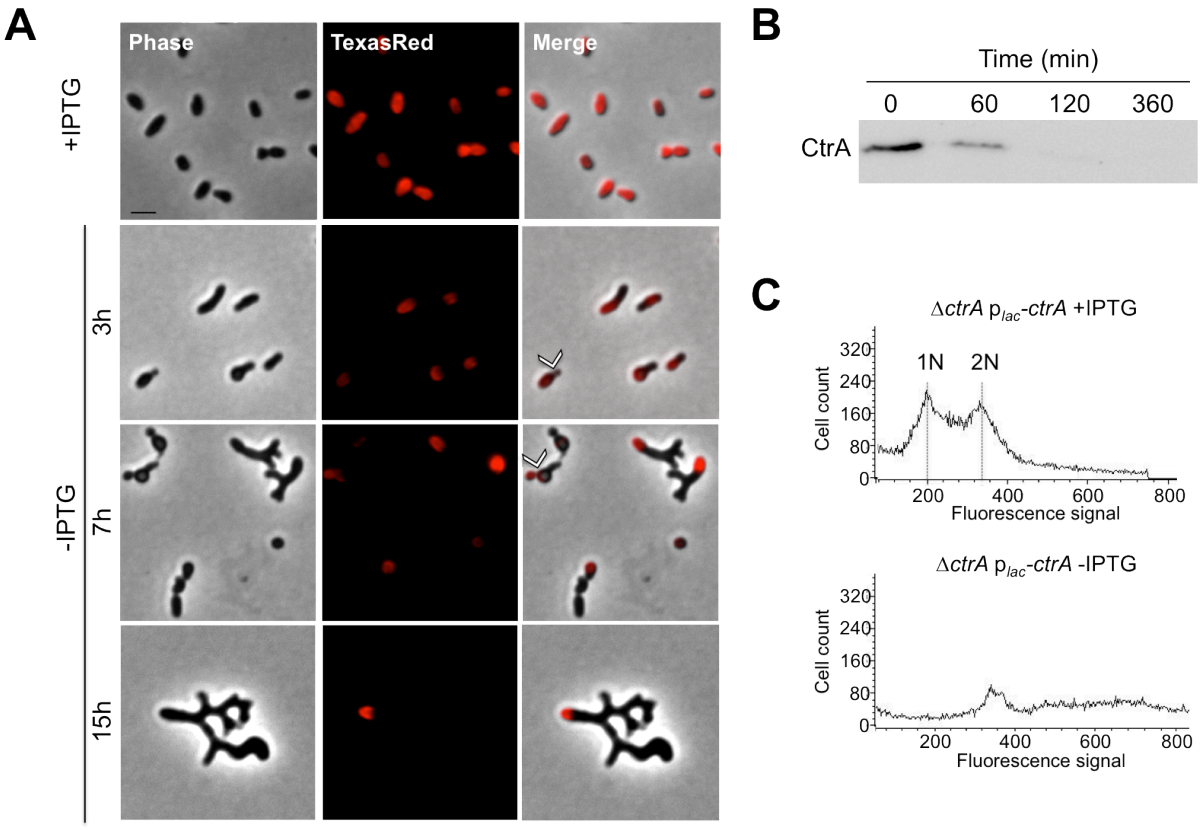

Fig 2. Characterization of the morphology and DNA content of the CtrA depletion strain. (A) Phase contrast ("Phase") and fluorescence ("TexasRed") microscopy images of a CtrA depletion strain labelled with TRSE and grown with IPTG ("+IPTG") show that bacteria have a normal morphology. Upon IPTG removal ("-IPTG"), bacteria elongate (3 h), form chains and branch (7 and 15 h). TRSE allows covalent binding of amine groups present at the bacterial surface with Texas Red. Growth occurring after TRSE labelling results in the incorporation of unlabelled envelope material. The scale bar corresponds to 2 μm. (B) CtrA detection by Western blot shows a quick decrease in protein amount and apparent clearance 120 min post-IPTG removal. (C) Detection of DNA content by flow cytometry shows that 7 h post-IPTG removal, bacteria accumulate multiple copies of their chromosomes.

a WT copy of *ctrA* was cloned on a replicative plasmid as a fusion with an IPTG-inducible promoter; then the chromosomal *ctrA* deletion was obtained by allelic replacement in the presence of IPTG. When the growth medium was supplemented with IPTG, the Δ*ctrA* p_{lac}-*ctrA* strain harboured a WT morphology (Fig 2-A) (bacteria were stained with Texas-Red Succinimidyl ester (TRSE) to follow their unipolar growth [24]) and a normal DNA content, as shown by the classical 1N-2N peaks obtained by flow cytometry (Fig 2-C). Upon IPTG removal, CtrA was cleared within 2 hours from the cells as measured by immunoblotting (Fig 2-B). Abnormal morphologies appeared 3 h post IPTG removal and consisted of elongated cells and cells with mislocalized constrictions, i.e. detectable septa located very close to one pole, (Fig 2-A; white arrow heads). A fraction of CtrA-depleted bacteria (10.9 %) were longer than 2.75 µm while only 1.6% of WT bacteria and 1.3 % of the depletion strain grown with IPTG exceeded this size ($p < 0.05$ in pairwise comparisons according to Scheffe analysis). A highly significant proportion of CtrA-depleted bacteria (6.3%) had a mislocalized constriction compared to the WT strain (0.88%) and to the CtrA depletion strain grown with IPTG (1.33%) (Fig 2-A) ($p < 0.01$ in pairwise comparisons according to Scheffe analysis). Seven hours after IPTG was removed from the culture, we observed bacteria that grew to form multiple branches while others generated small "chains" (Fig 2-A). If the incubation in a CtrA-depleted state is prolonged (15 h), bacteria kept on branching. These results suggest that in the absence of CtrA, bacterial elongation is maintained but division is highly perturbed: it is either abolished (there are no visible constriction sites in branching bacteria) or division is initiated at various positions but it is often not completed since bacteria form chains.

In *C. crescentus*, an important function of CtrA is to control replication by binding to the chromosomal replication origin (*oriC*) [19]. *In vitro*, *B. abortus* CtrA does not bind to the replication origin of chromosome I (*oriI*) [21] but a CtrA binding site is predicted in the promoter of *repAB*, which is thought to control the segregation of chromosome II origins (*oriII*). In order to detect a possible effect of CtrA on chromosomes replication, we analysed the DNA content of the CtrA depletion strain, 7 hours post-IPTG removal. At this time point, bacteria accumulated several copies of their genome (Fig 2-C). This indicates that CtrA depletion does not impair the chromosomes replication. It also indicates that inhibition of cell division does not prevent the initiation of a new round of chromosomes replication, nor cell elongation as a matter of fact. These data suggest that

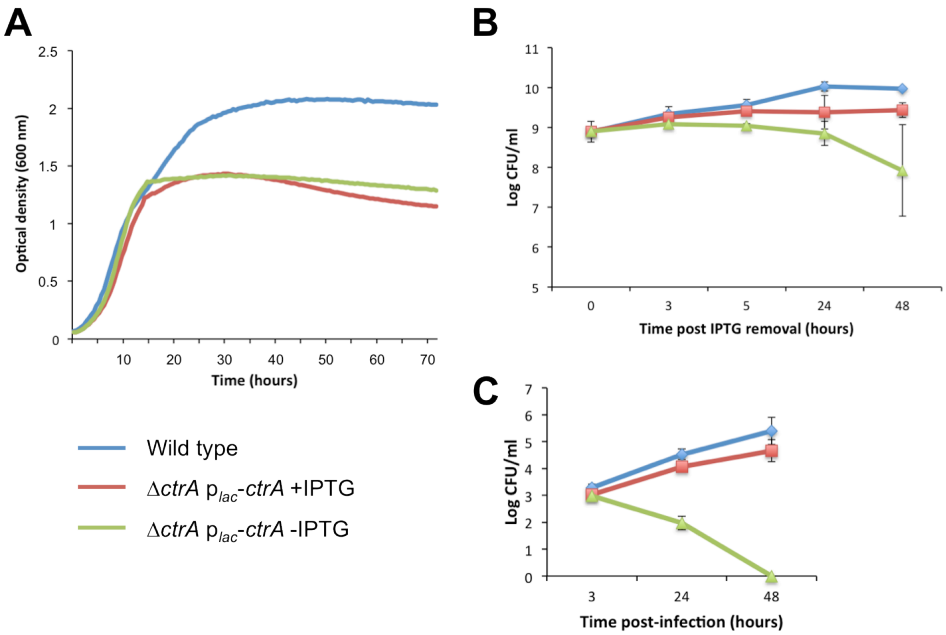

Fig 3. Growth curve and viability of the CtrA depletion strain in rich medium and infection. (A) OD_{600} measurements of the wild type and CtrA depletion strain (Δ*ctrA* p_{lac}-*ctrA)* cultivated with or without IPTG (+IPTG or –IPTG, respectively). (B) CFU count of the same strains in rich medium and (C) during a HeLa cell infection over a 48 h period of time.

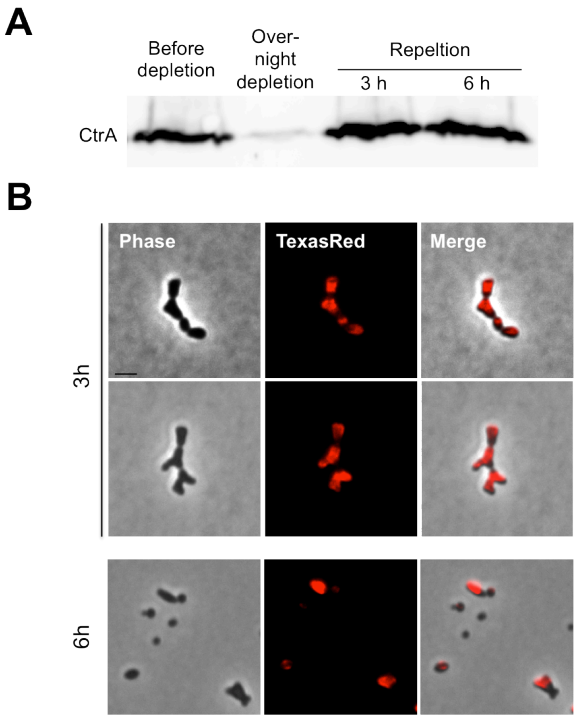

Fig 4. Characterization of *B. abortus* morphology after an overnight CtrA depletion followed by a repletion of 3 h and 6 h. (A) A CtrA Western blot showing the protein level after the depletion and after the addition of IPTG. (B) Fluorescence images of bacteria depleted of CtrA for one night, labelled with TRSE and grown for 3 and 6 h in IPTG-supplemented medium. The scale bar corresponds to 2 µm.

there is no checkpoint at division coordinating the event of daughter cell separation with cell elongation and initiation of chromosome replication. Alternatively, this checkpoint could exist but it would be altered in the absence of CtrA.

We next characterized growth and viability of the CtrA depletion strain. In the presence of IPTG, this strain grew but reached a plateau earlier than the WT (Fig 3-A). This profile was very similar for the culture in the absence of IPTG (Fig 3-A), but in this case bacterial morphology is very different (Fig 2-B). The viability of the CtrA depletion strain in rich culture medium was assessed by counting the number of colony forming units (CFU) (Fig 3-B). In the presence of IPTG, a stable number of CFU was reached earlier than the WT control, and the plateau was lower (Fig 3-B). In the absence of IPTG, the number of CFU did not increase, and remained constant for 24 h before dropping between 24 and 48 h. The high variability of CFU numbers harvested on IPTG-supplemented plates after 48 h of depletion could be due to a high variability in the capacity of branched bacteria to divide and release viable bacteria. These data suggest that CtrA is essential for *B. abortus* growth and long-term survival in rich medium.

To test the reversibility of the CtrA depletion on cell division, the CtrA depletion strain was grown overnight without IPTG, labelled with TRSE and inoculated in fresh medium supplemented with IPTG. A CtrA Western blot shows the accumulation of the transcription factor in bacteria grown in IPTG-supplemented medium (Fig 4-A). After 3 h of repletion, several unlabelled constriction sites were visible (Fig 4-B). Six hours after IPTG was added to the medium, several division events were completed as shown by the release of unlabelled or partially labelled bacteria (Fig 4-B). Those bacteria were of different size and shapes, demonstrating that the septa were formed at ectopic sites. These results further confirm that CtrA is essential for division in *B. abortus,* and that CtrA depletion effect is reversible for the generation of cell division events, but not for their correct positioning in the cell. It also indicates that large branching bacteria generated in the absence of IPTG are not dead, at least after an overnight depletion of CtrA.

CtrA is required for *B. abortus* survival in HeLa cells

To assess the role of CtrA during infection, the depletion strain was used to infect HeLa cells. Bacteria were incubated with HeLa cells for one hour with IPTG. Cells were then

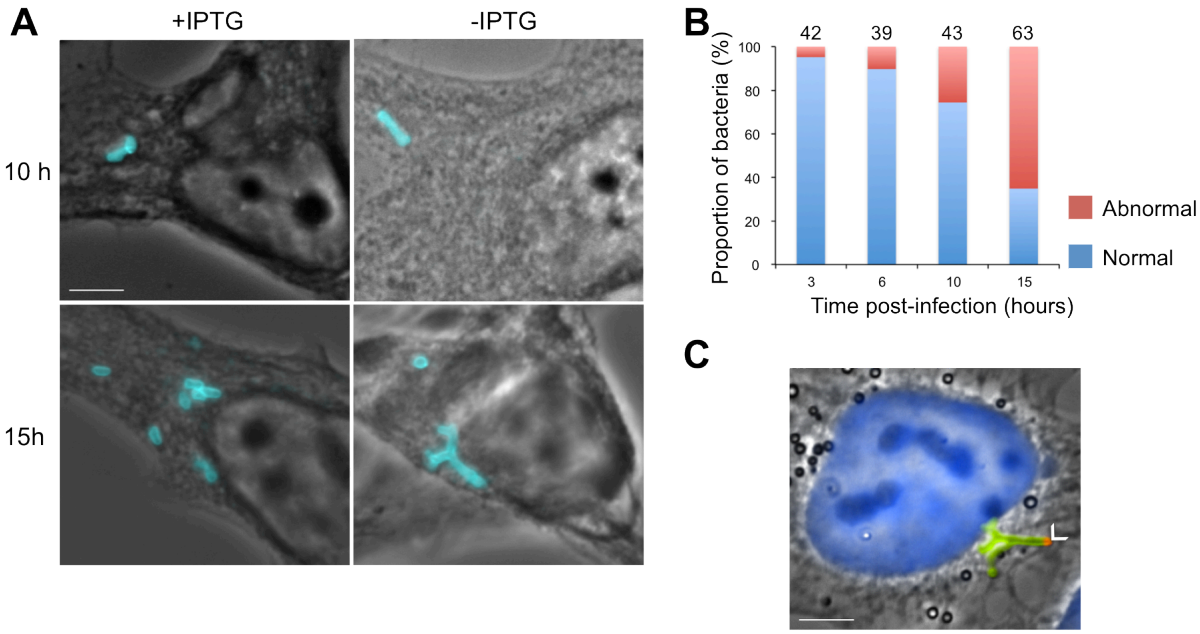

Fig 5. Characterization of the CtrA depletion strain morphology during infection. (A) Immunofluorescence microscopy of HeLa cells infected for 10 and 15 h with the depletion strain in presence or absence of IPTG. Phase contrast images were merged with anti-*Brucella* staining (cyan) to detect intracellular bacteria. The scale bar corresponds to 5 µm. (B) Quantification of bacteria with aberrant morphologies between 3 and 15 h post-infection. (C) Typical image of an abnormal morphology generated by the CtrA depletion strain 15 h post-infection in HeLa cells, with bacteria labelled with TRSE before infection. The TRSE-labelled pole corresponds to the old pole of the initial bacterium that invaded the host cell (white arrow head). DAPI (staining the nucleus in blue), anti-*Brucella* (green) and Texas Red are merged.

washed and gentamycin was added to kill extracellular bacteria. The CtrA depletion strain was able to infect HeLa cells and to replicate intracellularly almost to the same extent as the WT when IPTG was kept in the medium (Fig 3-C). When IPTG was removed after the initial hour of internalization, a similar number of CFU was recovered 3 h PI, and then the CFU counts dropped dramatically and went below the sensitivity threshold 48 h PI. We checked that the presence of Triton X-100, used for the extraction from host cells, did not decrease the CFU counts for the CtrA depletion strain in the absence of IPTG (data not shown). Altogether, these data suggest that CtrA is crucial for *B. abortus* viability during HeLa cells infection.

Similarly to the rich medium condition, we analysed the morphology of the CtrA depletion strain during infection. As expected, this strain had a WT morphology when IPTG was kept in the medium and showed several rounds of division 15 h PI (Fig 5-A). When IPTG was removed from the medium, bacteria with aberrant morphologies appeared around 10h PI and started to accumulate at 15 h PI (Fig 5-A-B). At 10 h PI, abnormal morphologies mainly consisted of elongated bacteria, as observed 3 h post-IPTG removal in rich culture medium while at 15 h PI, branched bacteria were observed (Fig 5-A). The intracellular branched morphologies are strikingly similar to those observed after a long depletion in culture (Fig 2). If bacteria are labelled with TRSE prior to infection, they also display a Texas Red fluorescence at the base of the branched morphology 15 h PI (Fig 5-C; white arrow head). The emergence of abnormal morphologies coincides with the time at which WT bacteria resume their growth during their intracellular trafficking [11]. This suggests that CtrA is not crucial to control the timing of the intracellular growth recovery.

We also investigated the intracellular trafficking of the CtrA depletion strain by monitoring the co-localization of bacteria with Lamp1 marker. As a first control, we infected HeLa cells with the WT strain known to reside in Lamp1+ compartments at early hours PI and to leave these compartments when proliferation starts [25]. As a second control, we used a Δ*virB* strain known to stay in Lamp1+ compartments for up to 12 h PI [8,26]. Our results showed indeed a low proportion of Lamp1+ vacuoles at 10 and 15 h PI (26 and 13% respectively) for the WT strain compared to Δ*virB* (66% at both times PI) (Fig 6-A-B). The CtrA depletion strain supplemented with IPTG had a similar proportion of Lamp1+ vacuoles compared to the WT (Fig 6-A), suggesting that

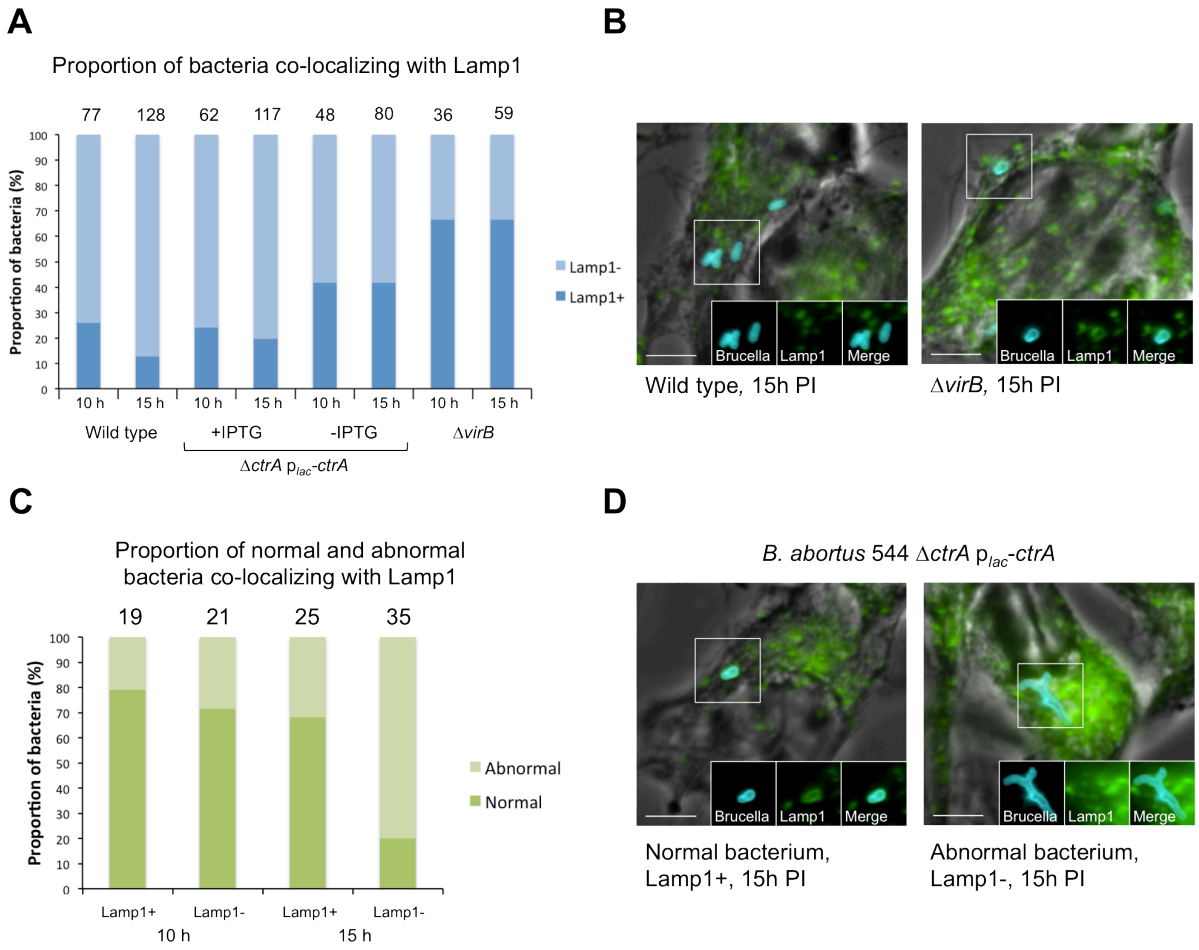

Fig 6. Characterization of the CtrA depletion strain intracellular trafficking. (A) Histogram showing the proportion of bacteria in Lamp1+ and Lamp1- compartments in a wild type, Δ*virB* and the depletion strain with and without IPTG. (B) Representative immunofluorescence images of the wild type and Δ*virB* controls (known to remain associated to the Lamp1 marker 15 h PI). The bacteria are labelled in cyan, and Lamp1 in green. At 15 h PI, most of the wild type bacteria do not co-localize with Lamp1, while Δ*virB* bacteria are observed in Lamp1+ compartments. (C) Histogram showing the proportion of bacteria with normal and abnormal morphologies co-localizing with the Lamp1 marker. (D) Representative immunofluorescence images of bacteria with normal (left panel) and abnormal (right panel) morphology of the CtrA depletion strain in the absence of IPTG.

its intracellular trafficking is comparable to the WT. The same strain depleted in CtrA had an intermediate phenotype between the WT and Δ*virB* strains, with 40% of bacteria still in Lamp1+ compartments at 10 and 15 h PI (Fig 6-A), suggesting an alteration of the intracellular trafficking in the absence of CtrA. Despite the apparent "stability" of the CtrA depleted strain localization between 10 and 15 h PI, the analysis of the morphology of bacteria associated or not with the Lamp1 marker revealed the presence of at least two localization patterns. Indeed, bacteria with an abnormal morphology were mostly located in Lamp1- compartments at 15 h PI (Fig 6-C-D). On the contrary, bacteria with a normal morphology remained in Lamp1+ compartments. Since bacteria with an abnormal branched morphology are those that have resumed their elongation (Fig 6-D), the strong correlation between the presence of Lamp1 and cell shape suggests that trafficking and elongation of individual bacteria are synchronous.

Investigating the CtrA regulon by ChIP-seq

A chromatin immunoprecipitation followed by deep sequencing (ChIP-seq) was performed to map CtrA binding sites on *B. abortus* genome. From this analysis, 105 CtrA binding regions were selected (S4 Table). Their distribution on the two chromosomes was heterogenous (S2 Fig). Of these regions, 71% had a predicted 9-mer or 8-mer consensus binding site with 0, 1 or 2 mismatches, and 97% map to intergenic regions. Among the CtrA-bound sequences with no predicted 9-mer or 8-mer box, 57% had at least one "TTAA(C)" half site. CtrA bound sequences upstream of genes involved in the CtrA phosphorylation pathway (*divJ, divK, chpT* and *ctrA*), as well as *ccrM*, a gene coding for an essential DNA methyltransferase [27], and genes coding for proteins known to be involved in CtrA proteolysis in *C. crescentus* (*cpdR, rcdA* and *clpX*) (S4 Table). CtrA also bound regions upstream of several operons, such as the *mraW* operon involved in peptidoglycan (PG) synthesis, the *minCD* operon involved in division [17], the *repAB* operon coding for the chromosome II segregation machinery and the *tolQ* operon known to be important for membrane homeostasis and division in *E. coli* [28,29]. Furthermore, CtrA bound intergenic regions upstream of many genes coding for outer-membrane proteins (OMP) such as *omp2b, omp25, omp16, omp19* and *bamA* (also called *omp89* or *omp1*) [30-32]. Finally, a CtrA binding site was located upstream of *lptA*, coding for a homolog of a component of the machinery involved in LPS translocation to the outer membrane [33].

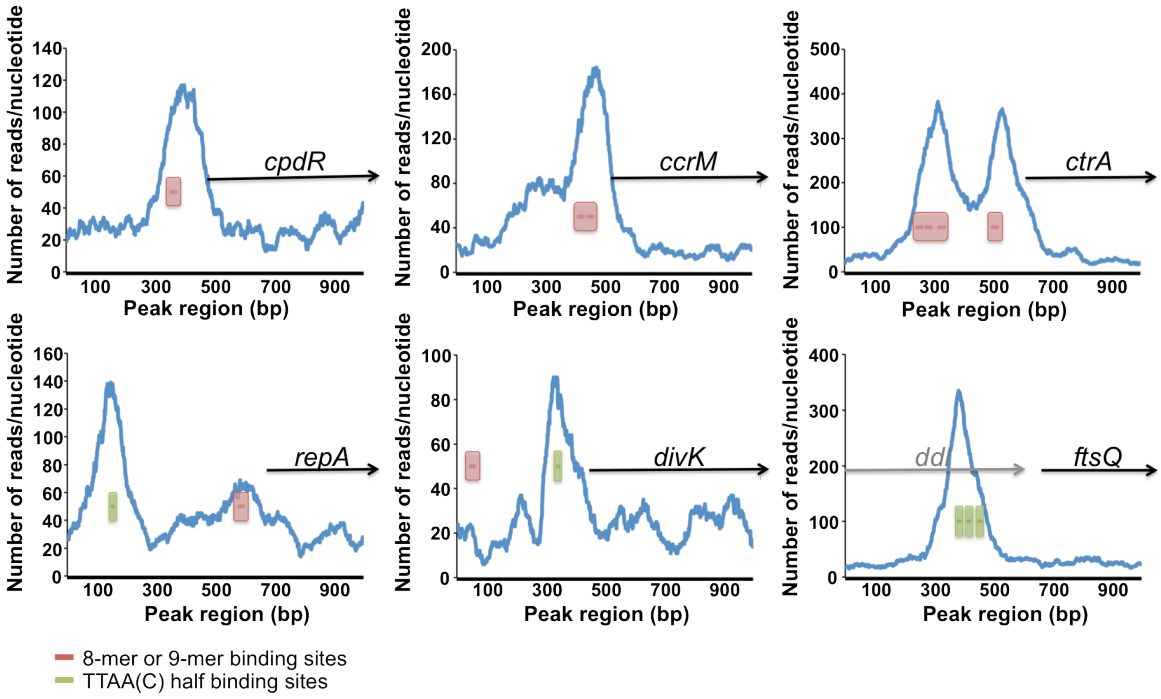

Fig 7. *In vivo* CtrA binding sites detected by ChIP-seq. The number of reads per nucleotide is plotted for 6 promoter regions enriched by CtrA pull-down. Red bars surrounded by red rectangles represent predicted 8-mer and 9-mer binding sites. Green bars surrounded by green rectangles represent TTAA(C) half binding sites. Arrows under gene names represents the start of the coding sequences.

CtrA binding pattern to DNA showed a single peak coinciding with a predicted binding site upstream of *cpdR* (BAB2_0042) and *ccrM* (BAB1_0516) (Fig 7). CtrA binding upstream of its own promoter showed two peaks of equal size overlapping multiple consensus sequences (Fig 7). These peaks corresponded to the regions protected from DNase I digestion by purified phosphorylated CtrA in an *in vitro* assay [21]. It should be noted that this intergenic region bound by CtrA could also serve to regulate the expression of another gene (BAB1_1615), which has an opposite orientation to *ctrA* (BAB1_1614). Similarly, CtrA binding between BAB2_1162 and *repA* (BAB2_1163) had a double peaks pattern, but the peaks were of unequal size, and the apparently strongest binding site contains a half site TTAAC (Fig 7). Some other CtrA binding patterns to DNA were less expected. For instance, CtrA bound a region upstream of *divK* (BAB2_0628) at the level of a TTAAC half site despite the presence of a 9-mer box around 300 base pairs upstream the actual binding site (Fig 7). Also CtrA bound a region inside the *ddl* open reading frame (BAB1_1447), which is in operon with *ftsQ, ftsA* and *ftsZ*. Interestingly, this binding site overlaps three TTAAC half sites. A similar binding profile was observed in *C. crescentus*, where CtrA also bound a sequence within the *ddl* gene upstream of the *ftsQA* operon [18].

In summary, CtrA binds to regulatory regions upstream of genes involved in growth (PG synthesis and insertion of LPS into the envelope via *lptA* gene), envelope homeostasis and cell cycle itself (division, chromosome replication) and its control. Genes involved in envelope biogenesis/homeostasis and those associated to cell cycle regulation are highly significantly ($p < 0.001$ in a χ^2 analysis) enriched among CtrA targets, as they constitute 33.3% and 11.5% of CtrA regulon respectively compared to 3.3% and 2.6% of the whole genome of *B. abortus*.

As CtrA binding to a given promoter does not necessarily modulate the transcription level of the downstream gene in all conditions, in order to understand the behaviour of CtrA, the CtrA depletion strain was used to perform RT-qPCR on selected target genes identified by ChIP-seq. A mRNA fraction was extracted (*i*) from the CtrA depletion strain grown to mid-exponential phase in the presence of IPTG and (*ii*) from the same strain grown without IPTG for 4h. Genes were selected from five different functional categories: envelope synthesis (PG and LPS), division, cell cycle control, OMP,

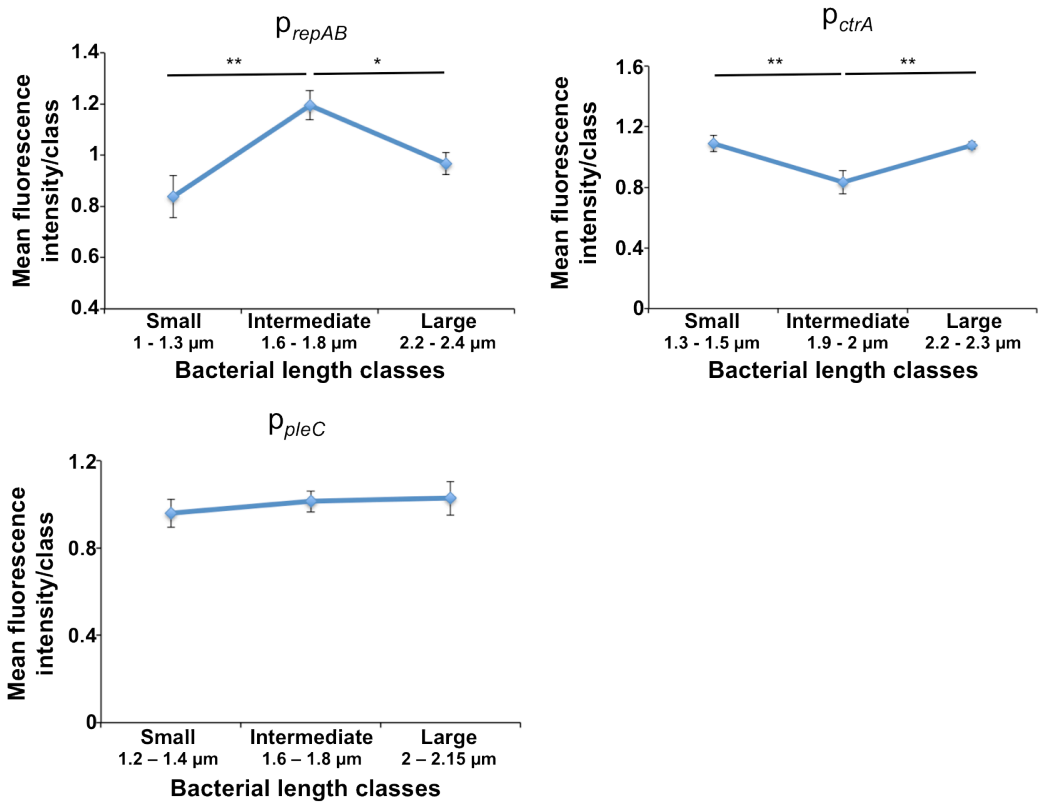

Fig 8. Activity profile of *repAB, ctrA, ccrM* and *pleC* promoters according to cell length. Normalized mean fluorescence intensity is represented as a function of the bacterial length classes, as determined by a MicrobeTracker analysis of 700 to 2000 bacteria per sample in three biological replicates (Sliusarenko et al., 2011). These classes were defined according to the fluorescence profile shown in Figure S4. Error bars represent the standard deviation (n = 3 biological replicates) to the average fluorescence intensity of each class. The significant pairwise comparisons are indicated by * ($p < 0.05$) and ** ($p < 0.01$).

chromosome replication and segregation (S3 Fig). RT-qPCR results showed that the expression level of genes involved in the synthesis of the envelope (*lptA* and *murD*) remained unchanged in the absence of CtrA compared to the control condition (culture supplemented with IPTG) while the *minCD* operon involved in Z-ring positioning was overexpressed in the absence of CtrA, as also found in *S. meliloti* [34]. These results are in agreement with the phenotype of the CtrA depletion strain, since in the absence of CtrA, elongation is maintained but division is prevented (Fig 2-B). The *bamA* and *omp19* genes were significantly downregulated ($p < 0.05$ in a Student *t* test) while *omp16* and *repAB* operon expression level was not changed in the absence of CtrA. Analysing the expression level of genes involved in the phosphorylation pathway upstream of CtrA suggested that CtrA might exert several feedback loops on its own phosphorylation and proteolysis. Indeed, in the CtrA-depleted culture *divK* and *cpdR* were downregulated ($p < 0.01$ in a Student *t* test). Finally, *ccrM* expression level did not change in absence of CtrA.

The activity of CtrA target promoters varies in function of bacterial cell size

RT-qPCR data suggest *repAB* and *ccrM* expression levels do not vary in the absence of CtrA. However, mRNA levels are measured at the level of the whole population, and despite the apparent stability in the expression of these CtrA target genes in the CtrA depletion strain, they could still be regulated in a cell cycle-dependent manner. To test this hypothesis, a reporter system was designed to monitor the activity of *ccrM* (p_{ccrM}), *repAB* (p_{repAB}), *ctrA* (p_{ctrA}) and *pleC* (p_{pleC}) promoters by fusing each of them to a gene coding for an unstable GFP (GFP-ASV) [35] on a medium-copy replicative vector [36]. The *ccrM* and *ctrA* transcription follows a tightly regulated profile throughout *C. crescentus* cell cycle while PleC protein amount remains stable [16,37,38]. Fluorescence intensity of the *B. abortus* reporter strains was measured in three independent experiments (S4 Fig) and mean fluorescence intensity was plotted against bacterial cell size, since until now *B. abortus* is not synchronizable (Fig 8). The p_{ctrA} and p_{repAB} activities have opposite profiles as maximal fluorescence intensity was measured in intermediate bacteria for p_{repAB} and in small and large bacteria for p_{ctrA} reporters. These data suggest that p_{ctrA} activity is maximal in large dividing bacteria, and this activity decreases after division (Fig 8). The maximal activity of p_{ctrA} in large bacteria is consistent with cell division defect in the CtrA depletion strain. On the contrary, p_{repAB} seems to be turned on early in the cell cycle, leading to an accumulation of GFP-ASV in

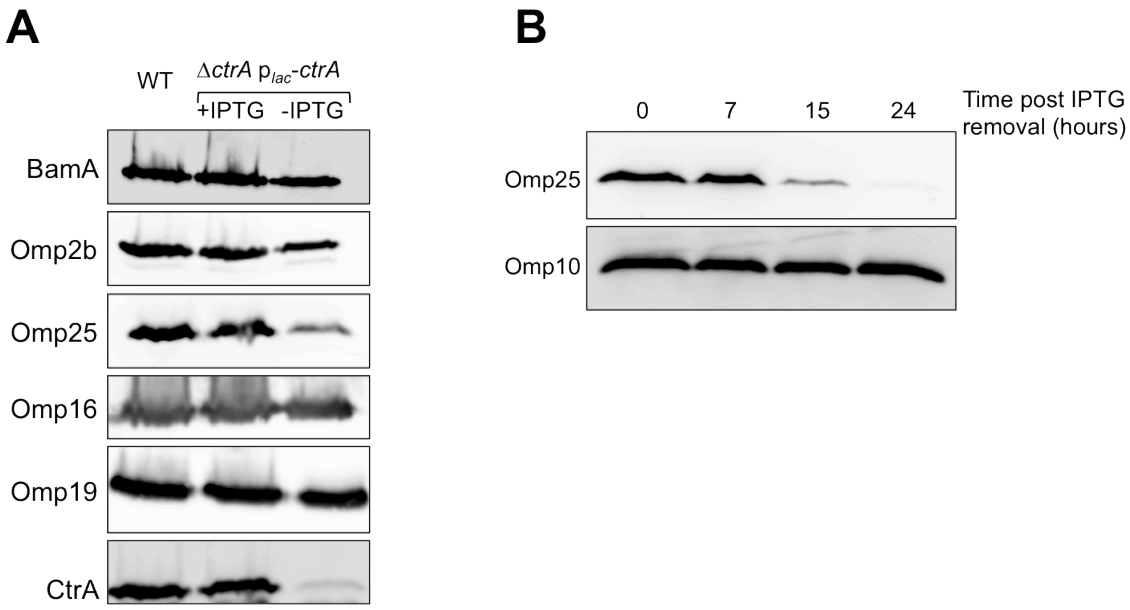

Fig 9. Western blots using monoclonal antibodies against *B. abortus* OMPs. (A) Western blots on *B. abortus* lysates of the wild type (WT) strain and the CtrA depletion strain grown with or without IPTG for one night, using monoclonal antibodies recognizing OMPs whose genes were identified by ChIP-seq as being potentially regulated by CtrA. (B) Western blots on lysates of the CtrA depletion strain grown without IPTG for 0, 7, 15 and 24 h, using anti-Omp25 antibodies. Omp10 was detected by Western blot as a loading control.

intermediate bacteria (Fig 8). These data correlate with the initiation of replication of chromosome II at about half of the cell cycle of *B. abortus* [11]. The p_{ccrM} activity profile is similar to p_{ctrA} (S4 Fig); differences between bacterial length classes are however not significant (data not shown), probably due to the high variability in the fluorescence intensity from one experiment to another (S4 Fig). The p_{pleC} did not show any significant variation in its activity according to bacterial cell size (Fig 8), which is consistent with the constant PleC amount in *C. crescentus* and the absence of CtrA binding in its promoter, at least in the conditions tested here. All together, these data suggest that two promoters bound by CtrA *in vivo* are differentially regulated during *B. abortus* cell cycle.

CtrA depletion affects OMP amounts

One surprising feature of the CtrA regulon, according to ChIP-seq data (S4 Table), is the high proportion of direct targets corresponding to genes encoding outer membrane components, particularly outer membrane proteins (OMPs). In order to reveal a possible impact of CtrA depletion on the abundance of some of these OMPs, Omp2b of the group 2 porins, Omp16 and Omp19 lipoproteins, Omp25 of group 3 OMP and BamA of the minor group 1 OMP were detected by Western blot on a *B. abortus* wild type strain, on the CtrA depletion strain cultivated with IPTG and on the same strain depleted in CtrA overnight. According to ChIP-seq data, CtrA bound the promoter region of genes encoding Omp2b, Omp25, Omp16, Omp19 and BamA and RT-qPCR showed a significant decrease ($p < 0.05$ in a Student t test) in *bamA* and *omp19* mRNA levels (S3 Fig). While the amount of Omp16 and Omp19 did not change in the absence of CtrA, a slight decrease in the amount of Omp2b and BamA was observed (Fig 9-A). Omp25 abundance was decreased in the absence of CtrA, and almost disappeared at longer depletion times (Fig 9-B). Given that OMPs of group 2 and 3 are the major OMPs in *Brucella* envelope [40], their reduced abundance in the absence of CtrA could lead to the perturbation of the envelope, which could have dramatic consequences for the bacterium when it is inside host cells (Fig 3-C).

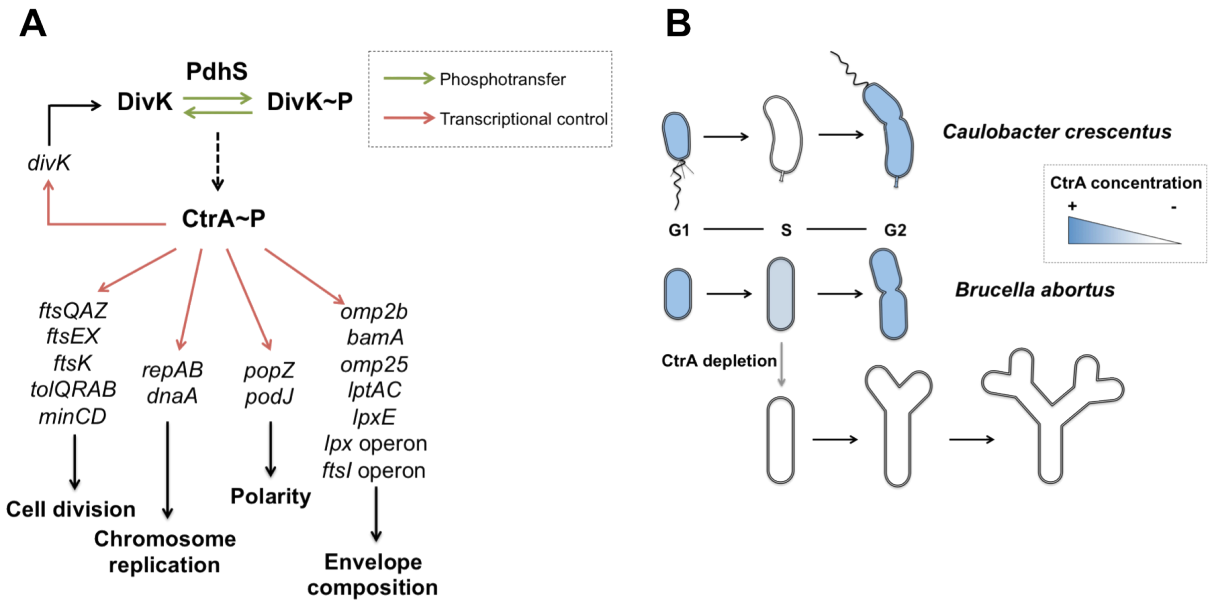

Fig 10. Model for the PdhS-DivK-CtrA phosphorelay and CtrA regulon (A) and for CtrA oscillation during *B. abortus* cell cycle (B). (A) DivK phosphorylation status is regulated by the histidine kinase PdhS. This two-component system regulates CtrA phosphorylation indirectly (dotted arrow) through the CckA-ChpT phosphorelay. As suggested by the ChIP-seq data, CtrA could regulate division, chromosome replication, polarity and envelope composition in *B. abortus*. Green arrows represent phosphorylation or dephosphorylation; red arrows represent transcriptional regulation (B) In *Caulobacter crescentus*, CtrA protein amount is known to oscillate during cell cycle; it is degraded during the differentiation of the flagellated cell into a stalked cell and is resynthesized during S phase and accumulates in predivisional cells. In *B. abortus*, the activity profile of *ctrA* promoter suggests CtrA amount could also be cell cycle regulated. The branched phenotype of CtrA-depleted bacteria further suggests it is present in predivional cells where it is required for septation. Different shades of blue represent varying concentrations of CtrA. White bacteria are cleared of CtrA.

Discussion

The DivK-CtrA regulation network controls cell cycle progression and polar morphogenesis in the model bacterium *C. crescentus* and in the plant symbiont *S. meliloti*. The conservation of this network in *Alphaproteobacteria* could suggest that its function remained unchanged along evolution. However, previous observations made on the pathogen *B. abortus* revealed that this regulation network has been adapted at least at two levels [13]. First, at the top of the cascade, the phosphorylation of DivK is controlled by the essential kinase PdhS, an atypical member of the PleC and DivJ family of HK that control DivK phosphorylation in *C. crescentus*. *B. abortus* PdhS being able to phosphorylate and dephosphorylate DivK *in vitro* (Fig 1 and 10-A), this suggests that PdhS could be sufficient to control DivK phosphorylation level *in vivo*, and would explain why *pleC* and *divJ* genes are not essential in *B. abortus* [22] while *pdhS* and *divK* are essential [23]. Second, at the bottom of the DivK-CtrA cascade the abundance and the phosphorylation of CtrA allows the control of target genes, among which some were proposed to be distinct from those described in *C. crescentus* [21]. For example, the *minCD* operon, participating in the positioning of the Z ring at the time of division, is a target of CtrA in *B. abortus* but this operon is absent in *C. crescentus* [17,21]. In *S. meliloti*, CtrA also represses the expression of the *min* operon [34]. Here we report that, on top of being essential for division as it was described for *C. crescentus* CtrA, *B. abortus* CtrA could be crucial for controlling envelope composition as exemplified by the regulation of *omp25* gene (Fig 9 and 10-A).

As implied earlier by the conservation of the DivK-CtrA pathway, alteration of PdhS amount results in a modification of CtrA abundance and phosphorylation (Fig 1-E), suggesting that the whole DivK-CtrA pathway is functional in *B. abortus*. Reconstitution of the CckA-ChpT-CpdR and CckA-ChpT-CtrA phosphorelays *in vitro*, and the analysis of *chpT, cpdR* and *ctrA* conditional mutants, already demonstrated that this part of the pathway is conserved in *B. abortus* [15]; indeed it controls phosphorylation and proteolysis of CtrA. Further work is needed to identify the role of DivL in the DivK-CtrA pathway, and to identify the signals sensed by PdhS and the other possible sensors of this pathway.

Here we report that depletion of CtrA results in an inhibition of cell division (Fig 2-A and 10-B), explaining why it was not possible to delete the *ctrA* gene in *B. abortus* [15,21]. The inhibition of cell division results in branched morphology and in small chains, the latter being probably produced by incomplete cell division. It is noteworthy that induction of *ctrA* expression after depletion results in the reactivation of cell division (Fig 4). Perturbation of division in the CtrA-depleted condition is likely explained by the presence in the CtrA predicted regulon of numerous genes and operons involved in division. Indeed, the *minCD* operon is involved in Z ring placement, and many genes and operons proposed to be involved in the cell division process, like *ftsQAZ*, *ftsEX*, *ftsI*, *ftsW*, *ftsK* and the *pal(omp16)-tolQRAB* locus are detected as possible direct targets of CtrA in *B. abortus* (S4 Table). The deregulation of only a fraction of these genes is probably sufficient to block the whole cell division process.

In HeLa cells, abnormal morphologies of the CtrA depletion strain appeared around 10 h PI (Fig 5-B), mainly consisting of elongated cells resembling bacteria 3 h post-IPTG removal in rich culture medium (Fig 5A). At 15 h PI, branched bacteria were observed, similarly to the 7 h depletion in culture. *B. abortus* was shown to resume its intracellular growth around 8 h PI in HeLa cells [11]. Such a correlation between cell growth resumption at 8 h PI and emergence of abnormal morphologies at 10 h PI suggest that CtrA might have been cleared from bacteria earlier during the trafficking but effects of this depletion on morphology are visible only after bacteria have restarted their growth. This observation also suggests that the absence of CtrA does not impair the growth arrest during the first 8 h PI, or the restart of growth during infection. Another correlation was made between bacterial growth and localization in Lamp1+ compartments. Earlier work showed that *B. abortus* growth is resumed in Lamp1+ compartments and that daughter cells are found almost exclusively in Lamp1- compartment [11]. Here we showed that CtrA-depleted *B. abortus* had a delay in its intracellular trafficking at 10 and 15 h PI, given the high proportion of bacteria still in Lamp1+ compartments (Fig 6-A). However, most unexpectedly, bacteria located in Lamp1- compartments at 15 h PI were in majority branched while most bacteria with a normal morphology were in Lamp1+ BCV. One possible way to interpret these observations would be that the ability to elongate is required for the bacterium to progress in its intracellular trafficking. The dramatic drop of the CFU counts at 48 h PI (Fig 3-C) suggests that the branched bacteria are unable to restore viable progeny when

plated on IPTG-supplemented medium. These branched bacteria could be redirected towards degrading compartments. Concerning bacteria with a normal morphology located in Lamp1+ BCV at 15 h PI, they could be blocked for their intracellular trafficking, and eventually destroyed later in phagolysosomes as well. There is currently no explanation for these two distinct phenotypes. One possibility could be that CtrA depletion is effective when bacteria reach different stages of their intracellular trafficking, yielding two different kinds of morphologies. Another possibility could be that the generation of distinct morphologies is the indirect consequence of the heterogeneity of the composition of the BCV along trafficking. The generation of non-growing bacteria intracellularly is interesting because it could be linked to persistence of bacteria inside the host, as it was proposed for *Salmonella* [41].

Among the direct targets of CtrA found in the conditions tested here, cell cycle-related genes are not restricted to division. Indeed, genes linked to replication (*dnaA*, *repAB* and *ccrM*), the DivK-CtrA regulation network (*divJ*, *mopJ*, *divK*, *chpT*, *sciP*, *rcdA* and *ctrA* itself) and the recruitment of proteins to the poles (*popZ*) have also their promoter enriched by ChIP-seq. Besides cell cycle-related genes, one obvious conclusion of the ChIP-seq experiment reported here is the high proportion of genes involved in envelope biogenesis or homeostasis. Indeed, CtrA predicted regulon is enriched in genes coding for LPS biosynthesis and export (e.g. *lptAC*, *lptFGD*, *lpxD-fabZ-lpxAB* and *lpxE*), peptidoglycan synthesis (e.g. *ftsI-murEF-mraY-murD*), outer membrane proteins (e.g. *omp2b*, *omp19* and *omp25*, also called *omp3a* in *B. abortus*) and outer membrane proteins export (*bamA*, also called *omp89* or *omp1* in *Brucella*) (Fig 10-A). The presence of CtrA is crucial for the production of normal amounts of Omp25 (Fig 9). Interestingly, the two-component system BvrRS also controls the expression of *omp25* [42]. A *B. abortus* deletion strain for *omp25* was attenuated in cattle [43]. More recent data suggested that this attenuation could be explained by a higher internalization and a higher intracellular killing of the Δ*omp3a* mutant compared to the wild type strain [44]. The exact role of the highly abundant Omp25 is still unknown; it was shown to inhibit TNFα production in human macrophages [45] and it could be involved in defining the properties of the outer membrane by interacting with the LPS [46]. Interestingly, in *S. meliloti*, CtrA binds to the promoter of *ropB* gene [34], encoding an Omp25 homolog involved in outer membrane stability in *Rhizobium leguminosarum* [47]. It is thus possible that in *Rhizobiales*, CtrA controls factors involved in outer membrane

biogenesis or homeostasis. Their control by CtrA would have been acquired after the divergence from the common ancestor with *C. crescentus*, since CtrA regulon is not particularly enriched in genes involved in outer membrane biogenesis or homeostasis [18,48]. Finally, the outer membrane properties of *B. abortus* are a crucial determinant of its virulence [49], and the proposed control of outer membrane composition by CtrA correlates with the strong attenuation of the CtrA depletion strain in HeLa cells. Further work is needed to better characterize the molecular mechanisms linking cell cycle control and virulence.

The GFP-based reporter system results hint towards a "*Caulobacter*-like" oscillation profile of CtrA along *B. abortus* cell cycle (Fig 8 and 10-B). Combined with the branching phenotype of the CtrA-depletion strain, we propose that CtrA presence in predivisional cells is crucial for septation.

Combining data obtained for several members of the *Alphaproteobacteria* class shows how a single phosphorylation cascade and a single transcription factor were conserved but adapted to diverse lifestyles during evolution. While PdhS is essential in *B. abortus*, CbrA, its homologue in the plant symbiont *S. meliloti*, is not [50]. Instead PleC is crucial for *S. meliloti* viability [51]. In *S. meliloti*, *cbrA* and *divJ* deletions are co-lethal [14]. Actually, CbrA and DivJ have redundant activities, both of them being kinases for DivK while PleC is the only known phosphatase for DivK [14]. Like in *C. crescentus*, the way DivK phosphorylation is regulated at the top of the cascade could impact CtrA activity and subsequently the expression level of target genes in *Rhizobiales*. It is indeed interesting to compare CtrA role in *B. abortus* pathogenesis to its role in *S. meliloti* symbiosis in plants. Data presented here suggest CtrA presence is crucial for *B. abortus* to accomplish a successful infection of host cells. On the contrary, CtrA has to be cleared from *S. meliloti* cells in order for them to differentiate into nitrogen-fixing bacteroids inside host plants [14]. Comparative analysis of several *Alphaproteobacteria* with distinct lifestyles will help us to understand how natural selection shaped the conserved DivK-CtrA pathway along evolution.

Material and methods

Bacterial strains

E. coli strains DH10B, BL21 (DE3) and DB3.1 were grown in Luria-Bertani (LB) medium at 37°C. Derivatives of the *Brucella abortus* 544 Nal^R strain were cultivated in 2YT rich medium (1% yeast extract, 1.6% peptone, 0.5% NaCl) at 37°C. Antibiotic concentrations are the following: ampicillin, 100µg/ml; kanamycin, 20 or 50 µg/ml; chloramphenicol, 20 µg/ml; nalidixic acid, 25 µg/ml; rifampicin, 20 µg/ml; gentamycin, 50 µg/ml.

Cloning of the pBBR-MCS1-p_{lacI}-*lacI*-p_{lac}-*ctrA*. The p_{lacI}-*lacI*-p_{lac} sequence was amplified from the pSRK-Kan vector using Phusion High-Fidelity DNA Polymerase (New England BioLabs) and *Sac*I-Kan3' and p_{lac}-R1 primers (See S2 Table). The *ctrA* coding sequence was amplified from *B. abortus* 544 purified genomic DNA using *ctrA*-F2 and *Kpn*I-*ctrA*-R2 primers. The PCR product was fused to the p_{lacI}-*lacI*-p_{lac} sequence by joining PCR. The p_{lacI}-*lacI*-p_{lac}-*ctrA* insert was then cloned in the pBBRMCS1 using *Sac*I and *Kpn*I restriction enzymes. By using these enzymes, the insert was cloned in the opposite orientation to the p_{lac} promoter of the pBBRMCS1.

The *ctrA* deletion. The *ctrA* gene was deleted from *B. abortus* 544 chromosome by allelic replacement. A 750 base pair (bp)-region upstream and another one downstream of *ctrA* were amplified by PCR using *Pst*I-Up-*ctrA*-F/Up-*ctrA*-R and Down-*ctrA*-F/*Sal*I-Down-*ctrA*-R pairs of primers respectively and both PCR products were fused together by joining PCR. The PCR product was first cloned in pGEMT digested with *Eco*RV, generating blunt ends, and sequenced. A *Pst*I-*Kpn*I restriction allowed the cloning of the insert in the pNPTS 138 vector (M. R. K. Alley, Imperial College of Science, London, UK) carrying a kanamycin resistance cassette and a sucrose sensitivity cassette.

Cloning of expression vectors. DNA sequences coding for the full version of the proteins of interest were amplified by PCR and *attB1* and *attB2* sequences were added upstream and downstream the coding sequences. A complete list of the used primers is detailed in S2 Table. A BP reaction was performed by incubating 4 µl of purified PCR product with 150 ng of pDONR vector at 18°C overnight. LR reaction was performed by incubating 150 ng of insert-pDONR vector with 150 ng of pML310 expression vector at 18°C overnight.

Cloning of reporter vectors. Promoter regions were amplified from *B. abortus* 544 purified genomic DNA using Phusion High-Fidelity DNA Polymerase and fused by joining

PCR to *gfp*(ASV). The pairs of primers used to amplify the promoter regions are *Xba*I-p_{ctrA}-F1/p_{ctrA}-R1, *Xba*I-p_{repAB}-F1/p_{repAB}-R1, *Xba*I-p_{ccrM}-F1/p_{ccrM}-R1 and *Xba*I-p_{pleC}-F1/p_{pleC}-R1. The pair of primers used to amplify the *gfp*(ASV) gene is *gfP*(ASV)-F2/*Xho*I-*gfp*(ASV)-R2. *Xba*I and *Xho*I restriction sites were added to the upstream and downstream primers. The fusion was first cloned in pGEMT digested with *Eco*RV, generating blunt ends, and sequenced. A *Xba*I-*Xho*I restriction allowed the transfer of the insert to a pBBRMCS1 vector, in the opposite direction to the *lac* promoter of the vector.

TRSE labelling

Bacteria were harvested by centrifugation at 7000 rpm for 2 min. They were then washed thrice with phosphate-buffered saline (PBS) and incubated with Texas Red succinimidyl ester (TRSE) (Invitrogen) diluted to 1µg/ml in PBS for 15 min at room temperature (RT) in the dark. Bacteria were then washed once with PBS and twice with the appropriate medium, 2YT for growth assays and Dulbecco's Modified Eagle's Medium (DMEM) (Invitrogen) for HeLa cells infections.

HeLa cells culture and infection

HeLa cells (from the Centre d'Immunologie de Marseille-Luminy, Marseille, France) were cultivated at 37°C and in a 5% CO_2 atmosphere in DMEM supplemented with 10% fetal bovine serum (Gibco), 0.1 g/l non-essential amino acids and 0.1 g/l sodium pyruvate (Invitrogen). For the infection, HeLa cells were seeded in 24-well plates (on cover-slips for immunolabelling) at a concentration of 4.10^4 cells/ml. On the day of the infection, an overnight culture of *B. abortus* was diluted in DMEM to reach a multiplicity of infection (MOI) of 300. Bacteria were added to HeLa cells and the 24-well plates were centrifuged at 1200 rpm for 10 min at 4°C. Cells were then incubated at 37°C in a 5% CO_2 atmosphere for one hour. Cells were washed twice in PBS and fresh medium supplemented with 50 µg/ml gentamycin was added.

Immunolabelling of infected HeLa cells

Cells were fixed in PBS 2% paraformaldehyde (Prolabo) for 20 min at RT then permeabilized in PBS 0.1% Triton X-100 for 10 min. Cells were incubated for 45 min with primary and secondary antibodies supplemented with 0.1% Triton X-100 and 3%

bovine serum albumin (BSA, Sigma Aldrich). *Brucella* were detected with the A76-12G12 monoclonal antibody (non-diluted hybridoma culture supernatant) followed by a secondary anti-mouse antibodies coupled to Alexa-488 diluted 500 times (Sigma Aldrich). Coverslips were washed thrice with PBS and once with $_{dd}H_2O$ and mounted with Mowiol (Sigma).

For Lamp1 labelling, cells were fixed in methanol-acetone (80%-20%) for 20 min at RT. Bacteria and Lamp1 were labelled with a rabbit anti-*Brucella* serum diluted 2000 times and mouse anti-Lamp1 antibodies diluted 200 times in PBS 2% BSA. Secondary anti-rabbit antibodies coupled to Pacific Blue and anti-mouse antibodies coupled to Alexa-488 (Sigma Aldrich) were diluted 500 times in PBS 2% BSA. Coverslips were washed thrice in PBS 2% BSA and mounted with Mowiol.

Protein purification

The DNA sequences coding for PdhS, DivK and CpdR as well as for the non-phosphorylatable versions of PdhS and DivK were cloned in a pML310 vector using the Gateway technique. This cloning allows the fusion of the proteins to a thioredoxin and poly-histidine tag at the N-terminus. Proteins were overproduced in *E. coli* BL21(DE3) strain. Cultures were grown to an OD_{600} of 0.6-0.8 at 37°C. Overexpression was induced by adding 300 µM isopropyl-b-D-thiogalactoside (IPTG) for 3 hours at 30°C. bacteria were harvested by centrifugation at 5000 rpm for 20 min at 4°C. Pellets were resuspended in lysis buffer (20 mM Tris-HCl pH 8.0, 500 mM NaCl, 10% glycerol, 10 or 20 mM imidazole, 0.1% TritonX-100, 1 mM DTT, 1 mg/ml lysozyme supplemented with Dnase I and Complete Protease inhibitor Cocktail) and lysed by sonication (Branson Sonifier 150) (8 cycles of 30 s).

Tandem purifications were performed. The first step consisted of an affinity purification on a Ni^{2+}-nitrilotriacetate affinity resin (Ni-NTA from Qiagen) equilibrated with lysis buffer and eluted with an imidazole gradient from 10 or 20 mM to 250 mM. The second step of purification consisted of a gel filtration on a HiLoad 16/60 Superdex 75 or 200 prep grade (GE healthcare) equilibrated with storage buffer (10 mM HEPES pH 8.0, 50 mM KCl, 10% glycerol, 0.1 mM EDTA, 1 mM DTT).

In vitro kinase assays

Autophosphorylation of histidine kinases (5 µM) was performed in storage buffer supplemented with 2 mM DTT, 5 mM $MgCl_2$, 500 µM ATP and 5 µCi γ^{32}P-ATP (3000 Ci/mmol) (PerkinElmer) for 40 min at 30°C. Response regulators were prepared at 5 µM in storage buffer supplemented with 5 mM MgCl2 and incubated with the phosphorylated histidine kinase for one to 30 min at RT.

In vivo Phostag assay

Bacteria were grown to mid-exponential phase, harvested by centrifugation and lysed in a lysis buffer (10 mM Tris-HCl pH 7.5, 2% SDS) for 5 min at RT. Loading buffer was added and lysates were kept on ice and directly loaded on a SDS gel supplemented with 25 µM Phostag (Nard Chemicals, Japan) and 1 mM $MnCl_2$. Samples heated at 80°C for 2 min were used as negative control. Migration was performed at 4°C for 3 hours and proteins were transferred to a nitrocellulose membrane for Western blotting.

Western blot analysis

One ml of a *B. abortus* culture was concentrated to an OD_{600} of 10 in PBS. Bacteria were inactivated for one hour at 80°C and loading buffer was added. Fifteen µl of bacterial lysate was loaded in each well. After migration, proteins were transferred onto a nitrocellulose membrane which was blocked in PBS supplemented with 0.05% Tween and 5% milk for at least one hour. The membrane was incubated for 1 h with the appropriate serum (diluted 10, 100 or 1000x depending on the serum) and secondary antibodies coupled to HRP (diluted 5000x) (Dako Denmark) diluted in PBS 0.05% Tween 1% milk. The membrane was washed 3 times for 5 min. The Clarity Western ECL Substrate (Biorad) and Image Quant LAS 4000 (General Electric) were used to reveal the bands.

Flow cytometry

One ml of bacteria grown in rich culture medium until an OD of 0.3-0.4 were washed once with PBS and fixed in 9 ml of ice-cold 77% ethanol. One ml of fixed bacteria were permeabilized in fluorescence-activated cell sorting (FACS) staining buffer (10 mM Tris-HCl pH7.2, 1 mM EDTA, 50 mM sodium citrate, 0.01% TritonX-100) and incubated with

0.1 mg/ml RNase A for 30 min at RT. Bacteria were washed with the FACS staining buffer and incubated with 0.5 µM Sytox Green for 15 min before analysing the samples (200,000 events) with a FACScalibur using CellQuest software (Becton Dickinson) with excitation at 495 nm and emission at 519 nm.

Growth curve and CFU counts

Growth curves were performed by using Bioscreen C from Oy Growth curves. Overnight cultures were diluted to an OD of 0.1 and the OD was measured every 30 min during 70 hours.

For CFU counts in culture, wild type (WT) *B. abortus* 544 and the CtrA depletion strain cultivated with IPTG were diluted to 10^{-6} or 10^{-7} in 2YT and 100 µl were plated on 2YT, supplemented with chloramphenicol and 1 mM IPTG for the depletion strain. The depletion strain grown without IPTG was diluted to 10^{-4} or 10^{-5}.

For CFU counts after infection, HeLa cells were lysed with 0.01% TritonX-100 PBS for 10 min at RT. Several dilutions were plated on 2YT supplemented with chloramphenicol and IPTG if needed. Plates were incubated for 3 to 4 days at 37°C.

Chromatin immunoprecipitation with anti-CtrA antibodies

An 80 ml culture of *B. abortus* 544 at an OD_{600} of 0.8 was centrifuged to harvest the bacteria. Protein-DNA crosslinking was performed in 10 µM sodium phosphate buffer (pH 7.6) and 1% formaldehyde for 10 min at RT and 30 min on ice. Bacteria were harvested by centrifugation at 8500 rpm for 5 min at 4°C, washed twice in cold PBS and resuspended in lysis buffer (10 mM Tris-HCl pH 7.5, 1 mM EDTA, 100 mM NaCl, 2.2 mg/ml lysozyme, 20 µl protease inhibitor solution). Zirconia/Silica beads (Biospec Products) of 0.1 and 0.5 mm diameter were added. Bacteria were lysed in the cell Disruptor Genie from Scientific Industries at maximal amplitude (2800) for 25 min at 4°C. ChIP buffer was added (1.1% TritonX-100, 1.2 mM EDTA, 16.7 mM Tris-HCl pH 8.0, 167 mM NaCl, protease inhibitors) and bacteria were incubated at 37°C for 10 min for further lysis. In order to obtain DNA fragments of about 300 base pairs, the lysate was sonicated on ice (Branson Sonifier Digital cell disruptor S-450D 400W) by applying 15 bursts of 20 sec (50% duty) at 30% amplitude and centrifuged at 14,000 rpm for 3 min to pellet the debris. The supernatant was normalized by protein content by measuring the absorbance at 280 nm. A sample corresponding to 7.5 mg of bacterial proteins was

diluted in 1 ml of ChIP buffer supplemented with 0.01% SDS and pre-cleared in 80 µl of protein A-agarose beads (Roche) and 100 µg BSA. Polyclonal anti-CtrA antibodies [21] were added to the supernatant (dilution 1:1000) and incubated for one night at 4°C to form immune complexes which were then incubated with 80 µl of protein A-agarose beads pre-saturated with BSA for 2 h at 4°C. Beads were then washed once with low salt buffer (0.1% SDS, 1% TritonX-100, 2 mM EDTA, 20 mM Tris-HCl pH 8.1, 150 mM NaCl), high salt buffer (0.1% SDS, 1% TritonX-100, 2 mM EDTA, 20 mM Tris-HCl pH 8.1, 500 mM NaCl) and LiCl buffer (0.25 M LiCl, 1% NP-40, 1% sodum deoxycholate, 1 mM EDTA, 10 mM Tris-HCl pH 8.1) and twice with TE buffer (10 mM Tris-HCl pH 8.1 and 1 mM EDTA). Protein-DNA complexes were eluted with 500 µl of elution buffer (1% SDS and 0.1M $NaHCO_3$). Reverse crosslinking was performed in presence of 300 mM of NaCl overnight at 65°C. Samples were treated with 2 µg of Proteinase K for 2h at 45°C in 40 mM EDTA and 40 mM Tris-HCl pH 6.5. DNA was extracted using QIAgen MinElute kit and resuspended in 30 µl of Elution Buffer. ChIP DNA was sequenced using Illumina MySeq.

Analysis of the sequencing data

Sequencing data consisted of a number of reads per nucleotide. Computing of average and variance in a window of 1 million base pairs allowed the calculation of a *Z* score for each base pair (i.e. the number of standard deviation from the average). Genomic regions with reads numbers above the threshold ($Z > 4$) were kept and considered to be bound by CtrA. These regions were mapped to the genome of *Brucella abortus* 2308, a close relative to the *B. abortus* 544 strain.

mRNA extraction and RT-qPCR

Fifty ml of a mid-exponential phase ($OD_{600} = 0.8$) culture of the Δ*ctrA* p_{lac}-*ctrA* strain grown with IPTG or without IPTG for 4 h were centrifuged to harvest bacteria that were lysed with 100 µl of SDS 10% in the presence of 20 µl of proteinase K for one hour at 37°C with shaking. Five ml of Tripure isolation reagent (Roche) were added and tubes were vortexed briefly and incubated for 10 min at 65°C. One ml of chloroform was added and tubes were inverted and incubated 10 min at RT. Lysates were centrifuged at 14,000 rpm for 15 min at 4°C and the aqueous phase was harvested and mixed with 2.5 ml of isopropanol. Samples were stored at -20°C. RNA was harvested by centrifugation

at 14,000 rpm for 30 min at 4°C and washed with 200 µl of 75% RNAse-Free ethanol. RNA was harvested by centrifugation at 8500 rpm for 5 min at 4°C. The pellet was kept to dry at RT and was solubilized in 50 µl of water treated with diethylpirocarbonate (DEPC) at 55°C for 10 min. RNA concentration was measured using the Nanodrop and 2 to 5 µg were incubated with 3 µl of DNAseI (1U/µl) (Fermentas) and the corresponding buffer in a total volume of 20 µl for 30 min at 37°C. Two µl of 50 mM EDTA were added and the mix was incubated 10 min at 65°C. The mix was split in two tubes of 10 µl each to perform reverse transcription (RT) and its negative control. First a hybridization step is performed by incubating the mix with 1 µl of oligo dT $_{12\text{-}18}$ Random Primers (500ng/ul) (Invitrogen) at 65°C for 5 min. Then were added to the mix 4 µl of 5x First Strand Buffer (Invitrogen), 2µl of 100 mM DTT (Invitrogen), 1 µl of a dNTP mix (containing 10 mM of each nucleotide) (Invitrogen) and 1 µl of H_2O treated with DEPEC. The obtained mix was incubated for 2 min at 42°C and 1 µl of SuperScript II (200 U/µl) (Invitrogen) was added to reverse transcribe RNA to DNA at 42°C for 50 min. The enzyme was then inactivated at 70°C for 15 min. The remaining RNA after RT was degraded by incubating the mix with 1 µl of Ribonuclease H (2U/µl) (Invitrogen) for 20 min at 37°C. qPCR was performed on 10 ng of cDNA using Fast Start Universal SYBRGreen Master Rox (Roche). Primers were designed to generate 100-150 base pair-long amplicons. The $2^{-\Delta\Delta CT}$ method was used to determine the fold induction of genes of interest in the CtrA depletion strain grown without IPTG in comparison to the same strain cultivated in the presence of IPTG. Ribosomal 16S RNA served as an internal control to normalize gene expression data.

Acknowledgements

We thank Véronique Dhennin from the UMR8199 sequencing service LIGAN-PM Equipex (Lille Integrated Genomics Advanced Network for personalized medicine). We thank Aurélie Mayard for assistance in protein purification and Kévin Willemart for help in mRNA extraction. We thank UNamur for financial and logistic supports.

References

1. Moreno E, Moriyon I (2006) The Genus *Brucella*. Prokaryotes 5: 315-456.
2. Detilleux PG, Deyoe BL, Cheville NF (1990) Penetration and intracellular growth of *Brucella abortus* in nonphagocytic cells in vitro. Infect Immun 58: 2320-2328.
3. Archambaud C, Salcedo SP, Lelouard H, Devilard E, de Bovis B, et al. (2010) Contrasting roles of macrophages and dendritic cells in controlling initial pulmonary Brucella infection. Eur J Immunol 40: 3458-3471.
4. Chaves-Olarte E, Guzman-Verri C, Meresse S, Desjardins M, Pizarro-Cerda J, et al. (2002) Activation of Rho and Rab GTPases dissociates Brucella abortus internalization from intracellular trafficking. Cell Microbiol 4: 663-676.
5. Pizarro-Cerda J, Meresse S, Parton RG, van der Goot G, Sola-Landa A, et al. (1998) *Brucella abortus* transits through the autophagic pathway and replicates in the endoplasmic reticulum of nonprofessional phagocytes. Infect Immun 66: 5711-5724.
6. Starr T, Ng TW, Wehrly TD, Knodler LA, Celli J (2008) *Brucella* intracellular replication requires trafficking through the late endosomal/lysosomal compartment. Traffic 9: 678-694.
7. Salcedo SP, Chevrier N, Lacerda TL, Ben Amara A, Gerart S, et al. (2013) Pathogenic *brucella*e replicate in human trophoblasts. J Infect Dis 207: 1075-1083.
8. Celli J, de Chastellier C, Franchini DM, Pizarro-Cerda J, Moreno E, et al. (2003) *Brucella* evades macrophage killing via VirB-dependent sustained interactions with the endoplasmic reticulum. J Exp Med 198: 545-556.
9. Celli J, Salcedo SP, Gorvel JP (2005) Brucella coopts the small GTPase Sar1 for intracellular replication. Proc Natl Acad Sci U S A 102: 1673-1678.
10. Starr T, Child R, Wehrly TD, Hansen B, Hwang S, et al. (2012) Selective subversion of autophagy complexes facilitates completion of the Brucella intracellular cycle. Cell Host Microbe 11: 33-45.
11. Deghelt M, Mullier C, Sternon JF, Francis N, Laloux G, et al. (2014) G1-arrested newborn cells are the predominant infectious form of the pathogen *Brucella abortus*. Nat Commun 5: 4366.

12. Brilli M, Fondi M, Fani R, Mengoni A, Ferri L, et al. (2010) The diversity and evolution of cell cycle regulation in alpha-proteobacteria: a comparative genomic analysis. BMC Syst Biol 4: 52.
13. Hallez R, Bellefontaine AF, Letesson JJ, De Bolle X (2004) Morphological and functional asymmetry in alpha-proteobacteria. Trends Microbiol 12: 361-365.
14. Pini F, Frage B, Ferri L, De Nisco NJ, Mohapatra SS, et al. (2013) The DivJ, CbrA and PleC system controls DivK phosphorylation and symbiosis in Sinorhizobium meliloti. Mol Microbiol 90: 54-71.
15. Willett JW, Herrou J, Briegel A, Rotskoff G, Crosson S (2015) Structural asymmetry in a conserved signaling system that regulates division, replication, and virulence of an intracellular pathogen. Proc Natl Acad Sci U S A 112: E3709-3718.
16. Wheeler RT, Shapiro L (1999) Differential localization of two histidine kinases controlling bacterial cell differentiation. Mol Cell 4: 683-694.
17. Hallez R, Letesson JJ, Vandenhaute J, De Bolle X (2007) Gateway-based destination vectors for functional analyses of bacterial ORFeomes: application to the Min system in *Brucella abortus*. Appl Environ Microbiol 73: 1375-1379.
18. Laub MT, Chen SL, Shapiro L, McAdams HH (2002) Genes directly controlled by CtrA, a master regulator of the Caulobacter cell cycle. Proc Natl Acad Sci U S A 99: 4632-4637.
19. Quon KC, Yang B, Domian IJ, Shapiro L, Marczynski GT (1998) Negative control of bacterial DNA replication by a cell cycle regulatory protein that binds at the chromosome origin. Proc Natl Acad Sci U S A 95: 120-125.
20. Reisenauer A, Quon K, Shapiro L (1999) The CtrA response regulator mediates temporal control of gene expression during the Caulobacter cell cycle. J Bacteriol 181: 2430-2439.
21. Bellefontaine AF, Pierreux CE, Mertens P, Vandenhaute J, Letesson JJ, et al. (2002) Plasticity of a transcriptional regulation network among alpha-proteobacteria is supported by the identification of CtrA targets in *Brucella abortus*. Mol Microbiol 43: 945-960.
22. Hallez R, Mignolet J, Van Mullem V, Wery M, Vandenhaute J, et al. (2007) The asymmetric distribution of the essential histidine kinase PdhS indicates a differentiation event in *Brucella abortus*. EMBO J 26: 1444-1455.

23. Van der Henst C, Beaufay F, Mignolet J, Didembourg C, Colinet J, et al. (2012) The histidine kinase PdhS controls cell cycle progression of the pathogenic alphaproteobacterium *Brucella abortus*. J Bacteriol 194: 5305-5314.
24. Brown PJ, de Pedro MA, Kysela DT, Van der Henst C, Kim J, et al. (2012) Polar growth in the Alphaproteobacterial order Rhizobiales. Proc Natl Acad Sci U S A 109: 1697-1701.
25. Pizarro-Cerda J, Moreno E, Sanguedolce V, Mege JL, Gorvel JP (1998) Virulent *Brucella abortus* prevents lysosome fusion and is distributed within autophagosome-like compartments. Infect Immun 66: 2387-2392.
26. Comerci DJ, Martinez-Lorenzo MJ, Sieira R, Gorvel JP, Ugalde RA (2001) Essential role of the VirB machinery in the maturation of the *Brucella abortus*-containing vacuole. Cell Microbiol 3: 159-168.
27. Robertson GT, Reisenauer A, Wright R, Jensen RB, Jensen A, et al. (2000) The *Brucella abortus* CcrM DNA methyltransferase is essential for viability, and its overexpression attenuates intracellular replication in murine macrophages. J Bacteriol 182: 3482-3489.
28. Gray AN, Egan AJ, Van't Veer IL, Verheul J, Colavin A, et al. (2015) Coordination of peptidoglycan synthesis and outer membrane constriction during Escherichia coli cell division. Elife 4.
29. Lazzaroni JC, Dubuisson JF, Vianney A (2002) The Tol proteins of Escherichia coli and their involvement in the translocation of group A colicins. Biochimie 84: 391-397.
30. Cloeckaert A, de Wergifosse P, Dubray G, Limet JN (1990) Identification of seven surface-exposed Brucella outer membrane proteins by use of monoclonal antibodies: immunogold labeling for electron microscopy and enzyme-linked immunosorbent assay. Infect Immun 58: 3980-3987.
31. Cloeckaert A, Verger JM, Grayon M, Vizcaino N (1996) Molecular and immunological characterization of the major outer membrane proteins of Brucella. FEMS Microbiol Lett 145: 1-8.
32. Verstreate DR, Creasy MT, Caveney NT, Baldwin CL, Blab MW, et al. (1982) Outer membrane proteins of Brucella abortus: isolation and characterization. Infect Immun 35: 979-989.

33. Sperandeo P, Cescutti R, Villa R, Di Benedetto C, Candia D, et al. (2007) Characterization of lptA and lptB, two essential genes implicated in lipopolysaccharide transport to the outer membrane of Escherichia coli. J Bacteriol 189: 244-253.
34. Pini F, De Nisco NJ, Ferri L, Penterman J, Fioravanti A, et al. (2015) Cell Cycle Control by the Master Regulator CtrA in Sinorhizobium meliloti. PLoS Genet 11: e1005232.
35. Andersen JB, Sternberg C, Poulsen LK, Bjorn SP, Givskov M, et al. (1998) New unstable variants of green fluorescent protein for studies of transient gene expression in bacteria. Appl Environ Microbiol 64: 2240-2246.
36. Terwagne M, Mirabella A, Lemaire J, Deschamps C, De Bolle X, et al. (2013) Quorum sensing and self-quorum quenching in the intracellular pathogen *Brucella melitensis*. PLoS One 8: e82514.
37. Quon KC, Marczynski GT, Shapiro L (1996) Cell cycle control by an essential bacterial two-component signal transduction protein. Cell 84: 83-93.
38. Zweiger G, Marczynski G, Shapiro L (1994) A *Caulobacter* DNA methyltransferase that functions only in the predivisional cell. J Mol Biol 235: 472-485.
39. Sliusarenko O, Heinritz J, Emonet T, Jacobs-Wagner C (2011) High-throughput, subpixel precision analysis of bacterial morphogenesis and intracellular spatio-temporal dynamics. Mol Microbiol 80: 612-627.
40. Dubray G, Charriaut C (1983) Evidence of three major polypeptide species and two major polysaccharide species in the Brucella outer membrane. Ann Rech Vet 14: 311-318.
41. Helaine S, Cheverton AM, Watson KG, Faure LM, Matthews SA, et al. (2014) Internalization of *Salmonella* by macrophages induces formation of nonreplicating persisters. Science 343: 204-208.
42. Guzman-Verri C, Manterola L, Sola-Landa A, Parra A, Cloeckaert A, et al. (2002) The two-component system BvrR/BvrS essential for Brucella abortus virulence regulates the expression of outer membrane proteins with counterparts in members of the Rhizobiaceae. Proc Natl Acad Sci U S A 99: 12375-12380.
43. Edmonds MD, Cloeckaert A, Booth NJ, Fulton WT, Hagius SD, et al. (2001) Attenuation of a Brucella abortus mutant lacking a major 25 kDa outer membrane protein in cattle. Am J Vet Res 62: 1461-1466.

44. Manterola L, Guzman-Verri C, Chaves-Olarte E, Barquero-Calvo E, de Miguel MJ, et al. (2007) BvrR/BvrS-controlled outer membrane proteins Omp3a and Omp3b are not essential for Brucella abortus virulence. Infect Immun 75: 4867-4874.

45. Jubier-Maurin V, Boigegrain RA, Cloeckaert A, Gross A, Alvarez-Martinez MT, et al. (2001) Major outer membrane protein Omp25 of Brucella suis is involved in inhibition of tumor necrosis factor alpha production during infection of human macrophages. Infect Immun 69: 4823-4830.

46. Manterola L, Moriyon I, Moreno E, Sola-Landa A, Weiss DS, et al. (2005) The lipopolysaccharide of Brucella abortus BvrS/BvrR mutants contains lipid A modifications and has higher affinity for bactericidal cationic peptides. J Bacteriol 187: 5631-5639.

47. Vanderlinde EM, Yost CK (2012) Mutation of the sensor kinase chvG in Rhizobium leguminosarum negatively impacts cellular metabolism, outer membrane stability, and symbiosis. J Bacteriol 194: 768-777.

48. Fumeaux C, Radhakrishnan SK, Ardissone S, Theraulaz L, Frandi A, et al. (2014) Cell cycle transition from S-phase to G1 in *Caulobacter* is mediated by ancestral virulence regulators. Nat Commun 5: 4081.

49. Barquero-Calvo E, Conde-Alvarez R, Chacon-Diaz C, Quesada-Lobo L, Martirosyan A, et al. (2009) The differential interaction of Brucella and ochrobactrum with innate immunity reveals traits related to the evolution of stealthy pathogens. PLoS One 4: e5893.

50. Sadowski CS, Wilson D, Schallies KB, Walker G, Gibson KE (2013) The Sinorhizobium meliloti sensor histidine kinase CbrA contributes to free-living cell cycle regulation. Microbiology 159: 1552-1563.

51. Fields AT, Navarrete CS, Zare AZ, Huang Z, Mostafavi M, et al. (2012) The conserved polarity factor podJ1 impacts multiple cell envelope-associated functions in Sinorhizobium meliloti. Mol Microbiol 84: 892-920.

Supporting information

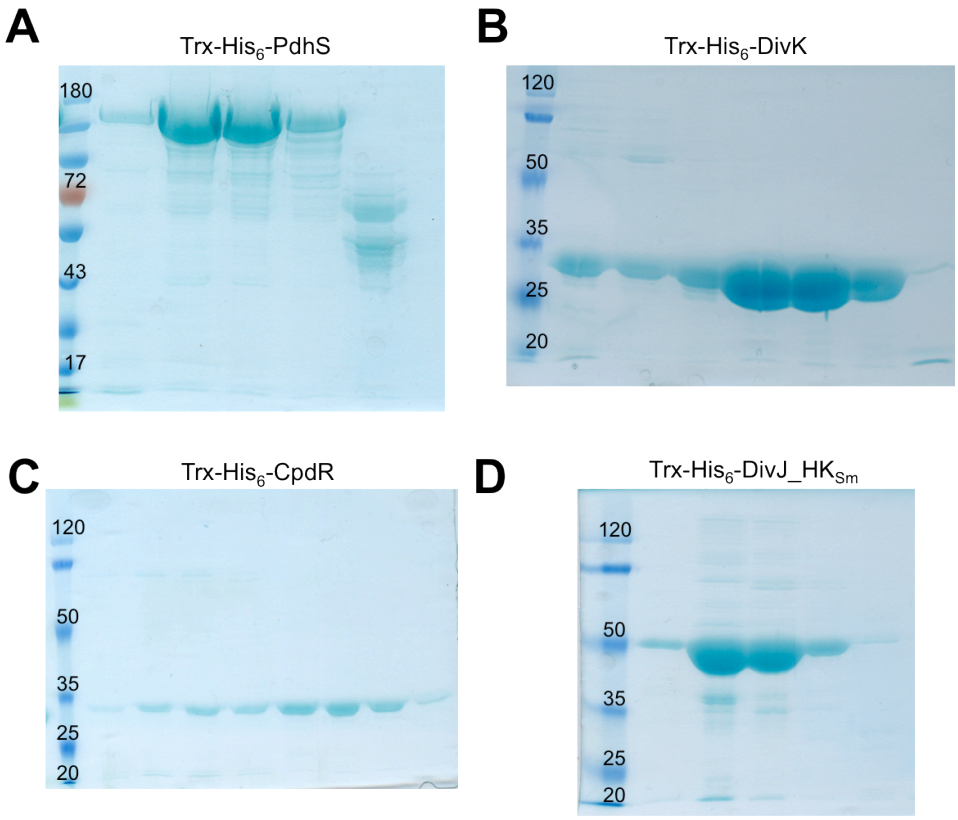

S1 Fig. Protein purification by gel filtration. Thioredoxin(Trx)-His_6 fusions to PdhS, DivK, CpdR and the histidine kinase domain of *S. meliloti* DivJ (DivJ_HK_{Sm}) were purified on a Ni-NTA column followed by gel filtration. The gel pictures show the elution fractions collected after size exclusion chromatography and corresponding to a single peak of elution measured at 280 nm.

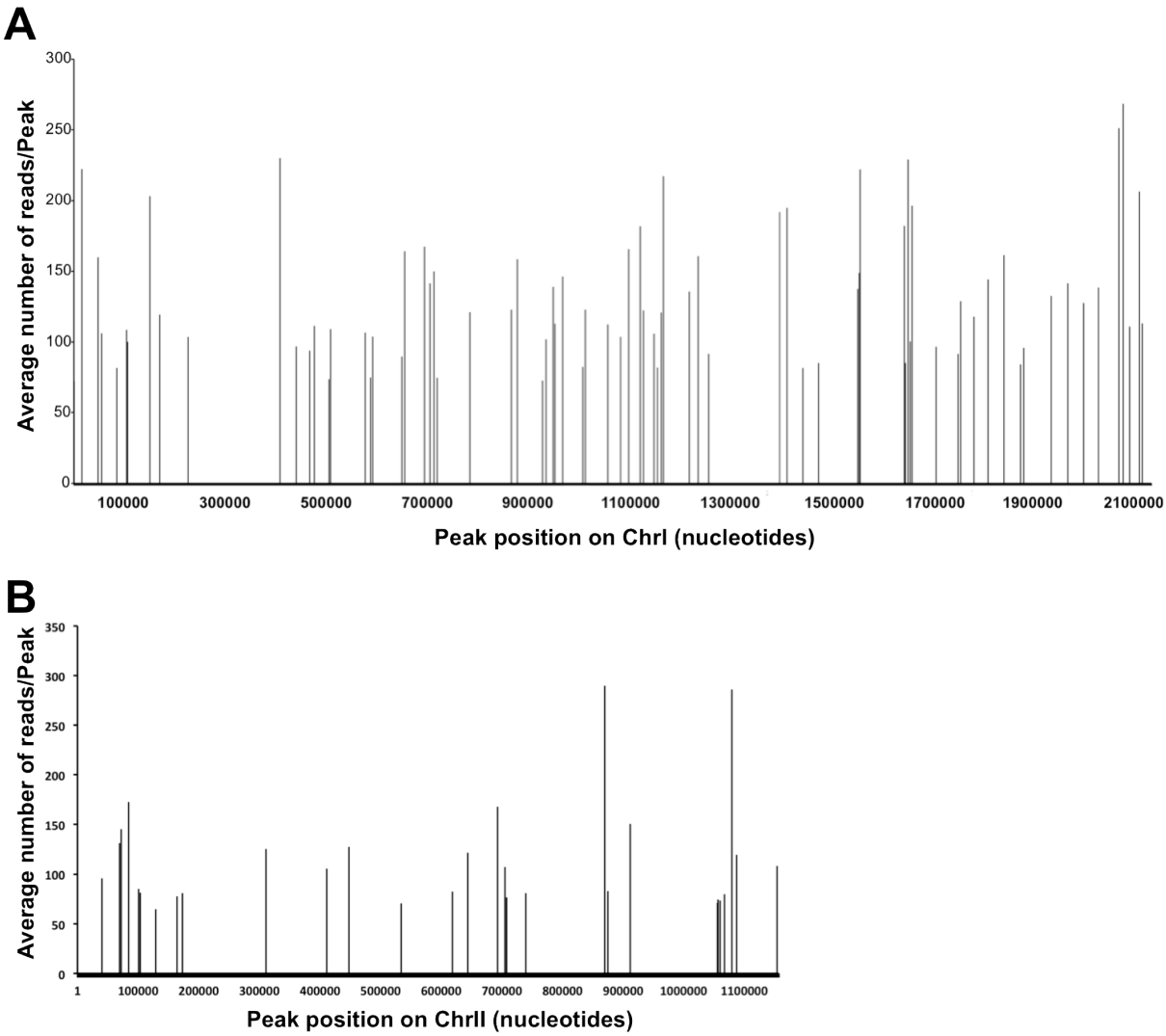

S2 Fig. CtrA binding sites on *B. abortus* chromosomes I and II. Histograms represent the average number of reads for each region immunoprecipitated with CtrA from chromosome I (ChrI) (A) and chromosome II (ChrII) (B). Only regions above the threshold (see material and methods) are shown.

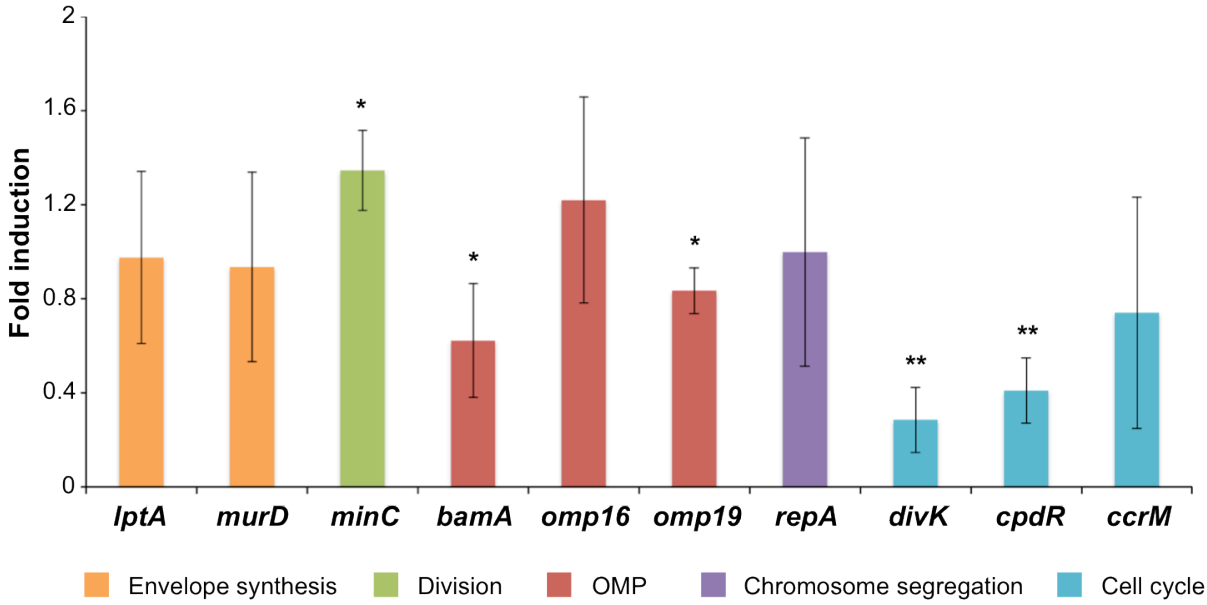

S3 Fig. Histogram showing the fold induction of potential CtrA target genes after a 4 h depletion. Potential CtrA target genes identified by ChIP-seq were classified in five functional categories and the relative expression of representative genes after 4 h of depletion was plotted in comparison with the non-depleted condition. The significant fold induction variations are indicated by * ($p < 0.05$) and ** ($p < 0.01$) (Student *t* test).

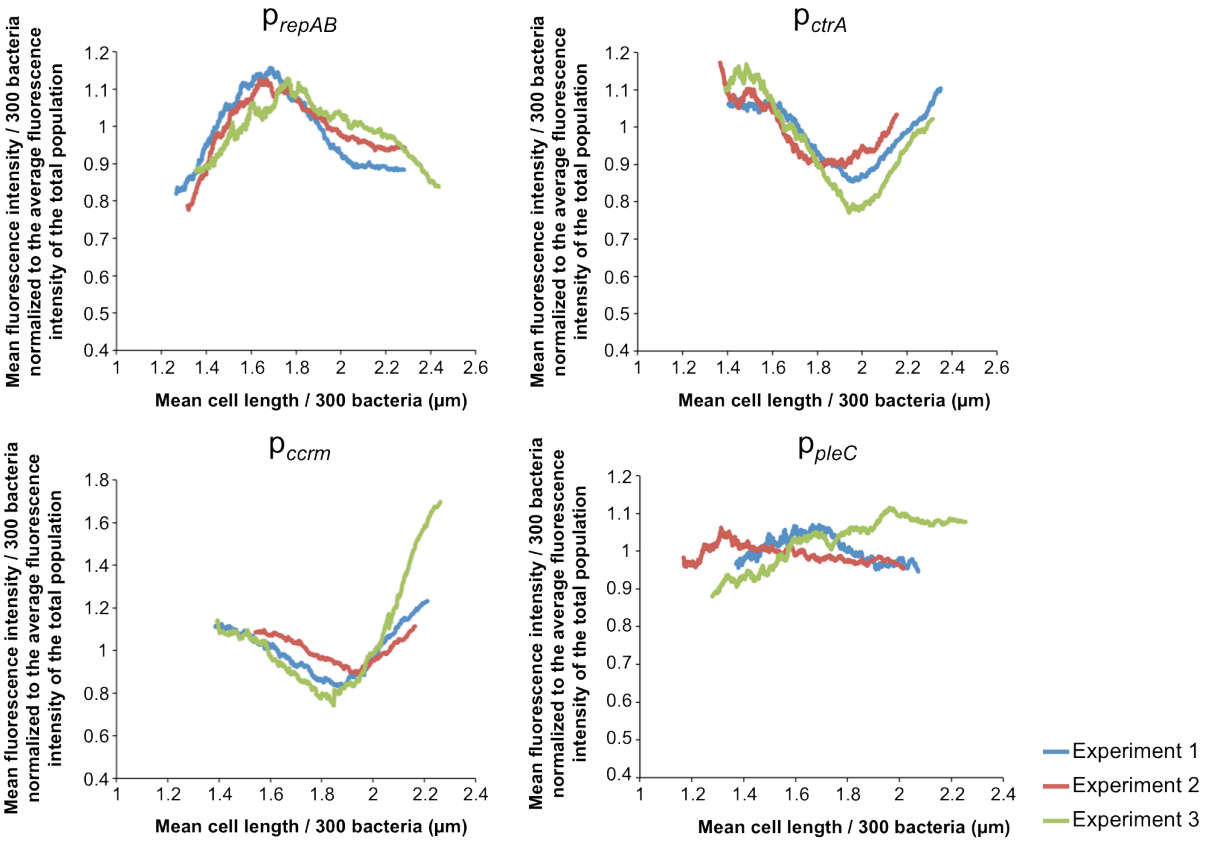

S4 Fig. Activity profiles of *repAB, ctrA, ccrM* and *pleC* promoters as a function of *B. abortus* cell length. Phase and fluorescence microscopy images of *B. abortus* reporter strains were analysed with the MicrobeTracker program. Bacteria were ordered according to their cell length and the mean cell length and mean fluorescence intensity was calculated for a sliding window (from smallest to largest bacteria) of 300 bacteria. The mean fluorescence intensities were normalized to the average fluorescence intensity of the whole population of a given experiment, allowing the representation of results from three independent experiments on the same plot. The number of bacteria analysed for p_{repAB} are 1632, 1402 and 2377; for p_{ctrA} 1456, 1487 and 1467; for p_{ccrM} 1446, 753 and 1678; for p_{pleC} 1888, 1297 and 1953.

S1 Table. List of plasmids

Plasmid name	Reference
pML310-TRX-His$_6$-*pdhS*	This study
pML310-TRX-His$_6$-*pdhS*(H805A)	This study
pML310-TRX-His$_6$-*divK*	This study
pML310-TRX-His$_6$-*divK*(D53A)	This study
pML310-TRX-His$_6$-*cpdR*	This study
pML310-TRX-His$_6$-*divJ*_HK$_{Sm}$	[1]
pET15b-MBP-*envZ*	[2]
pBBR-MCS1-p$_{lac}$-pdhS	[3]
pNPTS-Δ*ctrA*	This study
pBBR-MCS1-*lacI*-p$_{lac}$-*ctrA*	This study
pBBRMCS1-p$_{ctrA}$-*gfp*(ASV)	This study
pBBRMCS1-p$_{repAB}$-*gfp*(ASV)	This study
pBBRMCS1-p$_{ccrM}$-*gfp*(ASV)	This study
pBBRMCS1-p$_{pleC}$-*gfp*(ASV)	This study

S2 Table. List of primers

Primer name	5'-3' sequence
attB1-*pdhS*	GGGGACAAGTTTGTACAAAAAAGCAGGCTCCtcaggatcatacccttc atcga
attB2-*pdhS*	GGGGACCACTTTGTACAAGAAAGCTGGGtcaaacgcgggttggcggg
pdhS(H805A)-F	AgtCcggatttcagCgctgatg
pdhS(H805A)-R	cggAgtCcggatttcagCgctgatg
attB1-*divK*	GGGGACAAGTTTGTACAAAAAAGCAGGCTCCatgacgaaaagcgtaat gat
attB2-*divK*	GGGGACCACTTTGTACAAGAAAGCTGGGctaggcatcgcccag
attB1-*cpdR*	GGGGACAAGTTTGTACAAAAAAGCAGGCTCCATGAAGAGAATCC TTCTAGCTGAAG
attB2-*cdpR*	GGGGACCACTTTGTACAAGAAAGCTGGGTCAGGCGGCGATCAGC AT
*Pst*I-Up-*ctrA*-F	CTGCAGATGCCGGCCTTTTTC
Up-*ctrA*-R	tgatcgctggacatgAAAGGACGCGcatCTTT
Down-*ctrA*-F	catgtccagcgatcaCGCGAAAGCGCCtga
*Sal*I-Down-*ctrA*-R	GTCGACATCTGCCACGACATCATC
*Sac*I-Kan3'	GAGCTCcgccttcttgacgagttcttc
p$_{lac}$-R1	caatcaaaaggacgcgCATagctgtttcctgtgtgaaattg
ctrA-F2	ATGcgcgtccttttgattgaag
*Kpn*I-*ctrA*-R2	GGTACCTCAggcgctttcgcgcatct
*Xba*I-p$_{ctrA}$-F1	TCTAGAcccccaaatctcctcgcgatt
p$_{ctrA}$-R1	ttcttctcctttactCATcttttatccccttcc
gfP(ASV)-F2	ATGagtaaaggagaagaacttttcac
*Xho*I-*gfp*(ASV)-R2	CTCGAGTTAAACTGATGCAGCGTAGTTTTCG
*Xba*I-p$_{repAB}$-F1	TCTAGAcagaagcgttagactgccgtcta
p$_{repAB}$-R1	ttcttctcctttactCATtacttgggatccctagtgacggcactt
*Xba*I-p$_{ccrM}$-F1	GAGCTCtatcaaactacacccgacaggcactt
p$_{ccrM}$-R1	AGTTCTTCTCCTTTACTCATgggatactcgattacctgtgaacg
*Xba*I-p$_{pleC}$-F1	TCTAGAttcgcaaaatccgaaggtcga
p$_{pleC}$-R1	ttcttctcctttactCATctctcggcccctcttgaatc

S3 Table. Antibodies used for Western blots and immunofluorescence

Name	Produced in	Recognized structure/protein	Reference
A76/12G12	Mouse	*Brucella* LPS	[4]
A68/04B10/F05	Mouse	Omp25	[5]
A68/04G01/C06	Mouse	Omp16	[5]
A68/25H10/A05	Mouse	Omp19	[6]
A63/4D11/G01	Mouse	Omp2b	[7]
A68/07G11/C10	Mouse	Omp10	[5]
A53/10B2A01	Mouse	BamA	[5]
	Mouse	Lamp1	Developmental Studies Hybridoma Bank, University of Iowa
	Rabbit	CtrA	[8]

S4 Table. ChIP-seq data

Peak position	Open reading frame	Annotation*
Chromosome I		
376	BAB1_0001	*dnaA*
15383	BAB1_0012	
47939	BAB1_0045	
54961	BAB1_0047	
84533	BAB1_0075	
104209	BAB1_0099	
106422	BAB1_0102	
	BAB1_0103	
150501	BAB1_0137	
	BAB1_0138	
170171	BAB1_0155	*lptA*
408563	BAB1_0407	
	BAB1_0408	
440413	BAB1_0444	
	BAB1_0445	
466619	BAB1_0473	
476075	BAB1_0484	
505290	BAB1_0510	
	BAB1_0511	
508280	BAB1_0516	*ccrM*
577638	BAB1_0589	
587659	BAB1_0601	*divJ*
592031	BAB1_604	
650029	BAB1_0659	*omp2a*
	BAB1_0660	*omp2b*
655442	BAB1_0665	
694417	BAB1_0709	*lptF*
	BAB1_0710	*lptG*
705966	BAB1_0721	

	BAB1_0722	*omp25*
713901	BAB1_0729	
719706	BAB1_0735	
785187	BAB1_0804	
	BAB1_0805	
867579	BAB1_0896	
878925	BAB1_0907	
929503	BAB1_0953	
	BAB1_0954	
936336	BAB1_0964	*popZ*
950302	BAB1_0977	*fumA*
953710	BAB1_0981	
	BAB1_0982	
969790	BAB1_1009	
1009597	BAB1_1043	
	BAB1_1044	
1014411	BAB1_1052	
1058830	BAB1_1094	
1084215	BAB1_1119	
1100045	BAB1_1131	*clpX*
1123080	BAB1_1153	
1129350	BAB1_1159	
1150330	BAB1_1176	*bamA-lpxD-fabZ-lpxAB*
1157620	BAB1_1185	
1164924	BAB1_1192	*clpS*
	BAB1_1193	PBP6
1169289	BAB1_1198	
1220771	BAB1_1261	*rpsL*
	BAB1_1262	*rpsG*
1238318	BAB1_1277	*pipP*
1259719	BAB1_1302	*ropB*
1399918	BAB1_1447	*ftsQAZ*
1414746	BAB1_1458	*mraW-ftsI-murE-murF-mraY-murD-ftsW*
1446383	BAB1_1495	
1477542	BAB1_1526	
	BAB1_1527	
1555071	BAB1_1609	*sciP*
1557792	BAB1_1613	*chpT*
1559719	BAB1_1614	*ctrA*
	BAB1_1615	*picC*
1647366	BAB1_1701	
1649038	BAB1_1702	*glmM*
1655004	BAB1_1707	*omp16*
1659161	BAB1_1712	*tolQRAB*
1662896	BAB1_1717	*rcdA*
1710391	BAB1_1775	
1753997	BAB1_1818	
	BAB1_1819	

1759212	BAB1_1823	
1785299	BAB1_1846	
1813857	BAB1_1867	
1845254	BAB1_1895	*ftsK*
1877941	BAB1_1930	*omp19*
1884243	BAB1_1939	
1938421	BAB1_1997	*ftsEX*
1971825	BAB1_2034	
2002799	BAB1_2064	
2032666	BAB1_2099	
2072897	BAB1_2137	
2081502	BAB1_2147	
2093535	BAB1_2159	
2113650	BAB1_2177	
	BAB1_2178	
2118621	BAB1_2183	
	BAB1_2184	*mutM*
Chromosome II		
39884	BAB2_0042	*cpdR*
	BAB2_0043	
68915	BAB2_0069	
	BAB2_0070	
71756	BAB2_0071	
	BAB2_0072	
83509	BAB2_0082	
100320	BAB2_0099	
103279	BAB2_0104	
	BAB2_0105	
128782	BAB2_0131	*lpxE*
163741	BAB2_0170	
	BAB2_0171	
172554	BAB2_0178	
	BAB2_0179	
310706	BAB2_0314	
410426	BAB2_0413	*podJ*
	BAB2_0414	
447856	BAB2_450	
	BAB2_0451	
533985	BAB2_0535	*sodC*
617976	BAB2_0628	*divK*
643696	BAB2_0652	*lovK*
692300	BAB2_0658	*glmS*
705116	BAB2_0709	*ftsK*-like
707784	BAB2_0709	
	BAB2_0710	
739124	BAB2_0741	
	BAB2_0742	
868904	BAB2_0884	*minC*

874124	BAB2_0891	*nrdHIEF*
911086	BAB2_0930	
	BAB2_0931	
1059407	BAB2_1082	
1066673	BAB2_1083	
1078968	BAB2_1099	*ftcR*
1086928	BAB2_1106	*fliC*
	BAB2_1107	*bmaC*
1153945	BAB2_1163	*repA*

*The presence of multiple gene names indicates that CtrA binding was detected upstream an operon. The genes coding for hypothetical proteins are not indicated.

References

1. Pini F, Frage B, Ferri L, De Nisco NJ, Mohapatra SS, et al. (2013) The DivJ, CbrA and PleC system controls DivK phosphorylation and symbiosis in Sinorhizobium meliloti. Mol Microbiol 90: 54-71.
2. Huang KJ, Igo MM (1996) Identification of the bases in the ompF regulatory region, which interact with the transcription factor OmpR. J Mol Biol 262: 615-628.
3. Van der Henst C, Beaufay F, Mignolet J, Didembourg C, Colinet J, et al. (2012) The histidine kinase PdhS controls cell cycle progression of the pathogenic alphaproteobacterium *Brucella abortus*. J Bacteriol 194: 5305-5314.
4. Cloeckaert A, Zygmunt MS, Dubray G, Limet JN (1993) Characterization of O-polysaccharide specific monoclonal antibodies derived from mice infected with the rough *Brucella melitensis* strain B115. J Gen Microbiol 139: 1551-1556.
5. Cloeckaert A, de Wergifosse P, Dubray G, Limet JN (1990) Identification of seven surface-exposed Brucella outer membrane proteins by use of monoclonal antibodies: immunogold labeling for electron microscopy and enzyme-linked immunosorbent assay. Infect Immun 58: 3980-3987.
6. Cloeckaert A, Kerkhofs P, Limet JN (1992) Antibody response to Brucella outer membrane proteins in bovine brucellosis: immunoblot analysis and competitive enzyme-linked immunosorbent assay using monoclonal antibodies. J Clin Microbiol 30: 3168-3174.
7. Paquet JY, Diaz MA, Genevrois S, Grayon M, Verger JM, et al. (2001) Molecular, antigenic, and functional analyses of Omp2b porin size variants of Brucella spp. J Bacteriol 183: 4839-4847.
8. Bellefontaine AF, Pierreux CE, Mertens P, Vandenhaute J, Letesson JJ, et al. (2002) Plasticity of a transcriptional regulation network among alpha-proteobacteria is supported by the identification of CtrA targets in *Brucella abortus*. Mol Microbiol 43: 945-960.

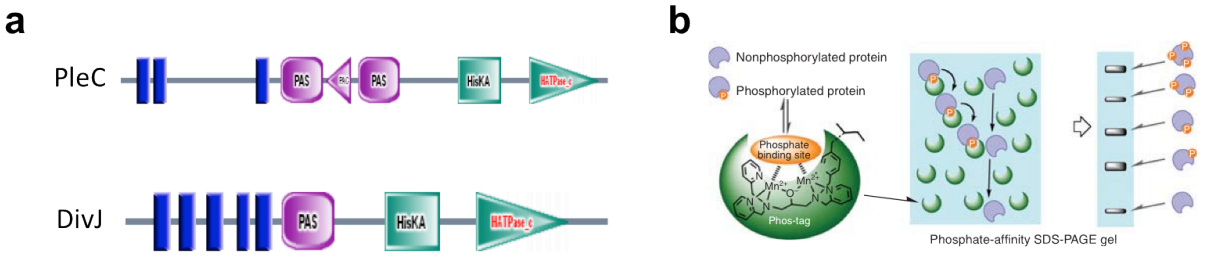

Figure 1- Domain prediction of PleC and DivJ and principle of a Phostag assay (Kinoshita et al., 2009)

a- Domain predictions of PleC and DivJ reveal the presence of several potential transmembrane domains as well as PAS domains at the N-terminus of the proteins (SMART prediction - http://smart.embl-heidelberg.de).

b- Schematic representation of a Phostag molecule chelating a phosphate group in presence of two Mn^{2+} ions incorporated in a polyacrylamide gel.

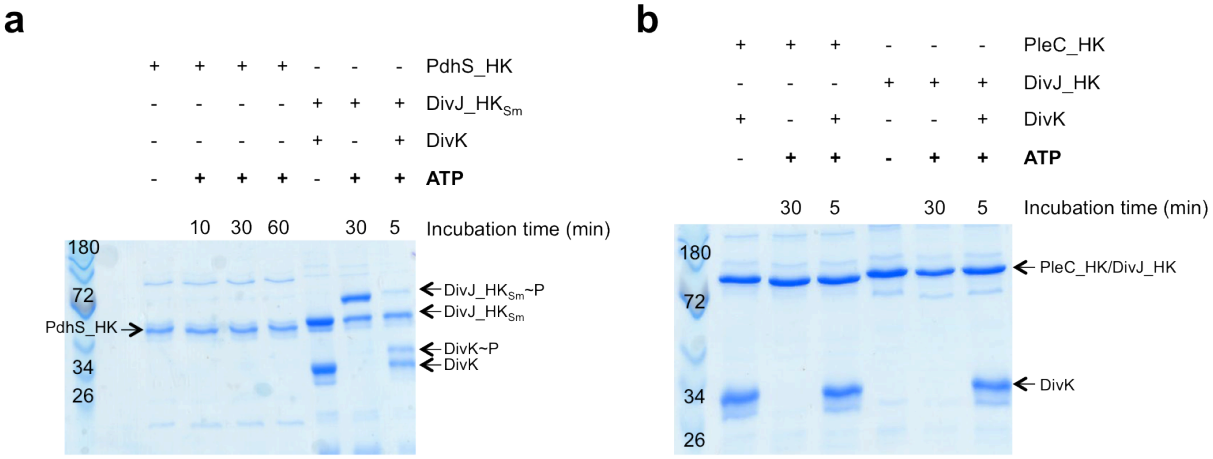

Figure 2- *In vitro* kinase assays on HK domains using Phostag gels

a- Lanes 1 and 5 are control lanes showing the migration of PdhS_HK (lane 1), DivJ_HK_{Sm} (lane 5) and DivK (lane 5) without ATP. Lanes 2, 3 and 4 show PdhS_HK migration profile after 10, 30 and 60 minutes of incubation with ATP. No difference is observed compared to lane 1. Incubating DivJ_HK_{Sm} with ATP resulted in a separation of the band into a phosphorylated form (upper band, DivJ_HK_{Sm}~P) and non-phosphorylated form (lower band) of the protein. When DivK is added to this mix, the band corresponding to DivJ_HK_{Sm}~P disappeared and concomitantly appeared a band corresponding to phosphorylated DivK (DivK~P).

b- Lanes 1 and 4 are control lanes showing the migration of PleC_HK (lane 1), DivK (lane 1) and DivJ_HK (lane 4) without ATP. Incubating either PleC_HK or DivJ_HK with ATP for 30 minutes did not change their migration profile. Adding DivK to either mix did not change its migration profile.

2. Attempts to investigate the activity of PleC and DivJ

A- Purification of the histidine kinase domains of PdhS, PleC and DivJ and kinase assays

As mentioned in the introduction, DivK phosphorylation status might be modulated not only by PdhS but also by PleC and DivJ membrane-associated HKs. Indeed, several transmembrane domains were predicted with SMARTool (Simple Modular Architecture Research Tool) for *B. abortus* PleC and DivJ (Figure 1-a). A first attempt to study the *in vitro* kinase activity of PdhS, PleC and DivJ was performed by purifying the histidine kinase domain (DHp+CA) of these proteins. Their autokinase activity was assayed using the Phostag technology (Barbieri and Stock, 2008). Phostag is a small molecule able to bind phosphate groups in the presence of Mn^{2+} or Zn^{2+} cations (Figure 1-b). When incorporated in a polyacrylamide gel, Phostag interacts with phosphorylated proteins and induces a shift in their migration (Figure 1-b). Migration on a Phostag gel of Trx-His_6-PdhS_HK (41.9 KDa), MBP-His_6-PleC_HK (72.84 KDa) and MBP-His_6-DivJ_HK (75.78 KDa) previously incubated with ATP did not induce a detectable shift of the band corresponding to each HK domain (Figure 2-a-b). Subsequently, no phosphotransfer to Trx-His_6-DivK (28.35 KDa) occurred either (Figure 2-b), suggesting that the purified kinase domains are not active. As a control for DivK phosphorylation, the purified Trx-His_6-DivJ_HK domain from *S. meliloti* (DivJ_HK_{Sm}) (45.57 KDa) was used as a phosphodonor. This kinase domain was able to autophosphorylate, as shown by the doubling of the corresponding band in presence of ATP, and to transfer the phosphate group to Trx-His_6-DivK from *B. abortus* (Figure 2-a). To rule out the possibility that the *B. abortus* purified HK domains might be active but lack a particular cofactor for their kinase activity, we checked whether they had a phosphatase activity towards DivK phosphorylated by DivJ_HK_{Sm}. No dephosphorylation of DivK~P was observed (data not shown), further confirming that the purified kinase domains are not active.

The lack of *in vitro* activity of these kinase domains is surprising, knowing that the autokinase activity of HKs is commonly tested on their purified HK domains. A possible explanation would be that the purified HK domains in our case are misfolded, resulting in inactive proteins. MBP-His_6-PleC_HK and MBP-His_6-DivJ_HK tended to precipitate quite easily. This observation is in line with the suggested hypothesis. Another explanation would be that a domain essential for the multimerization of these proteins is lacking in the purified truncated forms. This could indeed be the case for PdhS_HK as the D3 domain was shown to be involved in the interaction between two PdhS monomers (Van der Henst et al., 2012) and this domain is not present in the purified truncated form of PdhS (Introduction-Figure 20-b).

B- Purification of larger domains of PdhS, PleC and DivJ and kinase assays

Given the lack of activity of the HK domains, we went on and produced the full-length version of PdhS and the cytoplasmic domains of DivJ and PleC. Trx-His_6-PdhS (126 KDa) was readily soluble and easily purified (Manuscript-Figure S1). This was not the case for DivJ and PleC cytoplasmic domains. The solubility of several fusion proteins (His_6, Trx-His_6, MBP-His_6) was tested and several lysis methods were tried (sonication, cell disruptor, freezing-thawing cycles). Despite all these tested conditions, DivJ and PleC cytoplasmic domains were always collected in the insoluble fraction. Therefore their kinase activities could not be tested *in vitro*.

The kinase activity of the full-length version of Trx-His_6-PdhS was tested by Phostag. Although no shift in PdhS migration was observed after incubation with ATP, a short

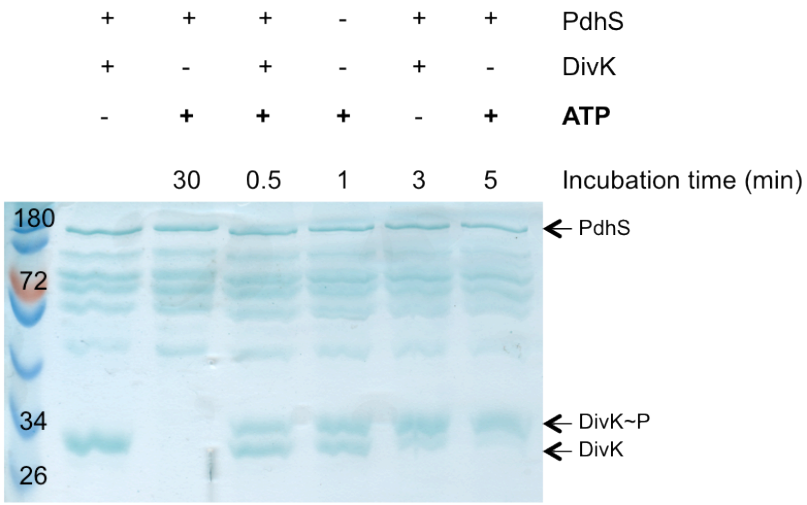

Figure 3- Autokinase assay on full-length PdhS and phosphotransfer to DivK
Lane 1 is a control lane showing the migration of PdhS and DivK without ATP. Incubating PdhS with ATP did not change its migration profile, but addition of DivK for 30 seconds induced a shift in DivK migration proving that PdhS can autophosphorylate and transfer its phosphate group to DivK.

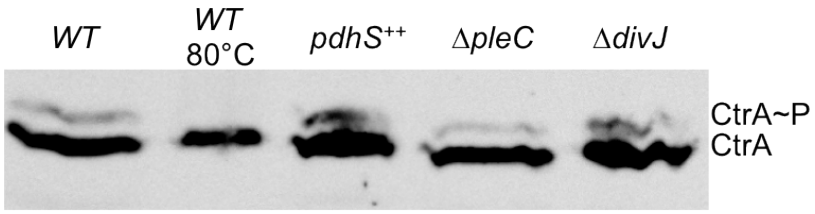

Figure 4- *In vivo* Phostag assay on *B. abortus* lysates and CtrA Western blot
Samples from four *B. abortus* strains were lysed and loaded on a Phostag gel without boiling. The upper band corresponds to phosphorylated CtrA as certified by the absence of this band when a sample of the WT strain was heated at 80°C.

incubation time (30 seconds) with Trx-His_6-DivK was sufficient to visualize a phosphorylation of the response regulator (Figure 3). This suggests that PdhS could autophosphorylate but the absence of a shift in its migration could be due to the big size of the protein. This Phostag assay on the full-length version of PdhS was performed before the radioactivity-based kinase assays presented in the paper.
Next we sought to determine the activity of PleC and DivJ *in vivo* by monitoring CtrA phosphorylation state (Figure 4). As already shown in the paper, overexpressing *pdhS* led to an increase in CtrA total amount as well as in the proportion of phosphorylated protein. These data suggest that PdhS could be a phosphatase for DivK, assuming that the TCS regulates the downstream phosphorelay in a similar manner to *C. crescentus*. Similar results are obtained in a Δ*divJ* strain, while deletion of *pleC* led to opposite results, with less phosphorylated CtrA compared to the WT (Figure 4). Two independent experiments were performed with the Δ*divJ* and the Δ*pleC* strains and the effects on CtrA amount and phosphorylation were reproducible. These observations suggest that DivJ might be a kinase for DivK while PleC might be its phosphatase, again assuming that the TCS regulates the downstream phosphorelay in a similar manner to *C. crescentus*. Quantitative Western blots should be performed to confirm these results.

3. The fumarase FumC interacts with PdhS and modulates its activity

PdhS has a long N-terminal cytoplasmic domain with no predicted function, except for a PAS domain. A combination of Y2H assays and a domain mapping of PdhS pointed out an interaction between domain D3 of PdhS and FumC (Introduction-Figure 20) (Mignolet et al., 2010; Van der Henst et al., 2012). FumC is a fumarase of the tricarboxylic acid (TCA) cycle catalysing the conversion of fumarate to malate by the incorporation of a molecule of water. The interaction between PdhS and FumC could serve as a link between cell cycle progression and metabolism. We sought to test whether FumC could affect PdhS autokinase activity by pre-incubating the two proteins together for 15 minutes prior to adding ATP. Given that PdhS phosphorylation cannot be visualized on a Phostag gel due to the absence of a shift in the migration, [^{32}γ-P]ATP was used instead to assay PdhS autokinase activity. The proportion of phosphorylated PdhS in the presence of FumC was quantified relatively to the condition without FumC (Figure 5). Pre-incubating PdhS with FumC reduced its autophosphorylation by 40%, suggesting that FumC inhibits PdhS autokinase activity. A pre-incubation of PdhS with either of FumC substrates (fumarate or malate) did not change its autokinase activity (data not shown). FumC did not prevent *E. coli* MBP-EnvZ autophosphorylation, showing that the effect on PdhS is specific. Given that the same domain (D3) is involved in PdhS multimerization and in its interaction with FumC, the fumarase could compete for the interaction with PdhS monomers. PdhS and FumC were mixed together at a 1:1 ratio. FumC forms homotetramers (Mignolet et al., 2010) while the multimerization status of PdhS is not known. A gel filtration should determine the multimerization status of PdhS and how the FumC and PdhS complexes are altered when both proteins are mixed together.

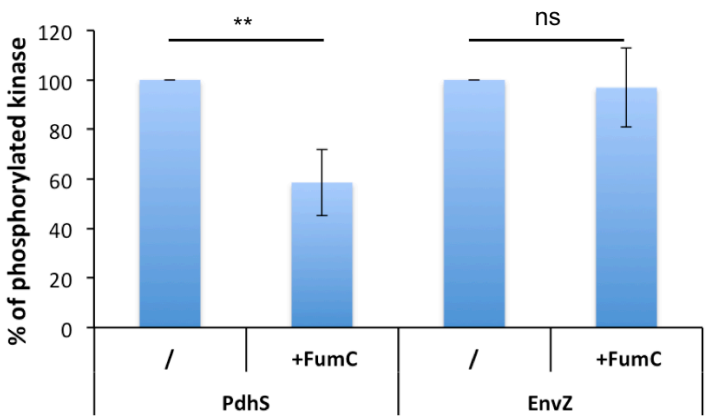

Figure 5- Relative quantification of PdhS and EnvZ autophosphorylation in presence of FumC

100% of autophosphorylation is attributed to the HK incubated by itself with ATP. The proportion of phosphorylated HK in presence of FumC is calculated relatively to the condition without FumC. PdhS autophosphorylation was highly significantly reduced in presence of FumC ($p < 0.01$ in a Student t test) while MBP-EnvZ activity remained unchanged (ns = not significant).

4. Monitoring the activity of CtrA target promoters in culture and infection

Most of the results presented in this section were obtained by Katy Poncin, a former master's student working under my supervision. Experiments related to *ctrA* promoter activity were performed by Luca Rappez, also a former master's student. One figure was taken from Katy's master thesis.

A- Constructing a reporter system

In *C. crescentus*, the activity of CtrA-regulated promoters varies during the cell cycle (Laub et al., 2000). For instance, *ccrM* and flagellar genes are expressed in the late S phase while *sciP* is transcribed in flagellated cells (Gora et al., 2010; Zweiger et al., 1994). It is easy to follow their activities along the cell cycle using *lacZ*-based reporter systems given that the *C. crescentus* strains used in the laboratories are synchronizable (Evinger and Agabian, 1977). In *B. abortus*, the absence of a synchronization protocol raises a real technical challenge to study cell cycle-related processes. In order to monitor the activity of CtrA target genes, we had to resort to a single-cell level technique. We fused promoters of interest to a gene coding for an unstable allele of GFP, the GFP-ASV, and monitored their activity by fluorescence microscopy. The C-terminal ASV tag (Alanine-Serine-Valine) is thought to be recognized by endogenous proteases in *E. coli* and *Pseudomonas putida,* rendering the GFP less stable (Andersen et al., 1998). The use of an unstable version of the GFP is important for monitoring promoter activity, as a stable fluorescent reporter will continue to emit a signal for a longer time after the promoter is turned off. The half-life of GFP-ASV is not known in *B. abortus* and it is likely that it is different from its half-life in *E. coli.* However, we reasoned that it should be degraded faster that the WT version of the protein.

Each target promoter p_{target}-*gfp*(ASV) construct was cloned in a pBBR-MCS1 vector, a replicative medium copy plasmid in *B. abortus*. The p_{target}-*gfp*(ASV) fusions were also cloned in the low copy vector pMR10 but the fluorescence signal produced was very low and could therefore not be analysed. The obtained *B. abortus* strains were imaged under the microscope and the mean fluorescence intensity was quantified in a large number of bacteria (Figure 6) using MicrobeTracker image analysis program (Sliusarenko et al., 2011). Briefly, this program defines the contours of bacteria and determines their cell length (in µm), divides each bacterium into segments and quantifies the fluorescence intensity associated to each segment. The mean fluorescence intensity for one bacterium can then be calculated.

B- Monitoring promoter activity in culture

We decided to monitor the activity of *repAB* (chromosome II replication and segregation), *ccrM* (DNA methyltransferase), *ctrA* (master regulator) and *pleC* (histidine kinase) promoters. We asked whether the activity of *ctrA* and *ccrM* promoters (p_{ctrA} and p_{ccrM}) oscillates during the cell cycle in a similar manner to *C. crescentus*. Given that chromosome replication is coupled to growth and division in *B. abortus*, we postulated that the expression of the genes coding for chromosome II replication and segregation machinery is also cell cycle regulated. Furthermore, it was already shown that chromosome II replication starts around the middle of the cell cycle (Deghelt et al., 2014). We chose to monitor the activity of *repAB* promoter (p_{repAB}) because it contains a conserved 9-mer box. Later, the ChIP-seq data showed that this region was weakly

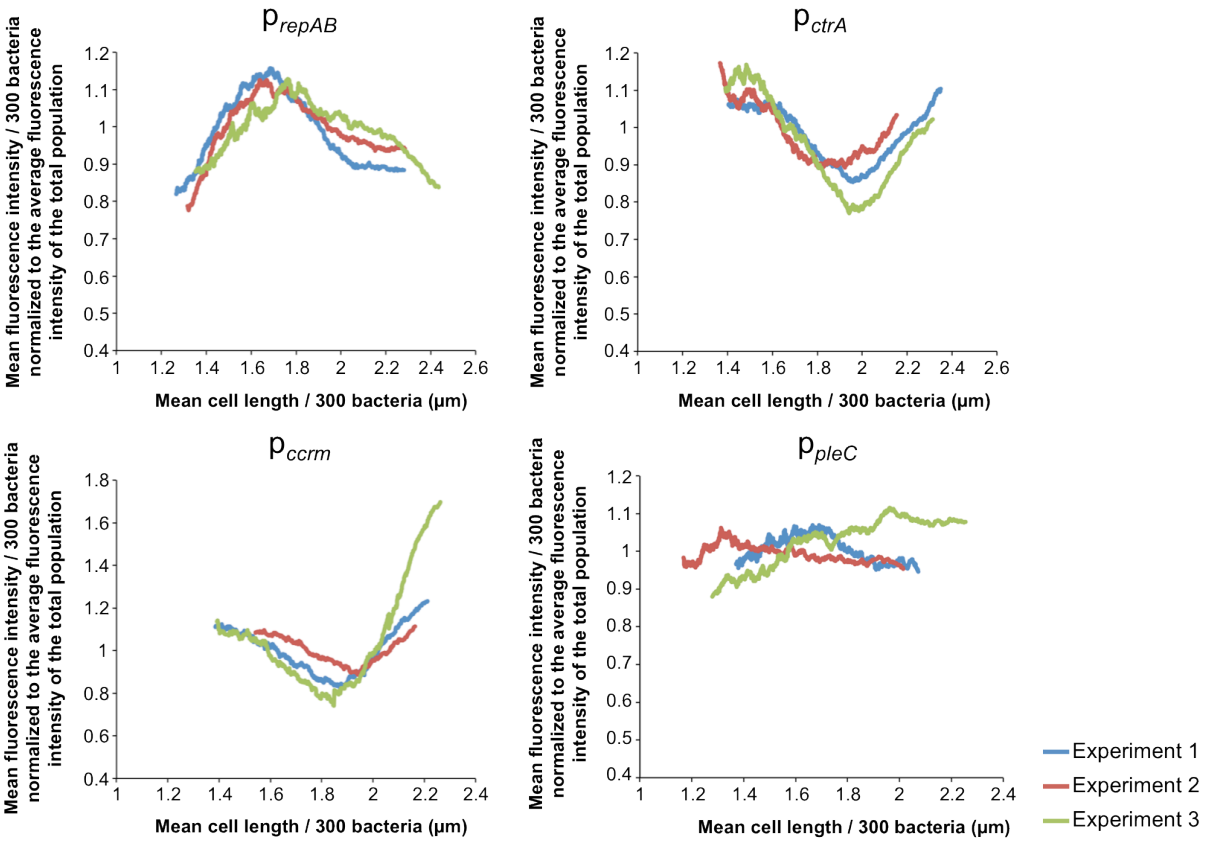

Figure 6- Activity profile of CtrA target promoters in culture

The plots represent the mean fluorescence intensity produced by a GFP as a function of bacterial cell length. The expression of the *gfp*(ASV) reporter is under the control of four promoters indicated above the plots. The results of three independent experiments are shown. The number of bacteria analysed for p_{repAB} are 1632, 1402 and 2377; for p_{ctrA} 1456, 1487 and 1467; for p_{ccrM} 1446, 753 and 1678; for p_{pleC} 1888, 1297 and 1953.

bound by CtrA *in vivo* (Manuscript-Figure 7). Finally, what prompted us to monitor *pleC* promoter (p_{pleC}) activity were the presence of a consensus 9-mer sequence and the fact that it was bound by phosphorylated CtrA *in vitro* (Bellefontaine et al., 2002). ChIP-seq data obtained later showed that CtrA did not bind p_{pleC} in an exponential phase culture of *B. abortus* grown in rich medium.

We had to face many technical challenges due to the asynchrony of the studied populations and to the high variability in the fluorescence intensity of the reporter strain. Figure 8 shows the standard deviation calculated for p_{repAB} reporter system as an example of the high variability in the measured fluorescence intensity. First, to bypass the problem of asynchrony, we ordered the bacteria according to their length, from the smallest to the largest and plotted the fluorescence intensity as a function of the cell length. We reasoned that bacteria of small size would be at the beginning of their cell cycle (that is in G1 phase) whereas the largest bacteria would be predivisional cells. Second, to analyse the fluorescence signal despite the high variability in the population, we plotted the mean fluorescence intensity for a sliding window of 300 bacteria. Finally, to compare independent experiments, we normalized the mean fluorescence intensity/300 bacteria to the average fluorescence intensity of the total population (Figure 6).
Several factors could have contributed to the high variability of the fluorescence intensity. First, the use of a replicative plasmid can lead to an unequal segregation of the vector between the daughter cells, and thus to a variable copy number of the p_{target}-*gfp*(ASV) fusion. Second, ordering bacteria according to their cell size does not account for the cell cycle stage in a precise way. Bacteria of the same size could be in different stages of their cell cycle.

The plots in Figure 6 show a reproducible variation of the fluorescence intensity for p_{ccrM}, p_{ctrA} and p_{repAB} but not for p_{pleC}. The p_{ccrM} and p_{ctrA} activity profiles are similar with a minimal fluorescence intensity in bacteria of intermediate cell length. p_{ccrM} activity profile is similar to the one in *C. crescentus* where CcrM is produced in late S phase to methylate the newly synthesized DNA strands. The high level of fluorescence intensity in small *B. abortus* cells could be due to residual GFP synthesized in the previous predivisional cells but not yet degraded. The decrease in the fluorescence intensity in bacteria of intermediate cell length suggests that the promoter is off during the early stages of the cell cycle. In *C. crescentus*, *ctrA* is transcribed during the S phase, first by the weak P1 promoter and then by the strong P2 promoter (Introduction paragraph A-2-e of Chapter II). *B. abortus* p_{ctrA} seems to be active in large bacteria. Bacteria of small size also harbour a high level of fluorescence, probably due, as for p_{ccrM}, to residual GFP. As for p_{repAB}, it seems to have an activity profile opposite to p_{ccrM} and p_{ctrA}, as a peak in fluorescence intensity is observed for bacteria of intermediate cell length. The profile suggests that the promoter is active in medium size bacteria probably allowing chromosome II replication and segregation. The promoter is probably less active later in the cell cycle as shown by a decrease in the fluorescence intensity. Finally, the p_{pleC}-*gfp*(ASV) fusion did not show a reproducible variation of the fluorescence intensity, suggesting that the activity of this promoter is not regulated throughout the cell cycle. In *C. crescentus*, p_{pleC} activity is directly or indirectly regulated by GcrA but the PleC protein amount remains stable throughout the cell cycle (Holtzendorff et al., 2004; Wheeler and Shapiro, 1999).

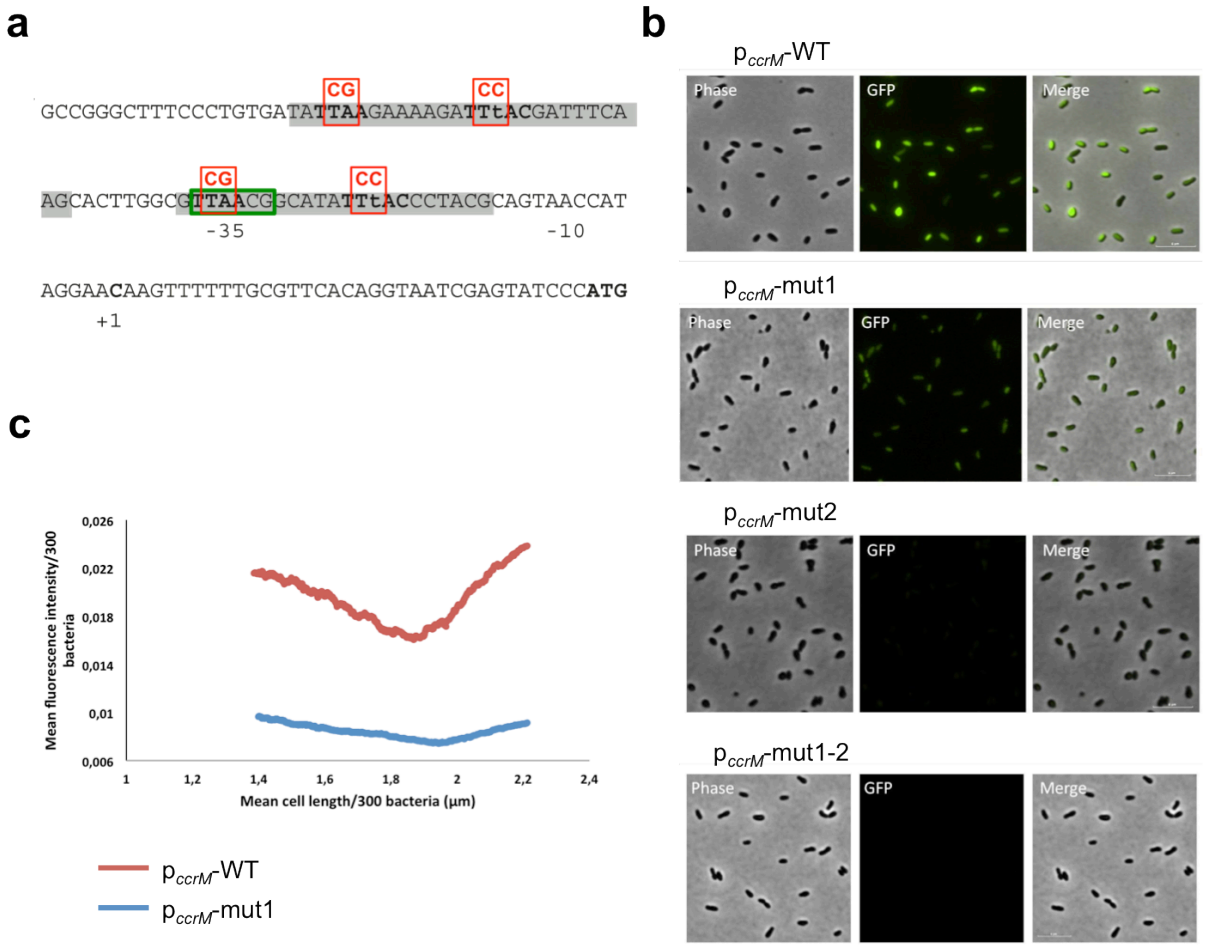

Figure 7- The *ccrM* promoter (p_{ccrM}) activity in culture

a) Sequence of *ccrM* promoter. Letters in bold correspond to the CtrA predicted 9-mer boxes. Shaded grey background highlights the regions protected by CtrA in a DNase I footprint assay. Red letters represent the mutations introduced in the reporter construct. The green box highlights the -35 box (Bellefontaine et al., 2002).

b) Images taken by fluorescence microscopy of the *B. abortus* p_{ccrM} reporter strains carrying the *WT* promoter (p_{ccrM} -WT), the promoter mutated in the first 9-mer box (p_{ccrM} -mut1), the promoter mutated in the second 9-mer box (p_{ccrM} -mut2) and the promoter mutated in both 9-mer boxes (p_{ccrM} -mut1-2). Scale bars = 5µm (Pictures taken from K. Poncin's master thesis).

c) Plot representing the activity profile of p_{ccrM} –WT and p_{ccrM} -mut1.

Next, we asked whether the differences in the fluorescence intensity observed for p_{ccrM}, p_{ctrA} and p_{repAB} between small, intermediate and large bacteria were significant (Manuscript-Figure 8). These classes were defined independently for each promoter based on the activity profiles shown in Figure 6. Fluorescence intensity was significantly higher in intermediate bacteria compared to small and large bacteria when *gfp*(ASV) was expressed under the control of p_{repAB} ($p < 0.05$ and $p < 0.01$ in pairwise comparisons according to Scheffe analysis). On the contrary, it was highly significantly lower in intermediate bacteria in the p_{ctrA} reporter strain ($p < 0.01$) (Manuscript-Figure 8). Differences in fluorescence intensity between length classes observed in the p_{ccrM} reporter strain were not significant, probably because of the high variability between the three independent experiments.
These data suggest that the activity of at least three CtrA-bound promoters are cell cycle-regulated, indicating that, as in *C. crescentus*, CtrA phosphorylation and amount could also vary along *B. abortus* development.

C- Monitoring promoter activity in culture with mutated CtrA binding sites

Next we asked whether the variations in the activity of p_{ccrM} and p_{repAB} were due to CtrA binding to the conserved consensus sequences present in these promoters. We thus disrupted the consensus binding sites by mutating the two central nucleotides of each of the TTAA half sites (Figure 7-a). T was replaced by C and A was replaced by G.
The p_{ccrM} has two predicted 9-mer binding sites and phosphorylated CtrA was previously shown to bind these sequences *in vitro* (Bellefontaine et al., 2002) (Figure 7-a). Therefore, we sought to mutate each of these consensus sequences separately (p_{ccrM}-mut1 and p_{ccrM}-mut2) and together (p_{ccrM}-mut1-2) in the reporter construct. Red letters above the sequence of the promoter indicate introduced mutations (Figure 7-a). The first TTAA half site of the second 9-mer box overlaps the -35 box highlighted by a green rectangle (Figure 7-a). We made sure that the introduced mutations were still consistent with -35 box consensus sequence known in *E. coli*.
Fluorescence microscopy images showed reduced fluorescence intensity when the first box was mutated and a complete loss of fluorescence when the second box or when both boxes were mutated (Figure 7-b). Plotting the mean fluorescence intensity of p_{ccrM}-mut1 together with p_{ccrM}-WT showed that the mutated version of the reporter system retained a "cell cycle"-regulated activity but with a general reduction of the *gfp*(ASV) expression level, suggesting a CtrA-dependent perturbation of the promoter activity (Figure 7-c). The absence of fluorescence in the p_{ccrM}-mut2 and p_{ccrM}-mut1-2 reporter constructs could be due to the disruption of the -35 box or to an abolishment of CtrA binding. We could indeed suggest a hierarchical cooperative binding of CtrA to p_{ccrM} similar to the one observed for binding sites [a] and [b] in *C. crescentus* origin of replication (Introduction-Figure 10-a). In *B. abortus* p_{ccrM}, the two regions protected by CtrA in the DNase I footprint assay are separated by 8 nucleotides (Figure 7-a). The dimers binding each consensus sequence could thus interact with each other and enhance their binding to DNA. The mutations introduced in our reporter system suggest that the second consensus sequence could be more important for CtrA binding to this promoter and that CtrA binding to the first 9-mer box is mediated by the second.

The p_{repAB} contains one 9-mer box that coincides with a region weakly bound by CtrA in the ChIP-seq assay (Manuscript-Figure 7). This consensus sequence was mutated in a similar manner to p_{ccrM} consensus sequences, where the central TA nucleotides of each TTAA half site were replaced by CG nucleotides. Mutating the 9-mer box in p_{repAB}

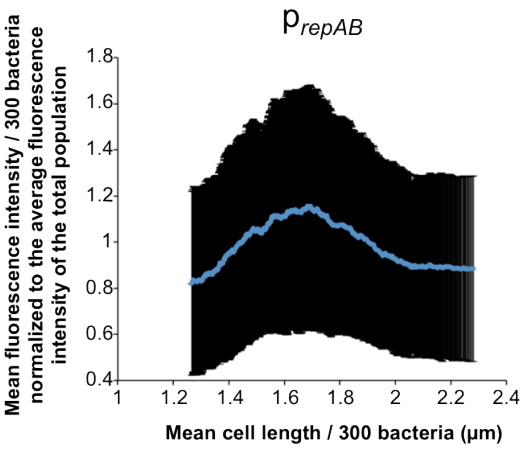

Figure 8- Normalized standard deviation of the p_{repAB} reporter system
Standard deviation of the mean fluorescence intensity was calculated in a sliding window of 300 bacteria and normalized to the average fluorescence intensity of the whole population.

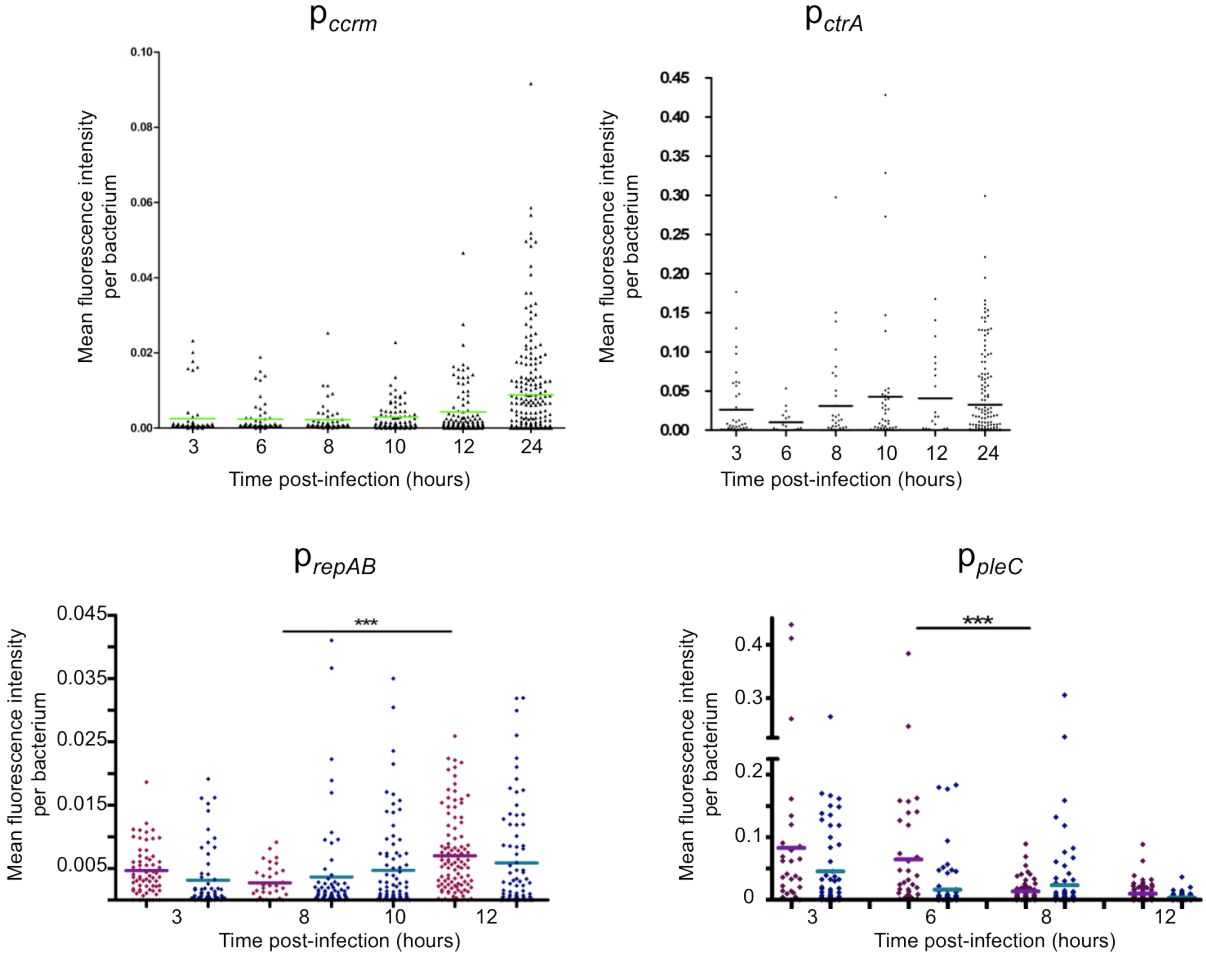

Figure 9- Activity profile of CtrA target promoters in a HeLa cell infection
These plots represent the variation of the fluorescence intensity during infection. Each dot represents the mean fluorescence intensity in one bacterium at a particular time of the infection. The results of two independent experiments are shown for p_{repAB} and p_{pleC} (pink and blue). Horizontal bars represent the average fluorescence intensity for a particular time PI.

resulted in a complete loss of the fluorescence signal, suggesting an important perturbation of the promoter activity (data not shown). The mutations could have perturbed the binding of CtrA as well as of other transcription factors to this promoter.

D- Monitoring promoter activity in infection

B. abortus strains carrying the reporter systems were used to infect HeLa cells. The mean fluorescence intensity was quantified for a number of bacteria (50 to 100) at different times post-infection (PI) (Figure 9). We chose early times PI (3 to 8 h) corresponding to the early non-proliferative phase and late times PI (10 to 24 h) corresponding to the proliferative phase of the infection. Each dot on the plots represents the mean fluorescence intensity measured in a single bacterium (Figure 9). As for the culture condition, the fluorescence intensity was highly variable in the population. No significant change in the activity of p_{ccrM} and p_{ctrA} was observed during infection suggesting that, unlike in culture, these promoters might not be subjected to a tight regulation during infection. Alternatively, the activity of these promoters could be differentially regulated in HeLa cells but the oscillations of the promoters activities are not detectable with our reporter system due to the variability in the fluorescence intensity in the population. This high variability in the fluorescence intensity could be due either to the reporter system itself or to different environmental conditions encountered by the intracellular bacteria that could lead to different expression levels of the *gfp*(ASV). Also, the GFP-ASV could be stabilized in infection, especially during the early hours. The results of two independent experiments show the activity profile of p_{repAB} and p_{pleC} (Figure 9-pink and blue). These two promoters seem to have opposite activities during infection, with p_{repAB} being mostly active in the late hours while p_{pleC} shows a maximal activity at 3 and 6 h PI. p_{repAB} activity increases between 8 and 10 h PI while p_{pleC} activity decreases between 3 and 8 h PI. The two independent experiments show a reproducible overall profile but the differences are not always significant, demonstrating again the limits of this reporter system. Finally, the presence of extracellular bacteria, not yet eliminated by the gentamycin treatment, can complicate the interpretation of the data collected at 3 h PI, maybe contributing to the high variability of the data at this time point.

5. Investigating the role of CtrA in maintaining the envelope homeostasis

The classification of CtrA potential target genes identified by ChIP-seq highlighted two highly represented functional categories: cell cycle and envelope biogenesis and homeostasis. Genes related to these two categories represent 2.6% and 3.3% of the whole *B. abortus* genome respectively. Among CtrA targets, they represent 11.5% and 33.3% of the total number of genes identified by ChIP-seq, showing a highly significant enrichment of genes belonging to these two functional categories among CtrA potential regulon ($p < 0.001$ in a χ^2 analysis). Among the targets related to envelope biogenesis and homeostasis were genes involved in peptidoglycan (PG) synthesis, LPS insertion in the outer membrane, the Tol-Pal system and outer membrane proteins (OMPs). Perturbing the expression of these genes could lead to important changes in the envelope composition and stability. We therefore sought to test the stability of *B. abortus* envelope after several hours of CtrA depletion by performing a polymyxin B

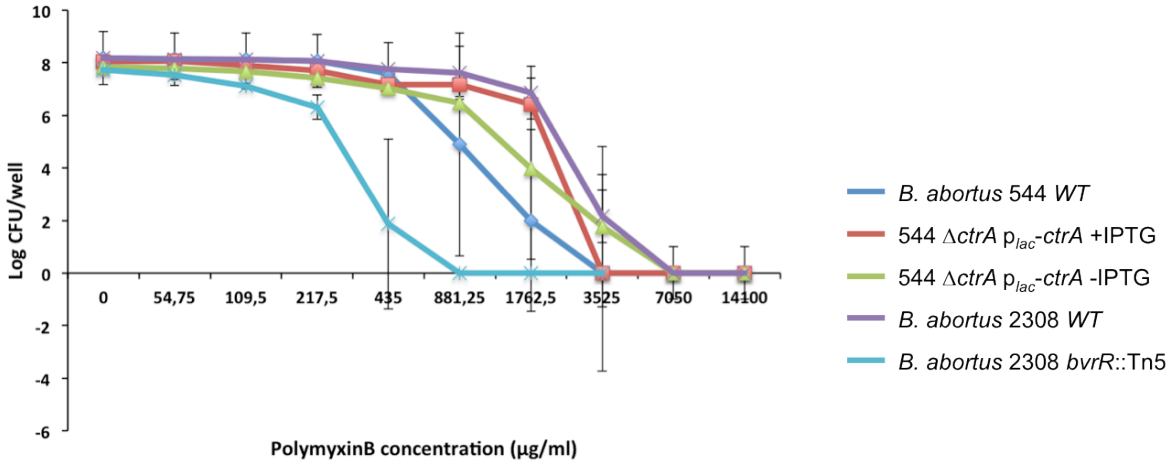

Figure 10- Survival curves of *B. abortus* 544 and 2308 WT and mutant strains to polymyxin B

The number of CFU collected from each well after a one-hour incubation with different concentrations of polymyxin B is represented on a logarithmic scale. Error bars represent the standard deviation from the average of a triplicate.

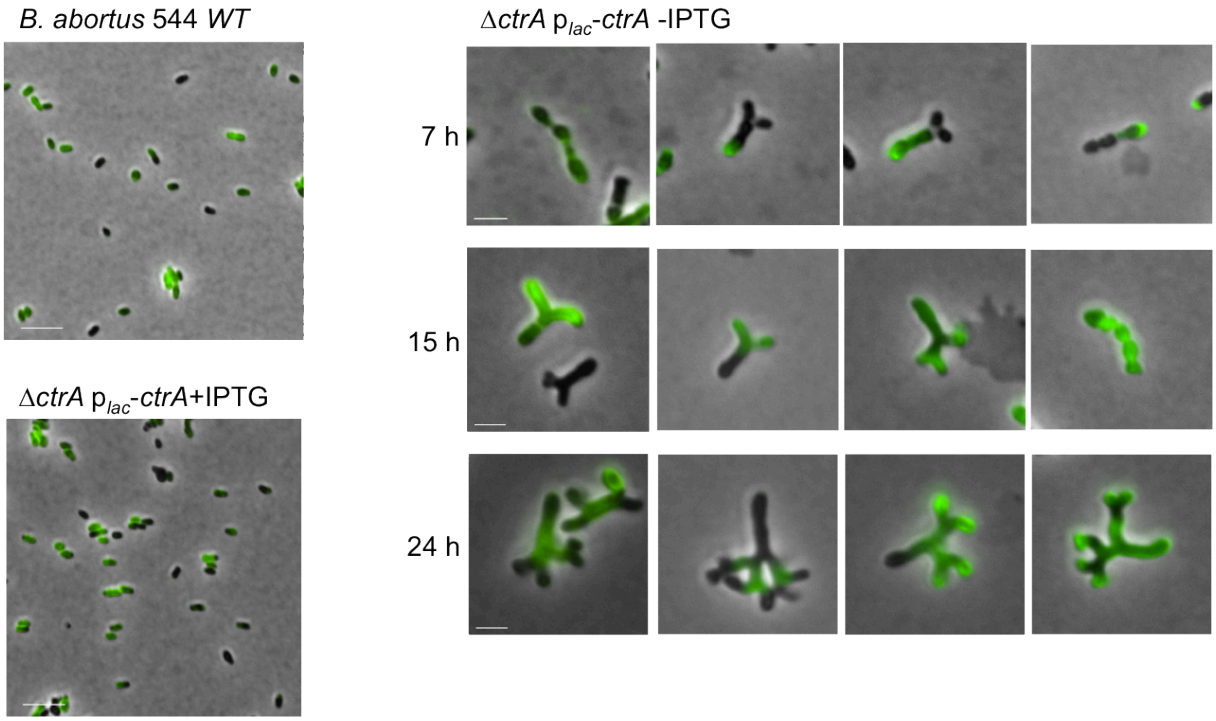

Figure 11- Omp25 localization in *B. abortus* 544 *WT* and the CtrA depletion strain

Phase contrast and fluorescence microscopy images of *B. abortus* cells labelled with an Omp25 monoclonal antibody. Scale bars of pictures on the left = 5µm; scale bars of pictures on the right = 2µm.

sensitivity assay. Western blots using monoclonal antibodies recognizing OMPs showed a decrease in Omp25 amount after an overnight CtrA depletion (Manuscript-Figure 9). We asked whether this decrease in the amount of protein was accompanied by an alteration of its localization pattern in the envelope.

A- Testing the sensitivity of the CtrA depletion strain to polymyxin B

B. abortus is known to have an envelope resistant to antimicrobial cationic peptides such as polymyxin B thanks to the unique composition of its LPS (Martinez de Tejada et al., 1995). We tested whether a 4-hour and an 8-hour CtrA depletion would render *B. abortus* less resistant to polymyxin B compared to the *B. abortus* 544 WT strain and the CtrA depletion strain cultivated in presence of IPTG. As a control of sensitivity to this cationic peptide, we performed the assay in parallel on a *B. abortus* 2308 *bvrR*::Tn5 strain (known to have an increased sensitivity to polymyxin B) and the corresponding WT strain *B. abortus* 2308 (Sola-Landa et al., 1998). In practice, a sample of each strain is collected at a given time, diluted in a saline buffer and incubated in a 96-well plate with increasing concentrations of polymyxin B for one hour at 37°C (for details, see protocol in the Material and methods section). Bacteria are then plated on rich medium supplemented with the appropriate antibiotic and IPTG if needed. Figure 10 represents the survival curves of the different strains to increasing concentrations of polymyxin B. As expected, the *bvrR* mutant is less resistant than the WT strain. Also, the *B. abortus* 2308 WT strain is more resistant than the 544 WT strain. However, the CtrA depletion strain grown with IPTG or without IPTG for 4 h does not show any decrease in its resistance to polymyxin B (Figure 10). On the contrary, it is even slightly more resistant than the 544 WT strain. An 8-h CtrA depletion did not increase *B. abortus* sensitivity to polymyxin B either (data not shown). Thus, in these conditions, bacteria lacking CtrA are not more sensitive to polymyxin B. Before excluding the possibility that *B. abortus* envelope is destabilized in absence of CtrA, we should test its resistance to other harmful agents such as the detergent deoxycholate or other cationic peptides such as poly L-lysine or poly L-ornithine.

B- Localizing Omp25 in the CtrA depletion strain

The decrease in Omp25 amount after 15 and 24 h of CtrA depletion (Manuscript-Figure 9) prompted us to check whether its localization in the envelope was also perturbed. Bacteria were labelled with monoclonal antibodies (MAb) A68/04B10/F05 recognizing Omp25 (Cloeckaert et al., 1990) and secondary antibodies coupled to Alexa Fluor 488 after 7, 15 and 24 h of CtrA depletion. *B. abortus* WT strain and the depletion strain grown with IPTG showed a heterogeneous expression of Omp25 in the population, some bacteria being completely or partially labelled while others had no Omp25 labelling at all (Figure 11). In the CtrA-depleted condition, Omp25 expression was also heterogeneous with some bacteria lacking any fluorescent signal while others were partially labelled with a segmented labelling pattern. However, the immunofluorescence labelling of Omp25 does not seem to confirm the dramatic decrease in Omp25 amount observed by Western blot as a high proportion of the population still showed at least partial labelling for Omp25 (73% and 70% of bacteria after 15 h and 24 h of depletion). The MAb used for immunofluorescence and Western blot is more efficient at recognizing a structural epitope of Omp25 presented at the surface of the bacterium than linear epitopes in the denatured form of the protein (Cloeckaert et al., 1996). Furthermore, *Brucella* are known to produce several homologs of Omp25 (OMPs of group 3)

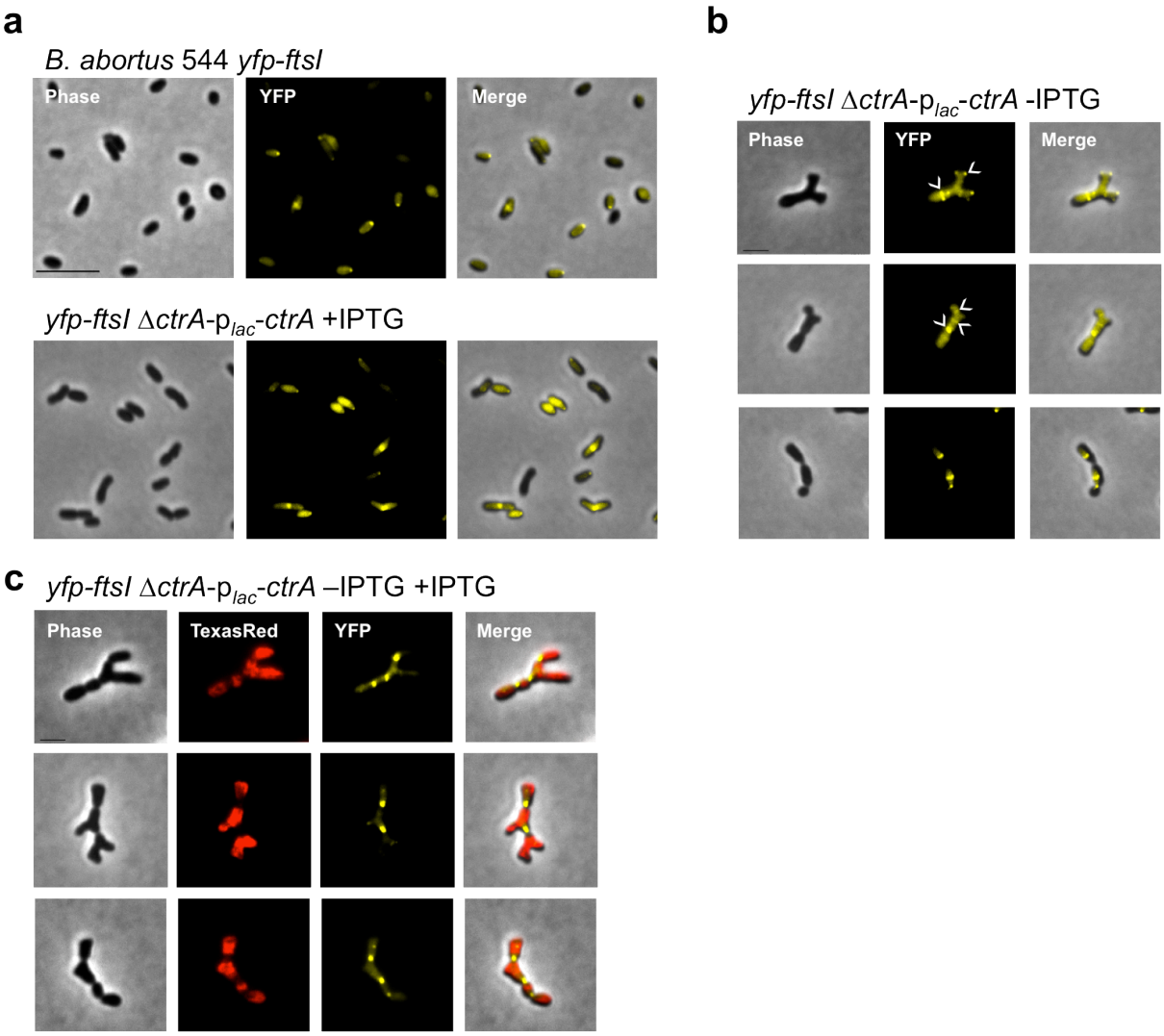

Figure 12- Localization of a YFP-FtsI fusion in *B. abortus* 544 and in the CtrA depletion strain

a) Phase contrast and fluorescence microscopy of the *B. abortus* 544 strain and the CtrA depletion strain grown with IPTG producing a YFP-FtsI fusion; scale bar = 5 µm.

b) Phase contrast and fluorescence microscopy of the CtrA depletion strain producing a YFP-FtsI fusion grown without IPTG for 7 h; scale bar = 2 µm.

c) Phase contrast and fluorescence microscopy of the CtrA depletion strain producing a YFP-FtsI fusion grown overnight without IPTG, labelled with TRSE and repleted with IPTG for 3 h; scale bar = 2 µm.

(Edmonds et al., 2002; Guzman-Verri et al., 2002) and another Omp25 MAb recognizes a similar structural epitope present in several Omp25 homologs (Salhi et al., 2003). It is thus possible that the MAb used here recognizes several Omp25 homologs on live bacteria but only the Omp25 of interest by Western blot. If this is the case, it is impossible to monitor the localization of the single Omp25 homolog (BAB1_0722) as a function of CtrA presence.
The segmented pattern of Omp25 homolog(s) labelling suggests that *omp25* gene(s) follow(s) an ON-and-OFF expression profile that is regulated in time as attested by the labelling of the bacterial branches 24 h post-IPTG removal (Figure 11). Indeed, this segmented pattern is identical in the different branches of a single bacterium, suggesting that the synthesis and the insertion of Omp25 into the outer membrane are synchronized in the different branches of the cell. Furthermore, these observations suggest that Omp25 does not move laterally in the outer membrane, which is in line with former suggestions that Omp25 might be anchored to the PG (Cloeckaert et al., 1995). This expression profile is probably independent of CtrA as it is different from one bacterium to another and could be due to a regulation coming from the BvrS/BvrR two-component system (Guzman-Verri et al., 2002).

C- Localizing the growth machinery in the CtrA depletion strain

Investigating *B. abortus* unipolar growth was part of a project conducted by Michael Deghelt, a former PhD student in the lab. He was interested in characterizing the mechanisms of *B. abortus* unipolar growth by localizing components of the growth machinery, in particular FtsI, the unique monofunctional penicillin binding protein (PBP) with a transpeptidase activity in *B. abortus*. In bacteria showing a dispersed mode of growth (along the cell body) such as *E. coli*, two paralogous monofuntional transpeptidases are present, PBP2 involved in elongation, and FtsI dedicated to division. *B. abortus* lacks a PBP2 homolog thus FtsI could be involved in both elongation and division. A chromosomal *yfp-ftsI* fusion shows a localization of the protein to the new pole and to the site of division, suggesting indeed a role of FtsI in elongation and division (M. Deghelt thesis). We decided to make use of the YFP-FtsI fusion to localize the growth machinery in a CtrA-depleted strain. In the *B. abortus* 544 WT strain and in the depletion strain grown with IPTG, bacteria displayed a single focus, either at the pole or at the septum (Figure 12-a). However, many bacteria did not show any fluorescence. In the CtrA-depleted condition, 7 h post IPTG removal, bacteria displayed several foci localized to the tip of the branches, to the base of the branches or along the cell body (Figure 12-b). They also localized to the septum and along the cell body of “chains”. As expected, localization of YFP-FtsI to the poles suggests the growth machinery is directed towards the elongating branches. Foci present along the cell body of chains and branched bacteria either co-localize with a visible constriction site or not. These foci probably correspond to division events that were initiated but blocked before completion. This hypothesis suggests that the Z ring was formed at these constriction sites and therefore that CtrA depletion does not result in the absence FtsZ, at least in these cells. Indeed, these localization patterns clearly show that at least part of the growth machinery is localized along the cell body to perform division. However, components essential for either constriction or daughter cell separation are missing. Furthermore, the growth machinery is often mislocalized. When TRSE-labelled bacteria are allowed to grow again in IPTG-supplemented medium for 3 h after an overnight CtrA depletion, they show constriction sites lacking TRSE labelling and co-localizing with YFP-FtsI foci (Figure 12-c). These data confirm that the CtrA “depletion phenotype” is reversible and that CtrA

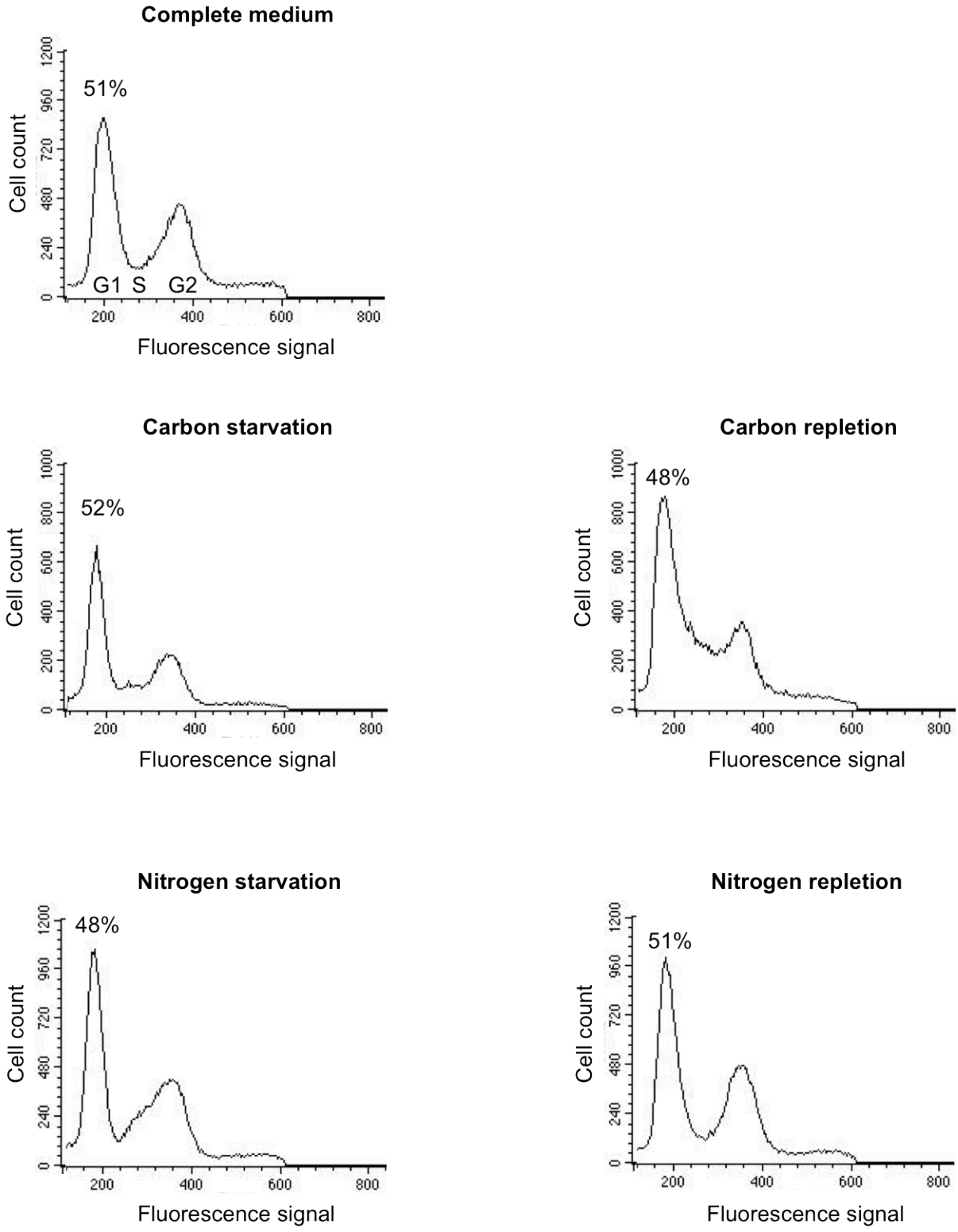

Figure 13- DNA content analysis of *B. abortus* 544 grown in Plommet defined medium depleted in nitrogen or carbon source

Flow cytometry results show the DNA content (Fluorescence signal) in *B. abortus* grown overnight in complete Plommet medium, then shifted for 3 h in the same medium depleted in nitrogen or carbon source (left panels). Bacteria are incubated again in complete Plommet medium for 3 h (right panels).

presence is essential for division. Interestingly, the YFP-FtsI foci found at the new division sites were brighter than those observed before repletion or even in the control conditions (Figure 12-a-b).

6. Attempts to synchronize *Brucella abortus*

Synchronizing *Brucella abortus* is essential to address questions related to cell cycle regulation. The technical difficulties we encountered while monitoring the activity of CtrA target promoters testify for the importance of a synchronization protocol. This is why we decided at the beginning of this project to develop a protocol allowing the enrichment of *B. abortus* cultures in G1 bacteria. In *C. crescentus*, the differential production of a capsule along the cell cycle renders flagellated cells more dense than stalked cells and predivisional cells (Ardissone et al., 2014; Evinger and Agabian, 1977). *B. abortus* cells do not display a difference in their buoyancy (J. Mignolet, unpublished); it is therefore impossible to separate bacterial subtypes on a density gradient. In *E. coli* and *C. crescentus,* nutrient starvation (carbon or nitrogen starvation) was shown to enrich the cultures in G1-phase bacteria (England et al., 2010; Lesley and Shapiro, 2008; Marsh and Hepburn, 1980). We decided to starve *B. abortus* for carbon and nitrogen sources separately and analyse their DNA content by flow cytometry to check for G1 enrichment. We cultivated *B. abortus* in a defined medium called Plommet containing phosphate, sodium and sulphate salts, vitamins and erythritol as sole carbon source (Plommet, 1991). After an overnight growth in complete Plommet medium, bacteria were diluted in Plommet lacking vitamins and salts containing nitrogen. In another experiment, erythritol was removed from the medium to induce carbon starvation. Bacteria were incubated in these nutrient-deficient media for 3 and 6 h and DNA content was analysed by flow cytometry. Data are shown for 3 h of nutrient starvation (Figure 13). After an overnight growth in complete Plommet medium, around 50% of bacteria were in G1 phase. After 3 or 6 h hours of nitrogen or carbon starvation, no enrichment in G1-phase bacteria was observed in the tested conditions (Figure 13). DNA content profiles suggest a complete arrest in the cell cycle, as most bacteria seem to remain in the same stage as prior to starvation induction. Adding back the missing nutrients and letting bacteria grow for 3 h did not change the DNA content profile of the population either (Figure 13). It could be that a 3-h repletion is too long, a steady state being already reached, and shorter times could be tested in the future.

Discussion and perspectives

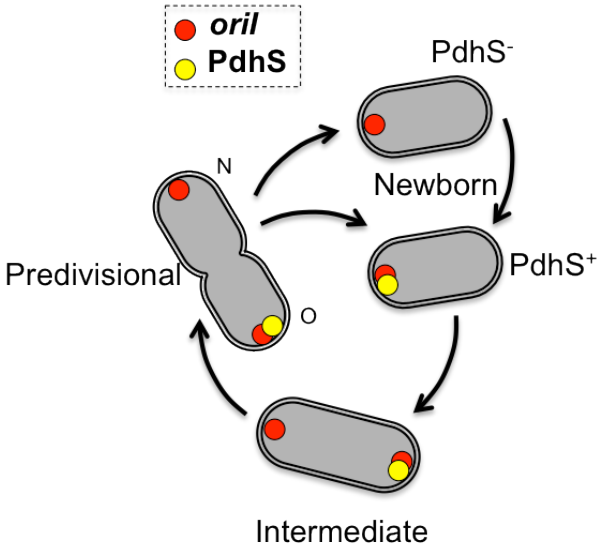

Figure 1- Polar localization of PdhS and the origin of replication of chromosome I
Schematic representation of *B. abortus* cell cycle and polar localization of the origin of replication of chromosome I (*oriI*) and PdhS. In newborn cells *oriI* is localized to the old pole of the two cells while PdhS is polarly localized in one of the two daughter cells immediately after division. The PdhS$^-$ cell acquires a polar focus after some time. In intermediate and predivisional cells, chromosome replication has started and the new *oriI* is segregated to the new pole (N) while a copy of the *oriI* remains at the old pole (O).

1. The PdhS/DivJ/PleC-DivK TCS

A- The TCS in *B. abortus*

The extensive study of the phosphorylation cascade upstream of CtrA in *C. crescentus* provided multiple evidences of the importance of dynamic protein localization for cell cycle progression. For instance, the localization of the hybrid histidine kinase CckA to the flagellated pole in predivisional cells is crucial for its activation. Predivisional cells harbour indeed a high level of phosphorylated DivK known to sequester DivL (Introduction-Figure 8-b). However, dephosphorylation of DivK by PleC at the flagellated pole frees DivL allowing its interaction with CckA in this specific "subcompartment" of the cells (Tsokos et al., 2011). The localization of PleC and DivJ to opposite poles ensures the inheritance by the daughter cells of distinct protein pools with distinct DivK phosphorylation states (Matroule et al., 2004).

In *B. abortus*, PdhS localizes to the old pole (Hallez et al., 2007). Thus after division, the large cell is the only daughter cell to inherit this polarly localized kinase and probably its activity (Figure 1). Figure 1 depicts the polar localization of PdhS and the origin of replication of chromosome I (*oriI*). The small cell generated after division is devoid of a focus of PdhS but acquires one at its old pole after some time (60-120 min in a time lapse performed at RT) (Figure 1) (Hallez et al., 2007). DivK co-localizes with PdhS to the old pole (Hallez et al., 2007) and when a *B. abortus* strain expressing a thermosensitive allele of *pdhS* is shifted to the restrictive temperature, DivK polar localization is lost (Van der Henst et al., 2012). These data clearly suggest that PdhS influences DivK localization *in vivo*. A non-phosphorylatable allele of DivK (D53A) fused to a fluorescent protein does not localize to the pole, suggesting that DivK polar localization depends on its phosphorylation (Hallez et al., 2007).
The loss of DivK focus in the PdhS thermosensitive strain highly suggests that PdhS is a kinase for DivK. Moreover, a Western blot analysis had previously shown that CtrA amount is decreased in a strain overexpressing *pdhS* (Hallez et al., 2007). If DivK regulates the CckA-ChpT-CtrA/CpdR phosphorelay in the same manner as in *C. crescentus*, these data would corroborate the hypothesis according to which PdhS is a kinase for DivK. Yet the *in vivo* Phostag results presented in the manuscript suggest the opposite (Manuscript-Figure 1-E). In the strain overexpressing *pdhS,* CtrA amount was increased and the proportion of phosphorylated protein as well suggesting an enhanced dephosphorylation of DivK in the *pdhS* overexpressing strain and thus an activation of the downstream phosphorelay. The Phostag assay was repeated three times and the results were reproducible. As shown by the *in vitro* phosphorylation assays, PdhS has a dual activity towards DivK (Manuscript-Figure 1-B-C). A switch from a kinase to a phosphatase activity *in vivo* could occur depending on the growth phase of the culture for instance, or on other cues sensed by the histidine kinase input domain, which could explain the contradictory observations.
Concomitantly, we investigated CtrA phosphorylation state in Δ*pleC* and Δ*divJ* strains (Hallez et al., 2007) by Phostag. In light of the CtrA Western blot results, CtrA seems to be less phosphorylated in the Δ*pleC* strain compared to the WT and an increase in the amount and in the phosphorylation of CtrA seems to occur in the Δ*divJ* strain (Results-Figure 4). A quantitative Western blot should be performed to confirm the observed data.

B- The TCS in Alphaproteobacteria

Paragraph II-B-1 of the introduction was dedicated to comparing the TCS between *C. crescentus* and *Rhizobiales*. The main ideas that came out of this comparison are that *Rhizobiales* encode one or two homologs of PleC and DivJ that are absent in *C. crescentus* (Introduction-Figure 16) and that unlike PleC and DivJ in the latter organism, all analysed *Rhizobiales* had one essential HK (Introduction-Table 1). It is interesting to notice that this essential HK is different from one organism to the other. Despite the differences in the essentiality of the TCS proteins, data obtained up to now on *S. meliloti, A. tumefaciens* and *B. abortus* highly suggest that the TCS and phosphorelay upstream of CtrA function in a similar manner to *C. crescentus* (Kim et al., 2013; Pini et al., 2013; Willett et al., 2015). So why is a protein essential in a particular organism and not in another? A possible explanation would lie in the particular need for a more or less active CtrA under laboratory conditions. In other words, accumulation of an excess of active CtrA or the lack of this transcription factor could be more or less tolerated by the bacteria. Alternatively, the essentiality of some HKs of this TCS could depend on the phosphorylation of a RR other than DivK. In *C. crescentus*, DivJ and PleC regulate the phosphorylation of an unorthodox RR called PleD (Jenal, 2004). PleD synthesizes cyclic di-GMP (c-di-GMP) from two molecules of GTP and this small signalling molecule regulates many processes such as adhesion, biofilm formation and virulence in animal and plant pathogens (Ryan, 2013). In *S. meliloti*, the inessentiality of DivJ and CbrA, two kinases of DivK, in culture is due to their redundant functions (a Δ*divJ*Δ*cbrA* double mutant being non-viable) while the essentiality of PleC, a DivK phosphatase, is linked to a deleterious effect of an accumulation of phosphorylated DivK in *S. meliloti* (Fields et al., 2012; Pini et al., 2013). Even if they are not strictly needed for bacterial survival in culture, DivJ and CbrA presence is essential for establishing a successful symbiosis with plants. In *A. tumefaciens*, the fact that DivK is dispensable while DivJ is essential remains unexplained and suggests that DivJ essential activity is exerted on another RR (Kim et al., 2013). Finally, PdhS in *B. abortus* is essential unlike CbrA in *S. meliloti* or PdhS1 and PdhS2 in *A. tumefaciens*. PdhS essentiality could reside in the fact that it can by itself monitor DivK phosphorylation status as it was shown to have a kinase and a phosphatase activity *in vitro*. Deleting *pleC* or *divJ* resulted in a slight variation in CtrA amount and phosphorylation while overexpressing *pdhS* clearly showed an increase in CtrA amount and phosphorylation (Results-Figure 4) suggesting that an alteration in PdhS amount can have a stronger impact on the downstream phosphorylation cascade. PdhS could have acquired increasing importance during evolution in *B. abortus* compared to other *Rhizobiales*.

It should be noted though that despite the non-essentiality of these HKs, deleting many of them is not without consequences for the bacteria. Indeed, many deletions resulted in aberrant morphologies and cell cycle defects. This is the case of Δ*pleC* and Δ*pdhS1* in *A. tumefaciens*; Δ*divJ* and *cbrA*::*tn5* in *S. meliloti* (Fields et al., 2012; Pini et al., 2013).

Finally, the signals sensed by these HKs are yet to be discovered. Even in *C. crescentus*, for which the phosphorylation cascade was thoroughly characterized, the cues recognized by PleC and DivJ are unknown. It is likely that these HKs sense an internal signal under laboratory conditions as their localization to the poles and their activities on DivK follow what seems to be a pre-defined program.

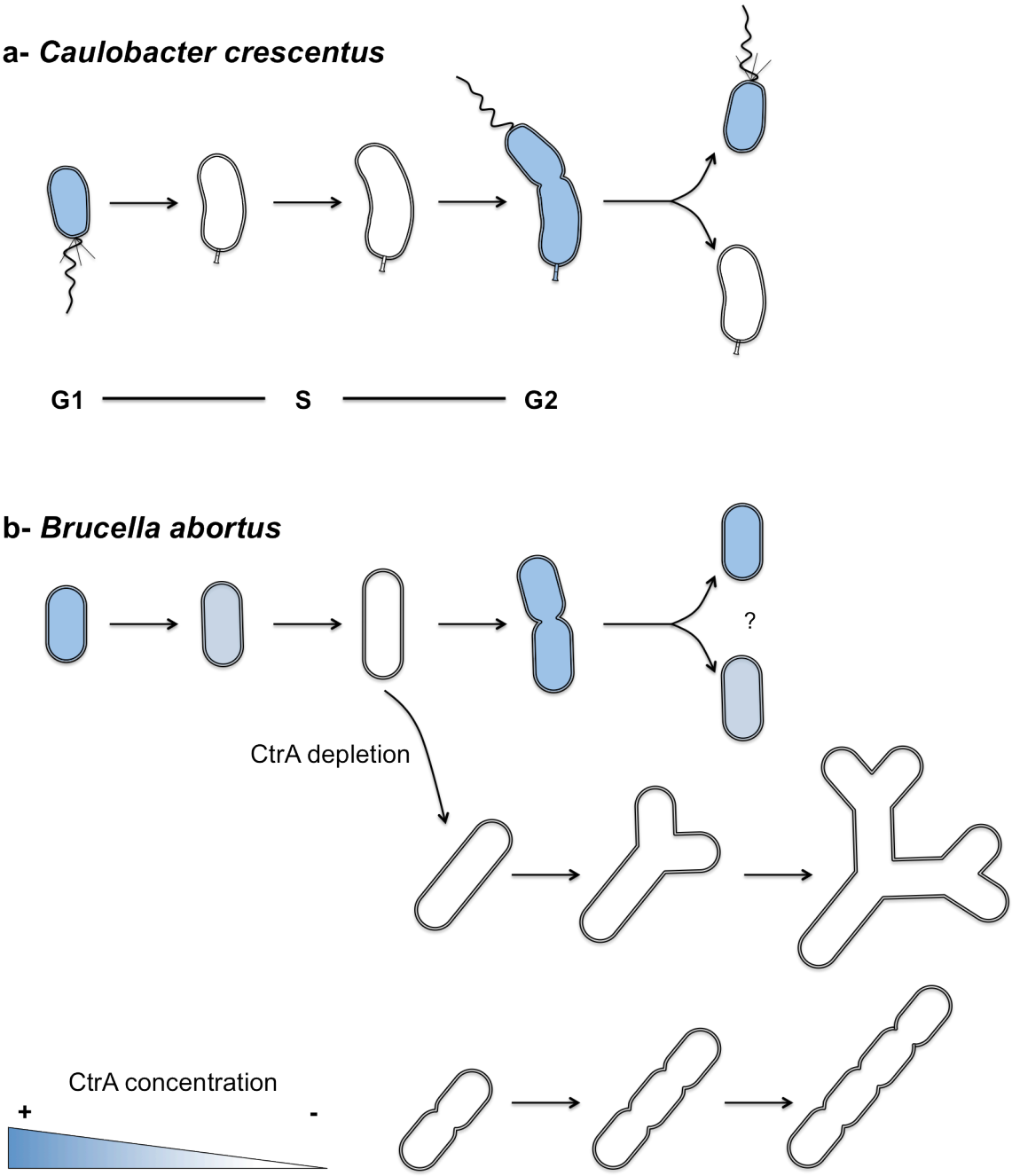

Figure 2- Variation of CtrA amount during *C. crescentus* and *B. abortus* cell cycle

a- In *C. crescentus*, CtrA is degraded at the G1-S transition, as depicted by a blue flagellated cell and a white stalked cell. CtrA is synthesized again in late S phase and accumulates in predivisional cells (blue). After septation, CtrA is maintained in the flagellated daughter cell and is cleared in the stalked cell.

b- The depicted model suggests that CtrA is also degraded during the S phase of *B. abortus* cell cycle and re-accumulates in predivisional cells where it is necessary for division. If this re-accumulation is prevented, division does not occur and bacteria keep on elongating, generating branched morphologies or chains. A fraction of the bacteria, not shown here, present intermediate phenotypes, harbouring initiated constriction(s) and a branched morphology.

2. CtrA, a versatile transcription factor

A- Is CtrA amount cell cycle-regulated in *B. abortus* as well?

Regulation of CtrA amount and phosphorylation along *C. crescentus* cell cycle is well established (Introduction-Figure 9). More recently, CtrA amount was shown to vary in a synchronized population of *S. meliloti* similarly to *C. crescentus*, with a decrease at the G1-S transition and an accumulation of CtrA during late S phase and G2 phase (Pini et al., 2015). In *B. abortus*, the lack of a synchronization protocol makes it impossible to monitor CtrA amount during cell cycle. However, two indirect observations hint towards a possible similar oscillating profile. First, the GFP-based reporter system shows a variation in the fluorescence intensity according to cell length, suggesting that the level of activity of *ctrA* promoter is not the same in bacteria of different cell length. Second, the maximal fluorescence intensity reached in large bacteria (presumably in G2 phase) suggests that CtrA might also accumulate in these bacteria where it is needed for division. This observation can be linked to the absence of division observed in the CtrA depletion strain (Manuscript-Figure 2). Combining these data, we suggest a model in which CtrA amount varies along *B. abortus* cell cycle similarly to *C. crescentus* (Figure 2). When CtrA is depleted, cells remain in an "S phase-like" state, during which division does not occur and chromosome replication is maintained and reinitiated as the cell grows.

B- CtrA in pathogenesis and in symbiosis

As already discussed in the introduction, an obvious link was highlighted between *B. abortus* cell cycle progression and its virulence (Deghelt et al., 2014). Indeed, bacteria in G1 phase are more infectious than the other subpopulations (S and G2). G1 bacteria regroup two distinct populations, large cells with a PdhS focus at their old pole and small cells lacking this focus (Figure 1). Infecting HeLa cells with a *B. abortus* strain carrying a YFP-PdhS fusion showed that a similar proportion of large $PdhS^+$ bacteria and small $PdhS^-$ bacteria enter HeLa cells, suggesting that there is no preferential internalization of these two bacterial subpopulations (C. Mullier thesis). Infection of HeLa cells with the CtrA depletion strain further confirms the connection between cell cycle and virulence of this pathogenic bacterium. Indeed, in the absence of CtrA, bacteria were unable to sustain their viability inside HeLa cells (Manuscript-Figure 3-C). Their intracellular trafficking also seems to be perturbed as a higher proportion of BCVs retained the Lamp1 marker for up to 15 h PI (Manuscript-Figure 6-A). Bacteria that excluded the Lamp1 marker from their BCV between 10 and 15 h PI had predominantly branched morphologies (Manuscript-Figure 6-B). This observation fits the data obtained by Deghelt-Mullier et al. who showed that *B. abortus* growth is resumed in $Lamp1^+$ compartments and that daughter cells are delivered in $Lamp1^-$ BCVs. Indeed, the fact that $Lamp1^-$ BCVs enclose mostly branched bacteria suggests that growth is an essential condition for bacteria to traffic out of the late endocytic pathway. However, cell division is certainly not required to proceed through the intracellular trafficking. Remains the question of whether the branched bacteria reach the secretory pathway and what happens to these bacteria between the moment they exclude the Lamp1 marker from their BCVs and the dramatic decrease in the CFU numbers at 24 and 48 h PI. Labelling BCVs for ER markers such as calnexin would answer the first part of this question. Could the BCVs be redirected to phagolysosomes later during infection? This is most probably the case for bacteria with a normal morphology that co-localize with the Lamp1 marker at 15 h PI (Manuscript-Figure 6-B). In the case of branched bacteria, the prolonged

absence of division or the alteration of outer membrane properties could be deleterious for the bacteria that might be subsequently redirected to phagolysosomes.

In *C. crescentus,* CtrA degradation in flagellated cells is essential for the initiation of the S phase and for the differentiation into stalked cells (Domian et al., 1997). In *S. meliloti,* CtrA proteolysis also occurs at the G1-S transition in culture and it is crucial for the differentiation into bacteroids inside plant host cells (Pini et al., 2013). In *B. abortus,* direct evidence of CtrA amount oscillation during the cell cycle is still missing due to the absence of a synchronization protocol. In order to follow CtrA amount in culture and during infection, a GFP-CtrA fusion could be helpful. Such a fusion was constructed during this thesis but no fluorescence was observed, suggesting instability or misfolding of the fusion protein. What can be concluded from the HeLa cell infections with the depletion strain is that, unlike in *S. meliloti* infection, CtrA is required for late phases of the infection. It is indeed required for bacterial division and survival. This difference in CtrA amount between the plant symbiont and the animal pathogen comes together with a difference in the outcome of each of these infections. In the case of *S. meliloti*, differentiation into nitrogen-fixing bacteroids is irreversible and can be considered as a "dead-end" for the bacteria. The accumulation of supernumerary copies of genomic DNA, the increased membrane permeability and the inability to resume growth and division make bacteroids non-viable outside the host plant (Mergaert et al., 2006). On the contrary, intracellular *B. abortus* grow and divide actively. They are also able to leave their replicative niche and to invade neighbouring mammalian cells. Thus, CtrA presence is crucial for *B. abortus* to accomplish its life cycle while its absence is essential for *S. meliloti* to establish a successful, irreversible symbiosis with host plants. This comparison allows us to appreciate how related organisms adapted the use of a single phosphorylation cascade and a single transcription factor to different lifestyles.
Not all plant-*Rhizobium* interactions lead to a cell cycle blockade in bacteria (Mergaert et al., 2006). In some symbiotic interactions, bacteria maintain a normal morphology, continue dividing and are viable if extracted from the nodules. It would be interesting to quantify CtrA amount during symbiosis in these *Rhizobiales.*

C- Other targets, other functions – Is CtrA a multifaceted transcription factor?

Whether CtrA is important for the initial non-proliferative phase of the infection is still not clear. At 3 h PI, a similar number of CFUs was collected from HeLa cells independently of the presence of IPTG in the medium (Manuscript-Figure 3-C). Given that the kinetics of CtrA proteolysis during infection is unknown, it is difficult to say whether a two hour-depletion is enough to clear CtrA from bacteria (the first hour of infection corresponds to the internalization of bacteria in presence of IPTG). The importance of CtrA for bacterial division was clearly shown in culture and during later hours of the infection. This role is most probably not important for the early hours of infection. However, ChIP-seq data suggest that CtrA might regulate other processes via different target genes. For instance, CtrA bound intergenic regions upstream of *sodC* and *mutM* (Manuscript-Table S4). The *sodC* gene codes for a superoxide dismutase. This enzyme converts highly reactive O_2^- superoxide ions into O_2 or H_2O_2. SodC protects *B. abortus* 2308 from respiratory burst in macrophages and is important to maintain a chronic infection in mice (Gee et al., 2005). In *E. coli,* MutM is involved in repairing DNA damages caused by oxidative stress (Michaels and Miller, 1992). The *B. abortus* BER (Base excision repair) system to which belongs MutM is currently under investigation in our laboratory (PhD thesis of Katy Poncin). Professional phagocytes produce reactive

oxygen species as a means of defence against invading pathogens. A correct expression, potentially mediated by CtrA, of *mutM* during the early hours of the infection could be crucial for bacterial viability. It would be interesting to deplete CtrA for a short time (3 to 4 h for example) prior to infection and assess bacterial survival in epithelial cells and professional phagocytes at early hours. Professional phagocytes could be activated by adding gamma interferon (INF-γ) prior to infection. INF-γ boosts the production of nictric oxide and renders macrophages more aggressive (Gross et al., 1998).

CtrA could also regulate the outer membrane (OM) properties of *B. abortus* and thus indirectly its virulence. Many genes coding for OMPs are targeted by CtrA and a CtrA depletion resulted in a dramatic decrease in Omp25 amount (Manuscript-Figure 9). As mentioned in the introduction (Paragraph III-C), Omp25 is essential for *B. abortus* viability in a mouse and a cattle infection model (Edmonds et al., 2001; Edmonds et al., 2002). Surprisingly, a Δ*omp25* mutant was shown to be as virulent as the WT when infecting HeLa cells and macrophages (Manterola et al., 2007). Therefore, the role of Omp25 in *B. abortus* virulence is not clear. BmaC is another potential target of CtrA which role is linked to *Brucella* OM. BmaC is a monomeric autotransporter implicated in *B. suis* adhesion to HeLa cells (Posadas et al., 2012). A Tn-seq experiment (transpositional mutagenesis followed by deep sequencing) performed in our laboratory suggests BmaC is also important for the late proliferative phase in RAW 264.7 macrophages (Thesis of Jean-François Sternon), where it could be involved in *Brucella* adherence to the internal face of its vacuole. Thus, CtrA could regulate the interactions between *B. abortus* and its host cell at the internalization step and during the intracellular trafficking.

CtrA regulon contains two genes coding for polarity determinants, PopZ (pole organizing protein) and PodJ (polar organelle development) (Manuscript-Table S4). In *C. crescentus*, PopZ interacts with the ParAB machinery and anchors the chromosome to the pole (Bowman et al., 2008; Ebersbach et al., 2008). It is localized to the old pole in G1 bacteria. PopZ focus duplicates during S phase and goes to the new pole where it anchors the newly segregated origin of replication to the pole. *C. crescentus* PodJ localizes to the new pole in predivisional cells and its presence at this pole is required for PleC localization to this pole and therefore for correct polar morphogenesis (Hinz et al., 2003). In *A. tumefaciens*, PopZ and PodJ have an opposite localization pattern compared to *C. crescentus* (Grangeon et al., 2015). PopZ displays a unique focus at the new growing pole while PodJ remains at the old pole during the whole cell cycle and only localizes to the new pole in the late stages of the cell cycle prior to division. It remains at this pole after division, probably marking the transition of the new pole into an old pole. Interestingly, PopZ in *B. abortus* also shows a single focus at the new pole (M. Deghelt thesis), suggesting a conservation of PopZ localization among *Rhizobiales*. The fact that CtrA binds upstream of *popZ, repAB* and to a lesser extent *dnaA* suggests that CtrA might coordinate the expression of these genes and hence the initiation of replication of chromosomes I and II and the anchoring of chromosome I to the new pole.

It should be noted that CtrA regulon most probably differs from one condition to another. It is therefore very likely that the promoters bound by CtrA during infection are different from the regions immunoprecipitated with CtrA in rich culture medium. As in *C. crescentus*, CtrA binding to DNA in *B. abortus* could be modulated by other transcription factors and cofactors, which amount and activity can highly vary

depending on the environment. It is noteworthy that *pleC* promoter is bound by CtrA *in vitro* (Bellefontaine et al., 2002) but not *in vivo* in the tested condition (ChIP-seq data). It is therefore tempting to suggest that this promoter might be bound in other conditions.

D- CtrA binding to DNA in *Brucella abortus* – Dissecting the ChIP-seq and reporter system data

CtrA binding to DNA was extensively studied in *C. crescentus.* Similarly to other members of the OmpR subfamily of RRs, CtrA binds DNA as a dimer and recognizes two direct repeats which consensus sequence in the case of CtrA is TTAA (Quon et al., 1998). These direct repeats are often separated by seven nucleotides (Quon et al., 1998). CtrA dimerization, and thus binding to DNA, is enhanced by phosphorylation (Reisenauer et al., 1999). When two binding sites are located close to each other, two dimers of CtrA recognize these sites and interact with each other, enhancing their binding to DNA in a cooperative manner (Siam and Marczynski, 2000). Many variations around this "TTAA(N_7)TTAAC" 9-mer consensus sequence are naturally present in *C. crescentus* genome, some implying base substitutions in the TTAA half sites and others including variations of the number of nucleotides separating the two half sites. These variations are thought to allow more flexibility in the regulation of the downstream genes by preventing CtrA from binding too tightly to DNA (Ouimet and Marczynski, 2000). A CtrA dimer is also able to bind the "TTAACCAT" 8-mer box, which is an extension of a single TTAA half site (Laub et al., 2002).

Around 70% of the DNA regions co-precipitated with CtrA in *B. abortus* had a sequence resembling the 9-mer or the 8-mer box. It is interesting to notice that a similar proportion (around 62%) of *C. crescentus* CtrA targets identified by microarray also had a consensus binding site (Laub et al., 2002). Among the remaining CtrA-bound regions in *B. abortus*, 57% had at least one "TTAA(C)" half site. In *C. crescentus*, disruption of a TTAA half site in a 9-mer box located in the origin of replication prevents the binding of a CtrA dimer to DNA suggesting that a single TTAA half site is not sufficient for CtrA binding (Siam and Marczynski, 2000). It is thus possible that the half sites identified in *B. abortus* genome are actually part of a degenerate 8-mer box or a "TTAA(N_X)TTAAC" 9-mer box where X is a number different from 7, explaining why these binding sites were not identified by our bioinformatics predictions. Alternatively, CtrA binding to these half sites could be stabilized by other transcription factors or cofactors such as SciP or by sigma factors. Ouimet and co-workers have indeed shown that the -10 box of a synthetic promoter carrying a 9-mer binding site can strengthen CtrA binding to this promoter and ensure a cell cycle regulation of the activity of this promoter (Ouimet and Marczynski, 2000). Nevertheless, both *C. crescentus* and *B. abortus* CtrA regulons include promoters with no predicted consensus sequence at all, suggesting that CtrA binding to DNA is not limited to the 8-mer and 9-mer boxes.

Genes downstream of the CtrA-bound intergenic regions can be classified in six main functional categories as follows: envelope synthesis (LPS incorporation and PG synthesis), division, outer membrane proteins (OMPs), chromosome replication and segregation, cell cycle regulation and genes with no predicted functions. A ChIP-seq assay performed on *S. meliloti* CtrA showed similar regulated functions with genes involved in motility (Pini et al., 2015). On the contrary, *C. crescentus* CtrA regulon has two major differences with *B. abortus* CtrA regulon: it includes less genes involved in envelope biogenesis and outer membrane homeostasis (10.6%) and more genes coding for regulatory proteins such as HKs, RRs and sigma factors (19%) compared to *B. abortus* CtrA regulon (33.3% and 4.9% respectively). These discrepancies exemplify the

adaptation of CtrA target genes to different lifestyles. The free-living bacterium *C. crescentus* living in oligotrophic environments is probably subjected to a wide range of stimuli and has to integrate a complex set of information into an adapted gene expression profile.

The GFP-based reporter system showed a variation in the activity of *repAB, ccrM* and *ctrA* promoters but not of *pleC* promoter in function of bacterial cell length. Classifying bacteria according to their cell length was the only means for us to monitor the activity of these promoters throughout *B. abortus* cell cycle. We are aware of the imperfections of this system as bacteria with the same length can be at different moments of their cell cycle. The *ctrA* and *ccrM* promoters harboured a similar activity profile with a maximal intensity for bacteria of small and large size and a minimal activity for bacteria of intermediate size (Results-Figure 6). The activity of *repAB* promoter had an opposite profile with a peak of fluorescence in bacteria of intermediate cell size. On the contrary, *pleC* promoter, which harbours a consensus binding site but was not bound by CtrA in the ChIP-seq, had a more or less stable activity for all bacterial sizes (Results-Figure 6). These data suggest that three promoters bound by CtrA *in vivo* could be cell cycle regulated. Interestingly, mutating the consensus sequences in *ccrM* and *repAB* promoters perturbed their activity. In the case of p_{ccrM}, the cell cycle regulation profile was maintained but the level of fluorescence was decreased when the first binding box was mutated (Results-Figure 7) while disrupting the 9-mer box in p_{repAB} resulted in a loss of fluorescence (data not shown). The possibility that these mutations disrupted the binding of other transcription factors should not be ruled out especially that the exact -10 and -35 boxes of p_{repAB} are not known.
If the activity profiles of p_{ctrA}, p_{ccrM} and p_{repAB} are indeed CtrA-dependent, this would mean that at least CtrA phosphorylation levels should also be cell cycle regulated in *B. abortus*. Overexpressing a non-phosphorylatable allele of *cpdR* (*cpdR*D52A) in *B. abortus* results in the clearance of CtrA from the cells, suggesting that a targeted degradation of CtrA in *B. abortus* is also occurring (Willett et al., 2015). Regulating the amount of active CtrA at the transcriptional, phosphorylation and proteolysis levels in *C. crescentus* is well established. A protocol based on nutrient starvation was developed to synchronize *S. meliloti* (De Nisco et al., 2014). It was recently shown that proteolysis contributes more than transcription to the regulation of CtrA amount in *S. meliloti* and that CtrA amount in a synchronized population oscillates in a similar manner to CtrA in *C. crescentus* (Pini et al., 2015).

3. The PdhS-FumC interaction, a potential link between cell cycle and metabolism

PdhS co-localizes with the fumarase FumC to the old pole, both proteins interact with each other in a Y2H assay (Mignolet et al., 2010) and our data suggest an alteration of PdhS autokinase activity in presence of FumC *in vitro* (Results-Figure 5). Yet FumC is not essential in *B. abortus* and deleting this gene does not induce any cell cycle defects (Mignolet et al., 2010). If FumC modulates PdhS activity *in vivo* too, this regulation must be dispensable under laboratory conditions. Actually, FumC is not essential because of the redundancy of its activity with FumA, another fumarase that does not interact with PdhS or localize to the old pole. This demonstrates that FumC binding to PdhS is not crucial for PdhS essential function(s). FumC could however modulate PdhS function at the old pole, where they co-localize.

The link between cell cycle and metabolism is a common subject in the literature and has been thoroughly investigated in *E. coli*, *B. subtilis* and *C. crescentus*. For instance, the initiator of chromosome replication DnaA constitutes a checkpoint for DNA replication depending of the nutrient availability (Wang and Levin, 2009). In *C. crescentus*, and in presence of nutrients, the glutamate dehydrogenase GdhZ and the oxidoreductase-like KidO destabilize the FtsZ ring in G2 phase to enhance constriction and promote division (Beaufay et al., 2015). In starvation conditions, the Z-ring is stabilized, preventing the release of the daughter cells in a hostile environment.

General conclusions and perspectives

The aim of this project was to decipher part of *Brucella abortus* cell cycle regulation. We decided to tackle this question at two levels: (1) at the top of the conserved phosphorylation cascade, by investigating the activity of the histidine kinase PdhS on the response regulator DivK; (2) at the bottom of this cascade, by investigating CtrA regulon and the effect of a CtrA depletion on *B. abortus* cell cycle. To address the first question, we performed *in vitro* kinase assays on purified proteins and showed that PdhS has a dual activity towards DivK: it is both a kinase and a phosphatase for this response regulator. When overproducing PdhS *in vivo*, CtrA amount and phosphorylation were modified compared to a WT strain, confirming that the two-component system and the phosphorelay are "wired" in *B. abortus*. PdhS autophosphorylation was partially inhibited in the presence of FumC fumarase, suggesting a potential link between cell cycle progression and central metabolism at the level of PdhS and FumC in *B. abortus*.
CtrA being essential, we constructed a CtrA depletion strain in *B. abortus* 544 strain. In absence of CtrA, *B. abortus* cells keep on elongating but stop dividing, forming branching phenotypes and "chains". When cells are repleted with CtrA, division is resumed and daughter cells are released in the medium again, clearly showing that CtrA is essential for the completion of division in *B. abortus*. However, this transcription factor seems to be dispensable for elongation as well as for the partial formation of septa, as shown by the presence of visible constriction sites and the presence of multiple YFP-FtsI foci in CtrA-depleted cells. CtrA is essential for *B. abortus* long-term survival in rich culture medium and in HeLa cells. When CtrA is depleted during *B. abortus* intracellular trafficking, part of the bacteria resume growth and form branches while another subgroup is arrested for its growth. A strong correlation was found between branching of bacteria and co-localization with the Lamp1 lysosomal marker. Indeed, most of the bacteria that were able to leave Lamp1+ compartments formed branches, suggesting that elongation is a necessary pre-requisite to go beyond the late endocytic pathway.
We performed a ChIP-seq assay to map CtrA binding sites on *B. abortus* chromosomes. Analysis of the data suggest CtrA regulon is enriched in cell cycle-related genes and in genes involved in envelope biogenesis and homeostasis, a feature that distinguishes *B. abortus* CtrA from *C. crescentus* CtrA, and to a lesser extent from *S. meliloti* CtrA. RT-qPCR data on the CtrA depletion strain show that CtrA might exert several feedback loops on the upstream phosphorylation cascade (particularly on *divK* and *cpdR*). Expression of genes involved in envelope synthesis remained unperturbed in the absence of CtrA, while some genes coding for OMP were downregulated. Using OMP MAb in Western blots, we showed a huge decrease in Omp25 amount in the CtrA depletion strain. However, we were not able to confirm this observation by immunofluorescence, probably because of a crosstalk of the antibodies with Omp25 homologs.

This work opens up many questions. Does SciP modulate CtrA transcriptional activity in *B. abortus*? Does CtrA coordinate the initiation of replication of the two chromosomes? Binding of CtrA, albeit it weak, upstream of *dnaA* and *repAB* suggests that CtrA might be involved in regulating the initiation of chromosome I replication before chromosome II (Deghelt et al., 2014). Is GcrA cell cycle regulated and does methylation by CcrM modulate GcrA binding to DNA and hence gene expression? Overexpressing *ccrM* results in aberrant morphologies and DNA content in *B. abortus* (Robertson et al., 2000) and *in vitro* assays show that the methylation state of DNA influences *B. abortus* GcrA binding (Fioravanti et al., 2013). A ChIP-seq assay was performed on *B. abortus* GcrA in parallel with CtrA. First analyses show an enrichment of GAnTC sites in the regions bound by

GcrA (K. Poncin). A deeper analysis of the data will provide us with information about GcrA role in *B. abortus.* The CtrA depletion strain highlighted a link between the onset of growth and the intracellular trafficking that was already suggested by the work of Deghelt-Mullier et al. (Deghelt et al., 2014). Why is resumption of growth important for *B. abortus* trafficking out of the late endocytic pathway? The development of a synchronization protocol will be a powerful tool to answer part of these questions and to address many other questions related to cell cycle regulation. Altogether, such projects will help us better understand how this pathogenic bacterium regulates its cell cycle in culture and when it encounters a mammalian host.

Material and methods

1. Protein purification

Cloning in expression vectors

DNA sequences coding for the proteins of interest were amplified from *B. abortus* 544 purified genomic DNA using Phusion High Fidelity DNA Polymerase (New England Biolabs). To the 5' end of forward and reverse primers were added attB1 and attB2 sequences respectively allowing the cloning of the amplicon in a pDONR entry vector by holmologous recombination, using BP clonase (Invitrogen). Around 4 µl of purified PCR product was incubated over-night at 25°C with 150 ng of pDONR vector, 1 µl of BP clonase and 2 µl of 5x BP buffer and the volume was brought to 10 µl with water. The BP reaction mix was transformed in *E. coli* DH10B strain and bacteria were plated on a selection medium containing kanamycin. Around three clones were screened for the presence of the insert by diagnostic restriction and one positive vector was sequenced. 150 ng of the entry vector containing the insert was incubated over-night at 25°C with 150 ng of expression vector, 2 µl of LR clonase (Invitrogen) and 2 µl of 5x LR buffer and the volume was brought to 10 µl with water. Expression vectors used in our experiments are pML310 and pML333 containing TRX-His_6 and MBP-His_6 tags respectively. The LR reaction mix was transformed in *E. coli* DH10B strain and bacteria were plated on a selection medium containing ampicillin. Plasmids from one or two clones were purified and directly transformed in *E. coli* BL21 DE3 strain for overexpression.

Overproduction of the fusion proteins

For an overproduction in a 1 L volume, a 40 ml pre-culture was prepared the day before and incubated at 37°C. In the morning, the over-night culture was diluted at an OD of 0.1 in a total volume of 1 L of LB supplemented with ampicillin and incubated at 37°C until OD reaches 0.6-0.8. Overexpression was induced by adding 300 µM of IPTG and the culture was incubated at 32°C for 3 to 3.5 hours. Bacteria were harvested by a centrifugation at 5000 rpm for 20 minutes at 4°C and stored at -20°C. A sample of the induced and non-induced fractions are kept to load on gel.

Bacterial lysis

A bacterial pellet corresponding to 1 L of culture was thawed on ice and resuspended in 50 ml of lysis buffer by agitating with a stir bar at 4°C for about 30 minutes. Bacteria were then lysed by applying 8 rounds of sonication of 30 seconds each with an input 4 using the Branson Sonifier 150. The lysate was centrifuged at 9500 rpm for 45 min at 4°C to separate the soluble fraction from the cellular debris. The supernatant was collected and passed through a 0.22 µm filter. A sample of each of the soluble and insoluble fractions are kept to load on gel.

The lysis buffer consisted of 20 mM Tris-HCl pH8 500 mM NaCl, 10% glycerol, 20 mM imidazole (10 mM in the case of TRX-His_6-PdhS), 0.1% Triton X-100, 1 mM DTT, 1 mg/ml lysozyme, 4 nM DNase I, one pill of complete protease inhibitor.

Note that the first time a fusion protein was produced, its overproduction and its solubility were tested on a 50 ml culture before scaling up to 1 L.

Protein purification on an affinity column and by gel filtration

The filtered supernatant was loaded on a Ni^{2+}-nitrilotriacetate affinity resin (Ni-NTA from Qiagen) previously washed with 10 column volumes (CV) of water then equilibrated with 10 CV of lysis buffer lacking DTT, DNase I and lysozyme. The flow through was collected and the column was washed with 10 CV of washing buffer. To elute the protein, a gradient was performed between the washing buffer and the elution buffer and fractions of 1 ml were collected in tubes. The column was then washed with 10 CV of water then 10 CV of ethanol 20% and stored at 4°C.

The washing buffer consisted of 20 mM HEPES pH8, 500 mM NaCl, 10% glycerol, 20 mM imidazole (10 mM in the case of PdhS), 0.1% Triton X-100 and 1 mM DTT. The elution buffer consisted of 20 mM HEPES pH8, 500 mM NaCl, 10% glycerol and 250 mM imidazole.

The flow through and the eluted fractions were loaded on gel. Fractions containing the protein were pooled, passed through a 0.22 µm filter and loaded onto a HiLoad Superdex 75 or 200 prep grade column (GE healthcare) previously equilibrated with storage buffer. Proteins with a molecular weight less than 70 KDa were loaded on a S75 column; those having a bigger size were loaded on a S200 column.
The storage buffer consisted of 10 mM HEPES pH8, 50 mM KCl, 10% glycerol, 0.1 mM EDTA, 1 mM DTT.

2. Phostag assays

Preparation of a Phostag gel
Running gel consisted of 10 or 12% acrylamide, 0.26 M Tris HCl pH8.8, 0.1% SDS, 50 µM Phostag and 100 µM $MnCl_2$ for *in vitro* assays, 25 µM Phostag 50 µM $MnCl_2$ for *in vivo* assays, 0.1% APS and 4 µl TEMED. Stacking gel was made of 5% acrylamide, 0.126 M Tris-HCl pH 6.8, 0.1% SDS, 0.1% APS and 6 µl TEMED. Each gel was kept to polymerize for one hour. Before loading the samples on gel, the wells are rinsed by flushing.

In vitro Phostag assays
Autophosphorylation assays were performed on 15 µM of kinase protein diluted in the storage buffer supplemented with 5 mM $MgCl_2$ and 10 mM ATP. A 30 minutes incubation was performed at room temperature (RT). 3 µl of this mix were added to 3 µl of storage buffer and 3 µl of 3x loading buffer and kept on ice. Another 3 µl of phosphorylated kinase were added to 3 µl of a mix containing the response regulator diluted in storage buffer at a final concentration of 15 µM and phosphotransfer was performed at RT for 5 minutes. 3 µl of 3x loading buffer were added and the mix was kept on ice.

In vivo Phostag assays
An over-night culture of *B. abortus* was diluted in the morning at an OD of 0.2 and incubated for five hours at 37°C. The OD was taken, 1 ml of culture was spun down at 7000 rpm for 2.5 minutes and the pellet was resuspended in the appropriate volume of lysis buffer to concentrate bacteria to an OD of 10. Bacteria were lysed for 5 minutes at RT, loading buffer was added and samples were kept on ice to be immediately loaded on gel. The lysis buffer consisted of 10 mM Tris-HCl pH7.5 and 2% SDS.

For *in vitro* and *in vivo* assays, migration was performed at 4°C in cold running buffer at 100V for three hours. For *in vitro* assays, the gel was coloured with Coomassie blue staining. For *in vivo* assays, the gel was rinsed in water, washed for 5 minutes in transfer buffer supplemented with 1 mM EDTA to remove the Mn^{2+} ions that can interfere with the transfer. The gel was then washed for 5 minutes in transfer buffer without EDTA to remove the EDTA-Mn^{2+} complexes and proteins were transferred to a nitrocellulose membrane by using the transfer system in Regis Hallez group.

3. *In vitro* kinase assays using radioactivity

Autophosphorylation was performed on 5 µM of kinase in storage buffer supplemented with 2 mM DTT, 5 mM $MgCl_2$, 500 µM ATP and 5 µCi ATP (3000 Ci/mmol) at 30°C for 40 minutes (Skerker et al., 2005). 5 µl of this mix were added to 5 µl of storage buffer and 5 µl of 3x loading buffer and kept on ice. Another 5 µl of phosphorylated kinase were added to 5 µl of a mix containing the response regulator diluted in storage buffer supplemented with 5 mM $MgCl_2$ at a final concentration of 5 µM and phosphotransfer was performed at RT for 5 minutes. 5 µl of 3x loading buffer were added and the mix was kept on ice. For testing the phosphatase activity of PdhS, the phosphotransfer was performed in a 50-µl volume and the kinase-response regulator mix was washed thrice of an amicon column with a 10 KDa cut off to remove the excess of ATP

by adding 450 µl of storage buffer and centrifuging 5 min at 10,000 rpm. Once the mix washed, PdhS was added at a final concentration of 5 µM and the mix was incubated for 30 minutes at RT. Migration in a pre-cast gel was performed at RT in a pre-cooled running buffer for 45 minutes at 250 V. The gel was dried and revealed on a Phosphoscreen.

4. Polymyxin B sensitivity assay

Bacteria in exponential phase culture were diluted 5.10^{-5} or 10^{-6} times (depending on the strain) in saline buffer (autoclaved 0.9% NaCl), an OD suitable for CFU counting after bacterial plating. A stock solution of polymyxin B is prepared in water at 150,000 U/ml and filter sterilized. Serial dilutions (2x) are then prepared in sterile cidal buffer (0.133M NaCl, 0.1M NaH_2PO_4 pH 5.5). Dilutions up to 2048x can be tested. 50 µl of the diluted bacterial suspension are dispatched in 96-well plates and 150 µl of polymyxin B are added to the bacteria. A triplicate is made for each bacterial strain – polymyxin B concentration pair. In practice, three subsequent lines of the 96-well plate correspond to one strain and each column of the plate corresponds to a different concentration of the cationic peptide. Bacteria are first mixed with the smallest concentration of polymyxin B. The plate is incubated at 37°C for one hour then bacteria are plated. To calculate the final concentration of polymyxin B to which a certain strain is resistant, it should be taken into account that one third of the total volume in each well (50 µl) consists of bacterial suspension.

5. Immunolabelling of *Brucella abortus* with anti-Omp25 antibodies

Bacteria grown in rich culture medium were washed twice in PBS by centrifugation at 4000 rpm for 2,5 min and resuspension. Washed bacteria were resuspended in non-diluted hybridoma culture supernatant containing monoclonal anti-Omp25 antibodies and with secondary anti-mouse antibodies coupled to Alexa-488 diluted 500 times in PBS for 40 min at RT on a wheel. Bacteria were washed twice in PBS and and 2 µl were dropped on an agarose pad (1% agarose in PBS) for microscopy.

References

Abel, S., Bucher, T., Nicollier, M., Hug, I., Kaever, V., Abel Zur Wiesch, P., and Jenal, U. (2013). Bi-modal distribution of the second messenger c-di-GMP controls cell fate and asymmetry during the caulobacter cell cycle. PLoS genetics *9*, e1003744.

Alves, R., and Savageau, M.A. (2003). Comparative analysis of prototype two-component systems with either bifunctional or monofunctional sensors: differences in molecular structure and physiological function. Molecular microbiology *48*, 25-51.

Anantharaman, V., and Aravind, L. (2000). Cache - a signaling domain common to animal Ca(2+)-channel subunits and a class of prokaryotic chemotaxis receptors. Trends in biochemical sciences *25*, 535-537.

Andersen, J.B., Sternberg, C., Poulsen, L.K., Bjorn, S.P., Givskov, M., and Molin, S. (1998). New unstable variants of green fluorescent protein for studies of transient gene expression in bacteria. Applied and environmental microbiology *64*, 2240-2246.

Anderson, T.D., Meador, V.P., and Cheville, N.F. (1986). Pathogenesis of placentitis in the goat inoculated with Brucella abortus. I. Gross and histologic lesions. Vet Pathol *23*, 219-226.

Archambaud, C., Salcedo, S.P., Lelouard, H., Devilard, E., de Bovis, B., Van Rooijen, N., Gorvel, J.P., and Malissen, B. (2010). Contrasting roles of macrophages and dendritic cells in controlling initial pulmonary Brucella infection. European journal of immunology *40*, 3458-3471.

Ardissone, S., Fumeaux, C., Berge, M., Beaussart, A., Theraulaz, L., Radhakrishnan, S.K., Dufrene, Y.F., and Viollier, P.H. (2014). Cell cycle constraints on capsulation and bacteriophage susceptibility. eLife *3*.

Atluri, V.L., Xavier, M.N., de Jong, M.F., den Hartigh, A.B., and Tsolis, R.M. (2011). Interactions of the human pathogenic Brucella species with their hosts. Annual review of microbiology *65*, 523-541.

Bachhawat, P., Swapna, G.V., Montelione, G.T., and Stock, A.M. (2005). Mechanism of activation for transcription factor PhoB suggested by different modes of dimerization in the inactive and active states. Structure *13*, 1353-1363.

Barbieri, C.M., and Stock, A.M. (2008). Universally applicable methods for monitoring response regulator aspartate phosphorylation both in vitro and in vivo using Phos-tag-based reagents. Anal Biochem *376*, 73-82.

Batut, J., Andersson, S.G., and O'Callaghan, D. (2004). The evolution of chronic infection strategies in the alpha-proteobacteria. Nature reviews Microbiology *2*, 933-945.

Beaufay, F., Coppine, J., Mayard, A., Laloux, G., De Bolle, X., and Hallez, R. (2015). A NAD-dependent glutamate dehydrogenase coordinates metabolism with cell division in Caulobacter crescentus. The EMBO journal *34*, 1786-1800.

Bellefontaine, A.F., Pierreux, C.E., Mertens, P., Vandenhaute, J., Letesson, J.J., and De Bolle, X. (2002). Plasticity of a transcriptional regulation network among alpha-proteobacteria is supported by the identification of CtrA targets in *Brucella abortus*. Molecular microbiology *43*, 945-960.

Billard, E., Dornand, J., and Gross, A. (2007). Interaction of Brucella suis and Brucella abortus rough strains with human dendritic cells. Infection and immunity *75*, 5916-5923.

Biondi, E.G., Reisinger, S.J., Skerker, J.M., Arif, M., Perchuk, B.S., Ryan, K.R., and Laub, M.T. (2006). Regulation of the bacterial cell cycle by an integrated genetic circuit. Nature *444*, 899-904.

Boschiroli, M.L., Ouahrani-Bettache, S., Foulongne, V., Michaux-Charachon, S., Bourg, G., Allardet-Servent, A., Cazevieille, C., Liautard, J.P., Ramuz, M., and O'Callaghan, D. (2002). The Brucella suis virB operon is induced intracellularly in macrophages. Proceedings of the National Academy of Sciences of the United States of America *99*, 1544-1549.

Bowman, G.R., Comolli, L.R., Zhu, J., Eckart, M., Koenig, M., Downing, K.H., Moerner, W.E., Earnest, T., and Shapiro, L. (2008). A polymeric protein anchors the chromosomal origin/ParB complex at a bacterial cell pole. Cell *134*, 945-955.

Brilli, M., Fondi, M., Fani, R., Mengoni, A., Ferri, L., Bazzicalupo, M., and Biondi, E.G. (2010). The diversity and evolution of cell cycle regulation in alpha-proteobacteria: a comparative genomic analysis. BMC Syst Biol *4*, 52.

Brown, P.J., de Pedro, M.A., Kysela, D.T., Van der Henst, C., Kim, J., De Bolle, X., Fuqua, C., and Brun, Y.V. (2012). Polar growth in the Alphaproteobacterial order Rhizobiales. Proceedings of the National Academy of Sciences of the United States of America *109*, 1697-1701.

Bruce, D. (1889). Observations on Malta Fever. British medical journal *1*, 1101-1105.
Cai, S.J., and Inouye, M. (2003). Spontaneous subunit exchange and biochemical evidence for trans-autophosphorylation in a dimer of Escherichia coli histidine kinase (EnvZ). Journal of molecular biology *329*, 495-503.

Carmany, D.O., Hollingsworth, K., and McCleary, W.R. (2003). Genetic and biochemical studies of phosphatase activity of PhoR. Journal of bacteriology *185*, 1112-1115.
Casino, P., Miguel-Romero, L., and Marina, A. (2014). Visualizing autophosphorylation in histidine kinases. Nature communications *5*, 3258.

Casino, P., Rubio, V., and Marina, A. (2009). Structural insight into partner specificity and phosphoryl transfer in two-component signal transduction. Cell *139*, 325-336.

Casino, P., Rubio, V., and Marina, A. (2010). The mechanism of signal transduction by two-component systems. Current opinion in structural biology *20*, 763-771.

Castaneda-Roldan, E.I., Avelino-Flores, F., Dall'Agnol, M., Freer, E., Cedillo, L., Dornand, J., and Giron, J.A. (2004). Adherence of Brucella to human epithelial cells and macrophages is mediated by sialic acid residues. Cellular microbiology *6*, 435-445.

Castaneda-Roldan, E.I., Ouahrani-Bettache, S., Saldana, Z., Avelino, F., Rendon, M.A., Dornand, J., and Giron, J.A. (2006). Characterization of SP41, a surface protein of Brucella associated with adherence and invasion of host epithelial cells. Cellular microbiology *8*, 1877-1887.

Celli, J., de Chastellier, C., Franchini, D.M., Pizarro-Cerda, J., Moreno, E., and Gorvel, J.P. (2003). *Brucella* evades macrophage killing via VirB-dependent sustained interactions with the endoplasmic reticulum. The Journal of experimental medicine *198*, 545-556.
Celli, J., Salcedo, S.P., and Gorvel, J.P. (2005). Brucella coopts the small GTPase Sar1 for intracellular replication. Proceedings of the National Academy of Sciences of the United States of America *102*, 1673-1678.

Chaves-Olarte, E., Guzman-Verri, C., Meresse, S., Desjardins, M., Pizarro-Cerda, J., Badilla, J., Gorvel, J.P., and Moreno, E. (2002). Activation of Rho and Rab GTPases dissociates Brucella abortus internalization from intracellular trafficking. Cellular microbiology *4*, 663-676.

Cheng, Z., Miura, K., Popov, V.L., Kumagai, Y., and Rikihisa, Y. (2011). Insights into the CtrA regulon in development of stress resistance in obligatory intracellular pathogen Ehrlichia chaffeensis. Molecular microbiology *82*, 1217-1234.

Cloeckaert, A., de Wergifosse, P., Dubray, G., and Limet, J.N. (1990). Identification of seven surface-exposed Brucella outer membrane proteins by use of monoclonal antibodies: immunogold labeling for electron microscopy and enzyme-linked immunosorbent assay. Infection and immunity *58*, 3980-3987.

Cloeckaert, A., Verger, J.M., Grayon, M., and Grepinet, O. (1995). Restriction site polymorphism of the genes encoding the major 25 kDa and 36 kDa outer-membrane proteins of Brucella. Microbiology *141 (Pt 9)*, 2111-2121.

Cloeckaert, A., Verger, J.M., Grayon, M., and Vizcaino, N. (1996). Molecular and immunological characterization of the major outer membrane proteins of Brucella. FEMS microbiology letters *145*, 1-8.

Cock, P.J., and Whitworth, D.E. (2007). Evolution of prokaryotic two-component system signaling pathways: gene fusions and fissions. Molecular biology and evolution *24*, 2355-2357.

Collier, J., Murray, S.R., and Shapiro, L. (2006). DnaA couples DNA replication and the expression of two cell cycle master regulators. The EMBO journal *25*, 346-356.

Comerci, D.J., Martinez-Lorenzo, M.J., Sieira, R., Gorvel, J.P., and Ugalde, R.A. (2001). Essential role of the VirB machinery in the maturation of the *Brucella abortus*-containing vacuole. Cellular microbiology *3*, 159-168.

Curtis, P.D., and Brun, Y.V. (2010). Getting in the loop: regulation of development in Caulobacter crescentus. Microbiology and molecular biology reviews : MMBR *74*, 13-41.

Czibener, C., and Ugalde, J.E. (2012). Identification of a unique gene cluster of Brucella spp. that mediates adhesion to host cells. Microbes and infection / Institut Pasteur *14*, 79-85.

de Barsy, M., Jamet, A., Filopon, D., Nicolas, C., Laloux, G., Rual, J.F., Muller, A., Twizere, J.C., Nkengfac, B., Vandenhaute, J.*, et al.* (2011). Identification of a *Brucella* spp. secreted effector specifically interacting with human small GTPase Rab2. Cellular microbiology *13*, 1044-1058.

De Nisco, N.J., Abo, R.P., Wu, C.M., Penterman, J., and Walker, G.C. (2014). Global analysis of cell cycle gene expression of the legume symbiont Sinorhizobium meliloti. Proceedings of the National Academy of Sciences of the United States of America *111*, 3217-3224.

Deghelt, M., Mullier, C., Sternon, J.F., Francis, N., Laloux, G., Dotreppe, D., Van der Henst, C., Jacobs-Wagner, C., Letesson, J.J., and De Bolle, X. (2014). G1-arrested newborn cells are the predominant infectious form of the pathogen *Brucella abortus*. Nature communications *5*, 4366.

Degnen, S.T., and Newton, A. (1972). Chromosome replication during development in Caulobacter crescentus. Journal of molecular biology *64*, 671-680.

Delrue, R.M., Deschamps, C., Leonard, S., Nijskens, C., Danese, I., Schaus, J.M., Bonnot, S., Ferooz, J., Tibor, A., De Bolle, X.*, et al.* (2005). A quorum-sensing regulator controls expression of both the type IV secretion system and the flagellar apparatus of *Brucella melitensis*. Cellular microbiology *7*, 1151-1161.

Delrue, R.M., Martinez-Lorenzo, M., Lestrate, P., Danese, I., Bielarz, V., Mertens, P., De Bolle, X., Tibor, A., Gorvel, J.P., and Letesson, J.J. (2001). Identification of *Brucella* spp. genes involved in intracellular trafficking. Cellular microbiology *3*, 487-497.

DelVecchio, V.G., Kapatral, V., Redkar, R.J., Patra, G., Mujer, C., Los, T., Ivanova, N., Anderson, I., Bhattacharyya, A., Lykidis, A.*, et al.* (2002). The genome sequence of the facultative intracellular pathogen *Brucella melitensis*. Proceedings of the National Academy of Sciences of the United States of America *99*, 443-448.

Detilleux, P.G., Deyoe, B.L., and Cheville, N.F. (1990). Penetration and intracellular growth of *Brucella abortus* in nonphagocytic cells in vitro. Infection and immunity *58*, 2320-2328.

Dohmer, P.H., Valguarnera, E., Czibener, C., and Ugalde, J.E. (2014). Identification of a type IV secretion substrate of Brucella abortus that participates in the early stages of intracellular survival. Cellular microbiology *16*, 396-410.

Domian, I.J., Quon, K.C., and Shapiro, L. (1997). Cell type-specific phosphorylation and proteolysis of a transcriptional regulator controls the G1-to-S transition in a bacterial cell cycle. Cell *90*, 415-424.

Domian, I.J., Reisenauer, A., and Shapiro, L. (1999). Feedback control of a master bacterial cell-cycle regulator. Proceedings of the National Academy of Sciences of the United States of America *96*, 6648-6653.

Ebersbach, G., Briegel, A., Jensen, G.J., and Jacobs-Wagner, C. (2008). A self-associating protein critical for chromosome attachment, division, and polar organization in caulobacter. Cell *134*, 956-968.

Edmonds, M.D., Cloeckaert, A., Booth, N.J., Fulton, W.T., Hagius, S.D., Walker, J.V., and Elzer, P.H. (2001). Attenuation of a Brucella abortus mutant lacking a major 25 kDa outer membrane protein in cattle. American journal of veterinary research *62*, 1461-1466.

Edmonds, M.D., Cloeckaert, A., and Elzer, P.H. (2002). Brucella species lacking the major outer membrane protein Omp25 are attenuated in mice and protect against Brucella melitensis and Brucella ovis. Veterinary microbiology *88*, 205-221.

England, J.C., Perchuk, B.S., Laub, M.T., and Gober, J.W. (2010). Global regulation of gene expression and cell differentiation in Caulobacter crescentus in response to nutrient availability. Journal of bacteriology *192*, 819-833.

Evinger, M., and Agabian, N. (1977). Envelope-associated nucleoid from Caulobacter crescentus stalked and swarmer cells. Journal of bacteriology *132*, 294-301.

Fields, A.T., Navarrete, C.S., Zare, A.Z., Huang, Z., Mostafavi, M., Lewis, J.C., Rezaeihaghighi, Y., Brezler, B.J., Ray, S., Rizzacasa, A.L.*, et al.* (2012). The conserved polarity factor podJ1 impacts multiple cell envelope-associated functions in Sinorhizobium meliloti. Molecular microbiology *84*, 892-920.

Fioravanti, A., Fumeaux, C., Mohapatra, S.S., Bompard, C., Brilli, M., Frandi, A., Castric, V., Villeret, V., Viollier, P.H., and Biondi, E.G. (2013). DNA binding of the cell cycle transcriptional regulator GcrA depends on N6-adenosine methylation in *Caulobacter crescentus* and other *Alphaproteobacteria*. PLoS genetics *9*, e1003541.

Fuller, R.S., Funnell, B.E., and Kornberg, A. (1984). The dnaA protein complex with the E. coli chromosomal replication origin (oriC) and other DNA sites. Cell *38*, 889-900.

Fumeaux, C., Radhakrishnan, S.K., Ardissone, S., Theraulaz, L., Frandi, A., Martins, D., Nesper, J., Abel, S., Jenal, U., and Viollier, P.H. (2014). Cell cycle transition from S-phase to G1 in *Caulobacter* is mediated by ancestral virulence regulators. Nature communications *5*, 4081.

Galibert, F., Finan, T.M., Long, S.R., Puhler, A., Abola, P., Ampe, F., Barloy-Hubler, F., Barnett, M.J., Becker, A., Boistard, P.*, et al.* (2001). The composite genome of the legume symbiont Sinorhizobium meliloti. Science *293*, 668-672.

Gao, R., and Stock, A.M. (2009). Biological insights from structures of two-component proteins. Annual review of microbiology *63*, 133-154.

Gee, J.M., Valderas, M.W., Kovach, M.E., Grippe, V.K., Robertson, G.T., Ng, W.L., Richardson, J.M., Winkler, M.E., and Roop, R.M., 2nd (2005). The Brucella abortus Cu,Zn superoxide dismutase is required for optimal resistance to oxidative killing by murine macrophages and wild-type virulence in experimentally infected mice. Infection and immunity *73*, 2873-2880.

Gibson, K.E., Campbell, G.R., Lloret, J., and Walker, G.C. (2006). CbrA is a stationary-phase regulator of cell surface physiology and legume symbiosis in Sinorhizobium meliloti. Journal of bacteriology *188*, 4508-4521.

Gibson, K.E., Kobayashi, H., and Walker, G.C. (2008). Molecular determinants of a symbiotic chronic infection. Annual review of genetics *42*, 413-441.

Goldstein, J., Hoffman, T., Frasch, C., Lizzio, E.F., Beining, P.R., Hochstein, D., Lee, Y.L., Angus, R.D., and Golding, B. (1992). Lipopolysaccharide (LPS) from Brucella abortus is less toxic than that from Escherichia coli, suggesting the possible use of B. abortus or LPS from B. abortus as a carrier in vaccines. Infection and immunity *60*, 1385-1389.

Gora, K.G., Cantin, A., Wohlever, M., Joshi, K.K., Perchuk, B.S., Chien, P., and Laub, M.T. (2013). Regulated proteolysis of a transcription factor complex is critical to cell cycle progression in Caulobacter crescentus. Molecular microbiology *87*, 1277-1289.

Gora, K.G., Tsokos, C.G., Chen, Y.E., Srinivasan, B.S., Perchuk, B.S., and Laub, M.T. (2010). A cell-type-specific protein-protein interaction modulates transcriptional activity of a master regulator in Caulobacter crescentus. Molecular cell *39*, 455-467.

Grangeon, R., Zupan, J.R., Anderson-Furgeson, J., and Zambryski, P.C. (2015). PopZ identifies the new pole, and PodJ identifies the old pole during polar growth in Agrobacterium tumefaciens. Proceedings of the National Academy of Sciences of the United States of America.

Gray, A.N., Egan, A.J., Van't Veer, I.L., Verheul, J., Colavin, A., Koumoutsi, A., Biboy, J., Altelaar, A.F., Damen, M.J., Huang, K.C.*, et al.* (2015). Coordination of peptidoglycan synthesis and outer membrane constriction during Escherichia coli cell division. eLife *4*.

Gross, A., Spiesser, S., Terraza, A., Rouot, B., Caron, E., and Dornand, J. (1998). Expression and bactericidal activity of nitric oxide synthase in Brucella suis-infected murine macrophages. Infection and immunity *66*, 1309-1316.

Guzman-Verri, C., Chaves-Olarte, E., von Eichel-Streiber, C., Lopez-Goni, I., Thelestam, M., Arvidson, S., Gorvel, J.P., and Moreno, E. (2001). GTPases of the Rho subfamily are required for Brucella abortus internalization in nonprofessional phagocytes: direct activation of Cdc42. The Journal of biological chemistry *276*, 44435-44443.

Guzman-Verri, C., Manterola, L., Sola-Landa, A., Parra, A., Cloeckaert, A., Garin, J., Gorvel, J.P., Moriyon, I., Moreno, E., and Lopez-Goni, I. (2002). The two-component system BvrR/BvrS essential for Brucella abortus virulence regulates the expression of outer membrane proteins with counterparts in members of the Rhizobiaceae. Proceedings of the National Academy of Sciences of the United States of America *99*, 12375-12380.

Hallez, R., Bellefontaine, A.F., Letesson, J.J., and De Bolle, X. (2004). Morphological and functional asymmetry in alpha-proteobacteria. Trends in microbiology *12*, 361-365.

Hallez, R., Mignolet, J., Van Mullem, V., Wery, M., Vandenhaute, J., Letesson, J.J., Jacobs-Wagner, C., and De Bolle, X. (2007). The asymmetric distribution of the essential histidine kinase PdhS indicates a differentiation event in *Brucella abortus*. The EMBO journal *26*, 1444-1455.

Harrison-McMonagle, P., Denissova, N., Martinez-Hackert, E., Ebright, R.H., and Stock, A.M. (1999). Orientation of OmpR monomers within an OmpR:DNA complex determined by DNA affinity cleaving. Journal of molecular biology *285*, 555-566.

Hecht, G.B., and Newton, A. (1995). Identification of a novel response regulator required for the swarmer-to-stalked-cell transition in Caulobacter crescentus. Journal of bacteriology *177*, 6223-6229.

Hernandez-Castro, R., Verdugo-Rodriguez, A., Puente, J.L., and Suarez-Guemes, F. (2008). The BMEI0216 gene of Brucella melitensis is required for internalization in HeLa cells. Microbial pathogenesis *44*, 28-33.

Hilbert, D.W., and Piggot, P.J. (2004). Compartmentalization of gene expression during Bacillus subtilis spore formation. Microbiology and molecular biology reviews : MMBR *68*, 234-262.

Hinz, A.J., Larson, D.E., Smith, C.S., and Brun, Y.V. (2003). The Caulobacter crescentus polar organelle development protein PodJ is differentially localized and is required for polar targeting of the PleC development regulator. Molecular microbiology *47*, 929-941.
Holtzendorff, J., Hung, D., Brende, P., Reisenauer, A., Viollier, P.H., McAdams, H.H., and Shapiro, L. (2004). Oscillating global regulators control the genetic circuit driving a bacterial cell cycle. Science *304*, 983-987.

Hottes, A.K., Shapiro, L., and McAdams, H.H. (2005). DnaA coordinates replication initiation and cell cycle transcription in Caulobacter crescentus. Molecular microbiology *58*, 1340-1353.

Hsing, W., and Silhavy, T.J. (1997). Function of conserved histidine-243 in phosphatase activity of EnvZ, the sensor for porin osmoregulation in Escherichia coli. Journal of bacteriology *179*, 3729-3735.

Iniesta, A.A., Hillson, N.J., and Shapiro, L. (2010). Cell pole-specific activation of a critical bacterial cell cycle kinase. Proceedings of the National Academy of Sciences of the United States of America *107*, 7012-7017.

Iniesta, A.A., McGrath, P.T., Reisenauer, A., McAdams, H.H., and Shapiro, L. (2006). A phospho-signaling pathway controls the localization and activity of a protease complex critical for bacterial cell cycle progression. Proceedings of the National Academy of Sciences of the United States of America *103*, 10935-10940.

Jacobs, C., Ausmees, N., Cordwell, S.J., Shapiro, L., and Laub, M.T. (2003). Functions of the CckA histidine kinase in Caulobacter cell cycle control. Molecular microbiology *47*, 1279-1290.

Jacobs, C., Domian, I.J., Maddock, J.R., and Shapiro, L. (1999). Cell cycle-dependent polar localization of an essential bacterial histidine kinase that controls DNA replication and cell division. Cell *97*, 111-120.

Jacobs-Wagner, C. (2004). Regulatory proteins with a sense of direction: cell cycle signalling network in Caulobacter. Molecular microbiology *51*, 7-13.

Jenal, U. (2004). Cyclic di-guanosine-monophosphate comes of age: a novel secondary messenger involved in modulating cell surface structures in bacteria? Current opinion in microbiology *7*, 185-191.

Jenal, U., and Fuchs, T. (1998). An essential protease involved in bacterial cell-cycle control. The EMBO journal *17*, 5658-5669.

Jones, S.E., Ferguson, N.L., and Alley, M.R. (2001). New members of the ctrA regulon: the major chemotaxis operon in Caulobacter is CtrA dependent. Microbiology *147*, 949-958.

Jubier-Maurin, V., Boigegrain, R.A., Cloeckaert, A., Gross, A., Alvarez-Martinez, M.T., Terraza, A., Liautard, J., Kohler, S., Rouot, B., Dornand, J.*, et al.* (2001). Major outer membrane protein Omp25 of Brucella suis is involved in inhibition of tumor necrosis factor alpha production during infection of human macrophages. Infection and immunity *69*, 4823-4830.

Judd, E.M., Ryan, K.R., Moerner, W.E., Shapiro, L., and McAdams, H.H. (2003). Fluorescence bleaching reveals asymmetric compartment formation prior to cell division in Caulobacter. Proceedings of the National Academy of Sciences of the United States of America *100*, 8235-8240.

Kim, J., Heindl, J.E., and Fuqua, C. (2013). Coordination of division and development influences complex multicellular behavior in Agrobacterium tumefaciens. PloS one *8*, e56682.

Kondorosi, E., Mergaert, P., and Kereszt, A. (2013). A paradigm for endosymbiotic life: cell differentiation of Rhizobium bacteria provoked by host plant factors. Annual review of microbiology *67*, 611-628.

Kozdon, J.B., Melfi, M.D., Luong, K., Clark, T.A., Boitano, M., Wang, S., Zhou, B., Gonzalez, D., Collier, J., Turner, S.W.*, et al.* (2013). Global methylation state at base-pair resolution of the Caulobacter genome throughout the cell cycle. Proceedings of the National Academy of Sciences of the United States of America *110*, E4658-4667.

Krell, T., Lacal, J., Busch, A., Silva-Jimenez, H., Guazzaroni, M.E., and Ramos, J.L. (2010). Bacterial sensor kinases: diversity in the recognition of environmental signals. Annual review of microbiology *64*, 539-559.

Lam, H., Matroule, J.Y., and Jacobs-Wagner, C. (2003). The asymmetric spatial distribution of bacterial signal transduction proteins coordinates cell cycle events. Developmental cell *5*, 149-159.

Lang, A.S., and Beatty, J.T. (2000). Genetic analysis of a bacterial genetic exchange element: the gene transfer agent of Rhodobacter capsulatus. Proceedings of the National Academy of Sciences of the United States of America *97*, 859-864.

Lapaque, N., Moriyon, I., Moreno, E., and Gorvel, J.P. (2005). Brucella lipopolysaccharide acts as a virulence factor. Current opinion in microbiology *8*, 60-66.

Laub, M.T., Chen, S.L., Shapiro, L., and McAdams, H.H. (2002). Genes directly controlled by CtrA, a master regulator of the Caulobacter cell cycle. Proceedings of the National Academy of Sciences of the United States of America *99*, 4632-4637.

Laub, M.T., McAdams, H.H., Feldblyum, T., Fraser, C.M., and Shapiro, L. (2000). Global analysis of the genetic network controlling a bacterial cell cycle. Science *290*, 2144-2148.
Lazzaroni, J.C., Dubuisson, J.F., and Vianney, A. (2002). The Tol proteins of Escherichia coli and their involvement in the translocation of group A colicins. Biochimie *84*, 391-397.

Leonardo, M.R., and Forst, S. (1996). Re-examination of the role of the periplasmic domain of EnvZ in sensing of osmolarity signals in Escherichia coli. Molecular microbiology *22*, 405-413.

Lesley, J.A., and Shapiro, L. (2008). SpoT regulates DnaA stability and initiation of DNA replication in carbon-starved *Caulobacter crescentus*. Journal of bacteriology *190*, 6867-6880.

Levine, B., Mizushima, N., and Virgin, H.W. (2011). Autophagy in immunity and inflammation. Nature *469*, 323-335.

Lopez-Goni, I., Guzman-Verri, C., Manterola, L., Sola-Landa, A., Moriyon, I., and Moreno, E. (2002). Regulation of Brucella virulence by the two-component system BvrR/BvrS. Veterinary microbiology *90*, 329-339.

Lori, C., Ozaki, S., Steiner, S., Bohm, R., Abel, S., Dubey, B.N., Schirmer, T., Hiller, S., and Jenal, U. (2015). Cyclic di-GMP acts as a cell cycle oscillator to drive chromosome replication. Nature *523*, 236-239.

Manterola, L., Guzman-Verri, C., Chaves-Olarte, E., Barquero-Calvo, E., de Miguel, M.J., Moriyon, I., Grillo, M.J., Lopez-Goni, I., and Moreno, E. (2007). BvrR/BvrS-controlled outer membrane proteins Omp3a and Omp3b are not essential for Brucella abortus virulence. Infection and immunity *75*, 4867-4874.

Manterola, L., Moriyon, I., Moreno, E., Sola-Landa, A., Weiss, D.S., Koch, M.H., Howe, J., Brandenburg, K., and Lopez-Goni, I. (2005). The lipopolysaccharide of Brucella abortus BvrS/BvrR mutants contains lipid A modifications and has higher affinity for bactericidal cationic peptides. Journal of bacteriology *187*, 5631-5639.

Marchesini, M.I., Herrmann, C.K., Salcedo, S.P., Gorvel, J.P., and Comerci, D.J. (2011). In search of Brucella abortus type IV secretion substrates: screening and identification of four proteins translocated into host cells through VirB system. Cellular microbiology *13*, 1261-1274.

Marczynski, G.T. (1999). Chromosome methylation and measurement of faithful, once and only once per cell cycle chromosome replication in Caulobacter crescentus. Journal of bacteriology *181*, 1984-1993.

Marquis, H., and Ficht, T.A. (1993). The omp2 gene locus of Brucella abortus encodes two homologous outer membrane proteins with properties characteristic of bacterial porins. Infection and immunity *61*, 3785-3790.

Marsh, R.C., and Hepburn, M.L. (1980). Inititation and termination of chromosome replication in Escherichia coli subjected to amino acid starvation. Journal of bacteriology *142*, 236-242.

Martinez de Tejada, G., Pizarro-Cerda, J., Moreno, E., and Moriyon, I. (1995). The outer membranes of Brucella spp. are resistant to bactericidal cationic peptides. Infection and immunity *63*, 3054-3061.

Mascher, T., Helmann, J.D., and Unden, G. (2006). Stimulus perception in bacterial signal-transducing histidine kinases. Microbiology and molecular biology reviews : MMBR *70*, 910-938.

Matroule, J.Y., Lam, H., Burnette, D.T., and Jacobs-Wagner, C. (2004). Cytokinesis monitoring during development; rapid pole-to-pole shuttling of a signaling protein by localized kinase and phosphatase in *Caulobacter*. Cell *118*, 579-590.

Mergaert, P., Uchiumi, T., Alunni, B., Evanno, G., Cheron, A., Catrice, O., Mausset, A.E., Barloy-Hubler, F., Galibert, F., Kondorosi, A.*, et al.* (2006). Eukaryotic control on bacterial cell cycle and differentiation in the Rhizobium-legume symbiosis. Proceedings of the National Academy of Sciences of the United States of America *103*, 5230-5235.

Merker, R.I., and Smit, J. (1988). Characterization of the adhesive holdfast of marine and freshwater caulobacters. Applied and environmental microbiology *54*, 2078-2085.

Michaels, M.L., and Miller, J.H. (1992). The GO system protects organisms from the mutagenic effect of the spontaneous lesion 8-hydroxyguanine (7,8-dihydro-8-oxoguanine). Journal of bacteriology *174*, 6321-6325.

Mignolet, J., Van der Henst, C., Nicolas, C., Deghelt, M., Dotreppe, D., Letesson, J.J., and De Bolle, X. (2010). PdhS, an old-pole-localized histidine kinase, recruits the fumarase FumC in *Brucella abortus*. Journal of bacteriology *192*, 3235-3239.

Mitrophanov, A.Y., and Groisman, E.A. (2008). Signal integration in bacterial two-component regulatory systems. Genes & development *22*, 2601-2611.

Mohapatra, S.S., Fioravanti, A., and Biondi, E.G. (2014). DNA methylation in Caulobacter and other Alphaproteobacteria during cell cycle progression. Trends in microbiology *22*, 528-535.

Moreno, E., and Moriyon, I. (2006). The Genus *Brucella*. Prokaryotes *5*, 315-456.

Moreno, E., Stackebrandt, E., Dorsch, M., Wolters, J., Busch, M., and Mayer, H. (1990). Brucella abortus 16S rRNA and lipid A reveal a phylogenetic relationship with members of the alpha-2 subdivision of the class Proteobacteria. Journal of bacteriology *172*, 3569-3576.

Mougel, C., and Zhulin, I.B. (2001). CHASE: an extracellular sensing domain common to transmembrane receptors from prokaryotes, lower eukaryotes and plants. Trends in biochemical sciences *26*, 582-584.

Myeni, S., Child, R., Ng, T.W., Kupko, J.J., 3rd, Wehrly, T.D., Porcella, S.F., Knodler, L.A., and Celli, J. (2013). Brucella modulates secretory trafficking via multiple type IV secretion effector proteins. PLoS pathogens *9*, e1003556.

Naroeni, A., and Porte, F. (2002). Role of cholesterol and the ganglioside GM(1) in entry and short-term survival of Brucella suis in murine macrophages. Infection and immunity *70*, 1640-1644.

Ninfa, E.G., Atkinson, M.R., Kamberov, E.S., and Ninfa, A.J. (1993). Mechanism of autophosphorylation of Escherichia coli nitrogen regulator II (NRII or NtrB): trans-phosphorylation between subunits. Journal of bacteriology *175*, 7024-7032.

Nixon, B.T., Ronson, C.W., and Ausubel, F.M. (1986). Two-component regulatory systems responsive to environmental stimuli share strongly conserved domains with the nitrogen assimilation regulatory genes ntrB and ntrC. Proceedings of the National Academy of Sciences of the United States of America *83*, 7850-7854.

O'Callaghan, D., Cazevieille, C., Allardet-Servent, A., Boschiroli, M.L., Bourg, G., Foulongne, V., Frutos, P., Kulakov, Y., and Ramuz, M. (1999). A homologue of the Agrobacterium tumefaciens VirB and Bordetella pertussis Ptl type IV secretion systems is essential for intracellular survival of Brucella suis. Molecular microbiology *33*, 1210-1220.

O'Hara, B.P., Norman, R.A., Wan, P.T., Roe, S.M., Barrett, T.E., Drew, R.E., and Pearl, L.H. (1999). Crystal structure and induction mechanism of AmiC-AmiR: a ligand-regulated transcription antitermination complex. The EMBO journal *18*, 5175-5186.

Ohta, N., Lane, T., Ninfa, E.G., Sommer, J.M., and Newton, A. (1992). A histidine protein kinase homologue required for regulation of bacterial cell division and differentiation. Proceedings of the National Academy of Sciences of the United States of America *89*, 10297-10301.

Ouimet, M.C., and Marczynski, G.T. (2000). Analysis of a cell-cycle promoter bound by a response regulator. Journal of molecular biology *302*, 761-775.

Pappas, G., Akritidis, N., Bosilkovski, M., and Tsianos, E. (2005). Brucellosis. The New England journal of medicine *352*, 2325-2336.

Pappas, G., Papadimitriou, P., Akritidis, N., Christou, L., and Tsianos, E.V. (2006). The new global map of human brucellosis. Lancet Infect Dis *6*, 91-99.

Park, S.Y., and Groisman, E.A. (2014). Signal-specific temporal response by the Salmonella PhoP/PhoQ regulatory system. Molecular microbiology *91*, 135-144.

Paul, R., Jaeger, T., Abel, S., Wiederkehr, I., Folcher, M., Biondi, E.G., Laub, M.T., and Jenal, U. (2008). Allosteric regulation of histidine kinases by their cognate response regulator determines cell fate. Cell *133*, 452-461.

Piggot, P.J., and Hilbert, D.W. (2004). Sporulation of Bacillus subtilis. Current opinion in microbiology *7*, 579-586.

Pini, F., De Nisco, N.J., Ferri, L., Penterman, J., Fioravanti, A., Brilli, M., Mengoni, A., Bazzicalupo, M., Viollier, P.H., Walker, G.C.*, et al.* (2015). Cell Cycle Control by the Master Regulator CtrA in Sinorhizobium meliloti. PLoS genetics *11*, e1005232.

Pini, F., Frage, B., Ferri, L., De Nisco, N.J., Mohapatra, S.S., Taddei, L., Fioravanti, A., Dewitte, F., Galardini, M., Brilli, M.*, et al.* (2013). The DivJ, CbrA and PleC system controls DivK phosphorylation and symbiosis in Sinorhizobium meliloti. Molecular microbiology *90*, 54-71.

Pinto, U.M., Pappas, K.M., and Winans, S.C. (2012). The ABCs of plasmid replication and segregation. Nature reviews Microbiology *10*, 755-765.

Pizarro-Cerda, J., Meresse, S., Parton, R.G., van der Goot, G., Sola-Landa, A., Lopez-Goni, I., Moreno, E., and Gorvel, J.P. (1998a). *Brucella abortus* transits through the autophagic pathway and replicates in the endoplasmic reticulum of nonprofessional phagocytes. Infection and immunity *66*, 5711-5724.

Pizarro-Cerda, J., Moreno, E., Sanguedolce, V., Mege, J.L., and Gorvel, J.P. (1998b). Virulent *Brucella abortus* prevents lysosome fusion and is distributed within autophagosome-like compartments. Infection and immunity *66*, 2387-2392.

Plommet, M. (1991). Minimal requirements for growth of Brucella suis and other Brucella species. Zentralblatt fur Bakteriologie : international journal of medical microbiology *275*, 436-450.

Porte, F., Naroeni, A., Ouahrani-Bettache, S., and Liautard, J.P. (2003). Role of the Brucella suis lipopolysaccharide O antigen in phagosomal genesis and in inhibition of phagosome-lysosome fusion in murine macrophages. Infection and immunity *71*, 1481-1490.

Posadas, D.M., Ruiz-Ranwez, V., Bonomi, H.R., Martin, F.A., and Zorreguieta, A. (2012). BmaC, a novel autotransporter of *Brucella suis*, is involved in bacterial adhesion to host cells. Cellular microbiology *14*, 965-982.

Quon, K.C., Marczynski, G.T., and Shapiro, L. (1996). Cell cycle control by an essential bacterial two-component signal transduction protein. Cell *84*, 83-93.

Quon, K.C., Yang, B., Domian, I.J., Shapiro, L., and Marczynski, G.T. (1998). Negative control of bacterial DNA replication by a cell cycle regulatory protein that binds at the chromosome origin. Proceedings of the National Academy of Sciences of the United States of America *95*, 120-125.

Reisenauer, A., Quon, K., and Shapiro, L. (1999). The CtrA response regulator mediates temporal control of gene expression during the Caulobacter cell cycle. Journal of bacteriology *181*, 2430-2439.

Reisenauer, A., and Shapiro, L. (2002). DNA methylation affects the cell cycle transcription of the CtrA global regulator in Caulobacter. The EMBO journal *21*, 4969-4977.

Rittig, M.G., Alvarez-Martinez, M.T., Porte, F., Liautard, J.P., and Rouot, B. (2001). Intracellular survival of Brucella spp. in human monocytes involves conventional uptake but special phagosomes. Infection and immunity *69*, 3995-4006.

Robertson, G.T., Reisenauer, A., Wright, R., Jensen, R.B., Jensen, A., Shapiro, L., and Roop, R.M., 2nd (2000). The *Brucella abortus* CcrM DNA methyltransferase is essential for viability, and its overexpression attenuates intracellular replication in murine macrophages. Journal of bacteriology *182*, 3482-3489.

Romling, U., Galperin, M.Y., and Gomelsky, M. (2013). Cyclic di-GMP: the first 25 years of a universal bacterial second messenger. Microbiology and molecular biology reviews : MMBR *77*, 1-52.

Ruiz-Ranwez, V., Posadas, D.M., Van der Henst, C., Estein, S.M., Arocena, G.M., Abdian, P.L., Martin, F.A., Sieira, R., De Bolle, X., and Zorreguieta, A. (2013). BtaE, an adhesin that belongs to the trimeric autotransporter family, is required for full virulence and defines a specific adhesive pole of Brucella suis. Infection and immunity *81*, 996-1007.

Russo, F.D., and Silhavy, T.J. (1991). EnvZ controls the concentration of phosphorylated OmpR to mediate osmoregulation of the porin genes. Journal of molecular biology *222*, 567-580.

Ryan, R.P. (2013). Cyclic di-GMP signalling and the regulation of bacterial virulence. Microbiology *159*, 1286-1297.

Sadowski, C.S., Wilson, D., Schallies, K.B., Walker, G., and Gibson, K.E. (2013). The Sinorhizobium meliloti sensor histidine kinase CbrA contributes to free-living cell cycle regulation. Microbiology *159*, 1552-1563.

Salhi, I., Boigegrain, R.A., Machold, J., Weise, C., Cloeckaert, A., and Rouot, B. (2003). Characterization of new members of the group 3 outer membrane protein family of Brucella spp. Infection and immunity *71*, 4326-4332.

Schell, M.A., Denny, T.P., and Huang, J. (1994). VsrA, a second two-component sensor regulating virulence genes of Pseudomonas solanacearum. Molecular microbiology *11*, 489-500.

Scholten, M., and Tommassen, J. (1993). Topology of the PhoR protein of Escherichia coli and functional analysis of internal deletion mutants. Molecular microbiology *8*, 269-275.

Schredl, A.T., Perez Mora, Y.G., Herrera, A., Cuajungco, M.P., and Murray, S.R. (2012). The Caulobacter crescentus ctrA P1 promoter is essential for the coordination of cell cycle events that prevent the overinitiation of DNA replication. Microbiology *158*, 2492-2503.

Shi, L., and Hulett, F.M. (1999). The cytoplasmic kinase domain of PhoR is sufficient for the low phosphate-inducible expression of pho regulon genes in Bacillus subtilis. Molecular microbiology *31*, 211-222.

Shimoda, N., Toyoda-Yamamoto, A., Aoki, S., and Machida, Y. (1993). Genetic evidence for an interaction between the VirA sensor protein and the ChvE sugar-binding protein of Agrobacterium. The Journal of biological chemistry *268*, 26552-26558.

Siam, R., and Marczynski, G.T. (2000). Cell cycle regulator phosphorylation stimulates two distinct modes of binding at a chromosome replication origin. The EMBO journal *19*, 1138-1147.

Singh, D.K., Kumar, A., Tiwari, A.K., Sankarasubramanian, J., Vishnu, U.S., Sridhar, J., Gunasekaran, P., and Rajendhran, J. (2015). Draft Genome Sequence of Brucella abortus Virulent Strain 544. Genome announcements *3*.

Skerker, J.M., Perchuk, B.S., Siryaporn, A., Lubin, E.A., Ashenberg, O., Goulian, M., and Laub, M.T. (2008). Rewiring the specificity of two-component signal transduction systems. Cell *133*, 1043-1054.

Skerker, J.M., Prasol, M.S., Perchuk, B.S., Biondi, E.G., and Laub, M.T. (2005). Two-component signal transduction pathways regulating growth and cell cycle progression in a bacterium: a system-level analysis. PLoS biology *3*, e334.

Skerker, J.M., and Shapiro, L. (2000). Identification and cell cycle control of a novel pilus system in Caulobacter crescentus. The EMBO journal *19*, 3223-3234.

Sliusarenko, O., Heinritz, J., Emonet, T., and Jacobs-Wagner, C. (2011). High-throughput, subpixel precision analysis of bacterial morphogenesis and intracellular spatio-temporal dynamics. Molecular microbiology *80*, 612-627.

Sola-Landa, A., Pizarro-Cerda, J., Grillo, M.J., Moreno, E., Moriyon, I., Blasco, J.M., Gorvel, J.P., and Lopez-Goni, I. (1998). A two-component regulatory system playing a critical role in plant pathogens and endosymbionts is present in Brucella abortus and controls cell invasion and virulence. Molecular microbiology *29*, 125-138.

Spencer, W., Siam, R., Ouimet, M.C., Bastedo, D.P., and Marczynski, G.T. (2009). CtrA, a global response regulator, uses a distinct second category of weak DNA binding sites for cell cycle transcription control in Caulobacter crescentus. Journal of bacteriology *191*, 5458-5470.

Starr, T., Child, R., Wehrly, T.D., Hansen, B., Hwang, S., Lopez-Otin, C., Virgin, H.W., and Celli, J. (2012). Selective subversion of autophagy complexes facilitates completion of the Brucella intracellular cycle. Cell host & microbe *11*, 33-45.

Starr, T., Ng, T.W., Wehrly, T.D., Knodler, L.A., and Celli, J. (2008). *Brucella* intracellular replication requires trafficking through the late endosomal/lysosomal compartment. Traffic *9*, 678-694.

Stephens, C.M., Zweiger, G., and Shapiro, L. (1995). Coordinate cell cycle control of a Caulobacter DNA methyltransferase and the flagellar genetic hierarchy. Journal of bacteriology *177*, 1662-1669.

Stewart, R.C. (2010). Protein histidine kinases: assembly of active sites and their regulation in signaling pathways. Current opinion in microbiology *13*, 133-141.

Tan, M.H., Kozdon, J.B., Shen, X., Shapiro, L., and McAdams, H.H. (2010). An essential transcription factor, SciP, enhances robustness of Caulobacter cell cycle regulation. Proceedings of the National Academy of Sciences of the United States of America *107*, 18985-18990.

Taylor, B.L., and Zhulin, I.B. (1999). PAS domains: internal sensors of oxygen, redox potential, and light. Microbiology and molecular biology reviews : MMBR *63*, 479-506.

Thanbichler, M. (2009). Spatial regulation in Caulobacter crescentus. Current opinion in microbiology *12*, 715-721.

Tibor, A., Decelle, B., and Letesson, J.J. (1999). Outer membrane proteins Omp10, Omp16, and Omp19 of Brucella spp. are lipoproteins. Infection and immunity *67*, 4960-4962.

Tibor, A., Wansard, V., Bielartz, V., Delrue, R.M., Danese, I., Michel, P., Walravens, K., Godfroid, J., and Letesson, J.J. (2002). Effect of omp10 or omp19 deletion on Brucella abortus outer membrane properties and virulence in mice. Infection and immunity *70*, 5540-5546.

Tibor, A., Weynants, V., Denoel, P., Lichtfouse, B., De Bolle, X., Saman, E., Limet, J.N., and Letesson, J.J. (1994). Molecular cloning, nucleotide sequence, and occurrence of a 16.5-kilodalton outer membrane protein of Brucella abortus with similarity to pal lipoproteins. Infection and immunity *62*, 3633-3639.

Tsokos, C.G., Perchuk, B.S., and Laub, M.T. (2011). A dynamic complex of signaling proteins uses polar localization to regulate cell-fate asymmetry in Caulobacter crescentus. Developmental cell *20*, 329-341.

Van der Henst, C., Beaufay, F., Mignolet, J., Didembourg, C., Colinet, J., Hallet, B., Letesson, J.J., and De Bolle, X. (2012). The histidine kinase PdhS controls cell cycle progression of the pathogenic alphaproteobacterium *Brucella abortus*. Journal of bacteriology *194*, 5305-5314.

Verstreate, D.R., Creasy, M.T., Caveney, N.T., Baldwin, C.L., Blab, M.W., and Winter, A.J. (1982). Outer membrane proteins of Brucella abortus: isolation and characterization. Infection and immunity *35*, 979-989.

von Bargen, K., Gorvel, J.P., and Salcedo, S.P. (2012). Internal affairs: investigating the Brucella intracellular lifestyle. FEMS microbiology reviews *36*, 533-562.

Wang, J.D., and Levin, P.A. (2009). Metabolism, cell growth and the bacterial cell cycle. Nature reviews Microbiology *7*, 822-827.

Wang, S.P., Sharma, P.L., Schoenlein, P.V., and Ely, B. (1993). A histidine protein kinase is involved in polar organelle development in Caulobacter crescentus. Proceedings of the National Academy of Sciences of the United States of America *90*, 630-634.

Watarai, M., Makino, S., Fujii, Y., Okamoto, K., and Shirahata, T. (2002). Modulation of Brucella-induced macropinocytosis by lipid rafts mediates intracellular replication. Cellular microbiology *4*, 341-355.

Wheeler, R.T., and Shapiro, L. (1999). Differential localization of two histidine kinases controlling bacterial cell differentiation. Molecular cell *4*, 683-694.

Whitworth, D.E., and Cock, P.J. (2009). Evolution of prokaryotic two-component systems: insights from comparative genomics. Amino acids *37*, 459-466.

Willett, J.W., Herrou, J., Briegel, A., Rotskoff, G., and Crosson, S. (2015). Structural asymmetry in a conserved signaling system that regulates division, replication, and virulence of an intracellular pathogen. Proceedings of the National Academy of Sciences of the United States of America *112*, E3709-3718.

Wood, D.W., Setubal, J.C., Kaul, R., Monks, D.E., Kitajima, J.P., Okura, V.K., Zhou, Y., Chen, L., Wood, G.E., Almeida, N.F., Jr.*, et al.* (2001). The genome of the natural genetic engineer Agrobacterium tumefaciens C58. Science *294*, 2317-2323.

Wright, R., Stephens, C., Zweiger, G., Shapiro, L., and Alley, M.R. (1996). Caulobacter Lon protease has a critical role in cell-cycle control of DNA methylation. Genes & development *10*, 1532-1542.

Yamamoto, K., Hirao, K., Oshima, T., Aiba, H., Utsumi, R., and Ishihama, A. (2005). Functional characterization in vitro of all two-component signal transduction systems from Escherichia coli. The Journal of biological chemistry *280*, 1448-1456.

Zhulin, I.B., Nikolskaya, A.N., and Galperin, M.Y. (2003). Common extracellular sensory domains in transmembrane receptors for diverse signal transduction pathways in bacteria and archaea. Journal of bacteriology *185*, 285-294.

Zweiger, G., Marczynski, G., and Shapiro, L. (1994). A *Caulobacter* DNA methyltransferase that functions only in the predivisional cell. Journal of molecular biology *235*, 472-485.

Zweiger, G., and Shapiro, L. (1994). Expression of Caulobacter dnaA as a function of the cell cycle. Journal of bacteriology *176*, 401-408.